ABSTRACT

Title of Dissertation: IMPACT OF CLIMATE CHANGE ON
WILDLAND FIRE THREAT TO THE AMUR
TIGER AND ITS HABITAT.

Tatiana V. Loboda, Ph.D., 2008

Directed By: Professor C.O. Justice, Department of
Geography

Global biodiversity is increasingly threatened by combined pressures from

human- and climate-related environmental change. Projected climate change

indicates that these trends are likely to continue and may accelerate by the end of this

century leading to large scale modification of species habitats. Such modification

will be amplified by an increase in catastrophic natural events such as wildland fire -

one of the dominant disturbance agents in boreal and temperate forests of the Russian

Far East (RFE). In the RFE, large fire events lead to abrupt, extensive, and long-term

conversion of forests to open landscapes, thus considerably impacting the habitat of

the critically endangered Amur tiger (*Panthera tigris altaica*). A remotely sensed

data-driven regional fire threat model (FTM) is developed to assess current and

projected fire threat to the Amur tiger under scenarios of climate change. The FTM is

parameterized to account for regional specifics of fire occurrence in the RFE and fire

impacts on the Amur tigers, their main prey, and their habitat. Fire regimes are

shown to be strongly influenced by anthropogenic use of fire and the monsoonal climate of the RFE, with large fire seasons observed during uncharacteristically dry years. Even with a large proportion of human ignition sources and periodic extreme events, fire currently poses a limited threat to the Amur tiger meta-population. The observed peaks in high fire threat conditions are localized in space and time and are likely to impact a small number of individual tigers. Under the wide range of the IPCC climate change scenarios, no considerable change in fire danger is expected by the mid-21st century. However, by the end of the 21st century under the A2 (regional self-reliance) scenario of the IPCC Special Report on Emissions, fire danger over the southern part of the RFE is predicted to increase by nearly 15%. An overlap of areas of likely increase in fire danger with areas of highest tiger habitat quality results in a 20% mean yearly increase in fire threat with a mean monthly increase of ~40% in August. The results have implications for conservation strategies aimed at securing long-term habitat availability.

IMPACT OF CLIMATE CHANGE ON WILDLAND FIRE THREAT TO THE
AMUR TIGER AND ITS HABITAT.

By

Tatiana V. Loboda

Dissertation submitted to the Faculty of the Graduate School of the
University of Maryland, College Park, in partial fulfillment
of the requirements for the degree of
Doctor of Philosophy
2008

Advisory Committee:
Professor Christopher O. Justice, Chair
Dr. Ivan A. Csiszar
Professor Ruth S. DeFries
Professor James M. Dietz
Dr. John Seidensticker
Professor John R.G. Townshend

Dedication

To my family,
Jim and Alex

Acknowledgements

Table of Contents

List of Tables

List of Figures

Chapter 3:

Chapter 4:

Chapter 6:

Chapter 7:

Chapter 1: Introduction

1.1. Background

Global biodiversity is increasingly threatened by combined pressures from human- and climate-related environmental change (Millennium Ecosystem Assessment, 2005). While it is widely accepted that human modification of species habitat may lead to species extinction (National Research Council, 1995; Lee and Jetz, 2007), new evidence shows that climate change alone can present a potent threat as well (Pimm, 2008). Thomas et al. (2004) estimate that under a suite of scenarios of climate change between 15 and 37% of species across various taxa and several geographic regions are likely to be 'committed to extinction' by 2050. A study by Sekercioglu et al. (in press) forecasts that a staggering 400 – 550 out of 8500 landbird species to be extinct by 2100. These and numerous other studies evaluate the gradual shift of species ranges under projected climate change (Pimm, 2008). However, little has been done to evaluate the threat posed to biodiversity by extensive and abrupt modifications of habitat under changing regimes of natural catastrophic events.

Wildland fire is one of the leading causes of land cover disturbance worldwide. The present global distribution of vegetation is nearly as much determined by fire occurrence as by climate (Bond et al., 2005). The extent of fire induced land cover disturbance is particularly pronounced in temperate and boreal forests of the Northern Hemisphere where it often represents an abrupt conversion of tree-dominated ecosystems to open landscapes over vast areas (Stocks 1991). In addition to the considerable spatial extent, fire induced land cover disturbance in

boreal forests is characterized by slow rates of vegetation regrowth. On average, secondary forests are established on burns within 50-75 years, and complete burn recovery to pre-fire conditions may take as long as 150-200 years (Sheshukov, 1996). The extent and persistence of land cover disturbance lead to significant and long-lasting changes in ecosystem functioning including nutrient cycling, microclimate, and species composition, distribution, and richness (Kielland et al., 2006; Harden et al., 2006; Vajda and Venalainen, 2005; Warren and Collins, 2007; Wein and de Groot, 1996).   It can also lead to regional climatic feedbacks through the increase in surface albedo associated with conversion of forest to open landscapes (Sirois and Payette, 1991, Chapin et al., 2000) triggering a chain of further changes in vegetation composition (Bonan et al., 1992).

The Sikhote-Alin ecoregion of the Russian Far East (RFE) is an area of high biological importance, part of which was designated by the United Nations Educational, Scientific and Cultural Organization (UNESCO) as a World Heritage Site (UNESCO, 2001) (Figure 1-1). The landscapes of the RFE present a mosaic of boreal and temperate forest rich in rare and endemic species (Astafiev and Potikha, 2006). These forests are considered the most diverse ecosystems of the north-western Pacific coastline, shared by subtropical and northern boreal species (IUCN, 2001). The World Conservation Union (IUCN) regards the protection of natural ecosystems of the RFE as highly important for both cultural and environmental reasons (2001). Forests of the RFE sustain the hunting culture of the Udege indigenous people. Additionally, this ecosystem is the only known habitat for several endangered species including the Far Eastern leopard and the Amur tiger.
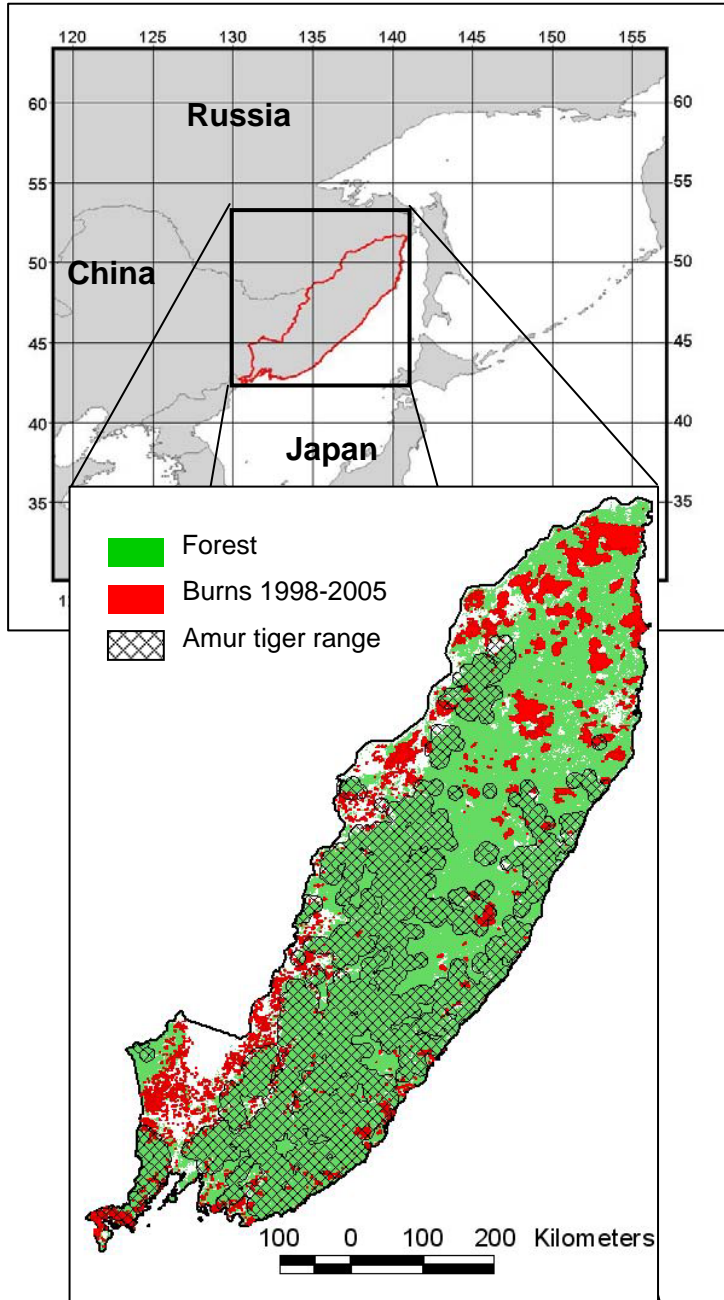
Figure 1-1. Map of study area showing distribution of forested landscapes in 2000, areas burned between 1998 (Sukhinin et al., 2004) and 2005 (chapter 4), and the range of the Amur tiger meta-population (Miquelle et al., 2005).

The Amur tiger (*Panthera tigris altaica)* is the northernmost subspecies of tiger. The entire tiger meta-population, which consisted of approximately 350 adult tigers remaining in the wild in 1998, is found within the Sikhote-Alin ecoregion of the RFE (Seidensticker et al, 1999). The Amur tiger population size has varied throughout the 20th century (Matyushkin, 2006). Although the forests of the RFE remained nearly pristine during the first half of the 20th century, unlimited tiger and ungulate hunting led to a deep depression in tiger population by mid 1960s. Between 1963 and 1966 tigers were extremely rare even within Sikhote-Alin Reserve, which is the largest reserve in the RFE established in 1935. The change in state policy and the inclusion of the Amur tiger in the protected species list resulted in a steady increase in the number of tigers first within the nature reserve and subsequently outside its boundaries.   In recent years tiger presence was noted north of the Amur River, which was previously considered to be beyond the tigers' northern ecological boundary (D. Miquelle and A. Kulikov, personal comm.).

While the tiger population is recovering (Matyshkin, 2006), it is yet far from the estimated 876 individuals – the minimal viable population (MVP) necessary to ensure the long-term species well-being and genetic diversity (Reed et al, 2003). Reaching the MPV of 876 individuals will not be possible without large continuous tracks of quality habitat. The Amur tiger has the lowest population densities and reproductive potential of all tiger subspecies even in high quality tiger habitat and thus requires extensive hunting areas for tigers (Smirnov and Miquelle, 1999). In the relatively undisturbed forests of the Sikhote-Aline reserve, Amur tiger home-ranges vary from 200-400km^2 for females to 800-1000km^2 for males (Matyushkin, 2006).

Male and female ranges often overlap, resulting in an estimated 500 km^2 hunting ground needed per tiger. Based on the size of the individual home ranges, the minimal dynamic area (MDA) required to sustain an MVP of 876 individuals is approximately 400,000 km^2. The MDA may be smaller in high quality habitats which can support higher prey densities. However, lower prey densities, resulting from over-hunting and habitat degradation and conversion, would require an even larger MDA to sustain the tiger meta-population.

Massive logging activities started in the second half of the 20th century in the highest quality tiger habitat – Korean pine stands (Matyushkin, 2006). By mid 1980s, nearly all Korean pine stands of the RFE were affected by industrial logging. Although the Korean pine harvest became illegal by early 1990s, the industrial logging did not diminish but was rather redirected to harvesting spruce, fir, and larch stands, further contributing to conversion of tree-dominated habitat to open landscapes. A comprehensive network of interconnected protected areas was designed to ensure the ecological corridors necessary to maintain the connectivity of fragmented landscapes (Miquelle et al., 1999). Although the proposed network of protected areas will mitigate against anthropogenic habitat disturbance, large fire events will continue tiger habitat conversion and fragmentation.

The RFE experiences a strong oceanic influence that is particularly well pronounced in the amount and regime of rainfall (Kotlyakov, 2003). The summer monsoon provides ample precipitation (500 mm/year in the lowlands and up to 1500 mm/year in the mountains) with the majority received during the June-August time period (Savin, 2003). The coincident peaks of large amounts of precipitation and

5

maximum annual temperatures determine lower frequency of large fire occurrence relative to the taiga forests of Central Siberia where large forest fires occur almost every year (Ivanova and Ivanov, 1999). Large and catastrophic fire events are recurring incidents in the RFE with a return interval of approximately 12-15 years (Sheingauz, 1996). Although fire occurrence is a natural component of this ecosystem, increased frequency of fire occurrence and amounts of burned area resulted in extensive and irreversible modifications of the Amur tiger habitat (Gromyko, 2006). Between 1977 and 2003 ~21% of spruce-fir forests and ~28% of Korean pine stands within the Sikhote-Alin reserve were killed by wildland fire. In addition, fires occurring within secondary forests impede regeneration of coniferous tree species leading to setbacks in forest restoration and potentially irreversible conversion of coniferous forests to other land cover types.

In the light of a considerable warming trend of the changing global climate with its particularly strong effect on the boreal regions, boreal ecosystems are changing rapidly (Barber et al., 2000; Soja et al., 2007). The projected trend towards higher temperatures in the boreal zone will affect vegetation flammability through its impact on fuel moisture, fire season length, and water levels (Stocks et al., 1998; Stocks, 1993; de Groot et al., 2003; Gillet et al., 2004). Even without accounting for these factors, burned area is expected to increase under changing climatic conditions (Flannigan et al., 2005). Additional changes in forest health due to increases in pest infestation (Logan et al, 2003) associated with a warming climate are expected to lead to fuel accumulation. Increases in hazardous fuel build-up results in a higher

frequency of fire occurrence and often changes the fire regime from low intensity ground fires to high intensity catastrophic fire events (Martell, 2001).

The changes in the natural fire cycle in the Amur tiger habitat, prompted by decades of intensive economic development and the rising frequency of large fires, necessitate the adoption of a proactive approach to resource protection from wildland fire impacts. The viability of such an approach is in part based on wildlife managers' ability to assess the potential threat posed by fire to the Amur tigers in spatially explicit and temporally dynamic framework. Fire risk or fire threat modeling addresses the likelihood and magnitude of fire impact on resources within a specific region and provides such a framework (Fairbrother and Turnley, 2005). Risk assessments are designed as decision tools in support of management activities. Fire risk modeling is particularly valuable for resource managers because of its ability to evaluate stress-induced ecological responses and subsequent resource recovery.

Although risk/threat modeling is the newest type of fire modeling, several approaches have been developed. The USDA Forest Service model is a probability based model designed to forecast the number of fires and particularly large fires over a given area during a particular time period (Preisler et al., 2004). The model output focuses on forecasting the likelihood of catastrophic fire occurrence rather than evaluation of expected impact. The fuzzy logic driven long-term risk fire model presented by Iliadis (2005) focuses on structural fire risk. In the context of wildland fire, structural risk implies long-term risk derived from parameters with slow dynamic ranges such as land cover type and topography. This model outputs spatially explicit but static maps of areas that can be potentially strongly affected by fire. A fire threat

assessment scheme (Solichin et al., 2003) introduces the temporal component of fire threat modeling and incorporates the notion of values at risk and fire suppression capabilities in addition to the overall topography related fire danger. Bonazountas et al. (2005) present a risk assessment model, forecasting integrated damage rate based on probability of fire ignition, socio-economic risk, land value, and potential fire spread rate. This model presents a similar approach to Solichin et al. but identifies values at risk more rigidly as socio-economic values.

The previously described models focus on the assessment of immediate post-fire impacts which are often transparent and are relatively easy to assess. However, these models do not balance the negative short-term effects with potentially positive long-term effects, which are highly important for natural resource management (Gossow, 1996). The approach to fire threat modeling introduced by Sampson and Sampson (2005) focuses on evaluation of long-term effects of fire occurrence as well as long-term effects of fire exclusion from the ecosystems. They examine ecosystem processes at landscape level to evaluate the benefits and potential damage from wildland fires to vegetative succession, watershed properties, and human life and property.

The overarching concern of above models with risk in relation to human life, property, or specific socio-economic values, makes them inapplicable to estimating threat posed by wildland fire to the Amur tiger. This threat is specific and includes a suite of direct and indirect fire effects on tigers that may not be explicitly linked to human well-being. The direct threats to tigers include flaming front-resultant tiger cub mortality and conversion of preferred tiger habitats to substandard habitat types.

8

Similarly, the indirect threats to the Amur tiger include flaming front induced mortality of the young of tigers' prey species and degradation or conversion of their preferred habitats. Additionally, the models described above do not account for ecological and socio-economic specifics of regional fire occurrence. Finally, the implementation of the evaluated models often relies on the availability of data sources which do not exist in many regions of the world (de la Riva et al, 2004: Vadrevu et al, 2006).

Data availability for fire threat modeling in the RFE is particularly limited. Fire records collected by the Russian federal aerial fire protection agency are highly inaccurate in both the position and estimated amounts of fire occurrence (Conard et al, 2002). Remote sensing presents the only viable source of timely, consistent, relatively unbiased, and spatially explicit data about wildland fires for the RFE. The Moderate Resolution Imaging Spectroradiometer (MODIS) instrument was in part designed for fire monitoring (Kaufman et al., 1998). The suite of standard MODIS products allows for high frequency observations of fire occurrence, land surface properties, and vegetation response at moderate (500 m) and coarse (1 km) spatial resolutions. Additional information used in fire modeling activities is available from global observations of terrestrial ecosystems from various satellite platforms (Amatulli et al., 2006; de la Riva et al, 2004; Chuvieco et al, 2004; Oldford et al, 2006).

The ability to model spatially explicit and temporally dynamic fire threat to the Amur tiger will enable the resource management community to develop short- and long-term plans, increasing the chances of maintaining tiger habitat quality,

9

availability, and connectivity under changing climate and/or land use. Fire threat modeling will also allow for testing various management approaches and evaluating scenarios beyond the current range of experience (Andrews and Queen, 2001). In addition to the operational value of fire threat modeling, this research contributes to addressing the scientific goals of the international Northern Eurasia Earth Science Partnership Initiative (NEESPI) by developing "predictive capability of terrestrial ecosystems dynamics over Northern Eurasia for the 21st century to support global projections as well as informed decision making and numerous practical applications in the region" (NEESPI, 2004).

1.2. Research Objectives

This research was designed to answer two major science questions: *How much threat does the wildland fire pose to the Amur tiger and its habitat* and *how will climate change affect fire threat to the Amur tiger by the end of 2100?* Two hypotheses were developed from the general body of knowledge in response to these science questions:

1. *Wildland fire presents a potent and wide spread threat to the Amur tiger and its habitat.*

2. *Climate change will increase fire threat to the Amur tiger and its habitat*

These hypotheses were tested within the framework of a spatially explicit and temporally dynamic Fire Threat Model (FTM) driven by remotely sensed data. The model was developed and parameterized to reflect regional specifics based on the analysis of fire occurrence in the RFE during 2001-2005 available from the MODIS record. The FTM was focused on assessing fire threat to the Amur tiger by modeling

potential impacts on the tigers, their main prey species (red deer, wild boar, and moose), and their habitat.

The specific sub-goals were as follows:

1. Develop a conceptual framework for fire threat assessment for resource managers.

2. Produce yearly burned area estimates for the RFE between 2001 and 2005 to facilitate the evaluation of drivers of fire occurrence.

3. Determine drivers of fire occurrence and quantify their contribution to fire danger.

4. Evaluate feasibility of using Global Circulation Model (GCM) data in projecting future trends in fire danger under various scenarios of climate change.

5. Develop an approach to evaluating fire driven ecological components of threat to the Amur tiger from qualitative assessments.

6. Map current levels of fire threat to the Amur tiger during 2005-2007.

7. Evaluate projected changes in fire threat to the Amur tiger through the year 2100 under climate change scenarios.

1.3. Outline of the Dissertation

This dissertation consists of seven chapters (Figure 1-2). Five chapters (Chapter 2 – Chapter 6) are presented in the self-contained format of journal articles. They are ordered in the sequence of project implementation where the subsequent analysis relies on the previously developed methodologies and data products. Chapter 7 concludes the dissertation with the discussion of the project's implications and future research directions.

Chapter 2 introduces the conceptual model of fire threat for resource management. The conceptual FTM presents a generic regional scale model that aims at identifying fire susceptible areas of high importance for a given resource. Additionally, it provides a framework for developing quantitative assessments of contributions from various parameters to the overall fire threat. The FTM is a fuzzy logic driven model designed to operate on spatially explicit data sources largely provided by remotely sensed data products. This chapter also includes assessment of the risk of ignition in the RFE as an example of model application.

Chapter 3 focuses on yearly burned area mapping for the RFE which is central to the analysis of fire occurrence in the RFE and the FTM parameterization. It describes a remote sensing/GIS-based algorithm for burned area mapping using MODIS data. This algorithm presents a novel approach to burned area mapping because it is adapted to ecosystem and regional specifics of fire occurrence in the area of interest. As a semi-automated algorithm, this methodology ensures consistent and reliable spatially explicit assessment of burned area for the RFE through 2001-2005.

Chapter 4 addresses the application of the FTM framework to assessing daily fire danger in the RFE during 2006. It describes the model parameterization based on the analysis of spatio-temporal patterns of fire occurrence as a factor of land cover and land use, topography, proximity to anthropogenic features, and previous disturbances. This analysis allowed for quantifying the relative contribution of various socio-economic and ecological parameters to fire danger in the RFE.

The fire danger modeling approach described in chapter 4 is extended to evaluate a broad range of potential scenarios of future trends in fire danger over the

Chapter 1: Introduction

Background, research objectives, and dissertation structure

Chapter 2: Conceptual Fire Threat Model (FTM) and risk of ignition

Assessing the risk of ignition in the Russian Far East within the modeling framework of fire threat
(Loboda and Csiszar, 2007a)

Chapter 3: Development of burned area product for the FTM parameterization

Regionally adaptable dNBR-based algorithm for burned area mapping from MODIS data
(Loboda et al., 2007)

Chapter 4: FTM application for modeling fire danger

Modeling fire danger in data-poor regions: a case study from the Russian Far East
(Loboda, in review)

Chapter 5: Projecting fire danger trends in the 21st century under climate change scenarios

Long-term forecasting of fire danger in the Russian Far East using climate change scenarios

Chapter 6: FTM application for modeling current and projected levels of fire threat to the Amur tiger

Estimating wildland fire threat to the Amur tiger: current levels and future scenarios under the influence of climate change

Chapter 7: Conclusion

Operational and scientific potential for fire threat modeling for the Amur tiger and its habitat and future research

Figure 1-2. Flow of the doctoral research project within the dissertation structure.

RFE (Chapter 5). This chapter addressed the feasibility of using very coarse resolution GCM outputs from the ECHAM5 model for fire danger modeling at the regional scale by comparing it to the observed meteorological conditions at the end of the 20th century. The potential changes in fire danger over the RFE are then analyzed for the B1 and A2 story lines of the Special Report on Emissions Scenarios (SRES) of the International Panel on Climate Change (IPCC) projected to the middle and the end of the 21st century.

Chapter 6 provides the connection between modeled fire danger levels and observed fire impacts on the vegetation of the RFE. This relationship presents the basis for evaluating fire threat to the Amur tiger. Direct impact of flaming front and smoke on the tigers and the major prey species is assessed together with the fire driven habitat conversion and fragmentation. These parameters are evaluated to present an integrated estimate of expected fire impact on the Amur tiger – Fire Threat. The current levels of Fire Threat to the Amur tiger modeled during 2005-2007 period are subsequently compared to the Fire Threat levels projected for 2096-2100 under the A2 scenario using the ECHAM5 model outputs.

Chapter 7 presents the overall conclusion of the doctoral research. It discusses the implications and opportunities provided by this research for the Amur tiger conservation, natural resource management, climate change science, and fire threat modeling. It also presents this project's contribution to the international NEESPI science program, strategic tiger conservation planning, and provides an overview of the future research directions.

Chapter 2: Assessing the Risk of Ignition in the Russian Far East within a Modeling Framework of Fire Threat[1]

This chapter presents a conceptual fire threat model as a resource oriented approach to assessing wildland fire impact. It identifies generic components of fire threat and provides a framework for building the model of fire threat to the Amur tiger in the RFE (finalized in chapter 6). The assessment of the risk of ignition describes the first step towards adapting the conceptual model to regional specifics of wildland fire in the RFE. This analysis is further used in chapter 4 to model fire danger.

2.1. Introduction

Considerable impacts on ecosystem functioning and human well-being, posed by wildland fire, necessitate adoption of proactive approaches to resource protection. The existing frameworks for assessment of fire threat commonly focus on wildland-urban interface and protection of human property (Cohen, 1999). This chapter presents a new conceptual model of fire threat designed for resource management rather than the fire management community and is aimed at evaluating spatio-temporal dynamics of fire threat to a given resource.

In this context, fire threat defines a combination of the expected probability and extent of fire occurrence, fire impact severity relevant to a specific resource, and the ability of the resource to recover within the time-frame of interest. The

---

[1] The presented material has been previously published in part in Loboda TV, Csisar IA (2007) Assessing the Risk of Ignition in the Russian Far East within a Modeling Framework of Fire Threat. *Ecological Applications*, 17(3), 791-805.

conceptual model is presented as a generic framework that can be applied to evaluating fire threat to a variety of specific (e.g. endangered species) or broad resource types (e.g. wetland ecosystems). For fire affected ecosystems, fire threat assessment provides critical information for short- and long-term strategic planning of resource protection, ranging from fire preventative measures to policy making and promoting fire-threat awareness among the population.

This chapter has a dual purpose. First, it introduces a spatially explicit and temporally dynamic model driven by remotely sensed data to assess quantitatively fire threat to a generic resource. Second, it presents an evaluation of the risk of ignition in the RFE within the framework of the presented model. This analysis demonstrates the functionality of the model and provides a brief assessment of temporal patterns of fire occurrence and how they relate to the patterns of fire ignition.

2.2. Dynamic Fire Threat Model

Fire threat modeling extends the predictive capabilities of fire danger assessment, which evaluates the ease of fire ignition and the difficulty of fire suppression for fire management purposes. The Fire Threat Model (FTM) presented here targets the resource management rather than the fire management community. The intent is to provide information on current and potential future wildland fire threat to a specific resource and to enable resource managers to make short and long-term decisions about the best approaches to protecting a particular resource from adverse wildland fire impact. Although the fire management community undoubtedly knows best how to reduce the threat of large fire impact, fire managers are often not

16

familiar with specific needs of a particular resource. The FTM output identifies areas where a given resource will be impacted the most at a specific period of time based on dominate weather patterns.

The FTM (Figure 2-1) has a number of advantages over the existing fire threat assessment schemes (e.g. Preisler et al., 2004; Iliadis, 2005; Solichin et al., 2003).
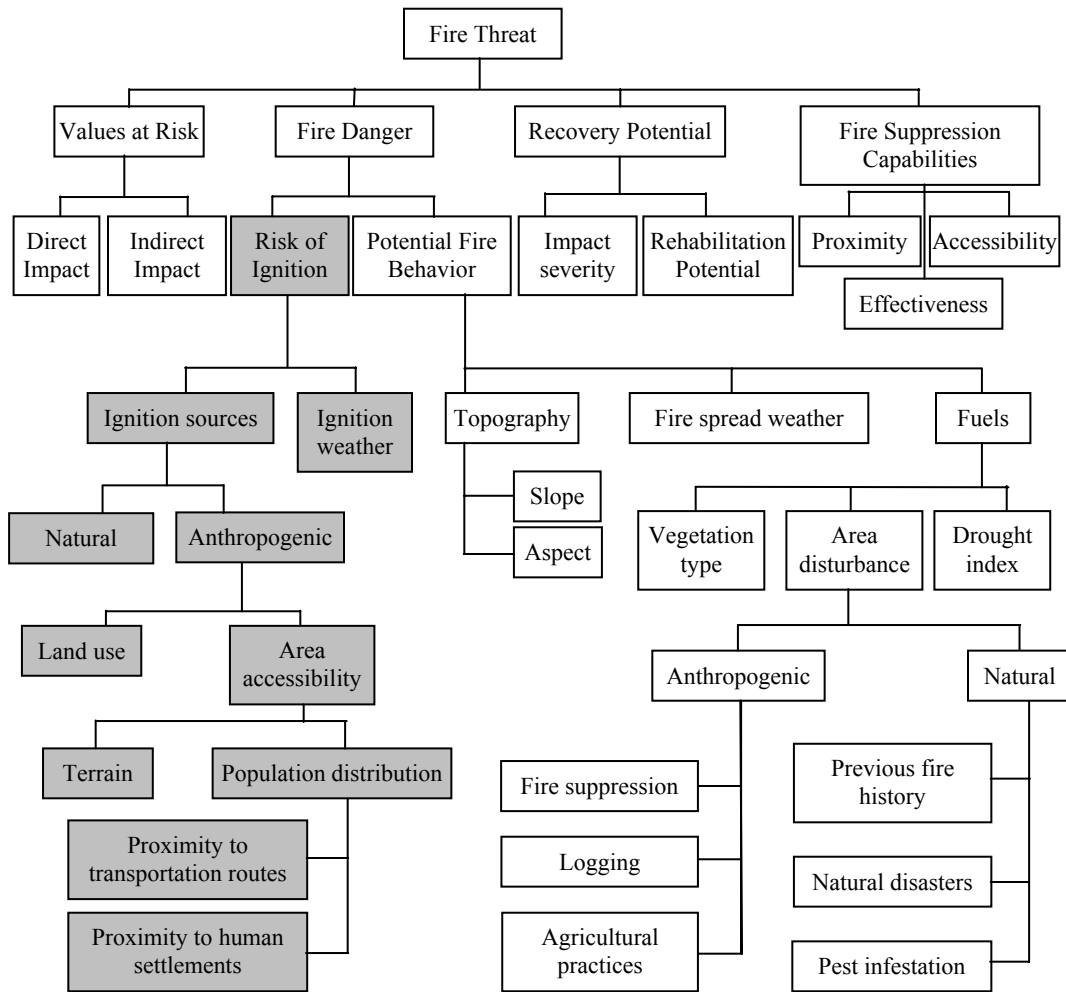
Figure 2-1. The conceptual Fire Threat Model for resource managers. The shaded areas show the components of the Risk of Ignition Module.

First, it is a highly generic model designed to operate at the regional scale. It presents

a skeleton of a system which can be populated and refined to meet the requirements

of a particular region and resource. Second, Geographic Information Systems (GIS)

and remotely sensed data sources enable spatially explicit and temporally dynamic

forecasting of fire threat to a given resource. Third, the FTM provides an opportunity

to evaluate "no-interference" fire threat scenarios. The flexibility of the FTM allows

for modifications of Fire Suppression Module parameterization not only as a factor of

a given area's proximity to fire suppression units (e.g. fire crew base station) and its

general accessibility, but also on the effectiveness of the fire suppression units

response.

2.2.1. The Fire Danger Module

The Fire Danger module is the most generic part of the FTM. It incorporates

two large components of fire occurrence: Risk of Ignition (ROI) and Potential Fire

Behavior (PFB). The relative importance of input variables is determined through

regional expert knowledge of fire regimes. The input variables are weighted

accordingly to simulate regional specifics of fire occurrence.

ROI evaluates the likelihood of fire ignition based on natural and human

causes of fire and the suitability of weather conditions. Lightning is the most

frequent natural cause of fire (Whelan, 1995). The anthropogenic influences on fire

regimes are evaluated through land use and area accessibility. Logging (both clear-

cutting and selective) affects the microclimate of forest stands directly by increasing

air temperature and reducing relative humidity (Whelan, 1995). Further, logging

debris presents hazardous dead fuels which can rapidly lose their moisture content

and facilitate fire ignition and propagation. In addition, logging introduces anthropogenic sources of ignition such as sparks from equipment and human negligence. Roads, railroads and human settlements and the complexity of the terrain strongly affect area accessibility and influence the likelihood of fire occurrence in Siberia (Kovacs et al., 2004). The third ROI component in the model is fire weather, which evaluates the possibility of fire ignition under specific weather conditions. Any of the weather indices currently used for fire danger assessment can be applied to the model.

Potential Fire Behavior at the regional scale is driven predominantly by terrain, fuel availability and condition. The Fuels component is composed of three major subcomponents: Vegetation Type (or Land Cover), Drought Index and Area Disturbance. At the regional scale vegetation type provides an approximation of fuel types/loading characteristics for a particular vegetation zone. Drought Index is of importance in relation to the condition of the fuels. Area Disturbance presents a combination of natural and anthropogenic causes. Previous fire history, natural disasters (e.g. hurricanes, tornadoes, etc.) leading to vegetation mortality and fuel accumulation, and pest infestation are the main natural disturbances influencing fuel availability. While natural disasters and pest infestation lead to an increase in fuel accumulation and therefore enhance fire occurrence and spread, previous fire history can have either enhancing or diminishing effects on fire behavior. Anthropogenic disturbance significantly changes the natural dynamics of fire. Complete fire suppression inside the US has led to high fuel loads leading to the uncontrollable spread of fire in many areas and, as a result, prescribed fire has been used in some

areas to decrease the fuel loads (Martell, 2001). Agricultural practices include a range of human activities affecting fire behavior. For example, management of pastures and open grasslands and prevention of brush encroachment by the use of fire changes considerably the fuel availability.

2.2.2. The Values at Risk Module

The Values at Risk module is designed to narrow the scope of the model to focus on the protection of a specific resource. This module reflects the current expert knowledge of the resource and the needs and potential impacts of wildland fire on various aspects of the resource environment. Fire threat to a resource can be modeled successfully as long as the fire impact and the feedbacks between the various components of a given resource are understood. Modeling fire threat to a complex resource with numerous feedbacks is significantly more difficult than a focused approach and may introduce a large amount of uncertainty into modeling results.

The two major components of the Values at Risk Module are assessments of direct and indirect fire impacts on a resource. The assessment of direct fire impacts on a resource is more straightforward than the assessment of the indirect impacts. Beside the fact that direct impacts are usually more obvious and therefore are easier to model, indirect impacts and their interactions are more complex. Therefore, it is practical to determine first, second, third, etc. order indirect impacts and, depending on the nature of the resource, limit the assessment to a specific order. While numerous parameters are likely to influence the resource in the long run, it is the short-term consequences which will affect the resource first and therefore require

immediate post-fire rehabilitation efforts. However, depending on the nature of a

resource, long-term impacts may be of higher importance to that particular resource.

2.2.3. The Recovery Potential Module

The FTM is the first threat/risk assessment scheme to incorporate a recovery

potential assessment. The Recovery Potential module provides information regarding

the ability of a given resource to return to its pre-burn condition and the time frame

for the recovery to occur. The recovery potential is estimated through the fire impact

severity and area rehabilitation potential. Similar to the Values at Risk component,

the Recovery Potential module is highly resource dependant. Recovery potential is

also important for natural resource management in terms of the possibility of

additional post-fire degradation of the resource/area due to the slow rates of area

recovery. For example, high intensity stand replacement fires can lead to soil erosion

which in turn leads to lower chances and slower rates of area recovery (Wirth and

Pyke, 2006).

2.2.4. The Fire Suppression Capabilities Module

The Fire Suppression Capabilities (FSC) module evaluates the ability to

mitigate against fire impacts on a given resource through fire suppression activities.

The FSC is assessed as a factor of area accessibility, proximity, and the efficiency of

the fire suppression unit's response. Area accessibility, defined as proximity to major

roadways, provides the possibility of using mechanized (fire trucks, bulldozers, etc.)

or aerial (aerodrome proximity) methods of fire suppression. The proximity, defined

as the distance between the fire event and the fire suppression unit base, allows for

evaluating the minimum time for the initial attack unit's arrival at the place of fire

21

occurrence. The likelihood of wildland fire suppression grows lower as the duration

of the fire event grows longer. A successful initial attack minimizes fire size and fire

impact. Additionally, it prevents wildland fires from reaching intensities that allow

the fire to spread uncontrollably.   The effectiveness of fire suppression unit response

also has a considerable effect on fire suppression success. Modification of the

response effectiveness parameter allows the resource managers to analyze a range of

potential outcomes of a fire event based on the FSC. The exclusion of this module

provides a "no interference scenario" which may be of great importance to resource

managers or within inaccessible areas. In some cases the impact of fire suppression

activities on a given resource may be greater than that caused by a fire event itself

(Backer et al., 2004). Therefore, evaluation of a range of fire threat levels based on

"no interference" and "fire suppression" scenarios will provide a basis for the

development of fire management strategies aimed at the needs of a given resource.

The evaluation of "no-interference" scenarios is also important because a given

resource will be impacted the most during large and catastrophic fire events when fire

is beyond any possibility of control by definition (Whelan, 1995). During these

events the Fire Suppression Capabilities module would artificially lower the output

fire threat level and provide misleading information on the security of the resource.

2. 3. Data and Methodology for Risk of Ignition Estimation

The MODIS (Moderate Resolution Imaging Spectroradiomenter) active fire

product (Giglio et al., 2003) from both the Terra (MOD14) satellite for the period of

2001 – 2004 and the Aqua (MYD14) satellite for the period of 2003 – 2004 was

included in the analysis. The active fire detections were processed through the Fire

Spread Reconstruction approach (Loboda and Csiszar, 2007b) to simulate development of fire events in space and time and identify points of ignition. Due to a considerable overlap of satellite orbits in the mid and high northern latitudes, the MODIS active fire product provides up to four observations of the study area daily from each of the two satellites. This high frequency of observation allows for the creation of algorithms which reconstruct fire development from the distribution of fire detections in three-dimensional space (x, y, and time). Individual fire detections were clustered into contiguous (in space and time) fire events. The earliest fire detection point(s) of individual fire events were considered ignition points. These points of ignition were later analyzed in the GIS environment in order to evaluate the frequency and distribution of fire ignitions as a factor of proximity to major roads, railroads, human settlements and rivers and as a factor of terrain complexity. The 2001 – 2004 fire seasons were not directly compared to each other but rather used to identify similar trends in the distribution of fire ignitions in space and time.

The GIS data for anthropogenic (roads, railroads and settlements) features in the RFE were acquired from the Digital Chart of the World (<www.maproom.psu.edu/dcw/>) and buffered in 1km increments. The road layer was classified into 11 zones based on the distance from major roads: 1) 0-1 km, 2) 1-2 km, 3) 2-3 km, 4) 3-4 km, 5) 4-5 km, 6) 5-6 km, 7) 6-7 km, 8) 7-8 km, 9) 8-9 km, 10) 9-10 km, and 11) outside 10 km buffer. The settlement and railroad layers were classified following the same approach into 21 zones (20 buffers and the rest of the area) and 31 zones (30 buffers and the rest of the area) respectively. Terrain was evaluated through 3 Arc Second Digital Elevation Models (DEM) from the data

23

acquired during the Shuttle Radar Topography Mission (USGS/GLCF, 2004). The terrain was classified into 5 zones based on slope gradient: 1) flat, 2) 1-10%, 3) 10-20%, 3) 20-30%, 4) 30-40%, and 5) over 40% slope. Land use was modeled using data from of the MODIS land cover product (Friedl et al., 2002), maps of land use (Stolbovoi and McCallum, 2003), and maps of protected areas (World Database on Protected Areas (WDPA Consortium, 2005; Miquelle et al., 1999b). The study area was classified into 8 land cover/land use zones: 1) croplands, 2) forest, 3) grasslands, 4) multiuse and traditional use areas, 5) protected natural areas, 6) shrublands, 7) other, and 8) water. The creation of a simplified but combined land cover/land use layer was necessary because land use of areas with different land covers varies even if their designation remains the same (e.g. federal lands). Cropland, grassland, shrubland, forest and water zones were extracted from the MODIS Land Cover Product. The "traditional and multi-use" zone was identified from the available maps of land use. Protected areas were mapped from a combination of WDPA data and available land use maps which were verified against the zones identified for the RFE in Miquelle et al. (1999b). All areas which were not included in the previously identified land cover/land use zones were assigned to the "other" category.

The risk of ignition was estimated through the evaluation of individual inputs for the FTM's ROI module (Figure 2-1 – shaded area) and their subsequent aggregation. The MODIS active fire product does not allow for differentiation between natural and anthropogenic sources of fire. Consequently, they are analyzed simultaneously under the Ignition Sources component. Additionally, the Fire Weather component of the ROI module was assessed qualitatively, to observe the

general trends in fire ignition rather than reconstruct specific conditions of fire occurrence.

Frequency of fire ignition, defined as an absolute or relative number of ignition points within a given buffer over a specific amount of time (e.g. monthly, yearly, etc.), was calculated for individual buffer zones from settlements, transportation routes, land use zones and different gradations of the steepness of terrain within the GIS environment. The calculated frequency of fire ignition was normalized by unit area through the *Ignition Load* coefficient (L) which presents a quantitative assessment of the relative frequency of ignition within a given parameter or zone.

$$L_y = \left(\sum_{i=1}^{4} f_{zi} / \sum_{i=1}^{4} f_{ti} \right) / \left(A_z / A_t \right)$$

(2.1)

where L_y is a yearly average *Ignition Load*, f_{zi} is the number of ignitions within a given buffer zone in year i, f_{ti} is the total number of ignitions within the study area in year i, A_z is the area of the given buffer zone, and A_t is the total area of the study area. The equation above shows calculation of yearly average ignition load (L_y) over four years (2001-2004). Similarly, monthly average *Ignition Load* (L_m) over the four year time period was calculated for each buffer and zone to observe temporal variability of ignition loading (Figure 2-2).
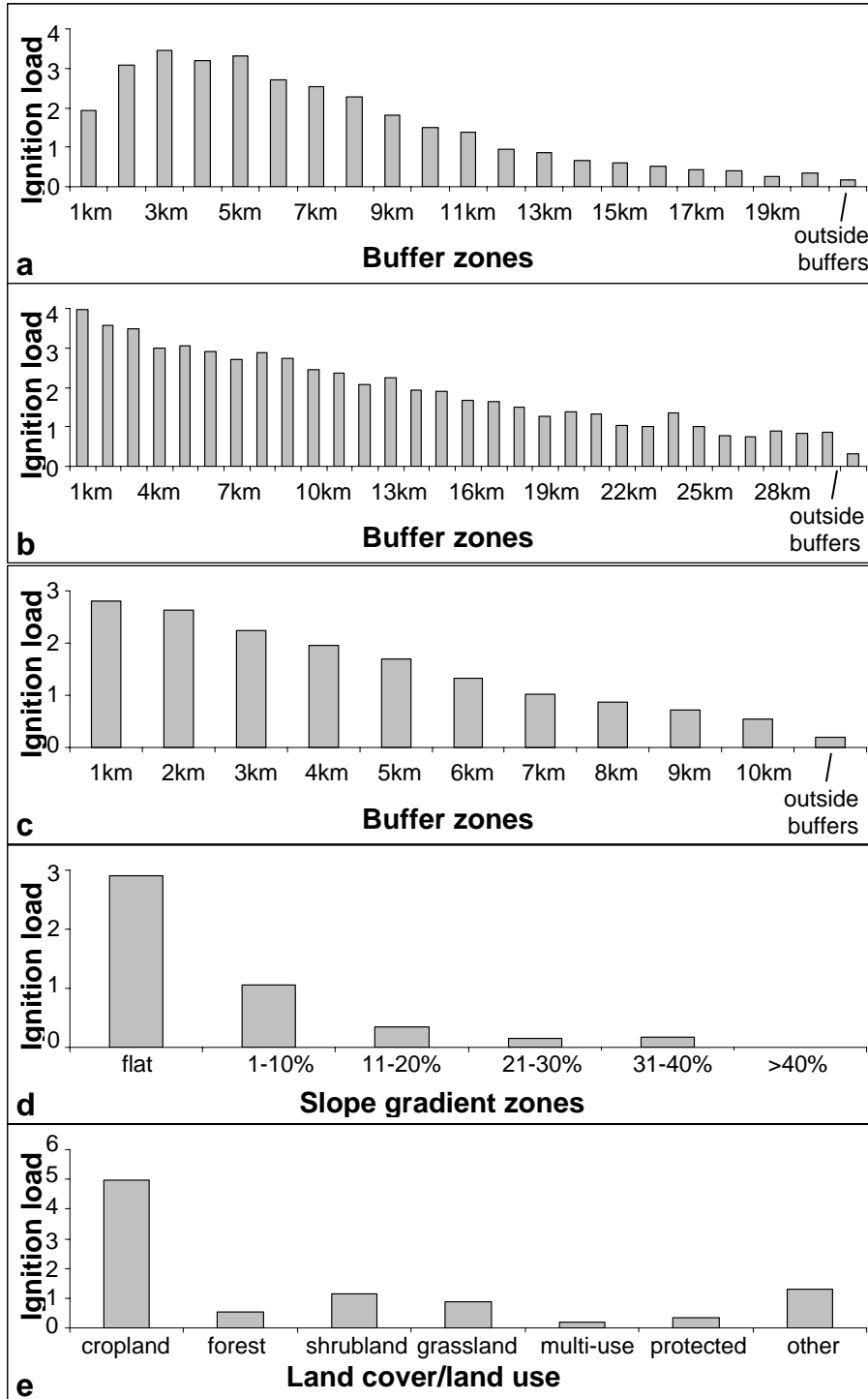
Figure 2-2. Distribution of average yearly *Ignition Load* (L_y) values by buffer zones

for: a) roads, b) railroads, c) settlements, d) slope, and e) land use.

Within this study the individual components of the ROI module were aggregated into the overall fire threat value based on fuzzy reasoning. While numerous methods of multi-criteria decision making are appropriate for evaluating the fire threat within the FTM framework, the fuzzy aggregation operations present significant advantages. The major advantage of fuzzy logic is the possibility of recreating complex scenarios based on a limited number of variables and rules. The ability to combine factors in a non-linear way and account for the inaccuracies of GIS information further advances the applicability of fuzzy logic to multi-criteria decision making in GIS (Sasikala et al., 1996). The disadvantage of the enhanced flexibility provided by the large range of fuzzy logic operators is the amount of fine tuning required to achieve high precision in the model output.

The L values were converted to fuzzy membership values (μ) which stretch between 0 and 1 where 0 implies no likelihood and 1 implies certainty. This conversion allows for developing a quantitative assessment scheme for evaluation of the likelihood of ignition as a factor of proximity to various anthropogenic (e.g. roads and settlements) and natural (e.g. flat terrain) geographic objects and phenomena. L_y values for each buffer zone were combined to create a range of values representing the frequency of fire ignition in the RFE. This range was subsequently used to develop equations to support conversion of the ignition load (L) to ignition likelihood (μ).

Conversion of the L_y values to μ was based on calculating several statistics. The first is the overall average of the L_y range which is considered to be equal to $\mu = 0.5$. The second is $\mu = 0.25$ which is represented by the average of all L_y values

below the average for the entire range. The same approach was used to identify

average L_y values corresponding to μ equal 0.75, 0.125, 0.375, 0.625 and 0.875. The

corresponding points, including the L_y value of 7 (the next full integer after the

maximum L_y zone value in the range) as the maximum fuzzy membership equal to 1,

are then plotted against each other and the best regression fit (with the intercept set at

0) is determined (Figure 2-3).
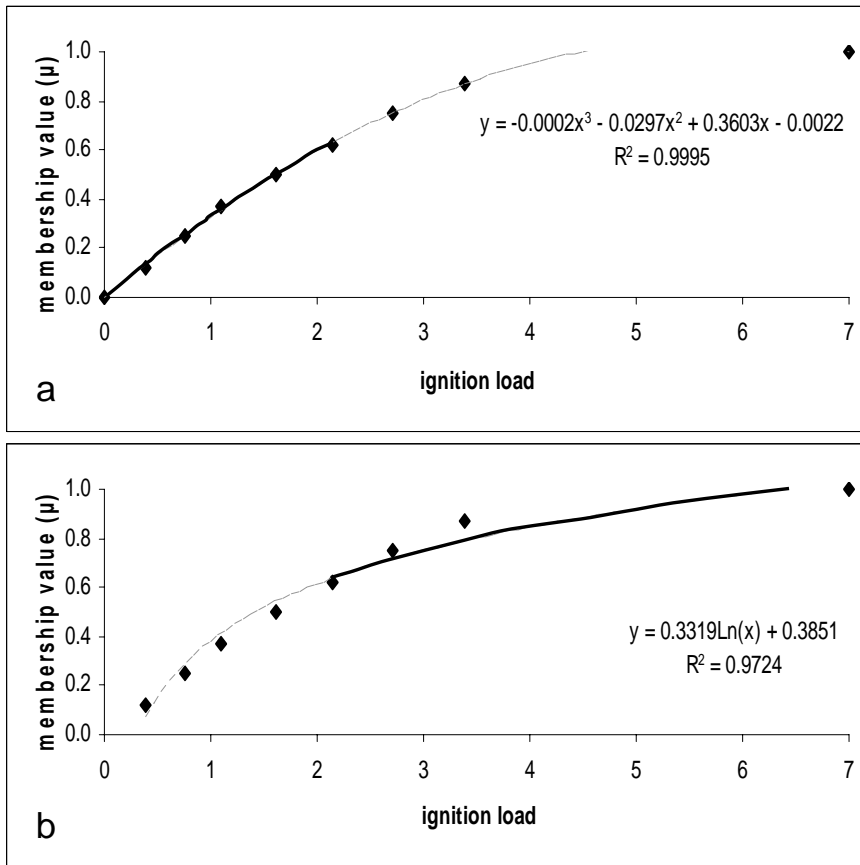
Figure 2-3. Regression equations for conversion of *Ignition Load* (L) values to fuzzy

memberships for: a) $\mu <= 0.625$, b) $\mu > 0.625$

Although the polynomial equation (Figure 2-3 a) provides the best fit for the majority of points, it quickly reaches saturation and therefore is not suitable for the higher L values. Instead, values of $\mu > 0.625$ are assigned following the logarithmic equation in Figure 2-3 b. Subsequently, the exact membership values of all individual L_m values are rescaled to the μ range following the combination of the two regression equations. The calculated μ values were further assigned to the respective buffer zones to create monthly maps of the likelihood of ignition as a factor of a given geographic phenomenon (roads, railroads, settlements, terrain, andland cover/land use). Each of these layers presents a continuous (with a value existing at each point of the surface) view of the likelihood of ignition based on a given parameter.

The overall risk of ignition is represented by a function of all the input likelihood values and can be presented as a spatial multi-criteria set of ROI = $(r_j, rr_j, s_j, t_j, lu_j)$, where r, rr, s, t, and lu represent the likelihood of ignition as a function of proximity to major roads, railroads, settlements, terrain and land cover/land use respectively for each jth point of the study area. The ordered weighted averaging (OWA) approach (Yager, 1988) was applied to aggregate this multi-criteria system with fuzzification using three sets of OWA operators: 1) MIN (intersection), 2) MAX (union), and 3) MEAN. The MIN operator allows for evaluating the ROI for "the best case scenario" where the lowest value of the input variables drives the overall output membership value without being mitigated by the other variables. The MAX operator outputs the "worst case scenario" where the overall ROI is driven by high likelihood of fire occurrence caused by one of the input parameters. The MEAN operator in this case presents a simple weighting additive decision rule where the ROI

presents a sum of all input variables multiplied by the weights assigned as w = [0.2, 0.2, 0.2, 0.2, 0.2]. It provides a trade-off environment for aggregating multi-criteria datasets where a positive compensation between the variables is realized (Malczewski, 1999). In this case equal importance was assigned to all input variables. The final output of this process presents a fuzzy set of ROI = (min, max, mean) values for each point within the set.

2.4. Results and Discussion

2.4.1. Fire Occurrence

Fire occurrence in the RFE, inferred from an analysis of the temporal distribution of fire detections in the RFE during the 2001-2004 period carried out outside the FTM framework, shows considerable interannual variations (Figure 2-4). The overall number of fire detections (Figure 2-4 a) shows a sharp contrast in the amount of fire occurrence between the years of high (2003) and low (2001, 2002 and 2004) fire activity as well as the variation in the temporal patterns of fire occurrence. During the low fire activity seasons, fire detections from MODIS demonstrate a bimodal distribution with a strong peak during spring months (April and May) and a much lower but still distinct peak in the fall (October and November). This distribution is characteristic for the area of Russia located between 40-48° latitudes (Korovin, 1996). However, during the large fire seasons of 2003 the bimodal distribution of the low fire activity years (2001, 2002, and 2004) is replaced by a strong dominating peak in fire occurrence in July. The seasonal distribution of fire ignitions in the RFE (Figure 2-4 b) mimics the bimodal distribution of fire occurrence during the low intensity fire years and is even more pronounced.
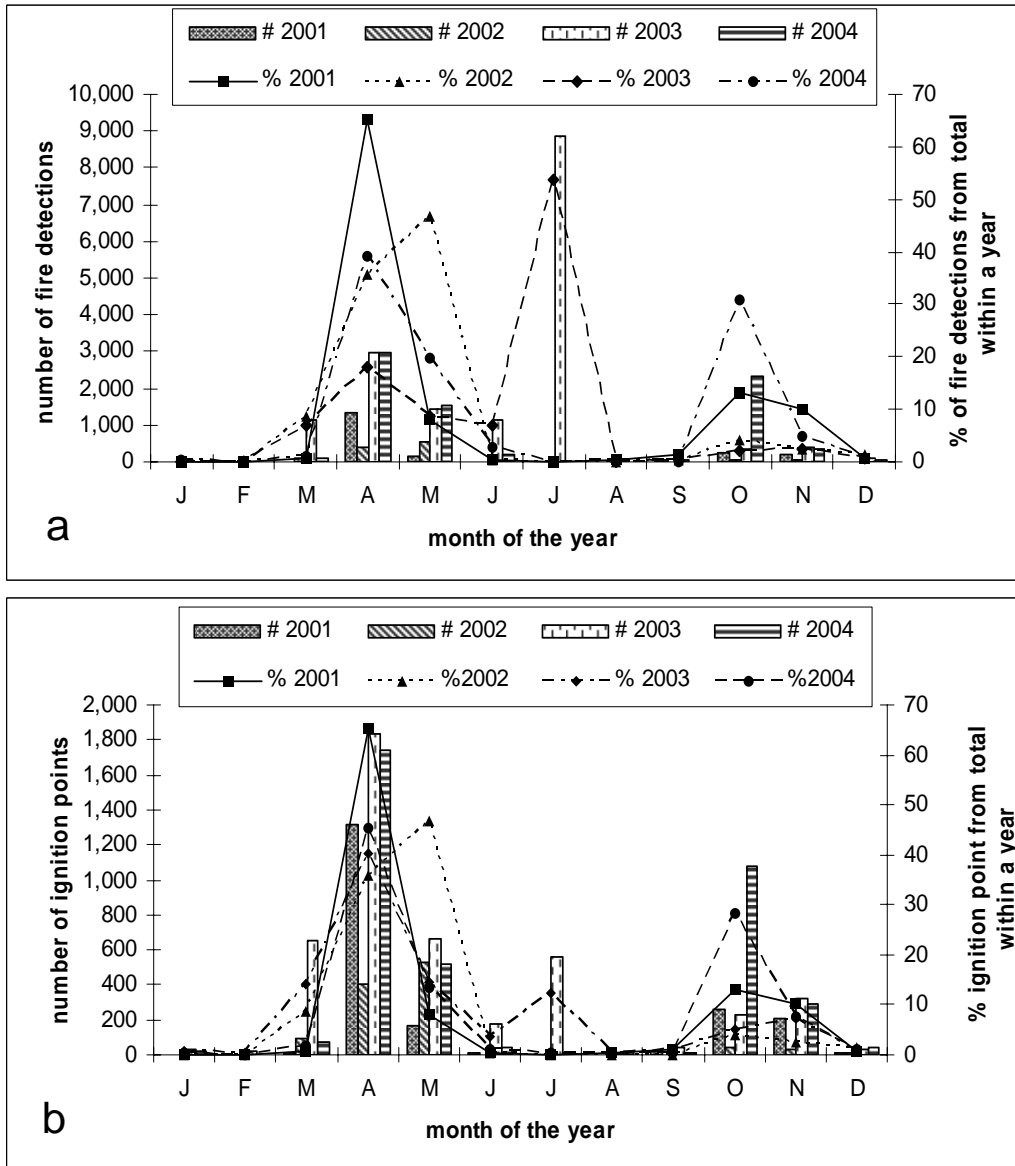
Figure 2-4. 2001-2004 absolute and relative numbers of: a) fire detections, b) fire ignitions.

The overwhelming majority (over 70%) of all individual fire events start in April - May and a smaller but still significant number (5-10%) start in October - November. Although July 2003 ignitions account for a comparatively larger portion of fire ignitions than usual (~14%), the bimodal spring/fall distribution of fire

31

ignitions remains largely unaffected. The overall comparison of the seasonal distribution of fire ignitions and fire detections implies that the high fire activity years are characterized by larger and longer burning fire events rather than a dramatic increase in the number of fire events.

2.4.2. Fire Ignitions

The analysis of fire ignition as a factor of proximity to various anthropogenic structures and land uses is an acceptable approach for the RFE due to low density of the transportation network in the area and uneven distribution of the population. Unlike the European part of Russia, the RFE has a very different pattern of transportation networks and population distribution which is determined by the complexity of terrain, history of the area's development and natural routes of transportation (large rivers and sea ports). Road, railroad, settlements, and river network densities were calculated for the RFE from the input GIS data layers and were compared with the statistics for other regions of Russia. There are comparatively fewer major roads going through the area with an average density of 0.04 km of roads per 1 km^2 of the study area, which is considerably lower than 0.2 km/km^2 found in European Russia (Stolbovoi and McCallum, 2003). The road network is considerably denser in the south-western part of the region with a higher percentage of population concentrated there. The network density of railroads is even lower than that of highways (0.01 km/km^2). In comparison, the river network in the RFE is fairly dense with 0.1 km of rivers per 1 km^2 of the area. Population density in the RFE is low - ~ 13 persons per km^2 (compared to 26.4 persons per km^2 in European Russia and 49.5 persons per km^2 in the Northern Caucasus) (Stolbovoi and

McCallum, 2003). Additionally, population distribution in this area is very uneven.

On average there is one settlement per over 700 km^2 of area, however the settlements

are concentrated along the Amur and Ussuri rivers, Lake Khanka and the coastline of

the Sea of Japan. The highly uneven distribution of population and low density of

transportation networks allow for a meaningful analysis of distribution of fire ignition

points as a factor of proximity to various anthropogenic structures. Due to the high

density of the river network in the RFE it was difficult to establish a connection

between the spatial patterns of fire ignitions and rivers as natural transportation

routes.

The analysis of fire ignitions as a factor of various components of the FTM

(Figure 2-1 – shaded area) has shown a significant connection between the

anthropogenic presence in the area and the frequency of fire ignitions. This result

supports the previous findings regarding the connection of fire occurrence and

anthropogenic activity characteristic for the Russian Federation (Korovin, 1996;

Kovacs et al., 2004). Population distribution, expressed through buffer zones from

human settlements and major transportation routes (highways and railroads), strongly

influences the number of fire ignitions in the RFE (Figure 2-2 a, b and c). The

number of fire ignitions decreases linearly as the distance from roads and railroads

increases. The highest number of fire ignitions is found within the 1 km buffer zone

along the transportation networks. The number of fire ignitions decreases more

rapidly with the increase in distance from highways, rather than railroads, where a

higher than average (L_y value of 1 representing 100% of fire ignition over 100% of

the area) number of fire ignitions is still found within the 24 km buffer. In contrast,

33

this number of fire ignitions is below average within the 8 km road buffer. The

frequency of fire occurrence as a factor of proximity to human settlements also

suggests a strong connection (Figure 2-2 c). The L_y values peak within the 3-5 km

buffers, then slope down considerably and go below average within the 12 km buffer.

Terrain expressed through slope gradient often determines the spatial

attributes of population distribution outside the settlements and transportation

networks and defines the accessibility of an area. The L_y values are the highest over

flat areas, drop rapidly with an increase in slope steepness, and fall far below average

($L_y = 0.35$) over areas where slope exceeds 20% (Figure 2-2 d). No fire ignitions

have been observed from the satellite data within areas with a slope over 40%.

An additional strong connection between the frequency of fire ignition and

land use has been established (Figure 2-2 e). The dominating source of fire ignitions

appears to be agricultural land use with $L_y \sim 5.1$ within agricultural areas.

2.4.3. Risk of ignition

There is considerable intra-annual variability in the risk of ignition in the

RFE. Figure 2-5 shows the spatial distribution of the ROI in the RFE for selected

months. During winter months (December – February) (not shown in Figure 2-5) the

ROI is very uniformly low across the entire study area for MAX ("worst case") and

MIN ("best case") scenarios. The MEAN ("trade-off case") shows an extremely low

ROI across the region with slightly higher levels (comparable to the MIN and MAX

scenarios) along transportation routes and within agricultural areas. The mean winter

temperatures range between -24°C (north-west and mountainous areas) and -7°C

(south-east) (NCEP/NCAR Reanalysis 1).
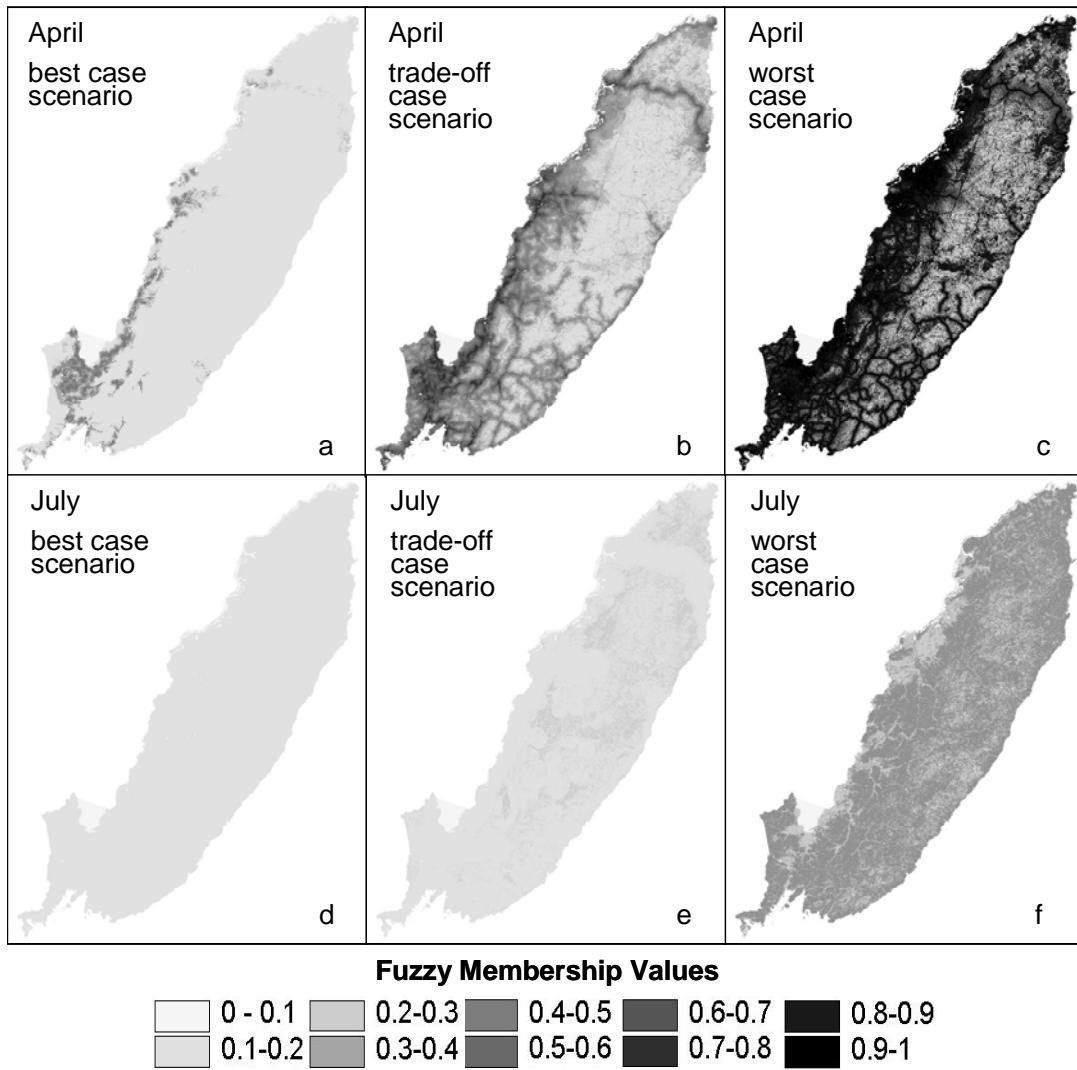
Figure 2-5. Monthly maps of Risk of Ignition (ROI) in the RFE: a) ROI in April calculated by MIN aggregation operator; b) ROI in April calculated by MAX aggregation operator; c) ROI in April calculated by MEAN aggregation operator; d) ROI in July calculated by MIN aggregation operator; e) ROI in July calculated by MAX aggregation operator; f) ROI in July calculated by MEAN aggregation operator.

At these temperatures there can be no natural sources of fire ignitions associated with lightning and therefore all sources are considered anthropogenic.

The ROI increases sharply in March around populated areas and along the transportation networks with a particularly noticeable increase in agricultural zones. While the MIN scenario associates the ROI increase exclusively with agricultural activity, the MAX and MEAN scenarios show a noticeable increase in wetlands, shrublands, forests and protected areas as well, primarily along the transportation network (Figure 2-5 a-c). This spatial distribution of the ROI is characteristic of the entire spring period (March through May) with a peak in April.

During the spring, croplands contain the majority of fire ignition points. This suggests that the majority of spring (and the overall yearly) fire activity in the RFE represents agricultural burning rather than forest fires (Figure 2-6). The temporal distribution of fire ignitions is consistent with the patterns of agricultural use of fire worldwide (Korontzi et al., 2006). Agricultural fire activities are often associated with removing crop residue from the fields either at the beginning or at the end of the growing season. Similar, although not as strong, a pattern of fire occurrence is observed in grasslands which are often used as pasture. The increase in spring fire detections in the RFE from 2001 and 2002 to 2003 and 2004 is caused by an increase in the frequency of MODIS fire detections after the launch of the Aqua satellite; however, the relative frequency of fire ignition through 2001-2004 remains constant. The high ratio of fire ignitions to all fire detections means that the agricultural fires are small in extent and short-lived. The overall ROI decreases in May and the spatial

distribution changes to resemble that of March. Higher levels of ROI are

concentrated along roads and settlements with a considerably lower ROI in croplands.
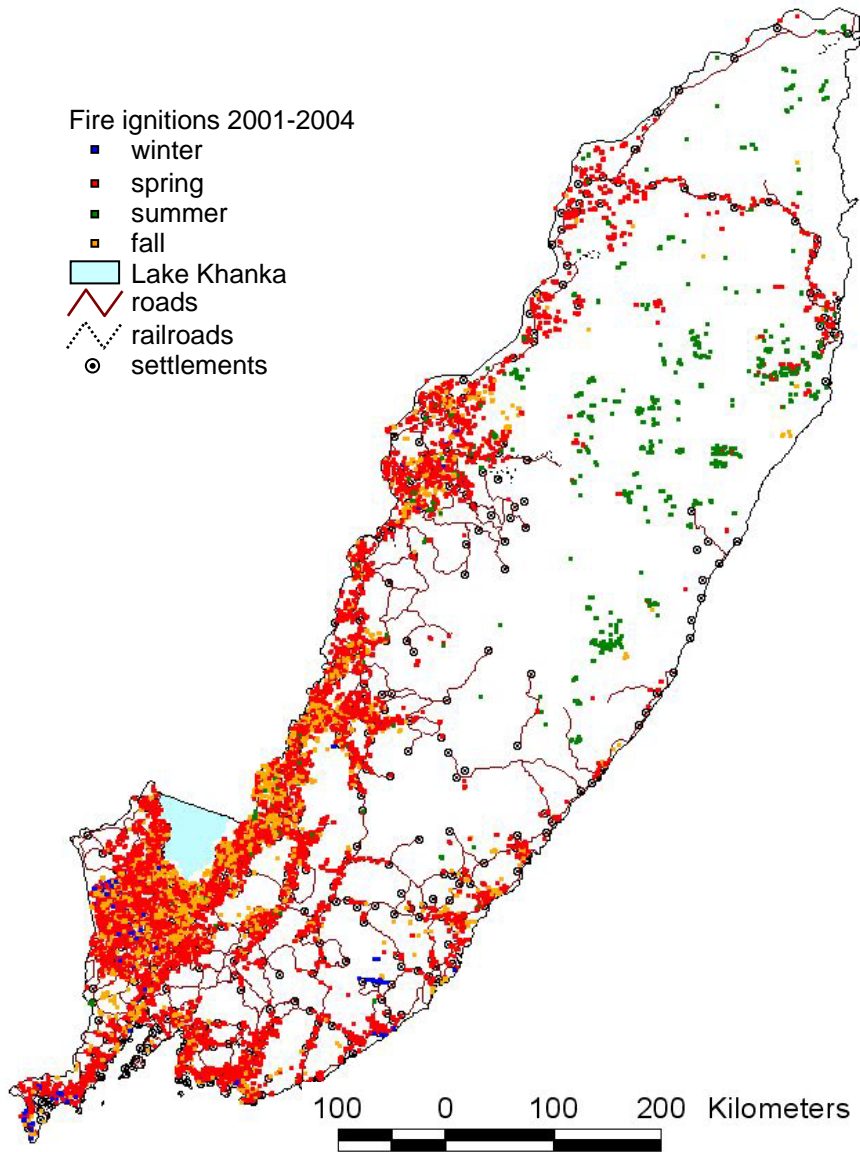
Figure 2-6. Spatial distribution of fire ignitions by seasons for 2001-2004.

The ROI continues to decline in June throughout the study area and remains

low overall throughout the summer (June - August). A slightly elevated ROI is

observed in remote areas and areas with complex terrain (Figure 2-5 d-f). This may be indicative of an addition of natural sources of fire ignition (e.g. lightning) to the existing anthropogenic sources. However, this premise requires further investigation involving extensive field work. In contrast with summer fires during seasons of low fire occurrence, summer fires during July 2003 have a considerably lower ratio of ignitions to all fire detections (Figure 2-6), suggesting an increase in the duration and spatial extent of these fire events. The ROI in agricultural areas during the summer months becomes very low. The higher ROI levels are observed in forested and shrubland landscapes. On average, protected areas with limited population access have fewer fires ignited within their territory.

During low fire activity years the proximity to highways – the first 6 km away from the road - becomes the most dominant factor in the distribution of ignition points (Figure 2-7). During high fire activity years the regular correlation between fire ignitions and major transportation routes breaks up. While some portion of fire ignitions during July of the high fire activity year (2003) occurred in a similar pattern compared to the fire occurrence during low fire activity years, the majority of large fires were initiated in areas distant from major roads, railroads and settlements. The slope gradient becomes the most dominant factor in the distribution of ignition points. Many of those fires were initiated near fairly large streams (Figure 2-8a), at previously disturbed sites (Figure 2-8c) and at logging concessions (Figure 2-8b). All of these factors are indicative of human-caused fire occurrence; however they do not provide solid support for this premise. High resolution up-to-date datasets of human

38

activities in the region are necessary to carry out a more detailed study targeting the

identification of sources of ignition during high fire activity years.
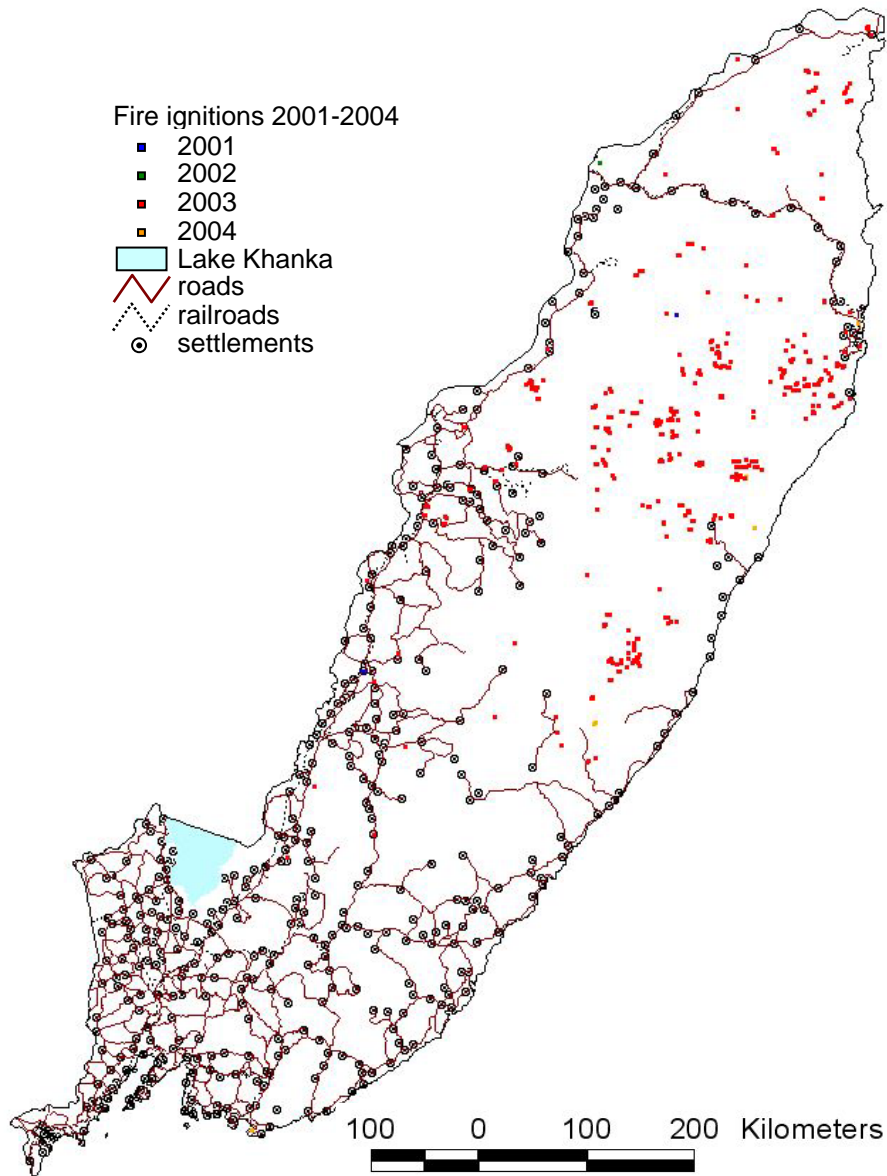
Figure 2-7. Spatial distribution of July fire ignitions for 2001-2004.
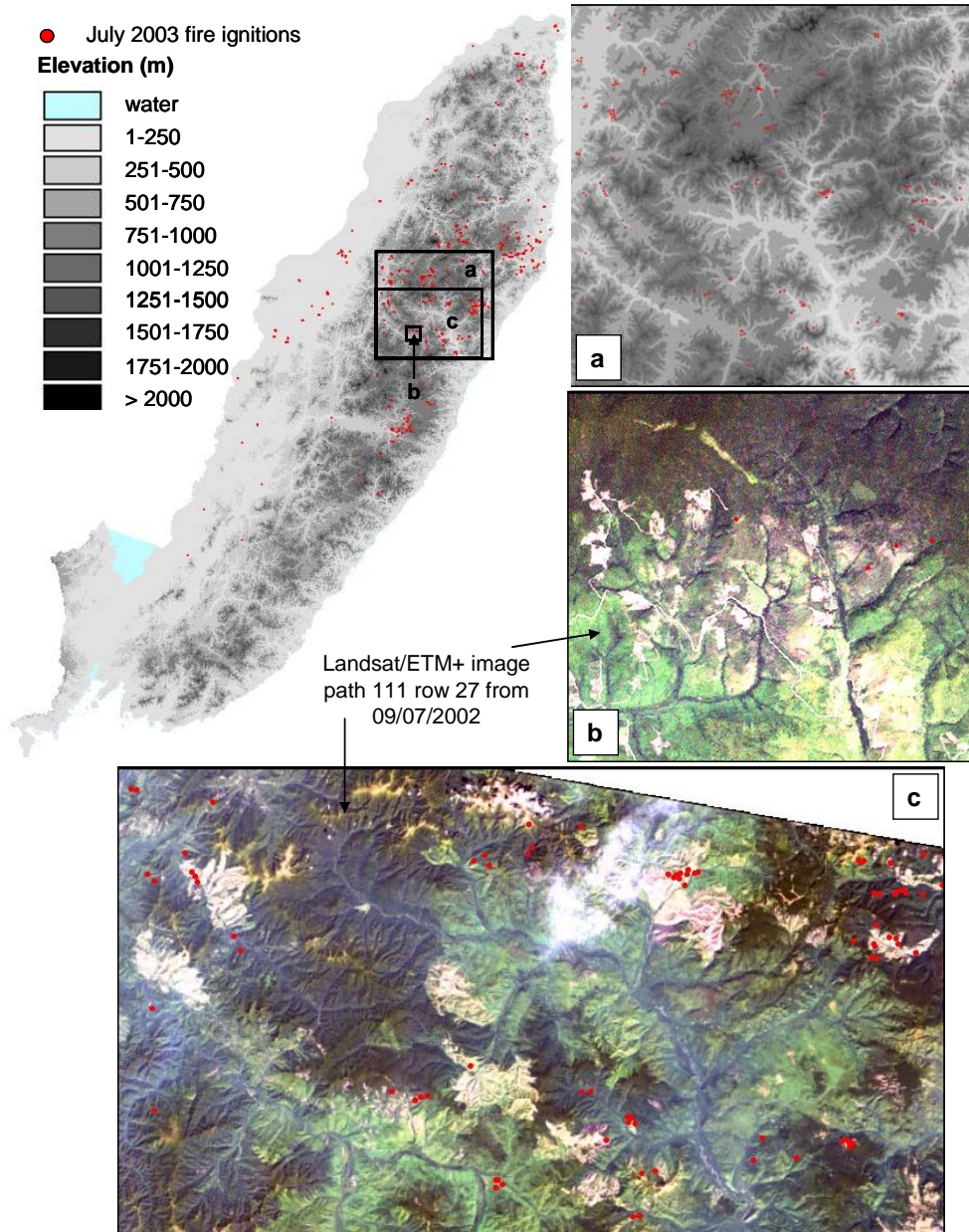
Figure 2-8. Examples of July spatial occurrence of July 2003 fire ignitions as a factor

of: a) elevation and proximity to large streams; b) proximity to logging sites; c)

proximity to previously disturbed areas.

   The increase in fire ignition in July of 2003 is more likely to have occurred in

connection with changes in weather patterns which created favorable conditions for

fire ignition rather than an increase in the available sources of fire. The climate of the study area is governed by a summer monsoon regime which causes increased amounts of precipitation and high levels of relative humidity in the area during the summer months (Stolbovoi and McCallum, 2003). In June-July of 2003 relative humidity over the area and the amount of precipitable water were uncharacteristically low (NCEP/NCAR Reanalysis 1) while at the same time there was an increase in the mean air temperature. The combination of higher than usual air temperatures and lower relative humidity leads to drier small fuels and creates potential for fire ignition.

The ROI begins to rise in September, peaks in October and declines by the end of November. The spatial patterns of ROI distribution are very similar to those during the spring months; however the levels of risk are considerably lower. The fall pattern of the ROI is also consistent with agricultural fire management of post-harvest crop residue.

The variability of fire ignitions in both the spatial and temporal domains shows that ROI is a highly dynamic factor which should be accounted for within a fire threat modeling framework. The observed monthly patterns of fire ignitions vary considerably intra-annually but show less variability inter-annually. The only noticeable difference is found during the summer period of years of low and high fire activity which is in part explained by changes in fire weather.

2.5. Conclusions

The Fire Threat Model is a new tool aimed at identifying fire susceptible areas of high importance for a given resource. It is a novel approach to spatially explicit and temporally dynamic modeling of fire threat designed to be used as a resource management tool. The FTM provides a framework for developing quantitative assessments of various parameters and their contribution to the overall potential impact of fire on a given resource. In addition to operational use of the FTM, the model provides the framework for predictive assessment of fire threat in the future and evaluation of potential resource management scenarios aimed at minimizing the fire threat to the resource of interest.

The analysis of fire occurrence in the RFE, described in this chapter, demonstrates considerable inter-annual variability of fire seasons. While average fire occurrence in this area is fairly low, large areas of the RFE become affected by fires during years of high fire activity. The findings show that the increase of fire activity during large fire years is not proportional to increase in the risk of ignition but is rather driven by enhanced propagation of fire linked to disruption of the monsoonal cycle in 2003.

The spatial and temporal patterns of fire ignition reveal a strong connection between human presence in the area and the risk of ignition. The intra-annual spatial variability of the risk of ignition also emphasizes the importance of developing temporally dynamic models in order to achieve better prediction of fire danger and fire threat.

The short record (four years) of fire detections from MODIS involved in this analysis presents a potential drawback due to the small sample size and the possibility of anomalous fire occurrence during all four years. However, the observed variability of fire occurrence during this time period indicates that the analysis included a set of different conditions and thus provides a reasonable range of possible outcomes.

Chapter 3: Regionally Adaptable dNBR-Based Algorithm for Burned Area Mapping from MODIS Data[2]

This chapter describes a burned area mapping algorithm necessary for assembling a record of fire activity in the RFE. Such record provides a baseline for developing an understanding of regional fire regimes and drivers of fire occurrence. It provides the inputs for parameterization of the potential fire behavior component within the fire danger module of the FTM (chapter 4). The available fire information in the RFE, collected by the Russian federal aerial fire protection agency, lacks spatial precision, reporting accuracy, and observational consistency (Conard et al., 2002), necessitating development of a multi-year record of burned area from satellite observations.

3.1. Introduction

The potential role of satellite imagery in monitoring and mapping wildland fire was recognized early on (Jayaweera and Ahlnas, 1974). The operational use of coarse resolution satellite information for active fire detection and monitoring was in place by the mid 1980s (Flannigan and Vonderhaar, 1986). A long term record of fire activity based on hotspot detections from satellite imagery is currently available for Along-Track Scanning Radiometer (ATSR) (Arino and Rosaz, 1999), Moderate Resolution Imaging Specroradiometer (MODIS) (Giglio et al., 2003), and Geostationary Operational Environmental Satellite (GOES) (Prins et al., 1998). At

---

the same time, development of a long-term record of global observations of burned area is lagging.

While numerous approaches demonstrated the feasibility of burned area mapping from Advanced Very High Resolution Radiometer (AVHRR) data (Chuvieco and Martin, 1994; Gutman et al., 1995; Rauster et al, 1997), they found a number of limitations which made AVHRR a less than ideal tool for fire observations. Recent advances in instrument design have led to considerable improvements in wildfire mapping at regional and global scales. The MODIS sensor on board the Terra and Aqua satellites was designed to enhance fire mapping capabilities (Kaufman et al., 1998) and to improve land surface monitoring (Justice et al, 1998). A suite of global MODIS products includes a burned area product (Roy et al, 2005a), however, the multi-year record has not yet become available to the public.

Other examples of global burned area mapping activities include GBA2000 (Tansey et al., 2004) and GLOBSCAR (Simon et al., 2004). Both products mapped the extent of burned area globally for the year 2000 using SPOT-Vegetation (GBA2000) and ATSR-2 (GLOBSCAR) data respectively. Unlike global active fire detection algorithms, these global burned area products take into account regional specifics to some degree. The GLOBSCAR processing mechanism involves identification of a "burnable zone" through application of a vegetation map. GBA2000 presents a combination of a series of regional burned area products developed through regional burned area algorithms. These algorithms are applied at continental and comparable scales covering various land cover types and biomes and therefore are insensitive to ecosystem level specifics of vegetative cover or fire

behavior. The MODIS Burned Area product is based on BRDF models which are contextually driven by vegetation type and therefore are more sensitive to spatial change of vegetative cover. However, the BRDF approach does not account for regional variability of fire occurrence and behavior which makes it difficult to differentiate between change due to burning and change caused by other reasons.

Numerous regional burned area mapping activities were also undertaken using SPOT-Vegetation (Gerard et al, 2003; Brivio et al, 2003; Zhang et al, 2003; Egorov et al., 2004) and AVHRR (Sukhinin et al., 2004) data. The majority of these regional products are hard-coded to the specifics of a given biome (e.g. boreal forest) and their mapping accuracy drops dramatically outside the intended area. The approach presented by Zhang et al (2003) has more flexibility to account for temporal changes in surface reflectance over various regions of the electro-magnetic (EM) spectrum as a function of forest/non-forest vegetative cover. The validation of this burned area dataset produced for the Russian Federation (at sub-continental scale) was performed over four Landsat 7 scenes positioned in pairs over 2 WRS paths (path 014 rows 14 and 15 and path 122 rows 15 and 16). This makes it difficult to draw conclusions about the reliability of algorithm performance over the broad range of ecosystems within the Russian Federation. Due to the natural variability of ecosystems, regional fire regimes, and land use practices, mapping burned area with high levels of accuracy requires development of a flexible approach which can be fine tuned to the regional/ecosystem level specifics.

This chapter describes a regionally adaptable semi-automated approach to mapping burned area using MODIS data. This is a flexible remote sensing/GIS based

46

algorithm which allows for easy modification of algorithm parameterization to adapt it to the regional specifics of fire occurrence in the biome or region of interest. The algorithm is based on Normalized Burned Ratio differencing (dNBR). The normalized differencing of TM bands 4 (0.76 - 0.90 μm) and 7 (2.08 - 2.35 μm) was introduced by Lopez-Garcia and Caselles (1991). The index is based on the independence of surface reflectance change in these ranges of the EM spectrum driven by fire effects on the land surface. The index, later named NBR by Key and Benson (2006), was originally developed specifically to map burned areas and more recently is used for burn severity assessment (Key and Benson, 2006; van Wagtendonk et al., 2004; Epting et al, 2005).

MODIS is presently the only moderate resolution instrument which allows for dNBR derivation. Other comparable sensors (e.g. SPOT-Vegetation and Medium Resolution Imaging Spectrometer - MERIS) do not collect spectral information in the 2.0 – 2.5 μm range of the EM spectrum. However, the Visible/Infrared Imager/Radiometer Suite (VIIRS) instrument developed for the future operational set of National Oceanic and Atmospheric Administration (NOAA) satellites will have a 2.25μm band. Therefore, the presented algorithm has the potential to be used with next generation satellite data to continue a long term record of fire impacts. While dNBR is currently used by the National Park Service, Burned Area Emergency Recovery (BAER) teams, and fire management agencies outside the US as an operational method for burn severity assessment (Cocke et al, 2005; van Wagtendonk et al., 2004; Howard and Lacasse, 2004), it may not be the optimal indicator of burn severity (Roy et al, 2006). Additionally, the potential applicability of dNBR as a

47

predictor of burn severity may be limited only to forested landscapes (Epting et al., 2005).

The burned area mapping approach presented in this paper was tested within three ecosystems (Figure 3-1): 1) boreal forest of Central Siberia, 2) Mediterranean-type ecosystem of California, and 3) sagebrush steppe of the Great Basin. Post-burn changes in surface reflectance are driven by pre-burn vegetation types as well as burn intensity. The presented approach includes threshold development based on an ecosystem's vegetation composition and more specifically percent tree cover. The test ecosystems differ substantially from each other in species composition, percent tree cover, and fire behavior. They represent a variety of land cover types in order to test algorithm adaptability to regional specifics and provide a reasonable evaluation of burned area mapping accuracy over a wide range of conditions.

3.2. Methodology

The input data for the algorithm include the MODIS Surface Reflectance 8-Day Composite product (Vermote et al, 2002) and the MODIS Active Fire product (Giglio et al, 2003). The approach is presented as a three-part procedure. The first part involves image processing and analysis of potential fire-induced changes in surface reflectance from remotely sensed data. The second part deals with development of thresholds based on ecosystem vegetation type, post-burn spectral signatures, and fire occurrence. The third part includes a GIS-based analysis of fire scar contiguity and inter-comparison with active fire detections (Figure 3-2).
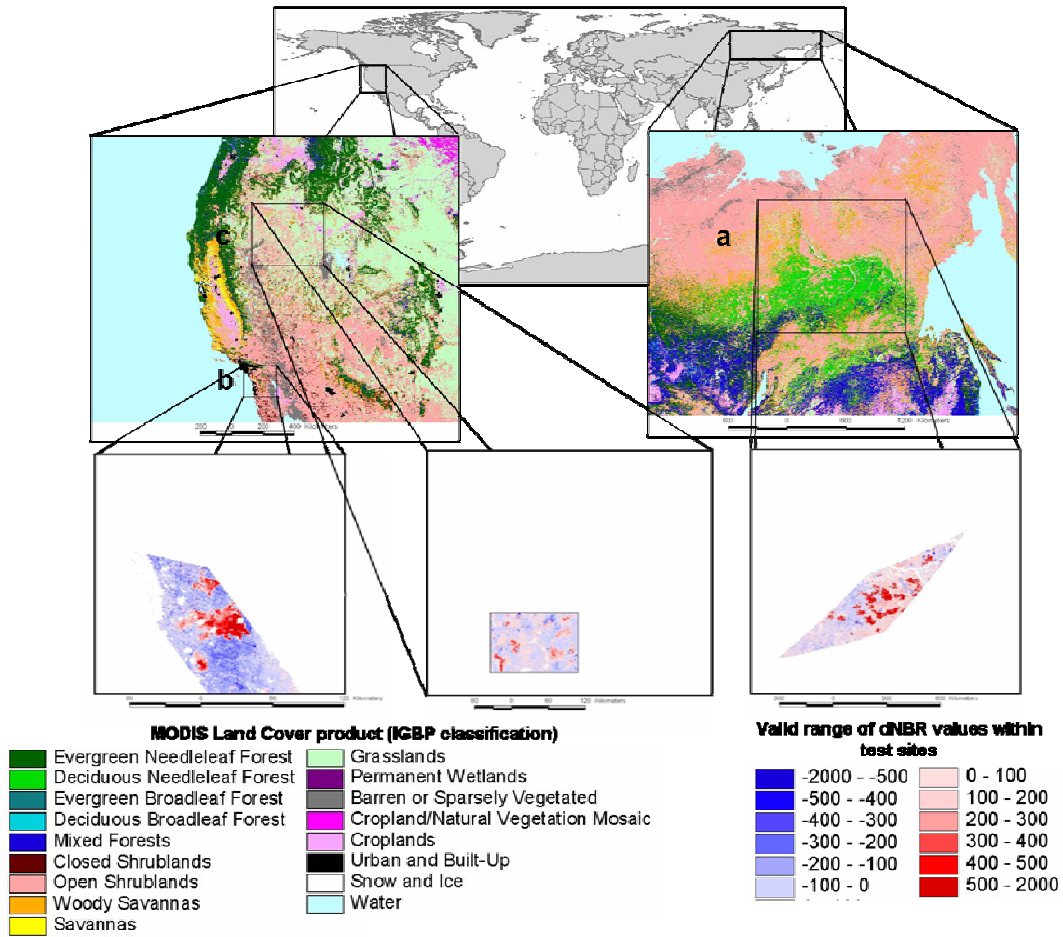
Figure 3-1. Distribution of test sites for the MODIS-based burned area assessment: a) Central Siberia boreal forests; b) Mediterranean-type ecosystem of California; c) Sagebrush steppe of the Great Basin. Enlarged boxes show the position of test windows over sample post-burn dNBR images used for burn threshold determination.

3.2.1. Image Processing

The analysis of fire induced change in surface reflectance is performed on the MODIS Surface Reflectance 8-day composites. Composites covering a full year (Jan 1 – December 31) are included in the processing. Only pixels of the highest quality are included in the analysis. Table 3-1 presents the image processing mask developed

based on the information contained in the packed quality bits which are found in the standard MODIS products. For further description of MODIS Surface Reflectance QA Science Data Set bits, see the MODIS Surface Reflectance User's Guide (<http://modis-sr.ltdri.org/html/guide.htm>).

```
┌─────────────────────────────────────────┐
│   NBR processing of surface reflectance 8-day │
│   composites with quality mask application:   │
│   ((band2-band7)/(band2+band7)) * quality mask│
└─────────────────────────────────────────┘
                    │
                    ▼
┌─────────────────────────────────────────┐
│   dNBR processing of 8-day composites:        │
│   NBRpre-burn – NBRpost-burn                  │
│   (i.e. previous year – current year)         │
└─────────────────────────────────────────┘
                    │
                    ▼
┌─────────────────────────────────────────┐
│   First dNBR threshold development            │
│   (based on dNBR histograms within the test windows) │
└─────────────────────────────────────────┘
                    │
                    ▼
┌─────────────────────────────────────────┐
│   Vegetation cover dependant dNBR thresholds  │
│   development (from histograms of ratio of MODIS BA to │
│   sample validation scar as a function of vegetation type) │
└─────────────────────────────────────────┘
                    │
                    ▼
┌─────────────────────────────────────────┐
│   dNBR thresholding on the 8-day dNBRs        │
└─────────────────────────────────────────┘
           │                      │
           ▼                      ▼
┌──────────────────────┐   ┌──────────────────────┐
│ Yearly max dNBR      │   │ 8-day potentially    │
│ composite            │   │ burned masks         │
└──────────────────────┘   └──────────────────────┘
           │                      │
           │                      ▼
           │           ┌──────────────────────┐
           │           │ Elimination of NBR change due │
           │           │ to reasons other than burning by │
           │           │ comparing with MODIS active │
           │           │ fire points for 8-day masks │
           │           └──────────────────────┘
           │                      │
           │                      ▼
           │           ┌──────────────────────┐
           │           │ Merge 8-day composites into │
           │           │ end-of-year burn coverage │
           │           └──────────────────────┘
           │                      │
           ▼                      ▼
┌─────────────────────────────────────────┐
│   End-of-year burned area product             │
└─────────────────────────────────────────┘
```

Figure 3-2. MODIS burned area algorithm processing stages.

Table 3-1.   MODIS Surface Reflectance QA Science Data Set bits used to mask out low quality data

sur_refl_state_500m bit id	0-1	2	3-5	6-7	8-9	10	12	15
Bit description	cloud state	cloud shadow	land/water flag	aerosol quality	cirrus detected	PGE11 internal cloud mask	Snow /ice flag	PGE11 internal snow mask
Value accepted	0	0	1	1-2	0-2	0	0	0

The uncorrelated response of the NIR and SWIR bands to post-fire effects is exploited in three different indices based on the different SWIR ranges of the EM spectrum. These indices are calculated according to the same equation (NIR – SWIR) / (NIR + SWIR) but differ in the range of SWIR band.   MODIS collects spectral information in three SWIR ranges (1.2, 1.6, and 2.1 µm). This allows for direct comparison of the performance of different indices used in burned area mapping. A time series of the Normalized Difference Water Index (NDWI) based on the 1.2 µm range (Gao, 1996), the Normalized Difference ShortWave Infrared Index (NDSWIR) based on the 1.6 µm range (Gerard et al., 2003), and NBR on MODIS data were compared over a known burned area in the Russian Far East boreal forest (located outside the validation sites used in this project).

Mean values of all pixels within the burned areas were calculated for all seven MODIS bands available in the standard MODIS Surface Reflectance 8-Day L3 Global 500m product (Vermote et al, 2002) during the time period 2002-2006. The pre-burn conditions were estimated from the 2002 MODIS data. The mean values were subsequently used to develop a time series of delta (preburn – postburn) NDWI,

NDSWIR, and NBR indices (Figure 3-3). While all these indices show a similar

pattern of change due to burning, dNBR (based on the 2.1 μm) has the largest

amplitude of values and the highest signal to noise ratio, particularly during the time

period immediately following burning.
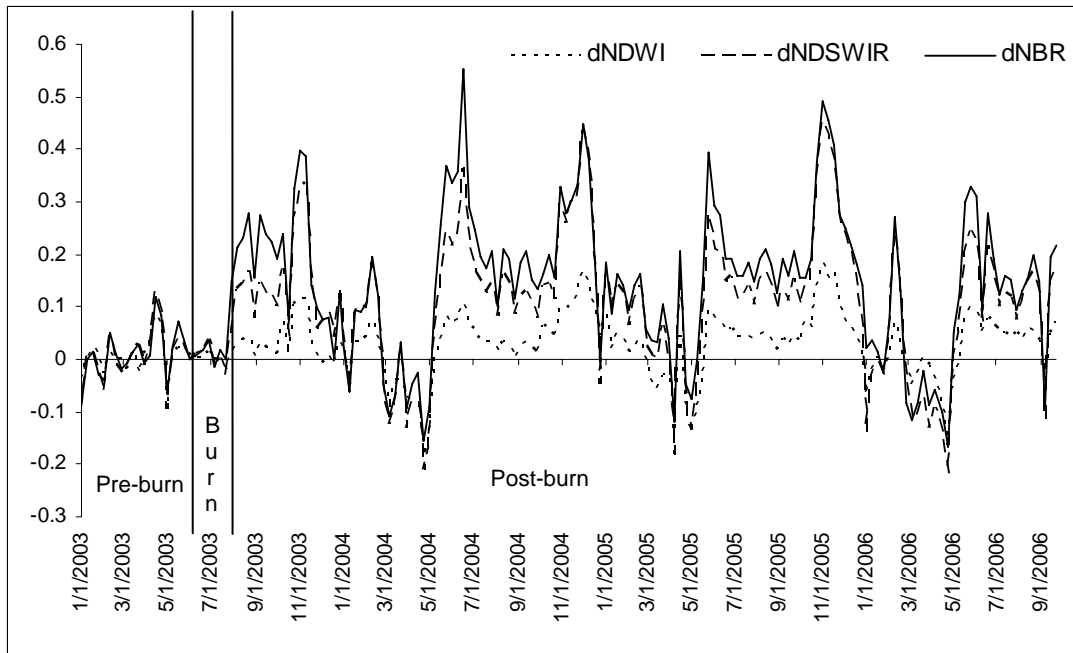
Figure 3-3. Time series of mean delta NDWI, NDSWIR, and NBR over the burned

areas in boreal forest during pre-burn, burning, and post-burn conditions. The X axis

shows the dates from January 1, 2003 through September 30, 2006. The Y axis

shows the range of dNDWI, dNDSWIR, and dNBR values. The vertical lines are

used to indicate the approximate time frames for pre-burn, burn, and post-burn

periods.

Within the processing algorithm the NBR is calculated using MODIS Surface

Reflectance product bands 2 (0.841-0.876 μm) and 7 (2.105-2.155 μm) following the

equation: NBR = (band2 – band7)/(band2 + band7). The NBR index was originally

developed for Landsat TM and ETM+ bands 4 (0.78–0.90 μm) and 7 (2.09-2.35 μm),

and therefore our selection of MODIS bands approximates spectral signatures

recorded by Landsat bands. Differenced NBR (dNBR) is calculated using the NBR

values in the compositing period containing the fire scar and the same compositing

period one year prior in order to account for phenology-driven intra-annual variability

of vegetation state. A set of 8-day dNBR composite images with values ranging from

-2000 to 2000 (dNBR * 1000 and converted to integers) and the "bad data quality"

fill value of -10000 is assembled for each year for further GIS analysis.

3.2.2. Threshold Development

Threshold development is the only analyst-driven part of the methodology.

There are two groups of thresholds used in the algorithm. The first group contains

dNBR-based thresholds developed through the manual selection of test sites within a

given region or ecosystem. The second group includes thresholds based on the

MODIS active fire product aimed at the elimination of fire scar false alarms caused

by land surface processes that generate a similar change in spectral response. While

dNBR provides a good measure of change in surface reflectance following a fire

event, inter-annual differences in the onset of greenup and senescence may cause a

non fire-related increase in dNBR values (van Wagtendonk et al., 2004). The

atmospheric correction procedure performed on MODIS data to produce the Surface

Reflectance products minimizes differences in atmospheric effects between pre- and

post-burn images, but does not account for BRDF effects (Epting et al., 2005) which

are particularly noticeable in mountainous areas. Additionally, anecdotal evidence

collected during algorithm development shows that dNBR may also be sensitive to changes in surface moisture following precipitation events or irrigation.

3.2.2.1. DNBR based thresholds

The masks of potentially burned areas are developed by thresholding the dNBR values at empirically-determined levels which differ for various biomes. This threshold is determined from the frequency distribution of dNBR values over a sample area with known fire activity based on the presence of MODIS Active Fire detections. It is important to select an area which includes a large sample of suspected burns (Figure 3-1) to ensure sufficient representation of dNBR burn values in the histogram. Although the size of the sample area is driven by the relative size of burns within a given ecosystem and therefore differs for various areas, the expected burns should constitute a minimum of 10% of the overall test site. The dNBR values from the best post-fire (determined from the dates of active fire detections) 8-day dNBR composite are evaluated. The histogram of dNBR values shows a near Gaussian distribution for unburned areas and an extended arm of positive values for burned areas (Figure 3-4). The first threshold, referred to as the burn threshold, is then set at the expected unburned pixels boundary which is defined by the fit of the Gaussian distribution at 95% of the range. The range of unburned dNBR values narrows as the percent tree cover diminishes from boreal forests (Figure 3-4 a) to grasslands (Figure 3-4 b), and subsequently the threshold slides from 300 to 75-100 (dNBR * 1000).

dNBR Frequency in Boreal Forests

dNBR Frequency in Sagebrush Steppe
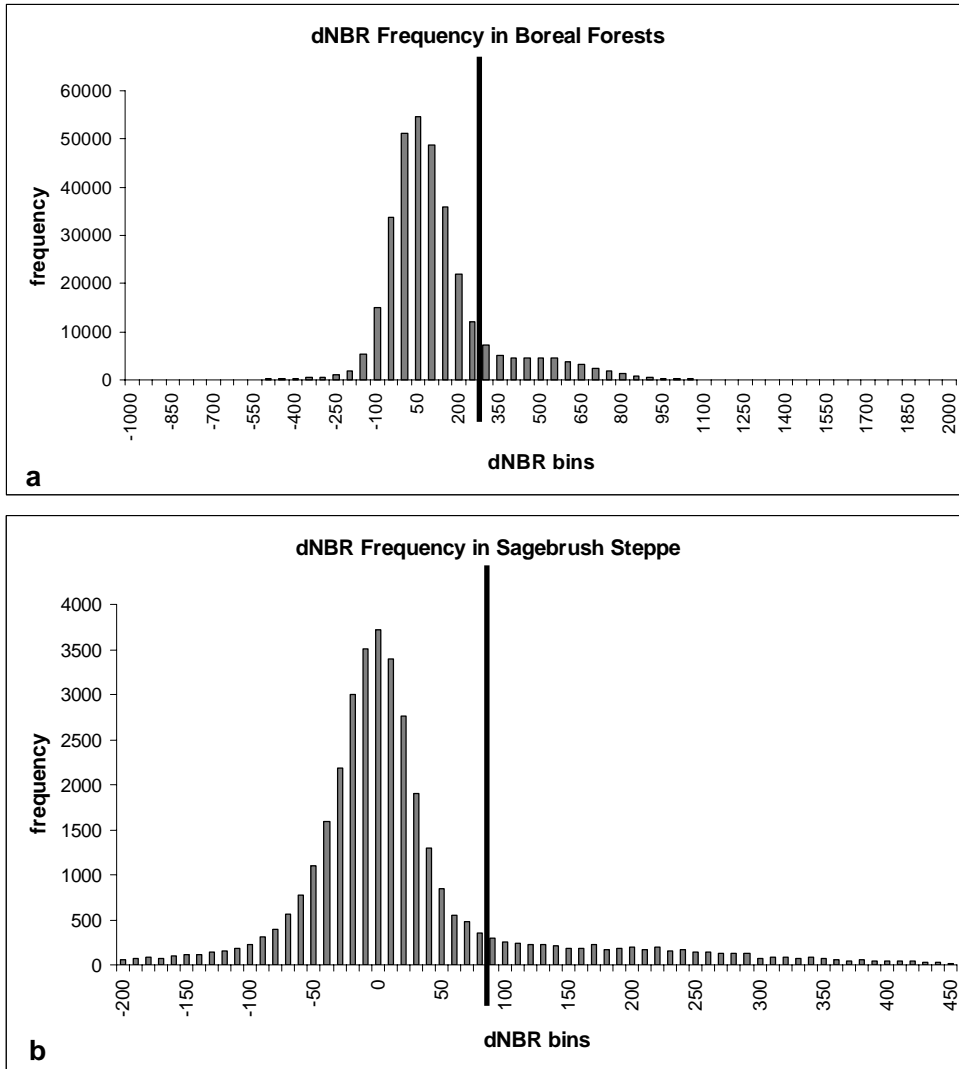
Figure 3-4. Frequency distribution of dNBR values for threshold development test windows in different ecosystems: a) Central Siberia boreal forest; b) Sagebrush steppe of the Great Basin. The test windows include a range of areas including burned as well as unburned areas. The vertical lines are used to indicate the placement of the burn thresholds. The difference in the scales of the presented graphs reflects the variability of dNBR range in various ecosystems.

The next stage of analysis allows for additional adjustment of the burn threshold based on the ecosystem of interest. The thresholds are adjusted manually based on the success rate of burned area masks mapped with the previously determined burn threshold. The MODIS Vegetation Continuous Fields (VCF) product (Hansen et al., 2003) provides important information about tree and herbaceous cover which is incorporated into additional thresholds within the GIS processing steps. A sample fire scar from the validation base is used to create a high confidence mask of a burned area. The distribution of MODIS post-fire dNBR values within the mask is then evaluated as a function of percent tree cover and percent herbaceous cover (Figure 3-5).

This evaluation yields vegetation cover thresholds subsequently used to adjust the burn thresholds. Within the sagebrush steppe test site, all areas with tree cover > 2% and areas with herbaceous cover > 72% performed adequately. However, areas with tree cover <= 2% and herbaceous cover <= 72% were not mapped well. Subsequently, the burn threshold for the underrepresented areas was moved to the lowest level of "potentially burned" pixels – a dNBR value of 75. Similarly, the burn threshold for boreal forests of Central Siberia with tree cover <= 10% was moved to 200 whereas the areas with tree cover > 10% were mapped with the original burn threshold of 300. All thresholds used in the burned area mapping within the three test ecosystems are summarized in Table 3-2.
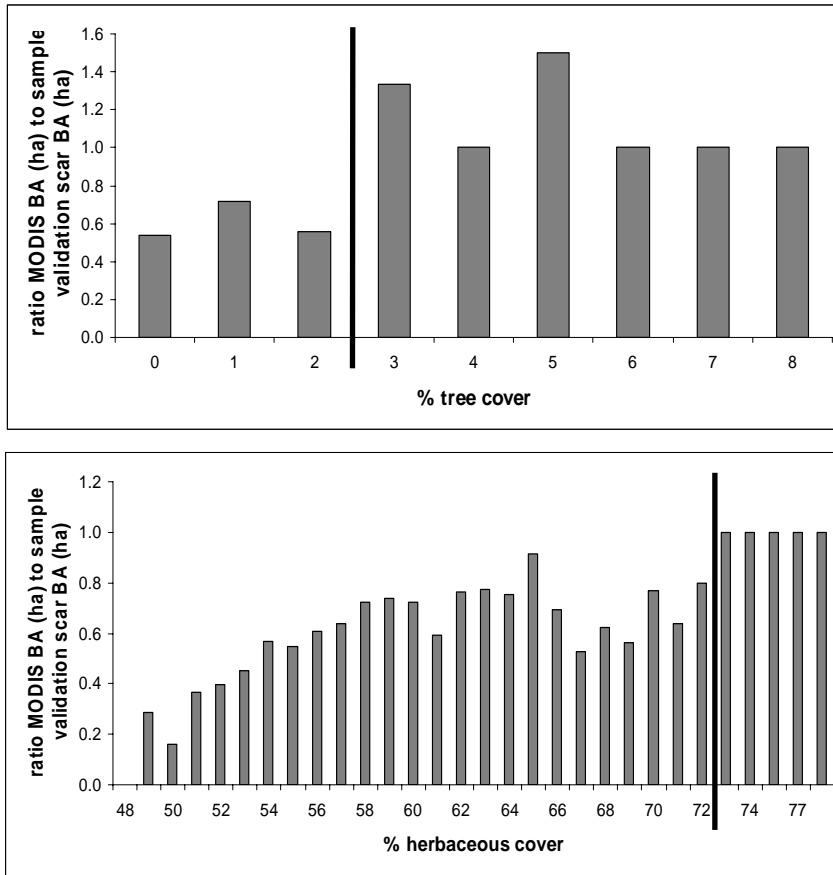
Figure 3-5. Ratio of MODIS burned area estimates mapped with the original threshold to burned area estimates in the reference database within the sagebrush steppe test site. The lines are used to indicate the placement of vegetation thresholds for: a) Percent tree cover; b) Percent herbaceous cover

3.2.2.2. Active Fire based Thresholds

The MODIS Active Fire product is included in the burned area mapping approach to provide a means to identify fire-induced changes in surface reflectance. An empirically-determined set of spatial and temporal thresholds is selected to account for fire spread specifics in the biome and latitude of the given region or ecosystem.

Table 3-2. Thresholds used for burned area mapping in the test ecosystems.

Thresholds	Boreal forest	Mediterranean-type ecosystem	Sagebrush steppe
Burn thresholds			
Tree cover threshold	10%	10%	2%
dNBR * 1000 (> high tree threshold)	300	150	100
dNBR * 1000 (<= tree threshold)	200	100	see herbaceous thresholds
herbaceous cover threshold	na	na	72%
dNBR * 1000 (> high herbaceous threshold)	na	na	100
dNBR * 1000 (<= low herbaceous threshold)	na	na	75
Active Fire thresholds			
Spatial	3 * 100ha	4*100ha	5*100ha
Temporal	64 days	32 days	32 days

The number of active fire detections increases in the northern latitudes due to overlap of the MODIS swaths, producing as many as four observations per day of the same area from each of the Aqua and Terra satellites (Giglio et al., 2006). In comparison, observations at the equator do not exceed twice per day from each satellite. In addition, fire spread rates and obstruction of fire detection due to heavy smoke lead to considerable gaps between consequent fire detections. Therefore a buffer is necessary for threshold development. Giglio et al. (2006) established a relationship between area burned and active fire detections count within several different biomes based on the mean percent tree cover. Their approach involved using regression trees to calibrate MODIS active fire detection counts and MODIS burned area estimates derived from 500m MODIS imagery in fourteen global regions. In their algorithm, the variability of the proportion of active fire detections count to burned area was driven by percent tree and herbaceous cover and mean fire cluster size. Their results show that in biomes with low percent tree cover, such as grasslands and shrublands, a

single 1 km^2 active fire detection represents 4–6 km^2 of burned area. However, in boreal forests the relationship is much closer where ~1 km^2 of active fire detection represents 1.5 km^2 of burned area.

In addition to the dependence on fractional tree cover, the relationship between active fire detections and burned area is affected by the mean size of the fire cluster. The amount of burned area per active fire detection increases with an increase in the mean fire cluster size. The increase is shown to be steepest in grassland ecosystems, reaching 8 km^2 of burned area per 1 km^2 of active fire detections in the arid grasslands of Central Asia (Giglio et al, 2006).

The coefficients developed by Giglio et al. (2006) are indicative of the thresholds used in our approach. However, since these coefficients were developed based on averaged 1 degree grid cell values they are not sufficiently precise for spatially explicit fire scar mapping. In addition, our previous research (Loboda and Csiszar, unpublished) has shown that MODIS Active Fire detections tend to omit considerable areas of burning in large scars, which is associated with the release of large quantities of smoke. Active fire detection count thresholds (spatial thresholds) for each test area were set based on the previously described trends and regression tree estimates of the relationship between active fire detection and burned area (Giglio et al., 2006).   The spatial threshold limits the extent of burned areas based on the biome-dependant coefficient applied to the number of active fire detections multiplied by 100 ha (1 km^2). These coefficients are described for each study area in the respective sections 3.4.1, 3.4.2, and 3.4.3 and summarized in Table 3-2.

In addition to the spatial threshold, a temporal threshold is introduced to limit the inclusion of active fire detections to those which were likely to produce a change in dNBR. The temporal threshold is based on the dates of active fire detections provided within the MODIS Active Fire product. Only fire detections observed prior to the date of the surface reflectance 8-day composite are included in the analysis. A sliding time window of X number of days prior to the date of fire scar mapping is set depending on the specifics of fire occurrence and vegetation response within the ecosystem of interest. Large forest fires often burn for extended periods of time, producing large smoke plumes which make the mapping effort impossible. However, these fire scars remain easily detectable in the imagery for a long time after burning is complete. Therefore the temporal threshold for forested areas was set at 64 days prior to the date of the analyzed surface reflectance 8-day composite. In contrast, it is extremely rare for fire events in grasslands and shrublands to last over that length of time. In addition, vegetation recovery is considerably quicker in these ecosystems and fire scars are easily masked by new vegetative growth. Subsequently, the temporal threshold was set at 32 days prior to the date of the analyzed surface reflectance 8-day composite. The spatial and temporal thresholds are adjustable and can be modified based on the expert knowledge of fire behavior within the ecosystem of interest.

3.2.3. Burned Area Mapping

The dNBR 8-day composites created during the image processing stage are processed to generate two outputs. The first output presents a set of 8-day composite-based masks of potentially-burned area based on thresholds at an ecosystem-

determined dNBR level (described in section 3.2.2.1). The second output presents the end–of–year maximum dNBR composite. The potential burn masks are evaluated as contiguous polygons against the MODIS Active Fire detections (thresholded as described in section 3.2.2.2). Active fire location points representing the center of MODIS Active Fire product pixels are buffered by a 500m radius to approximate the nominal 1km^2 area from which the radiometric signal is received by the satellite. The buffers are subsequently intersected with the potential burn polygons. If the area of the evaluated polygon is less than or equal to the spatial threshold value it is considered burned; otherwise the polygon is excluded from further consideration.

At the final stage of the process, the individually evaluated 8-day composite-based masks are merged into the end-of-year burn mask which is further used to clip the maximum dNBR composites. Each pixel in the output burned area product is assigned the beginning and ending date of fire scar mapping based on the date of the 8-day masks which detected the given pixel. The final burned area product presents a shapefile coverage which contains dNBR values ranging from 0-2000 and beginning and ending fire scar mapping dates. The end-of-year maximum dNBR represents an efficient way to map fire scars to their maximum extent (provided the burning did not occur in the time period December – January) while preserving dNBR values to indicate the largest recorded change in surface reflectance within the fire scar. The additional attributive information about the first and last date of mapping individual burned pixels allows for identification of areas of burning over a long period of time and areas which burned several times during a given year, which is characteristic for agricultural burning. However, the algorithm can be easily modified to output 8-day

(or multiples of 8 days) burned area composites with the dNBR values from the given compositing period.

3.3. Validation Datasets and Methodology

Two different validation reference bases were used to evaluate algorithm performance. The reference base used for validation of the MODIS burned areas in Central Siberia was created by mapping burned areas from single-date Landsat ETM+ data using the supervised Spectral Angle Mapper method (Kruse et al, 1993). Prior to classification the Landsat ETM+ data were converted to at sensor surface reflectance and aggregated to 100 m to account for the modulation transfer function (MTF) effect (Kaufman, 1988). Areas of significant cloud cover and cloud shadows were manually digitized and excluded from further consideration. The results of the classification were subsequently compared against active fire detections from MODIS and AVHRR (Sukhinin et al., 2004) and available quick look images of preceding dates to verify burned area assignment. Burn scars in boreal forests remain reliably detectable in the imagery for up to 10 years after the fire event. However, *a posteriori* identification of the time of burning can be successfully implemented through overlaying active fire detections with mapped burned areas (George et al., 2006). In the final step, the burned areas were manually selected and the false alarms were eliminated. Due to the nature of the burned areas developed from MODIS (end-of-year mapping), only fire scars with completed burning in the high resolution imagery were included in the analysis. The Landsat ETM+ validation reference base allows for conducting both inventory and geographic accuracy assessments. Inventory assessment is defined as a

comparison of burn scar area (ha) mapped by each product. Geographic accuracy is evaluated through confusion matrices.

The validation of the MODIS burned areas in the test sites located within the United States was performed using fire perimeter data obtained by federal and state interagency incident management teams. The dataset contains perimeters derived using different methods with different reference bases and therefore may include inconsistent data and contain errors due to misregistration of geographic information. To ensure accurate comparison of the burned areas with the reference database, only perimeters containing MODIS active fire locations were included in the analysis. The nature of this reference base allows only for providing the inventory accuracy assessment without true estimates of errors of commission and omission.

3.4. Results

This section presents the results of the described approach to burned area mapping in three unique case studies. The test sites are located in three distinct ecosystems (Figure 3-1) with considerable differences in vegetation composition and structure and fire regimes to demonstrate the versatility of the algorithm. Burned area was mapped in these test sites using thresholds adjusted for each ecosystem based on expert knowledge of fire characteristics and vegetation specifics. The resulting burned area maps were evaluated against fire scars mapped from Landsat ETM+ data and fire perimeter data derived from various methods by U.S. federal and state agencies and San Diego State University (<http://map.sdsu.edu>).

3.4.1. Boreal Forest of Central Siberia

Central Siberia is covered predominantly by boreal forests and shrublands (Figure 3-1). The tree cover density in these forests is relatively low (< 50%) and typical for mid-taiga stands (Stolbovoi et al, 1998). The northern part of the test site includes a northern taiga stand with short (< 5m) trees and minimal (< 30%) tree cover (Hansen et al., 2003). Due to these vegetation characteristics, northern taiga is identified in the MODIS land cover product as shrubland. None of the validation fire scars from Landsat scenes are found in tundra. Forests are predominately coniferous (larch, spruce-fir and pine) stands with considerable accumulation of plant litter. Fire scars are characterized by high dNBR values during the year of burning. Analysis of subsequent year green up using NDVI values produced from the MODIS 8-day surface reflectance composites showed very low levels of photosynthetic vegetation within the fire scars which can be indicative of high levels of tree mortality.

The Central Siberia boreal forest site covers the area of ~2.5 million km^2 (MODIS tiles h23v2 and h24v2). MODIS burned area was mapped for this site for 2001 and 2002. The dNBR thresholds were set at 300 (dNBR * 1000) for areas with tree cover > 10%, and 200 for areas with tree cover <= 10%. The spatial threshold for active fires was developed from the estimates provided by Giglio et al (2006) for boreal forests of North America. The spatial active fire threshold is primarily important for large clusters, therefore we followed the regression tree estimates for mean cluster size > 6.6 and high vegetation cover. The coefficient of 2.8 was rounded and the spatial active fire threshold were set at "3 times active fire pixel count * 100 ha". The temporal active fire threshold was set at 64 days prior to the

date of the compositing period due to the high frequency of cloud cover, large smoke

plumes, and long duration of fire events in this area.

The Central Siberia case study is the largest test site in this study. The high

resolution reference base includes ninety-nine fire scars from 11 Landsat ETM+

images acquired in 2001 and 2002 (Table 3-3). Five of these Landsat scenes

contained only scars with fully completed burning and the remaining scenes

contained a combination of fire scars with completed and on-going burning. The fire

scars with completed burning from all scenes were included in the evaluation of

burned area estimates.

Table 3-3. Landsat ETM+ scenes included in the reference database for Central
Siberia

WRS2 Path_Row	Acquisition date	Number of scars with completed burning	Included in geographic accuracy assessment
113_015	08/17/2001	1	no
117_016	07/28/2001	10	no
120_013	08/02/2001	10	yes
120_013	07/20/2002	6	no
120_014	07/20/2002	6	yes
120_015	07/17/2001	2	no
121_016	08/09/2001	22	no
121_017	08/09/2001	14	no
122_015	08/16/2001	16	yes
125_015	09/06/2001	6	yes
132_018	08/22/2001	4	yes

The results show that the MODIS burned areas provide accurate estimates

(slope = 0.89 with R^2 = 0.98) of burned area across a large territory (Figure 3-6 a).

The overall assessment is driven clearly by the largest fire scar mapped in Landsat

path 125 row 15 from 09/06/2001. However, the relationship remains strong (slope =

1.13 with $R^2 = 0.97$) for smaller fire scars (< 50,000 ha) and is not entirely dependant

on the largest fire scar (Figure 3-6 b). The MODIS burned areas missed nearly all

fire scars less than 100 ha (1 km^2). However, the overall contribution of the small fire

scars to the total area burned is negligible (0.31%). The MODIS burned areas have a

nearly 100% mapping rate for fire scars larger than 200 ha with only one fire scar

missed, which results in high accuracy of burned area estimates.
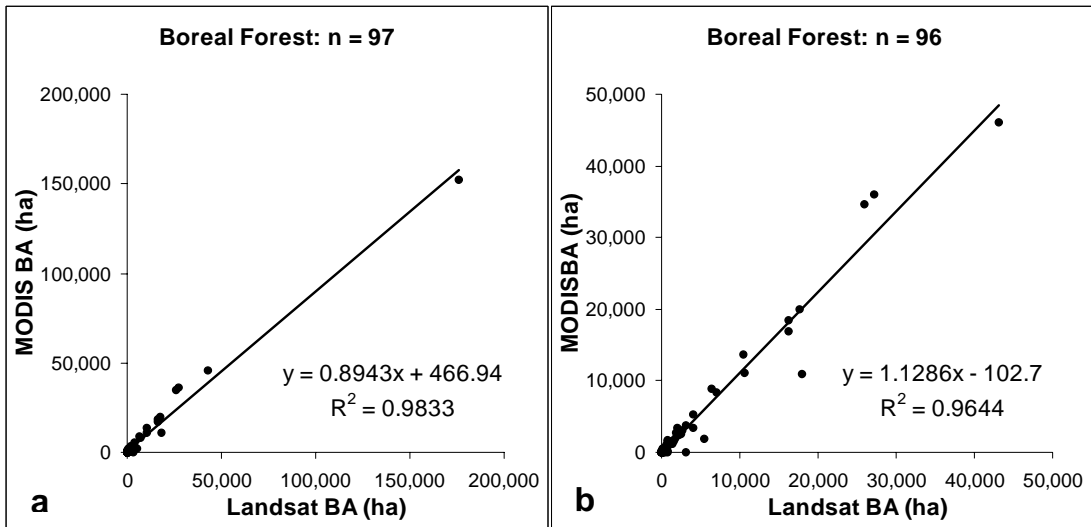
Figure 3-6. Inventory accuracy assessment for the Central Siberian test site compared

against Landsat ETM+ fire scars: a) all fire scars; b) fire scars less than 50,000 ha.

Geographic accuracy of burned area mapping is also reasonably high (Figure

3-9 a). Geographic accuracy assessment produced the lowest results for Landsat path

120 row 14 from 07/20/2002 with a Kappa value of 0.35. This is most likely due to

the fact that three of a total of six fire scars in this scene are less than 150 ha and the

only large fire scar missed contains a very heterogeneous burned surface. The next

lowest Kappa value was 0.69 for Landsat path 120 row 13 from 07/20/2002 which also contains small burn scars. Kappa values improve greatly in scenes containing larger fire scars – 0.76, 0.78 and 0.79 for Landsat path 132 row18 from 08/22/2001, path 122 row 15 from 08/16/2001, and path 125 row 15 from 09/06/2001, respectively.

3.4.2. Mediterranean-type Ecosystem of California

The southern coast of California is a Mediterranean-type ecosystem (MTE) consisting of dense thickets of chaparral and coastal sage scrub communities. Chaparral describes communities of highly flammable evergreen shrubs with sclerophyllous leaves found in more inland reaches at moderate elevations, while coastal sage scrub describes communities of drought deciduous shrubs found along the coastal margin in lower elevations (Rundel, 1998). These species lose most of their leaves during the summer drought as soil moisture is reduced. Fire is the dominant disturbance agent that determines structure and functions of vegetation in MTEs (Hanes, 1971), although fire suppression efforts have skewed fire regime toward longer return intervals, larger burn extent and greater fire intensity (Minnich, 1983). Fire spread is promoted by the dense shrub canopy, availability of fine fuels, and low fuel moisture during the summer drought (Davis and Burrows, 1994). Fires are typically intense and stand-replacing, and post-fire regeneration occurs within 3-7 years (Hanes, 1971) through resprouting and stored seeds (Moreno and Oechel, 1994).

The MODIS burned areas for this ecosystem were mapped over the total area of ~42,000 km^2 (MODIS tile h08v05) for 5 years (2001-2005). The thresholds were

set at 150 (dNBR * 1000) for areas with tree cover > 10% and 100 (dNBR * 1000) for areas with tree cover <=10%. The spatial active fire threshold was set at "4 times active fire pixel count * 100 ha" modeled from Giglio et al. (2006) estimates for Australia with percent tree cover < 18.5 and cluster size > 6.2. The temporal active fire threshold was set at 32 days prior to the date of compositing period.

The burned area estimates developed using MODIS were compared to the fire perimeters from federal and state interagency incident management teams. The MODIS burned areas showed a considerable overestimate of burned area (slope = 1.46 with R^2 = 0.99) (Figure 3-7 a). However, during the examination of potential reasons for such a large error it was determined that the error was caused by a large plume of particulate matter not detected by the quality bits in the input MODIS Surface Reflectance product for the compositing date 11/25/2003. The overall accuracy improved (slope = 0.92 with R^2 = 0.97) (Figure 3-7 b) once this date was excluded from the analysis. Similar to the Central Siberian test site, the relationship is driven by one very large fire scar. For fire scars less than 50,000 ha, the MODIS burned areas slightly overestimate the area (slope = 1.15) and have less consistency in the estimates with R^2 = 0.87 (Figure 3-7 c). Although the reference dataset does not allow for conducting full assessment of geographic accuracy of burned area mapping, the visual evaluation of mapped burns shows good spatial correspondence between the MODIS burned area and the fire perimeters (Figure 3-9 b).
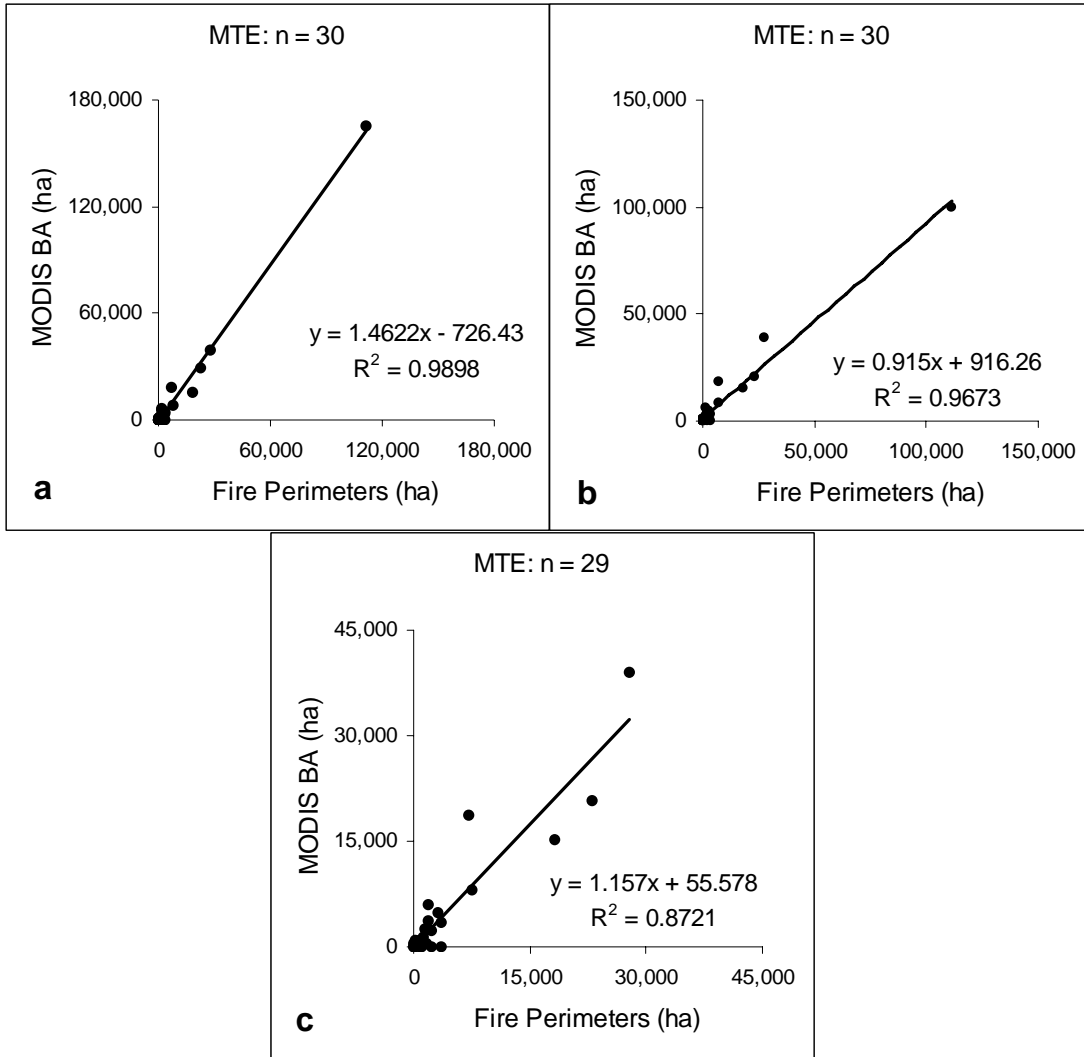
Figure 3-7. Inventory accuracy assessment for the Mediterranean-type ecosystem test site compared against fire perimeters: a) all fire scars; b) all fire scars mapped with composite 11/25/2003 excluded; c) fire scars less than 50,000 ha with composite 11/25/2003 excluded.

3.4.3. Sagebrush Steppe of the Great Basin

Sagebrush steppe is found in the northern-most reaches of the Great Basin desert region in the intermountain Western US. The region is predominantly open rangeland containing sparse shrub cover intermixed with grass cover and exposed

rocky soils. Historically, the ecosystem consisted of several sagebrush species and short perennial bunchgrasses and forbs (Young and Allen, 1997). Fires and widespread grazing were not initially part of the ecological disturbance regime (Harris, 1967). In the past century, there has been an invasion of exotic annual grasses that have altered the fire regime (Mack, 1981). The increase in fine fuels availability has facilitated fire spread and increased fire frequency. Repeated fires coupled with overgrazing have allowed for the replacement of sagebrush by exotic annual grasses (Prater et al., 2006), facilitating the overall dominance of annual grass cover and further altering the fire regime through a feedback loop. Post-fire regeneration of sagebrush is relatively slow as compared to other shrub communities, with regeneration often requiring 15 years or more to return to pre-burn conditions (Humphrey, 1984).

The sagebrush steppe site covers ~175,000 km^2 (MODIS tile h09v04), and the burned areas for this ecosystem were mapped for 2001. Herbaceous cover was incorporated in the dNBR threshold development in addition to tree cover. The threshold was set at 100 (dNBR * 1000) for areas with tree cover >2%. For areas with tree cover <= 2%, the thresholds were set at 100 (dNBR * 1000) for herbaceous cover > 72% and 75 (dNBR * 1000) for areas with herbaceous cover <= 72%. The spatial active fire threshold was set at "5 times active fire pixel count * 100 ha" based on the estimates of arid grasslands in Northern Africa for clusters > 2.3 and herbaceous cover < 73.5 %. The temporal active fire threshold was set at 32 days prior to the date of the compositing period.

The comparison of the MODIS burned area estimates with the fire perimeter data showed that MODIS burned areas only slightly overestimate the area burned (slope = 1.11 with R^2 = 0.92) (Figure 3-8). Visual evaluation of mapping accuracy also shows a good correspondence between the MODIS burned area and the reference burn scars (Figure 3-9 c). These results are very encouraging considering the difficulty of mapping burned areas with coarse and moderate resolution instruments in ecosystems with low biomass concentrations.
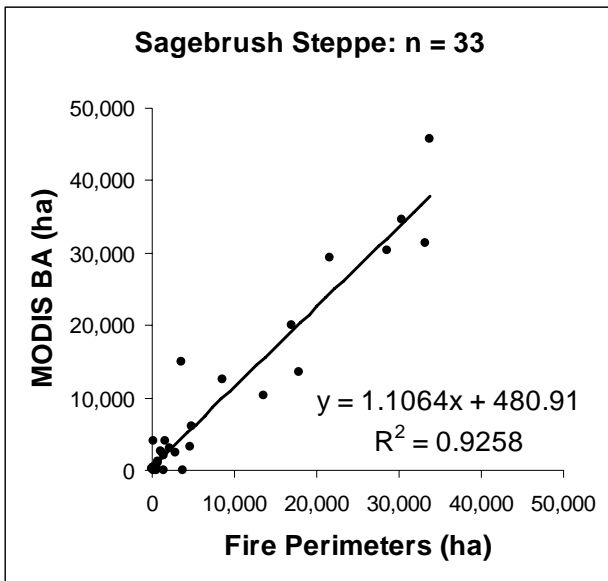
Figure 3-8. Inventory accuracy assessment for the Great Basin sagebrush steppe test site compared against fire perimeters.
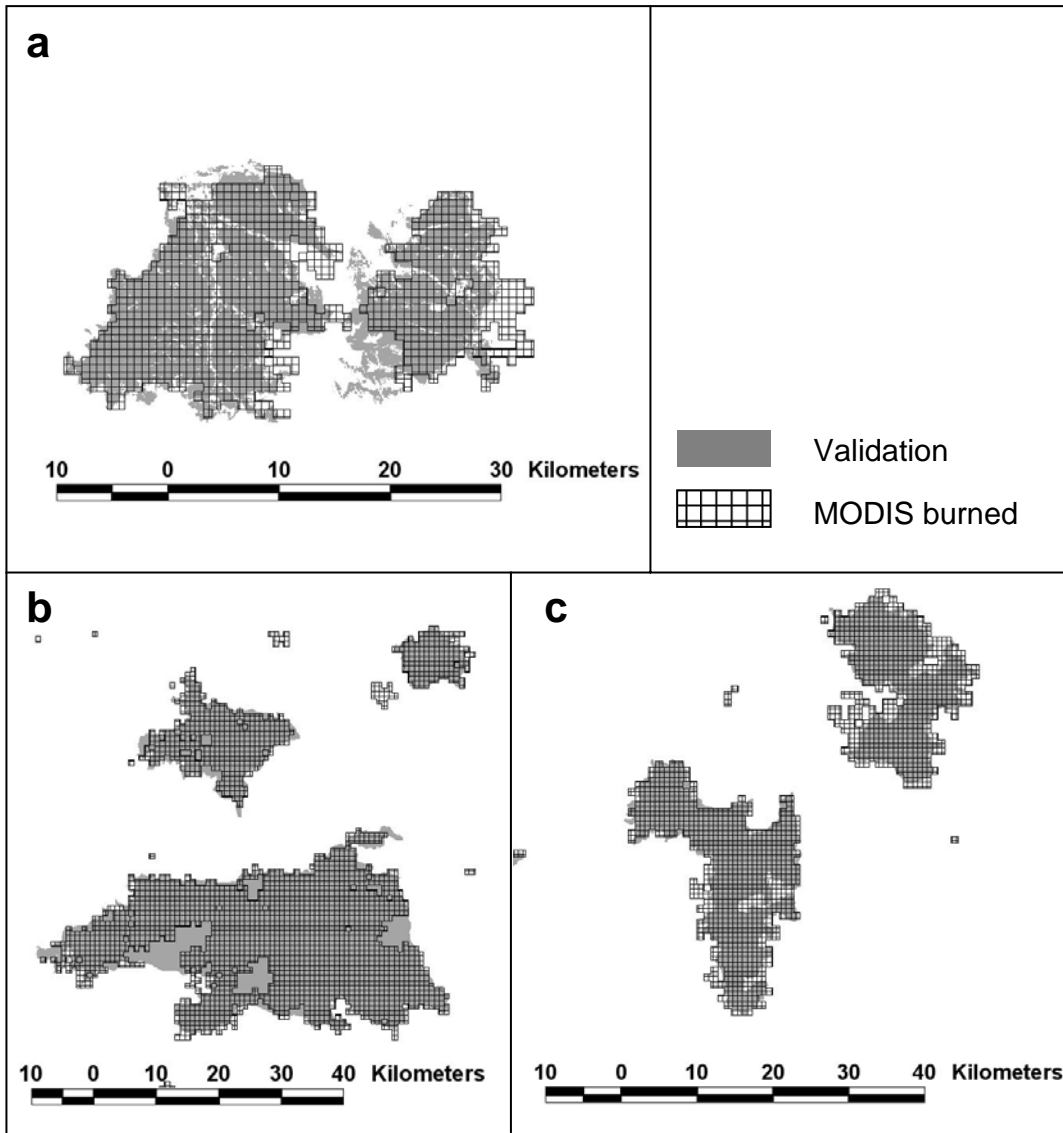
Figure 3-9. Examples of the MODIS-based burned areas overlaid on the validation

datasets in the three test ecosystems: a) Central Siberia boreal forest; b)

Mediterranean-type ecosystem of California; c) Sagebrush steppe of the Great Basin.

3.5. Discussion

The regionally adjustable burned area algorithm presents an innovative

approach which focuses on unique combinations of vegetative, fire progression, and

post-fire recovery characteristics for various biomes. The approach is straightforward and repeatable. Although the algorithm is not fully automated it does not rely on the analyst's knowledge of the regional specifics and eliminates subjectivity of threshold selection. The results of the MODIS burned area mapping approach across the three test ecosystems are encouraging (Figure 3-9). The flexibility of the algorithm allows for high levels of mapping accuracy across different ecosystems ranging from boreal forests to semi-arid grass and shrub lands with estimates falling within 15% of the validation base. The high accuracy of algorithm performance within individual regions and ecosystems also allows for cross-comparison of burned areas between regions and biomes of interest. In addition to the high accuracy of burned area estimates, the product demonstrated high levels of geographic accuracy for large fire scars (Kappa 0.76 – 0.79). The geographic accuracy for smaller fire scars was lower, but this is partially explained by the coarse mapping resolution (500m) of the MODIS burned areas. Among the most common sources of error introduced by the coarse resolution instruments are edge effects, where a burned MODIS pixel at the edge of the fire scar covers a combination of burned and unburned pixels in the validation dataset. The limitations arising from the instruments' spatial resolution are amplified by the heterogeneity of burned areas with numerous unburned inclusions within the fire scars which results in a considerable overestimate of the burned area (Loboda and Csiszar, 2005).

Several major problems found with mapping burned areas are related to the input data. The exclusion of atmospherically contaminated pixels leads to gaps in burned areas due to a lack of high quality surface observations. This problem is

particularly relevant for areas with high average percent cloud cover and areas where burning results in the release of large quantities of particulate matter into the atmosphere. Another problem is the existence of low quality input data missed by the quality assessment algorithm used on the MODIS Surface Reflectance product. Atmospheric contamination in the input data leads to a large error in burned area mapping. It is possible to reduce this error by visual inspection of input data. However, this solution is extremely time consuming and is only feasible for small projects. The burned area accuracy may also be further improved by the inclusion of MODIS products from the Aqua satellite in the processing chain.

Intra-annual and inter-annual variability of vegetative cover driven by phenology and differences in onset of green up and senescence presents a challenge for single "annual" threshold application in burned area mapping. This issue was particularly prominent in mapping burned areas in Mediterranean-type ecosystems where a large inter-annual difference in NBR values is observed during the spring (February through April). This problem leads to the identification of extremely large contiguous areas as being burned. While these areas were subsequently eliminated by the algorithm at later processing stages, true burned areas were also eliminated. Changing dNBR thresholds as a function of season of fire occurrence could present a solution to this issue and lead to considerable improvements in mapping burned areas. Two potential issues with the validation approach are the use of a single-date burned area mapping technique with the Landsat ETM+ imagery and the fire perimeters from the interagency incident command teams as the validation reference bases. Although multi-temporal change detection is a more commonly used approach to burned area

mapping, the persistent cloud cover over Northern Eurasia throughout the year (60-80% according to ISCCP-D2, mean monthly cloud products July, 1983 – December, 2004, <http://isccp.giss.nasa.gov/>) makes the availability of cloud-free image pairs rare. Single image classification enhances the possibility of creating burned area products over large geographic areas with a yearly temporal frequency. It also allows for mapping burned areas with a higher temporal frequency due to the availability of a larger number of single Landsat images per fire season compared to the number of multi-temporal Landsat image pairs. In addition to the Landsat validation base issues, the fire perimeters contain an archive of inconsistent sources with numerous errors of misregistration which significantly limit their use. In the future we plan to adapt fully the GOFC/GOLD validation protocol used by the Southern Africa Fire Network (SAFNet) and described by Roy et al. (2005b) wherever possible to produce consistent and full (inventory and geographic) accuracy assessments for this product.

3.6. Conclusions

The presented algorithm provides the basis for developing a long-term (based on the MODIS data record length) record of fire effects over the entire study region necessary for parameterization of the fire danger model. The algorithm is based on readily available operational MODIS products which ensure the availability and consistency of input data. As a semi-automated algorithm, this approach provides consistent estimates of burned area over time. At the same time, the flexibility of the approach presents an opportunity to adapt burned area mapping to the regional specifics of vegetation composition and structure and fire regime. Developed thresholds for mapping burned area in Siberian forests, produce accurate estimates of

the total amount of burned area ($R^2 \sim 0.97$, slope ~ 1.1) as well as reasonable geographic precision of mapping (kappa ~ 0.78 for larger scars).

In addition to the binary burned /unburned mask, the algorithm preserves the variability of change in surface reflectance compared to the pre-burn conditions, which provides valuable information about characteristics of burning and fire impact. While dNBR may not be a suitable index for burn severity assessment across various ecosystems, its variability within an individual fire scar may provide comparative estimates of fire impacts on a given area. The recorded spectral signature of the dNBR index may prove useful to differentiate fire impact severity levels within a single ecosystem or a single fire scar with proper field validation. However, additional work in developing understanding of dNBR as a measure of fire impact on land surface and severity is necessary.

Chapter 4: Modeling Fire Danger in Data-Poor Regions: A Case Study from the Russian Far East[3]

In this chapter, the generic conceptual framework of fire threat is adapted to regional specifics of fire occurrence in the RFE through parameterization of the fire danger module. As a region-specific but resource independent module (chapter 2), fire danger is presented at this stage as a stand-alone model. Here the predictive capability of the fire danger model is tested by comparing it to observed fire occurrence. The model is subsequently used in chapter 5 to evaluate climate driven changes in fire danger during the 21st century and is merged with other components to evaluate fire threat to the Amur tiger in chapter 6.

4.1. Introduction

Fire danger modeling, concerned with the spatio-temporal assessment of factors supporting initiation and influencing behavior of fires (Allgőwer et al., 2003; Lynham, 2005), presents the next step in parameterization of the Fire Threat Model to the regional fire specifics of the RFE. Despite the nearly global extent of fire, our ability to forecast fire danger using existing fire danger rating systems is limited to only a few regions where fire management is supported by a well developed scientific understanding of fire ecology, integrated with fire management experience (Taylor and Alexander, 2006). The most well developed and known systems include the Canadian Forest Fire Danger Rating System, National Fire Danger Rating System in the US, McArthur's Fire Danger Rating System in Australia (San-Miguel-Ayanz et

---

al, 2003), and European Forest Fire Information System (<effis.jrc.it>). These danger rating systems rely on information provided by long-term records of fire activity, a dense network of field sites and meteorological stations, and a large volume of supporting information, such as high resolution fuel maps and high precision topographic and digital elevation models.

The RFE lacks the required inputs necessary for applying the existing fire danger rating approaches. However, the FTM provides the necessary framework for development of fire danger models driven by remotely sensed data. This chapter details the development of inputs from remotely sensed data, provides an analysis of contribution from various factors to the potential fire behavior, describes parameterization of the Fire Danger module, and demonstrates its feasibility. It incorporates the understanding of the risk of ignition (described in chapter 2) with the potential fire behavior (based on the multi-year record of burned area described in chapter 3) and fire weather assessment into a comprehensive multivariate predictive systems of fire danger modeling.

4.2. Data sources and methodology

The conceptual framework of the FTM was adapted to fit the data availability and regional specifics of the RFE (Figure 4-1). Fire Danger is assessed through the evaluation of the Risk of Ignition, Potential Fire Behavior, and Fire Weather. The Risk of Ignition (ROI) module assesses the likelihood of fire initiation as a factor of landscape accessibility for people and potential for occurrence of natural sources of ignition (e.g. lightning). Potential Fire Behavior (PFB) evaluates the likelihood of fire spread over large areas based on the expected condition of fuels, assessed through

the combination of vegetation types and previous disturbances over the existing

terrain.
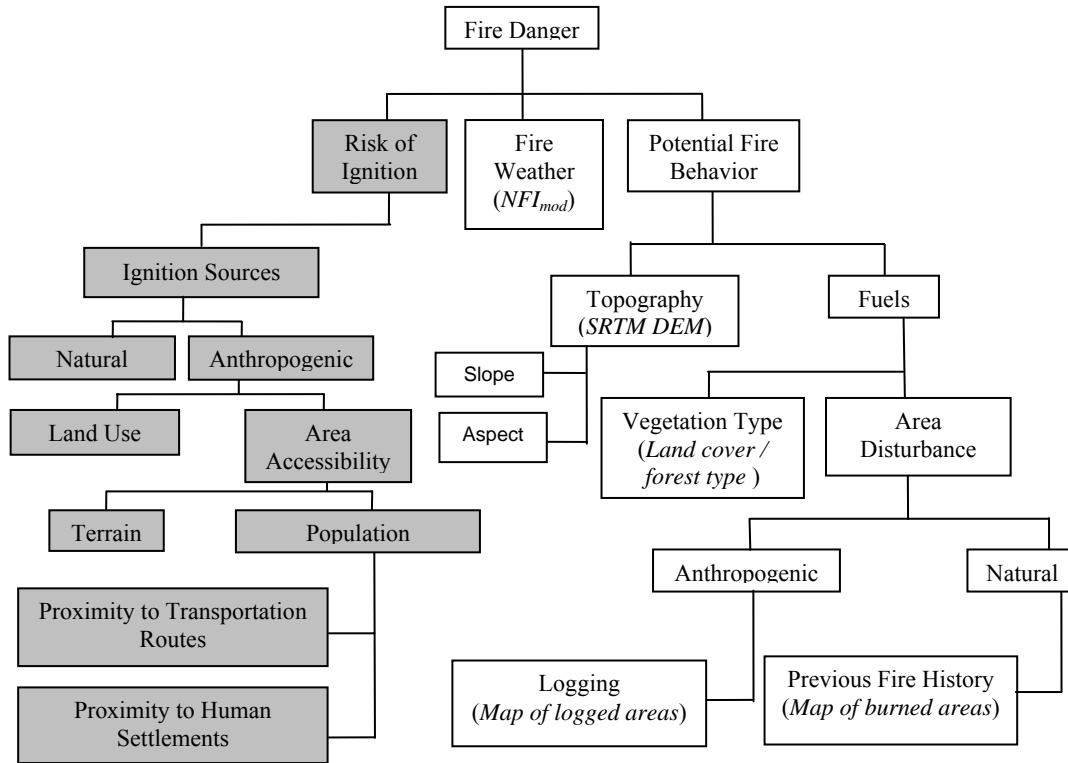
Figure 4-1. Input parameters for regional fire danger assessment for the Russian Far

East. The shaded area shows the assessment of the Risk of Ignition described in

chapter 2. The clear boxes indicate inputs described in this chapter with the name of

the product describing it in parentheses.

 Fire Weather (FW) provides daily estimates of likelihood that meteorological

conditions are optimal for fire ignition and spread over large areas.   These model

components are weighted based on the analysis of the MODIS record of fire

occurrence as a factor of parameters, such as seasonality, fuels, fire weather, and

topography, described later in turn. The predictive capabilities of fire danger modeling were evaluated during the 2006 fire season against known fire occurrence shown by MODIS active fire detections.

Data and derived data products from MODIS for 2001-2005 constitute the major portion of remotely sensed data used in the analysis. The MODIS instrument collected data aboard two satellites – Terra (launched in late 1999) and Aqua (launched in mid 2002). To ensure consistency of the fire data record during the entire 2001-2005 period, only MODIS Terra data products were included in the analysis. Publicly available products from other satellite platforms and archives were also used in the project for land cover, forest disturbance, and terrain assessment, and are referenced in their respective dataset descriptions.

4.2.1. Fire events characterization from MODIS active fire product

The MODIS Rapid Response System active fire product, obtained from Fire Information for Resource Management System (<maps.geog.umd.edu>), presents center points of pixels within the MODIS swath that were flagged as fire by its detection algorithm (Giglio et al., 2003). Due to considerable swath overlap in the high latitudes, the MODIS Terra can collect up to four daily observations of fire occurrence over the same area. This high frequency of observations provides a detailed view of fire development and was used as the basis for the Fire Spread Reconstruction approach (FSR) (Loboda and Csiszar, 2007b). This approach clusters individual fire observations into contiguous fire events in space and time and provides information on the number of fire events, their duration, and the average spread rate of fire between observations.

4.2.2. Burned area estimates

A regional burned area product from Surface Reflectance 8-Day L3 Global 500 m product (MOD09A1) was used to assess the annual amount of burned area (described in chapter 3). A problem associated with mapping burned area using this approach in the current study area impacted the mapping of early and late season fires due to presence of snow cover. Pixels affected by snow are masked out at the pre-processing stage. Subsequently many pre-burn and post-burn images were eliminated for early season and late season fires. This issue is particularly pronounced in mapping late season fires that may be large and produce considerable smoke plumes thus making mapping burned area during the on-going burning process unfeasible. Appearance of snow cover on the ground immediately after or possibly even before the burning is completed prevents such fires from being fully mapped. Two large fire events recorded by the MODIS active fire product in the northern part of the study during November 2005 were mapped using the same algorithm, but with relaxed data quality standards to ensure that these areas were included in further analysis. In particular, pixels with high concentrations of aerosols, which are normally masked out by the algorithm, were included in the processing chain. The results produced contiguous burned areas which were visually confirmed by the analyst.

4.2.3. Land cover/Forest type coverage

A land cover/forest type layer was developed by combining three coarse resolution datasets: 1) a map of Russia's forests (Bartalev et al., 2004), 2) a land cover map of Northern Eurasia from the Global Land Cover 2000 (GLC2000) Project (Bartalev et al., 2003), and 3) a MODIS land cover (MOD12Q1) in IGBP

classification (Friedl et al., 2002). Fusion of these data sources enhances advantages and minimizes disadvantages presented by the application of each individual dataset. This approach builds on consistency in mapping of highly important forest classes by independently produced datasets, translating generic MODIS IGBP legend classes to region specific legends for Northern Eurasia, and filling unspecified gaps (e.g. "recent burns") with meaningful land cover classes.   Incorporation of the map of Russia's forests, derived from two independently produced remote sensing datasets -land cover of Northern Eurasia and MODIS vegetation continuous fields product (Hansen et al., 2003) - provides a more detailed description of forest cover in the RFE, compared to either of the land cover maps. Unlike the MODIS land cover product, the map of land cover for the Northern Eurasia is based on a regionally adapted algorithm that differentiates land cover classes specific to Northern Eurasia better. However, the classification legend for this product contains classes that do not represent land cover (e.g. recent burns). The land covers for these spatial areas were identified from the MODIS land cover product. In addition, the intercomparison of independent land cover products allows higher confidence in identifying forest cover, which presents the single most important land cover type for the RFE.

The input data sources were combined over the study area following the overall scheme presented in Figure 4-2. The output coverage contains two large groups of classes, "forest" and "non-forest." Within the "forest" group, the output map contains six dominant forest types defined by the map of Russia's forests (larch, dark coniferous, pine, broadleaf, mixed, and Siberian dwarf pine) in dense (40-100 % crown cover) and sparse (10-39 % crown cover) categories.

82

Forest | Study Area + Russia's Forests | Non forest

larch (dense)
larch (sparse)
dark conifer (dense)
dark conifer (sparse)
pine (dense)
pine (sparse)
mixed (dense)
mixed (sparse)
broadleaf (dense)
broadleaf (sparse)
dwarf pine (dense)
dwarf pine (sparse)

Non forest + Land Cover of Northern Eurasia

palsa bogs
bare soil and rock
forest - natural vegetation
steppe, humid grasslands
needleleaf evergreen shrubs, broadleaf deciduous shrubs
open shrublands, closed shrublands, woody savannas
savannas, grasslands

recent burns + forests

unclassified + MODIS Land Cover

Forests: evergreen needleleaf, evergreen broadleaf, deciduous needleleaf, deciduous broadleaf, mixed

croplands, cropland/ natural vegetation mosaic
snow and ice, barren and sparsely vegetated

sedge tundra
urban
cropland - grassland complexes
riparian vegetation
water bodies
grasslands
shrubland
shrublands
grasslands
croplands
permanent wetlands
barren and sparsely vegetated
forest-natural vegetation complexes
urban and built-up

tundra
riparian vegetation
barren and sparsely vegetated
grasslands
shrublands
water
cropland and cropland complexes
wetlands
forest-natural vegetation mosaic
urban

Figure 4-2. Schematic description of assembling the land cover/forest type map for the RFE from three data sources: Russia's forests, Land cover of Northern Eurasia, and MODIS land cover (shown in shaded boxes). Italicized text shows the areas evaluated by using the data from one of the original land/forest cover products. The

diamond connections show processing data flow. The arrows indicate the contribution of original land/forest cover products to the final land cover map.

The "non-forest" group consists of 10 classes (combined and cross-referenced from the MODIS land cover product and the land cover of Northern Eurasia map): tundra, riparian vegetation, shrublands, grasslands, croplands and cropland complexes, forest-natural vegetation mosaic, wetlands, water, barren and sparsely vegetated, and urban.

4.2.4. Forest disturbance layer

The two major forest disturbance processes in the RFE are forest fires and logging (Sheingauz, 1996). These two disturbances impact forest fire susceptibility and forest structure differently. Logging often leads to fine fuel accumulation, changes in forest microclimate through full or partial removal of the canopy, and a rise in the risk of ignition due to improved accessibility and the introduction of anthropogenic sources of ignition (Whelan, 1995). The effects of fire on vegetation are generally more variable and complex. The type, intensity, and return interval of fire events within different vegetation types can produce drastically different results from improving forest productivity to replacing forests with brushwood or grasslands (Sheshukov, 1996).

A map of logged areas was obtained through visual evaluation of Landsat ETM+ imagery acquired between 1999 and 2002. The apparent areas of logging activities were delineated to include logging sites grouped into "clear cut" and "selective" logging categories. An additional class of "potential" logging was mapped from the "hot spot" areas of forest cover change (Achard et al., 2005). These

areas were identified by the local experts from satellite imagery mosaics as forest that experienced the most rapid rates of logging in the region since 2000. The "hot spots" of forest conversion due to logging mapped by Archard et al. (2005) delineate general areas rather than map forest conversion per pixel; therefore they include both logged and non-logged areas, and are considered "potential" areas of logging in this study. Since the majority of Landsat imagery used to map logging in the previous step was acquired prior to 2002, the "potentially" logged areas help to account for more recent logging activities in the RFE. In areas of spatial coincidence between the different logging categories the "clear cut" and "selective" (mutually exclusive) classes were assigned to the disturbance map instead of "potential" category. Forest disturbance due to burning was mapped annually between 2001 and 2005. The input sources include annual MODIS burned area product (described in section *Burned area estimates*) and large fire scars from fires of the 1998 fire season mapped with AVHRR imagery (Sukhinin et al., 2004). The scars were grouped into "recent burns" (less than 5 years old) and "old burns" (5 years old and greater) for each year.

4.2.5. Fire weather

Fire weather was assessed through the Nesterov Fire Index (NFI) (as shown in Buchholtz and Weidemann, 2000). The major advantage of the NFI is the simplicity of its calculation, which follows the equation:

$$NFI = \sum_{i=1}^{W}(T_i - D_i)*T_i \qquad (4.1.)$$

85

where NFI is the fire index, W is the number of days since the last daily rainfall greater than 3 mm, T is the temperature (°C), and D is the dew-point temperature (°C). Ideally, air temperature T and dew point temperature D are acquired mid day (Groisman et al., 2007) around the expected daily peak for both parameters. In this study, maximum daily temperature and dew point measurements were used to calculate NFI. The low number of readily available input parameters in this equation makes it possible to provide the daily coverage of NFI from remotely sensed or archived meteorological observations. One of the major disadvantages of the NFI is its inability to retain fire weather history because it zeroes out with cumulative 24-hour precipitation of 3mm or more. The modified NFI (NFI_{mod}), developed within this study, presents the sum of mean daily NFI values over the nine previous days and the actual NFI value of a given day. The average NFI over the previous 9 days allows retention of the previous fire history. However, while retaining the previous fire history, simple averaging leads to the creation of a time lag in the beginning of a given period of enhanced fire danger weather. This lag counterbalances one of the advantages of the NFI - its quick response to changes in fire weather (Buchholtz and Weidemann, 2000), which is important for fire ignition. The danger level assignment based on the NIF_{mod} index was adjusted from the original thresholds in order to account for the summation of 9-day average and the current day NFI values which nearly doubles the output numeric value of the fire index. The NFI_{mod} was converted to membership values μ through linear stretching of values between the identified thresholds in Table 4-1.

Table 4-1. Danger level assignment for the NFI and NFI$_{mod}$ values and fuzzy

membership (μ) assignment. Fire danger levels in bold show the original 4 step scale

developed by Nesterov (as shown in Buchholtz and Weidemann, 2000). Fire danger

levels in normal font were added to provide further differentiation at finer scales.

Fire Danger Level	NFI range	NFI$_{mod}$ Range	NFI$_{mod}$ μ
Nil (Very Low)	0-300	0-500	0-0.2
Low		501-1000	0.2-0.4
Moderate	300-1000	1001 - 2000	0.4-0.6
High	1000-4000	2001-8000	0.6-0.8
Very High		8001-15000	0.8-1
Extreme	4000+	> 15000	1

A gridded NFI$_{mod}$ product for the RFE was created following the approach

presented in Jolly et al (2005). Point source weather data collected at 23 weather

stations (archived at < www.wunderground.com/global/RS.html> and shown in figure

4-3) for maximum air temperature, maximum dew point temperature, and amount of

precipitation were interpolated over the study area. This approach is based on

interpolation of potential temperatures (recorded point source values converted to

values at 1000 mb) and subsequent conversion of interpolated potential temperature

surfaces using a fixed relationship between elevation and temperatures. The

interpolation of precipitation adopted by Jolly et al (2005) is based on the approach

described in Thornton et al (1997). In this method, the interpolation of the actual

precipitation value is preceded by evaluation of precipitation occurrence probability

(POP) defined as a likelihood of precipitation occurring at a given point.

Precipitation amounts were interpolated only within the areas with a probability over

0.54 (Jolly et al, 2005). The interpolation was done using a predefined spline routine in GIS software.
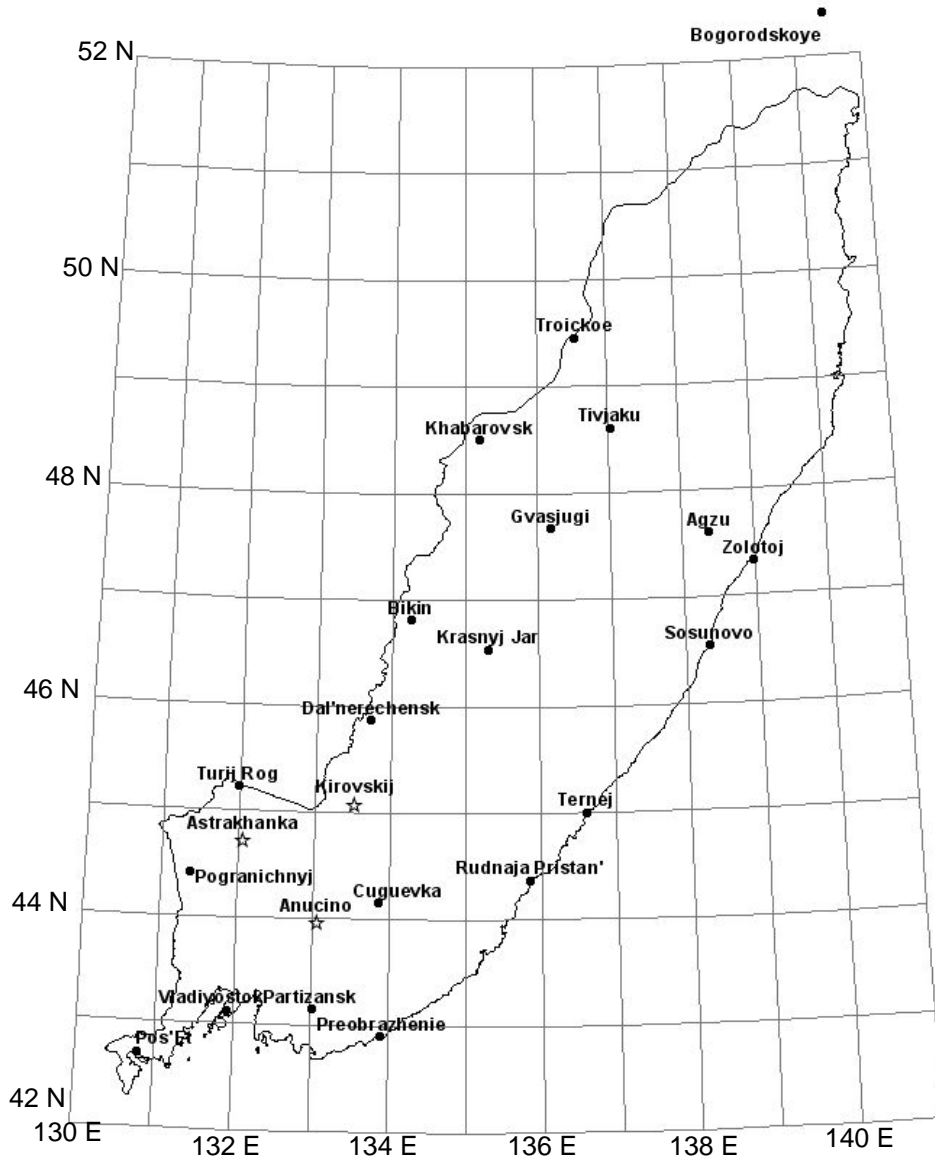
Figure 4-3. Distribution of weather stations used in interpolation of fire weather parameters. Stations shows as hollow stars used to test the stability of the interpolation methodology.

This interpolation approach was tested to evaluate its stability. The test included

removal of 3 stations from interpolation and comparison of the interpolated values to

the values recorded at these stations (Figure 4-4). The results show a significant but

not very strong relationship between the interpolated and recorded values ($R^2 \sim 0.57$).

With the removal of the three test stations, precipitation was interpolated between

stations ~200 km apart. Recognizing that rainfall is an atmospheric parameter with

high spatial variability, and that it operates at the level of weather cells considerably

smaller than the distance between stations, a strong correlation between the

precipitation recorded at different stations is not likely.
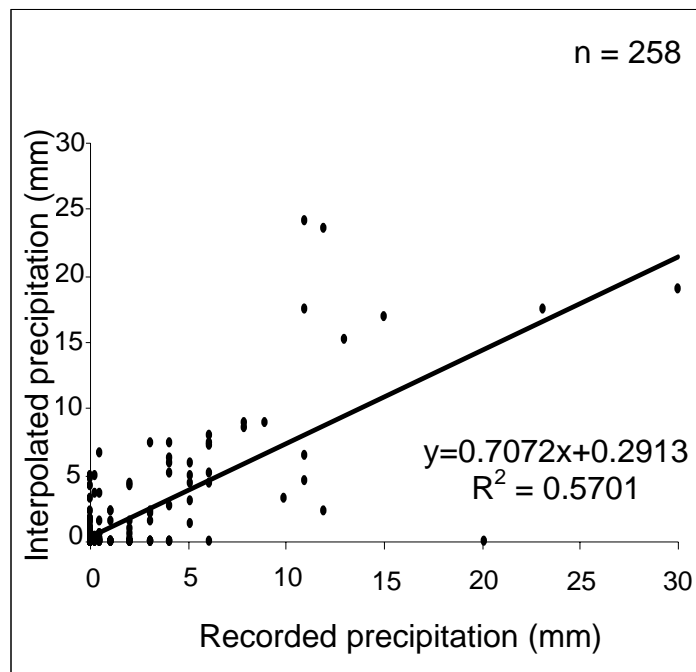
Figure 4-4. Amount of precipitation estimated by interpolation routine and recorded

at three test stations during March 1 – October 31.

The Global Precipitation Climatology Project's One-degree Daily

Precipitation Estimate product (<lwf.ncdc.noaa.gov/oa/wmo/wdcamet-ncdc.html>) is

the only available alternative to the interpolated product. Mean values for

interpolated precipitation amounts within 21 full 1 degree cells found within the study

area were calculated and compared with the amounts of precipitation derived from the

satellite observations. The results of the comparison showed no relationship between

the mean interpolated values and the GPCP data ($R^2 < 0.001$). A similar relationship

was established between the amounts provided within the GPCP and the amounts of

precipitation recorded at the stations. Although direct correlation between the

amounts reported within the GPCP product and the stations should not be expected,

there is an large number of points where a considerable (over 10mm) amount of

precipitation was recorded by one data source and registered as 0 by the other.

To evaluate the discrepancy further, one 1degree cell containing 2 weather

stations positioned at the southern and at the northern boundaries of the cell –

Partizansk and Anucino (Figure 4-3) was selected. Although the stations within this

cell are separated by a considerable distance (over 90 km) the comparison of

precipitation amounts recorded at these stations shows a significant relationship ($R^2 =$

0.68). However, no relationship was detected between the values reported by the

GPCP product and either of these stations ($R^2 = 0.0001$ and $R^2 = 0.0066$). These

findings prompted adopting point source interpolated datasets as a more reliable

source.

4.2.6. Terrain

Topography influences fire spread through slope, aspect and elevation (Whelan, 1995). Slope gradient affects fire behavior by preheating upper slopes through convective and radiant heat and through draft winds that increase fire spread capabilities. Aspect determines a slope's exposure to the sun and therefore influences fuel availability, fuel conditions and the slope's fire weather (i.e., air temperature and relative humidity). Elevation determines vegetation composition and is consequently evaluated through land cover analysis. Although aspect and slope are related, there is no dependence between the two and no direct connections. Each has a specific input to the potential fire spread rate that can be expressed through a matrix (Table 4-2).

Table 4-2. Matrix for evaluation of the potential fire behavior as a function of terrain for categories adapted from Solichin et al (2003): VL (very low), μ = 0.0-0.2; L (low), μ = 0.2-0.4; M (moderate), μ =0.4-0.6; H (high), μ = 0.6-0.8; and VH (very high), μ = 0.8-1.0. Fuzzy membership (μ) values are assigned to aspect by linearly stretching the values between 0 (0° aspect - north) and 1 (180° aspect – south), and to slope by linearly stretching the slope values between 0 (0%) and 1 (100%).

Fire spread as a function of					
slope \ aspect	**VL**	**L**	**M**	**H**	**VH**
VL	VL	VL	L	M	M
L	VL	L	L	M	H
M	L	L	M	H	H
H	M	M	H	VH	VH
VH	M	H	H	VH	VH

91

The terrain component of fire spread was modeled using the Shuttle Radar Topography Mission (SRTM) Digital Elevation Model (DEM). In the Northern Hemisphere south facing slopes receive the majority of the sun's warmth and the north facing slopes have little exposure to the sun. Consequently, the aspect values were converted into membership values (μ) and stretched linearly between northern (0° aspect - $\mu = 0.01$) and southern (180° aspect - $\mu = 0.99$). Slope gradient was converted into membership values by linearly stretching the slope steepness between 0 and 1.

4.3. Spatio-temporal patterns of fire occurrence in the RFE 2001-2005

4.3.1. General patterns of fire occurrence

The analysis of fire occurrence in the RFE was carried out using satellite data products described earlier in the paper to develop an understanding of regional fire dynamics and parameterize the Fire Danger model. Based on the satellite record from 2001-2005, fire occurrence in the study area varied in both the amount and seasonality of burning. During this period the RFE experienced a range of severity from low fire activity seasons in 2001 and 2002 (~263,921 ha and ~221,298 ha burned, respectively) to very the high fire activity season of 2003 (burned area ~972,795 ha) with 2004 and 2005 being moderate fire activity seasons (~544,716 and ~597,095 ha of burned area respectively). The division into "low", "moderate", and "high" fire activity seasons is conditional based upon the observed variability of fire seasons. Burned area estimates cover all fires during these seasons, which include detected agricultural burning and management fires as well as explicitly wildland fire.

Figure 4-5 shows the comparative severity of fire seasons. Although the number of fire detections or individual pixels flagged as "hotspots" in the MODIS active fire product in 2001 is similar to that of 2005 and the number of fire detections in 2002 is only slightly lower than that of 2004, the difference in area burned during these seasons is considerable (Table 4-3). An analysis of fire event duration (Figure 4-6), where a fire event is defined as a contiguous cluster of fire detections in space and time (see section *Fire events characterization from MODIS active fire product)*, shows that the majority of fire events are very short-lived (1 day).
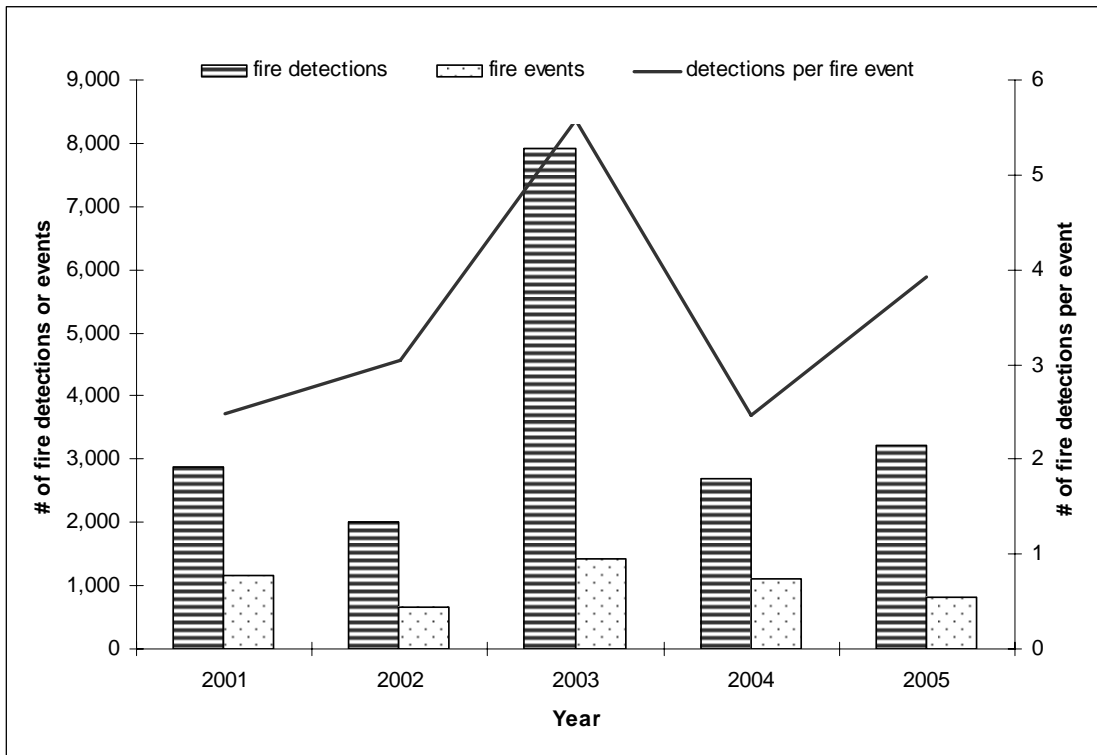
Figure 4-5. Observations of fire occurrence from the MODIS (Terra) during 2001-2005 shown as a comparison of the raw number of fire detections (1 fire detection = 1 "hot" pixel), number of fire events (clustered in space-time fire detections) and the number of detections per fire event.

Table 4-3. Seasonal and total amounts of burned area in the RFE during 2001- 2005.
The seasons are defined as early (March – May), mid (June – August), and late
(September – November).

Year	Burned area (ha)			
	early season	mid season	late season	total
2001	172,078	22,922	68,921	263,921
2002	51,762	159,336	10,201	221,298
2003	364,159	533,322	75,314	972,795
2004	268,015	47,946	228,754	544,716
2005	118,988	105,022	373,084	597,095
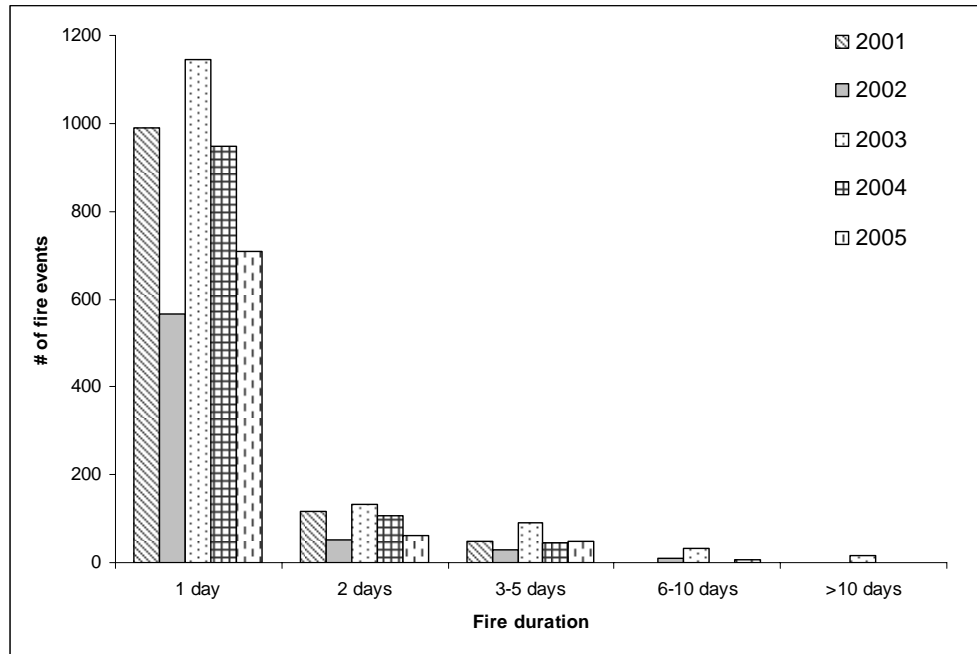
Figure 4-6. Frequency of occurrence of short- and long-lasting fire events in the RFE
during 2001-2005.

The fire detections/fire event ratio (Figure 4-7), indicative of long-burning
fires, explains the larger amount of area burned in 2005 compared to 2001 or 2002.

However, this ratio does not account for the increase in burned area during 2004. The increase in burned area during 2004 occurred due to the increases in number of fire events during the spring and fall seasons (Figure 4-8 and Table 4-3).
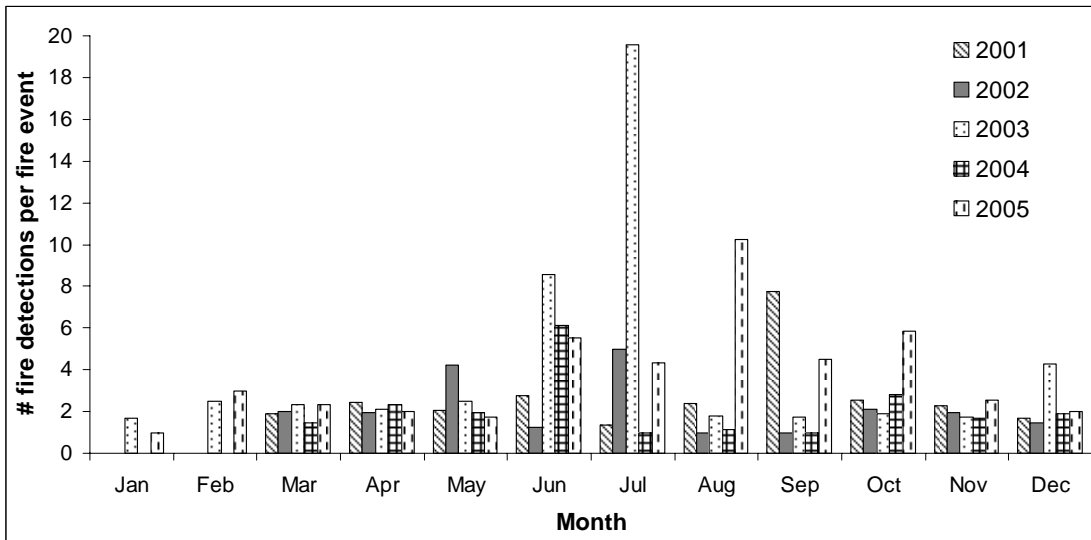
Figure 4-7. Ratio of fire detections to fire events shows the variability in size and duration of fire events monthly during 2001-2005.

In summary, the observed fire regime in the RFE is similar to the general pattern of fire activity in boreal forests where a small number of high intensity fire events account for the majority of burned area and a large number of smaller low intensity fires add little to the overall fire impacts on the region (Stocks, 1991). For example, in 2003 ~20% of all fire scars (scars > 1000 ha) account for over 76% of total burned area, while over 30% of all scars (scars < 300ha) account for just over 4% of the area burned.
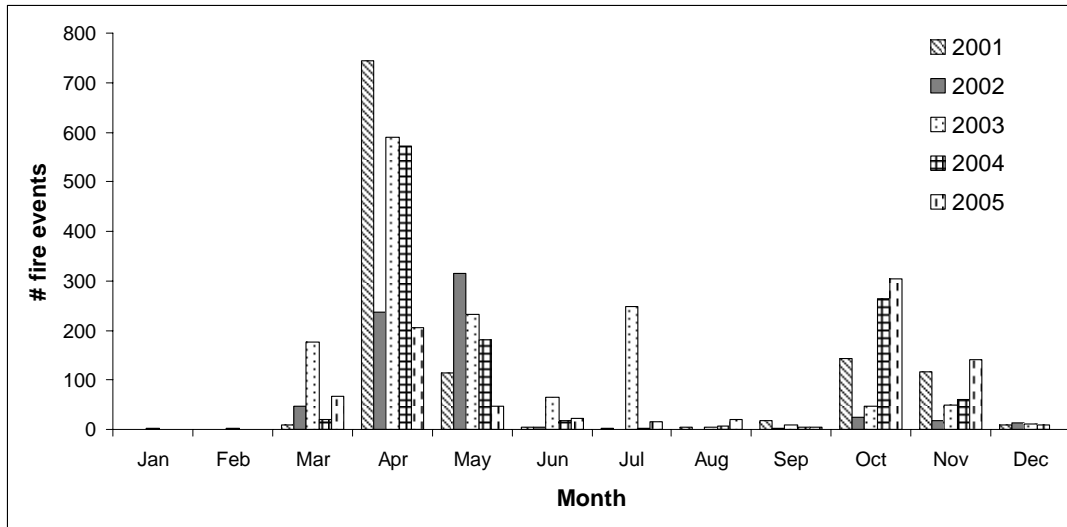
Figure 4-8. Monthly amount of fire occurrence in the RFE during 2001-2005.

Daily observations of fire show a distinct biannual pattern of fire occurrence (Figure 4-8). Fire occurrence starts in March, peaks in April, and drops later in May. The climate of the RFE is regulated by the summer monsoon, which brings abundant precipitation during summer month. The RFE receives 600 – 1200 mm of rainfall annually in the lowlands and mountainous regions respectively (Kotlyakov, 2003). Over 45% of the total yearly precipitation is received during June, July, and August (Savin, 2003). This explains overall very low fire occurrence during June, July, and August. Fire occurrence increases again during late September and lasts through November. During 2001-2005 this pattern was consistent, with the exception of 2003, when a considerable increase in fire occurrence was registered in July. Intra-annual pattern of fire occurrence identifies three periods of burning within a given year: early season (March –May), mid season (June – August), and late season (September – November).

In order to ensure eventual fire danger model parameterization, the three intra-annual fire seasons were compared between years. Although the majority of fire events occur during the early fire season, these fire events are small and short with two fire detections per fire event, on average (Figure 4-7).   Fires burn through cured vegetation leaving patchy scars that rapidly disappear with the onset of spring green-up.

On average, most burning during the early season happens in broadleaf forests, grasslands, and croplands (44, 25, and 13% of early season burned area, respectively). The spatial pattern of late season fires is similar to that of the early season, with broadleaf forests, grasslands, and croplands accounting for an average of 84% of burned area (28, 44, and 14% respectively). Fewer fires occur in the fall than in the spring (Figure 4-8); however, the number of fire events that burn longer and result in larger burned areas increases (Figure 4-7 and Table 4-3); the analysis shows that although the total ratio of fire detections to fire events does not change greatly, the actual number of larger fire events is greater in the fall than in the spring period.

Mid season fire characteristics differ from those of both spring and fall (Figure 4-8). There are generally very few fire events with the exception of 2003, when over 50% of burned area resulted from mid season fires. Mid season fire events are longer; they burn through live green vegetation, and leave long-lasting scars discernable in the remotely sensed imagery for decades. These fires burned predominantly in spruce-fir forests, larch forests, and grasslands, each of these types contributing around 20% of burned area in the mid season of 2003 and make up 11% of total burned area for the year.

4.3.2. Impact of forest disturbance on fire occurrence in the RFE

Fire occurrence was also evaluated as a function of previous area disturbance. The two major disturbances in the RFE are logging and fire. The analysis did not find a relationship between fire occurrence and logging during early and late fire seasons. The only strong relationship was established between clear cut logging and fire occurrence during mid season, particularly for long-burning fires. During the mid season of 2003, 63 fire events (~4.6% of the total burned area during 2003) occurred in clear-cut sites (~1% of total area of the RFE). Because the uncharacteristic summer conditions were observed only once during 2001-2005, this finding is based only on a very limited set of data. However, since there is no specific concentration of clear cut areas in only one geographic region of the study area, the observed relationship appears to be non-accidental.

Fire occurrence as a function of previous burning showed a more complex relationship. The data suggest that fires are the least likely (~2% from total on average) to occur on sites having older scars (> 5 years old) in all years and seasons. Fires are more likely (~4% from total on average) to occur on previously burned sites (≤ 5 years old) than in the previously unburned areas, particularly during early and, to a lesser extent, the late fire season (~5 and 3%, respectively). The latter finding may reflect the spatial proximity of areas previously burned to frequent fire ignition sources. Since a number of early and late season fires represent agricultural burning, it is expected that those areas would burn more frequently as a result of crop residue management practices. However, the spatial analysis showed that repeated burning is not limited to only agricultural areas.

Fires that occurred on previously burned area within different land cover types were analyzed for the period of 2002-2005. Burn scars for the time period prior to 2001 are only available for the northern part of the study area for the 1998 season. Analysis of repeated burns during 2001 would, therefore, be skewed towards the land covers present in northern areas. Consequently, burned areas of 2001 were excluded from further analysis. Although the amount of area reburned increased during 2002 – 2005 from 5000 km^2 to 95000 km^2, this increase reflects the improved record of obtaining burn area estimates during 2001-2005 rather than an increase in fire activity. Relative percentages of reburned areas by land cover types were calculated for each year between 2002 and 2005 and averaged over the 4 years of observation (Figure 4-9).
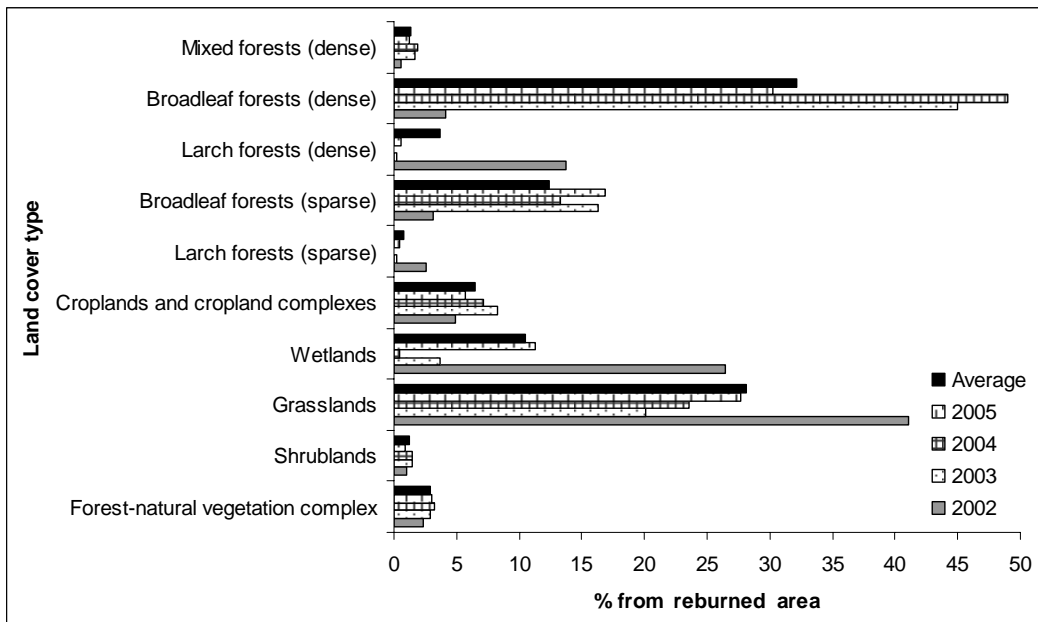
Figure 4-9. Relative amounts of reburned areas over recent burns (<= 5 year old burns) within different land cover types during 2002 – 2005.

The results show that the majority of reburning occurs within dense broadleaved

forests and grasslands (32% and 28% of reburned areas, respectively) followed by

sparse broadleaved forests and wetlands (12% and 10% respectively) whereas

croplands and cropland complexes account on average for 7% of reburned areas.

4.4. Model parameterization

The analysis of fire occurrence in the RFE demonstrated that characteristics of

fire occurrence vary intra-annually. Similar intra-annual variability in distribution of

fire ignitions in the RFE was noted in chapter 2. This temporal variability is

preserved in model parameterization through introduction of temporal thresholds set

for the three major components of the fire danger model – the Risk of Ignition (ROI),

Potential Fire Behavior (PFB), and Fire Weather (FW) (Figure 4-1). The thresholds

change at a monthly time scale for the ROI module and at a seasonal time scale

(early, mid, late) for the PFB module. FW is evaluated daily; however, the thresholds

identifying the ranges of fire weather severity remain constant throughout the year.

All model input parameters were weighed through a set of *Fire Occurrence*

Load coefficients (*FOL*), which evaluate the likelihood of a single fire's occurrence

and extent, driven by a given parameter. For example, the *FOL* coefficient was

evaluated as a function of land cover following the equation:

$$FOL_s = (\sum_{i=1}^{5} f_{zi} / \sum_{i=1}^{5} f_{ti})/(A_z / A_t) \tag{4.2}$$

Where *FOL*$_s$ is a seasonal average *Fire Occurrence Load*, f_{zi} is the area burned within a

given land cover zone z in year i, f_{ti} is the total area t burned within the study area in year

i, A_z is the area of the given land cover zone z, and A_t is the total area of the study area

over five years (2001-2005). When the *FOL* coefficient equals 1, it indicates that fire

occurrence in the given land cover is average for the region equivalent of the

distribution of 100% of fires over 100% of area. For land covers with *FOL* greater

than 1, the recorded occurrence is greater than average; and for *FOL* less than 1, the

recorded fire occurrence in less than average. Table 4-4 shows the *FOL* for all

evaluated parameters.

In order to assign weights to the model input parameters, the *FOL* coefficients

were stretched between 0 and 1 to convert them to membership values (μ) following

the methodology described in chapter 2. A range of *FOL* values for all parameters

within the PFB component was established and used to develop equations for

membership value assignment. The mean value for the entire range of *FOL* values

was set to $\mu = 0.5$. The mean of *FOL* values below and above the mean for the entire

range correspond to $\mu = 0.25$ and $\mu = 0.75$, respectively. Following the same

approach, corresponding *FOL* values for $\mu = 0.125, 0.375, 0.625$, and 0.875 were

calculated. The relationships were fitted with a regression equation that was then

used to translate each *FOL* to μ. The calculated μ values were further assigned to

respective land covers, terrain gradient zones, and disturbance layers to create a

continuous (a value existing at each point in space) grids of PFB as a factor of these

individual parameters for 3 seasons (early - March – May, mid - June – August, and

late - September – November).   The list of resultant membership values is presented

in Table 4-4.

Table 4-4. Conversion of *FOL* coefficient to membership values (μ) for model parameterization.

Parameter	early season		mid season		late season	
	FOL	μ	*FOL*	μ	*FOL*	μ
Landcover / Forest Type						
Barren and sparsely vegetated	0.27	152	0.36	193	0.17	97
Broadleaf forests (dense)	0.69	343	0.03	19	0.13	76
Broadleaf forests (sparse)	2.79	794	0.17	95	0.90	422
Croplands and cropland complexes	1.08	484	0.51	267	0.68	339
Dark coniferous forests (dense)	0.01	7	0.20	114	0.13	73
Dark coniferous forests (sparse)	0.06	35	0.42	224	0.27	151
Forest-natural vegetation complex	0.68	336	0.33	182	0.31	169
Grasslands	1.04	471	0.47	247	1.75	653
Larch forests (dense)	0.21	118	0.42	225	0.09	52
Larch forests (sparse)	0.70	348	0.70	348	0.22	124
Mixed forests (dense)	0.14	80	0.09	51	0.06	37
Mixed forests (sparse)	0.36	194	0.22	121	0.22	125
Pine forests (dense)	0.00	0	0.00	0	0.00	0
Pine forests (sparse)	0.00	0	0.00	0	0.00	0
Riparian vegetation	1.30	500	1.30	500	1.30	500
Shrublands	0.38	206	0.23	128	0.24	132
Siberian dwarf pine forests (dense)	0.00	0	0.13	74	0.11	61
Siberian dwarf pine forests (sparse)	0.00	0	0.23	130	0.29	161
Tundra	0.00	0	0.00	0	0.34	187
Unclassified	0.02	12	0.00	1	0.16	92
Urban	0.02	14	0.07	43	0.04	24
Water bodies	0.00	0	0.00	0	0.00	0
Wetlands	1.77	658	0.79	381	1.91	683
Burns						
Old burns	0.09	52	0.11	61	0.18	100
New burns	1.43	583	0.26	145	0.76	372
Non-burned	0.48	249	0.19	109	0.28	156
Logging						
Clearcut logging	0.15	85	1.76	656	0.21	116
Selective logging	0.05	26	0.07	40	0.04	21
Potential logging	0.01	5	0.13	76	0.06	33
Non-logged	0.57	292	0.19	106	0.34	184

4.5. Evaluation of fire danger within the modeling framework of the Fire Threat

Model

Fire danger (FD) is calculated as a sum of its major components. ROI and PFB are evaluated through the ordered weighted averaging (OWA) approach (Yager, 1988) to model fire danger with fuzzification. In this approach, PFB is treated as a fuzzy set $PFB = (lc_j, terr_j, d_j)$ where *lc* is land cover, *terr* is terrain, *d* is disturbance for each pixel *j*. Fuzzy logic driven approach to combining input parameters in a quantitative assessment of fire danger accounts for non-linearity of the interaction among the input parameters and provides a built-in method for assessing the range of uncertainty. The OWA with fuzzification outputs a fuzzy set FD = (minimum, mean, maximum) which can be viewed as 3 potential *PFB* scenarios. The scenarios are built using the following weightings (w): 1) "best case" scenario (fuzzy intersection - w = [1,0,0] with the weight of 1 assigned to the lowest input value), 2) "worst case" scenario (fuzzy union – w = [0,0,1] with the weight of 1 assigned to the highest input value), and 3) "trade-off" scenario (arithmetic mean – w = [0.33, 0.33,0.33] with equal weights assigned to all inputs). The "best case" scenario implies that fire susceptibility of a given area is mitigated by the lowest value of the three input parameters providing the low boundary of the range of uncertainty. For example, if terrain has the lowest input value of the three, the situation can be interpreted as "although this type of vegetation can support fast moving fires that spread over large areas and there is additional dead fuel from a previous disturbance, the flatness of terrain will minimize the rate of spread of the fire". Similarly, the "worst case" scenario defines the upper boundary of the range of uncertainty. In the same example, if terrain has the highest membership value of the three inputs, the situation can be interpreted as "no matter

what land cover type is present, steep slopes will increase preheating of the fuels and, in combination with slope driven wind effects, will aid in fast movement of the fire upslope resulting in more severe fire effects". The "trade off" scenario provides an estimate of combined effects from all three inputs on fire danger.

Similarly, ROI presents a fuzzy set $ROI = (r_j, rr_j, s_j, t_j, lu_j)$, where r, rr, s, t, and lu represent the likelihood of ignition as a function of distance from major roads, railroads, and settlements, terrain gradient, and land cover/land use, respectively, for each jth point of the study area (chapter 2). The Fire Danger for date i is then calculated as $FD_{if} = Sum(ROI_{mf}, PFB_{sf}, FW_i)$, where f is one of the three output scenarios, ROI_m is the monthly risk of ignition index relevant to date i, PFB_s is the seasonal potential fire behavior index relevant for date i, and FW_i is the daily fire weather index for date i. Values for the three inputs, ranging between 0 and 1, are converted for computational purposes to integer values by rounding off the floating point value multiplied by 1000 and effectively stretching the range of individual inputs between 0 and 1000. Consequently, the output fire danger range is stretched between 0 and 3000.

Fire Danger model performance was evaluated against the MODIS fire detections during March10 – October 30 of 2006 fire season. Maps of Fire Danger were produced and evaluated against MODIS active fire detections at a daily time step (Figure 4-10). The MODIS daily fire detection points were buffered to a 1 km diameter to approximate the MODIS pixel size. It was assumed that all the area within the buffered fire detections was burned.
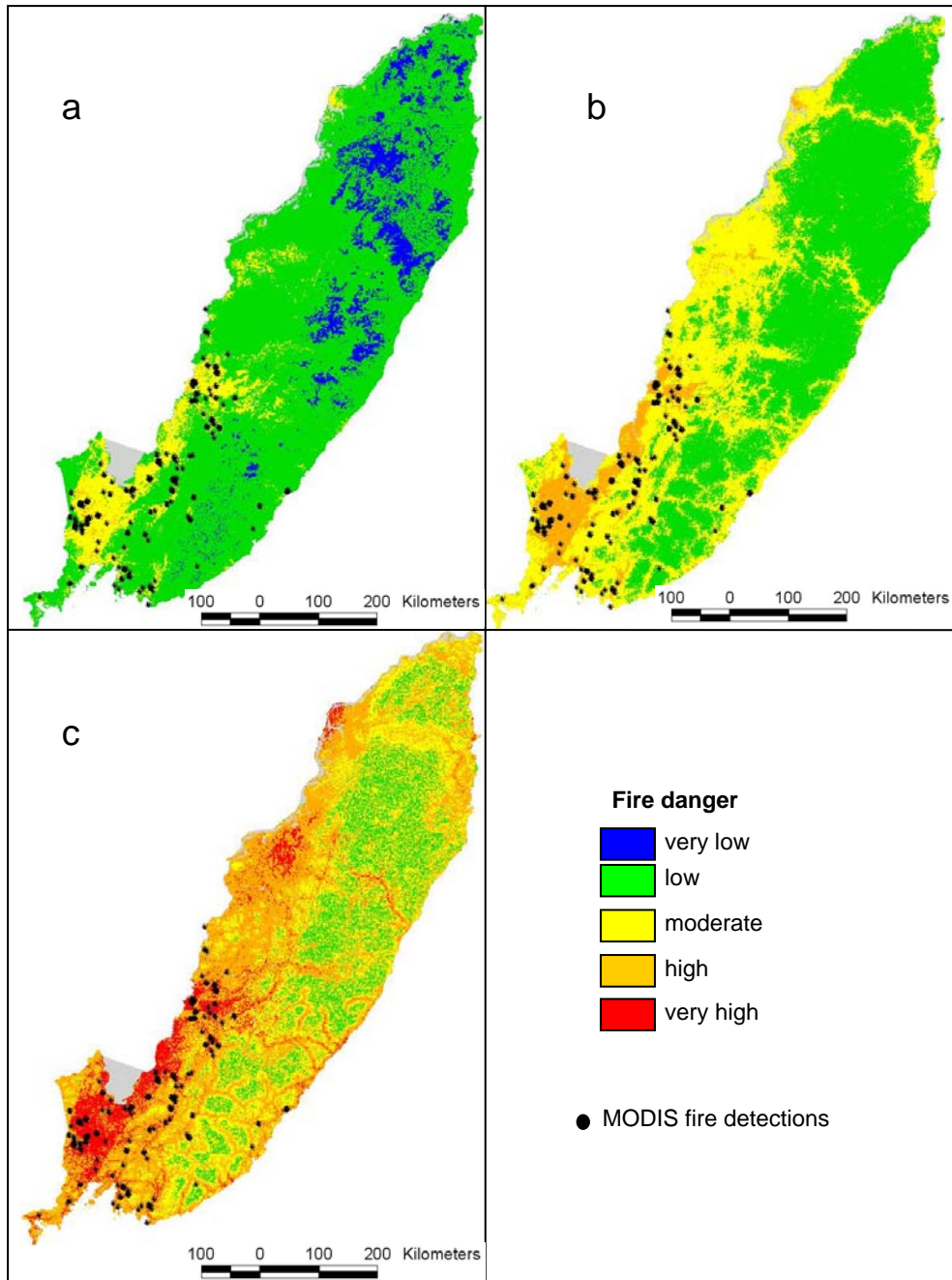
Figure 4-10. Maps of fire danger ratings for April 14, 2006 and corresponding fire occurrence on that date for three scenarios: a) "best case" scenario, b) "trade-off" scenario, c) "worst case" scenario.

All three scenarios present meaningful evaluations of fire danger in the RFE but differ from each other, to a certain degree, in spatial distribution and the amplitude of danger levels (Figure 4-11). Each of the scenarios operates within a different range of fire danger values with the "best case" scenario gravitating towards the lower range of fire danger and the "worst case" scenario towards the upper range of values. The two parameters graphed in figure 4-11 show the overall distribution of values binned by fire danger levels as well as the ratio of the number of pixels within MODIS fire detection buffers to the total number of pixels within a given fire danger range for the study area (fire/total ratio). The cumulative yearly frequency distribution of values shows the dynamic range of the model output and the proportion of elevated levels of fire danger (upper range of moderate, high and very high). This parameter helps to ensure that the relationship between observed fire occurrence and fire danger level is not driven by overestimated fire danger throughout the year. The fire /total ratio demonstrates the relative frequency of fire occurrence as a function of the modeled fire danger levels by calculating the fraction of "burned" pixels (as defined by the 1km MODIS buffers) within a group of pixels of the same fire danger level.

All three scenarios show that the fire/total ratio increases sharply through moderate to high ranges of fire danger (or high to very high levels for the "worst case" scenario). This increase indicates that the fires are more likely to be found within areas identified as high fire danger zone than low.

The "worst case" scenario (Figure 4-11 c) outputs a wide range of fire danger values with the majority of areas falling within moderate and low fire danger levels.
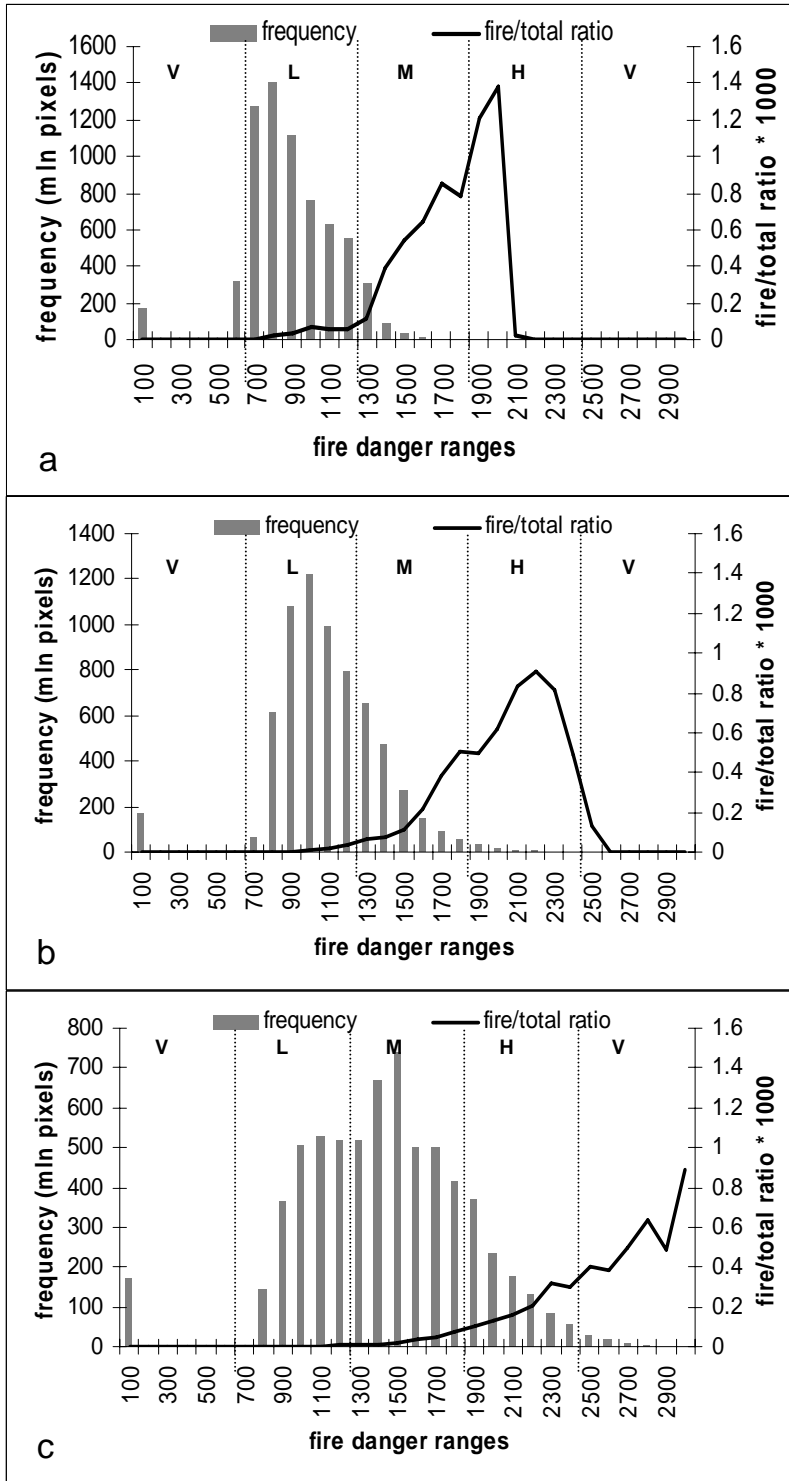
Figure 4-11. Frequency distribution of fire danger values during March10 – October

31 of 2006 and the ratio between the number of fire danger values within buffer zones

from the MODIS active fire detections and the total number of fire danger values for

three scenarios: a) "best case" scenario, b) "trade-off" scenario, c) "worst case" scenario. The first bin (100) includes fire danger value of "0" over water bodies.

A considerable (16%) number of values fall within high danger levels, which somewhat contradicts the actual fire activity levels in the RFE during 2006. In addition the ratio of pixels within fire buffers to the total number of pixels of a given range of fire danger values appears to saturate. This indicates a limited applicability of this scenario for high fire activity seasons.

The "best case" scenario (Figure 4-11 a) has the narrowest dynamic range of fire danger levels with the majority of values falling within the low fire danger zone. The number of pixels mapped as high fire danger is extremely low and the maximum fire danger values do not exceed 2000. This scenario has the sharpest increase in the fire/total ratio demonstrating the highest likelihood of fire occurrence within areas classified as high fire danger levels.

The "trade-off scenario (Figure 4-11 b) has a relatively wide dynamic range. While the majority of values are found within the low fire danger zone, many pixels are identified as moderate fire danger and some as high fire danger, a designation that can support multi-day fire events. The fire/total ratio is extremely low within the low fire danger zone. It sharply increases throughout the upper range of the moderate fire danger zone and peaks in the high fire danger zone. It further declines towards the very high danger zone due to a very low number of pixels identified as very high fire danger areas.

Based on the fire occurrence of 2006 fire season the "trade-off" scenario presents the optimal choice for mapping fire danger in the RFE during low fire activity seasons. The "best case" scenario is the most appropriate evaluation of fire danger levels for applications focused on identification of areas likely to support large and catastrophic fire events (undetected during 2006). The "worst case" scenario may be best suited for applications supporting early signs of increase in fire danger. Since 2006 was a year of relatively low fire occurrence with nearly complete absence of fire during mid season, further evaluation of model performance during high fire activity years and during mid season is necessary.

4.6. Conclusions

The presented approach demonstrates feasibility of successful fire danger assessment in the RFE within the framework of Fire Threat Modeling. The model parameterization, driven by remotely sensed data, allows for incorporation of anthropogenic influences on fire ignition and propagation. The ability to account for human impact on fire is particularly relevant for the RFE where the distribution of fire ignitions is closely connected with human presence (chapter 2) and large fire occurrence during dry years is enhanced in logged areas (this chapter).

The modeled fire danger levels are supported by observation of actual fire activity in the RFE during the 2006 fire season. The three output scenarios provide an estimate of uncertainty associated with modeling outputs. While all three modeled scenarios provide meaningful evaluations of fire danger in the region, selection of an appropriate scenario may be determined by the risk tolerance of decision makers and fire season severity. During low fire activity seasons similar to 2006, the "trade-off"

scenario appears to be the most appropriate for mapping fire danger at a daily time scale.

The parameterization of the model is highly dependent on the accuracy and resolution of the input data. Each individual data source introduces a number of uncertainties into the modeled scenarios. However, parameterization of the model using knowledge of the relationship between fire occurrence and related parameters gained by using remotely sensed data products can help to minimize the error associated with converting biophysical relationships previously established during field studies at the local scale to regional applications.

Based on the 2006 assessment, the predictive capabilities of the model can be applied for operational applications and scientific research. Daily scenarios of fire danger can be created using observed, forecasted, or modeled meteorological conditions. The flexible model structure and minimized requirements for input weather parameters allow for evaluating long-term scenarios of potential climate induced change in regional fire danger from the outputs of General Circulation Models.

Chapter 5: Long-Term Forecasting of Fire Danger in the Russian Far East Using Climate Change Scenarios

In this chapter, the predictive capability of the fire danger module is used to evaluate a range of potential change in fire danger under several scenarios of climate change during the 21st century. The research presented here builds the capacity for coupling the regional fire danger and fire threat models with outputs of the Global Circulation Models, thus extending the models' predictive capabilities. Because the fire danger module is a stand-alone component within a more complex structure of fire threat modeling, it allows for more efficient processing of a variety of climate change scenarios aimed at narrowing the suite of potential model runs to a subset of relevant scenarios. The resultant subset is further used in chapter 6 to assess potential change of fire threat to the Amur tiger by the end of the 21st century.

5.1. Introduction

Global climate warming is now recognized as unequivocal by the international scientific community (Intergovernmental Panel on Climate Change (IPCC), 2007). Systematic observations of climatic trends show a net increase in global air and ocean temperatures with a particularly pronounced increase in higher northern latitudes of Northern Eurasia (Groisman et al., 2007). Following the warming climate, there has been a considerable increase in frequency, extent, and severity of wildland fire in boreal forests worldwide (Stocks et al., 1998; Conard et al., 2002; Kasischke et al., 2004). Moreover, under the further developing conditions of climate change the

frequency of large severe fire occurrence in Russia is predicted to rise (Stocks et al., 1998; Malevsky-Malevich et al., 2008).

The borderline position between temperate and boreal zones makes the RFE especially sensitive to climate change. A mosaic of boreal and temperate species provides a readily available seed bank which can respond to changing climate faster than areas of uniform boreal or temperate forests as broadleaved species generally outcompete needleleaved species (Shao et al., 2003; Shriner and Street, 1998). The rate of change in vegetation composition is likely to be enhanced by stand replacing disturbances such as fire. Therefore, understanding potential changes in future fire regimes under the changing climate will provide a basis for understanding the potential change in fire impacts on the Amur tiger habitat.

Several studies have previously analyzed changes in fire weather over Russia under the changing climate during the 20th century (Groisman et al., 2007) and during the 21st century under various scenarios of climate change produced by Global Circulation Models (GCM) (Malevsky-Malevish et al., 2008). However, these studies considered fire weather outside of a fire danger rating system providing estimates of separate uncoupled components. The fire danger model developed within the fire threat modeling framework (chapter 4) provides an approach for evaluating future change in fire danger under the projected scenarios of climate change in spatial relation to the risk of ignition and potential fire behavior, thus providing a more explicit set of scenarios of expected change compared to the previous studies.

This chapter presents an evaluation of future trends in fire danger in the RFE and the uncertainties in our estimates associated with our ability to forecast climate change. This analysis aims at answering three major questions: 1) how suitable are the GCM predicted parameters for evaluation of potential climate change at a regional (sub-continental) scale; 2) how do GCM data driven fire danger estimates compare to those driven by observed weather parameters; and 3) what are the expected trends in fire danger in the RFE under the IPCC scenarios of climate change during the 21st century.

5.2. Data and Methodology

This chapter is designed as a three part study. First, GCM based meteorological parameters including temperature, humidity, and precipitation are compared with the same parameters derived from observations at meteorological stations over a 5-year period (1996 – 2000) to evaluate the ability of very coarse resolution (~1.85 X 1.85 degrees) GCM data to reproduce observed weather patterns within a relatively small region. Second, fire danger predictions, developed using the fire danger model presented in chapter 4, from observed and modeled meteorological conditions are evaluated over the 1996-2000 time period. This comparison provides an opportunity to assess fire danger model sensitivity to various meteorological inputs as well as determine if GCM outputs can be used to model fire danger within a coupled system that includes risk of ignition and potential fire behavior with reasonable accuracy. During the third stage, GCM based estimates of fire danger were modeled under two different Special Report on Emissions Scenarios (SRES). These GCM-based estimates were compared for three 5-year periods – end of the 20th

century (1996-2000), mid 21st century (2046-2050), and end of the 21st century (2096-2100). This analysis furthers our understanding of trends in potential climate impact on wildland fire in the RFE during the 21st century.

5.2.1. Meteorological Data for Fire Danger Modeling

Meteorological observations for the study area during 1996 – 2000 were obtained from the National Climatic Data Center (NCDC) datasets 9290c and 9813 (NCDC, 2005 A and B). These datasets include point source observations of temperature, relative humidity, air pressure, air pressure at sea level (dataset 9290c), and daily amount of precipitation (dataset 9813). These parameters were collected for 36 stations in the study area and further interpolated to create gridded products at 1km resolution using the methodology of Jolly et al. (2005) described in detail in chapter 4.

The NCDC dataset 9290c includes several daily observations of meteorological parameters. Maximum daily air temperatures were selected as inputs for the fire danger model to maintain consistent daily GCM outputs. Measured air temperature and dew point temperature derived from recorded relative humidity were converted to potential temperatures in accordance with the Jolly et al. (2005) methodology as inputs to the fire danger model.

Although NCDC datasets 9290c and 9813 present the most complete and detailed archive of meteorological data available for the study area outside Russia, there are considerable gaps in data record from individual stations. Missing observations from individual stations were removed from the dataset at a daily time step by subsequently removing the station points from the interpolation routine.

Therefore, some daily gridded temperature and air pressure products were interpolated from fewer than the total available 36 stations. There were no missing records in the precipitation dataset and it was interpolated into gridded products separately. The data record for year 1997 was affected particularly strongly: during this year daily data interpolation was performed from as few as 24 of the 36 available stations.

5.2.2. Climate Model Selection

Scenarios of change from various Global Circulation Models (GCMs) often differ in their estimates of change in temperature and precipitation for different regions of the world (Williams et al., 1998). Temperature and precipitation trends analysis for the SRES A2 greenhouse gases and aerosol precursor emissions scenario (a description of this scenario is provided below in section 5.2.3) during the 21st century was conducted for the study area relative to 1961-1990 for six major GCMs (<www.ipcc-data.org/cgi-bin/ddcvis/gcmcf>): 1) CCCma (Canada), 2) CSIRO (Australia), 3) ECHAM4 (Germany), 4) GDFL99 (USA), 5) HadCM3 (UK), and 6) NIES99 (Japan). The comparison included the magnitude of change averaged over the entire study region as well as a visual assessment of spatial patterns of change (Figure 5-1). The general trends produced by the analyzed GCMs are relatively consistent in both magnitude and spatial pattern. This allowed us to select one model representative of a general trend for fire danger modeling.

The ECHAM5 model was selected because it is representative of the averaged trends, it has comparatively high spatial resolution of ~1.875 degrees, and daily outputs of the necessary parameters including air temperature, specific humidity, air
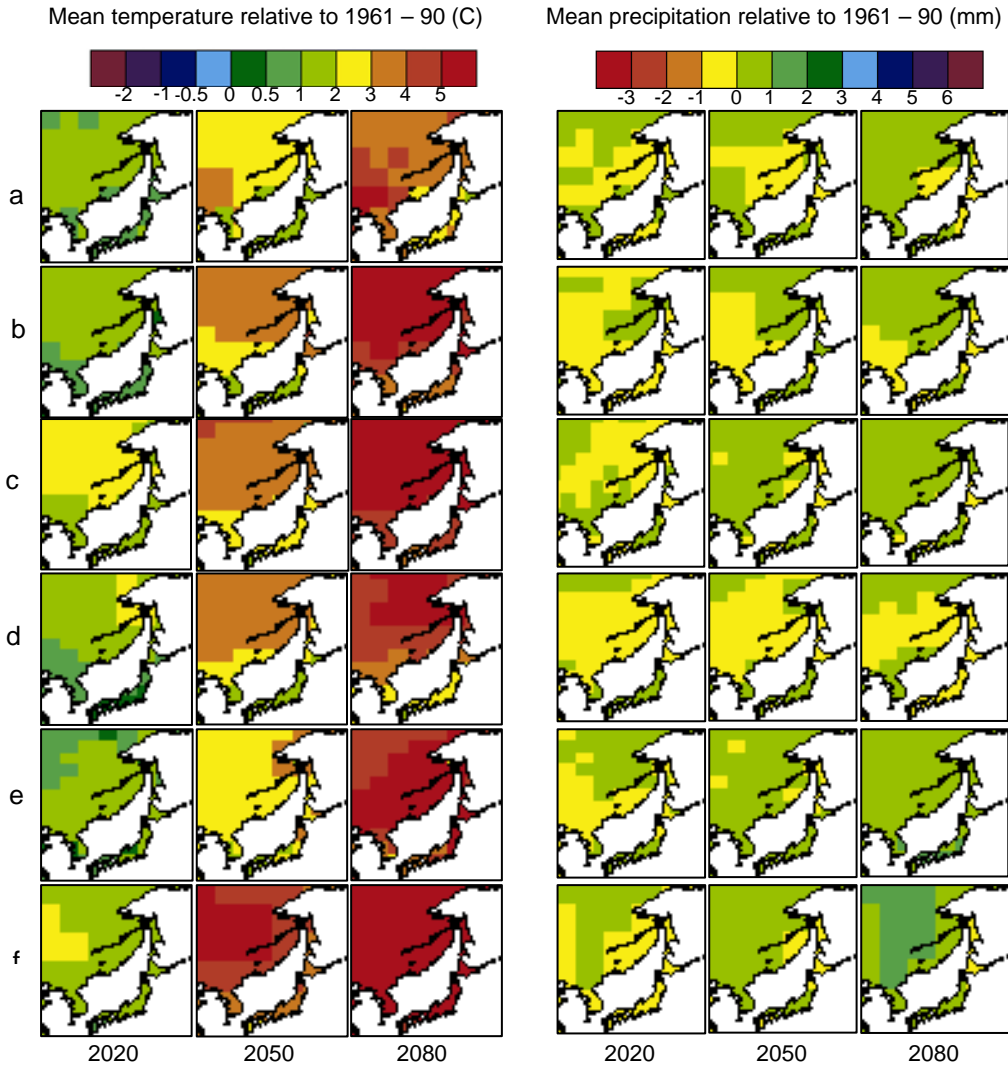
Figure 5-1. General climatic trends and spatial patterns for temperature and precipitation over the RFE in the 21st century relative to 1961 – 1990 produced by major General Circulation Models: a) CCCma, b) CSIRO, c) ECHAM4, d) GDFL99, e) HadCM3, and f) NIES99.

pressure, and precipitation for 7 different climate change scenarios are available from the World Climate Research Programme's (WCRP) Coupled Model Intercomparison Project (CMIP3) Multi-Model Database archive at Program for Climate Model

Diagnosis and Intercomparison (PCMDI) (<www-pcmdi.llnl.gov>). The higher

spatial resolution of the ECHAM5 is important considering the relatively small size

of the region (~300,000 km^2) as compared to GCM cell size (~8,000 km^2).

5.2.3. Climate Change Scenario Selection

The design of this project required the evaluation of scenarios that overlap

with the existing data record and cover a broad range of potential future

developments. Data overlap is provided by the climate of the 20th Century

experiment (20C3M) where daily ECHAM5 modeled outputs are available for 1961 –

2000. The SRES A2 and B1 experiments represent the best and worst potential future

conditions, respectively (Meehl, 2007). Their selection met the requirement for

covering a broad range of potential developments. Both SRES A2 and B1 initialize

with conditions from the end of the 20C3M experiment and run at least through 2100.

The A2 and B1 storylines of the SRES experiments present opposites for the

emissions associated with two sets of divergent tendencies between economic -

environmental values on the Y axis and globalization – regionalization values on the

X axis (Nakicenovic et al., 2000). The A2 scenario is based on highly fragmented

and regionally oriented economic growth and continuously increasing population.

Inclusion of this scenario is of particular importance in the RFE because this area is

close to South and South-East Asia which are the most rapidly growing regions in

terms of their economies and populations.

The B1 emissions scenario is based on a projected stabilization of the world's

population by the middle of the 21st century with a subsequent decline by the end of

the 21st century. In addition, this story line includes conversion of the economic

117

structure to a service and information oriented economy and development of clean

and efficient technologies. The B1 story line presents the greatest reduction in

pressure from population growth accompanied by very high rates of economic

development. In summary, the A2 – B1 range presents a reasonable estimate of the

wide range of uncertainly associated with the potential future climate change in the

RFE.

5.2.4. Conversion of GCM Outputs for Fire Danger Modeling

Daily outputs for maximum daily surface air temperature, specific humidity,

precipitation flux, and air pressure at sea level from the ECHAM5 model were

acquired from WCRP CMIP3 Multi-Model Database. Air temperature and specific

humidity were collected at 1000hPa range to develop gridded products for potential

air temperature and dew point temperature. Specific humidity (kg/kg) was converted

to vapor pressure following the equation of Gill (1982):

$$q = (0.622*e) / (p - 0.378 * e) \qquad (5.1)$$

where q is specific humidity (kg/kg), e is vapor pressure in Pa, and p is air pressure

(=1000hPa). Vapor pressure was subsequently converted to dew point temperature

using (<www.srh.noaa.gov/elp/wxcalc/formulas/vaporPressure.html>):

$$e = 6.11*10^{(7.5*Td/(237.3+Td))} \qquad (5.2)$$

where e is vapor pressure in hPa and Td is dew point temperature in °C .

Maximum air temperature and the resultant dew point temperature were

converted to K. Precipitation flux (kg/m^{2}s) was converted to mm/day multiplying the

flux by 8.64 * 10^4 (Roads et al., 2002). The resultant grids including temperatures,

precipitation, and sea level pressure were regridded to 1km resolution consistent with

the fire danger model resolution and then processed by the same algorithms used for converting the interpolated meteorological station data.

5.3. Results

5.3.1. Comparison of Temperature, Humidity, and Precipitation Estimates from Observational and ECHAM5 Modeled Data

Comparison of estimates for weather parameters from observed and modeled data provides a basis for further assessment of uncertainty introduced by those parameters into fire danger estimates. Methodologies for creating gridded datasets from the observed and modeled data at the potential temperature, potential dew point temperature, and precipitation differ. The point observations at the meteorological stations are interpolated creating highly variable potential temperatures or precipitation surfaces, as opposed to highly uniform surfaces created by the ECHAM5 model grid. In addition, point source precipitation interpolation involved setting a probability threshold below which the actual interpolated precipitation values are converted to 0, whereas the modeled dataset inputs the uniformly distributed precipitation over each ECHAM5 model grid cell. Based on these fundamental differences, a strong relationship between estimated temperature, humidity (expressed through dew point temperature), and precipitation from the two datasets is not expected. The focus is rather shifted to evaluation of the magnitude and spatial patterns of differences in order to assess their potential to influence fire danger estimates in the subsequent analysis.

Average regional temperatures estimated from the two datasets differ considerably (Figure 5-2). The amplitude of meteo-stations based estimates is much

119

greater than that of the ECHAM5 driven estimates: the observational data driven outputs show much lower winter and much higher summer temperatures. ECHAM5 driven estimates show a slower increase in temperatures in spring and early summer with a peak in September as opposed to a peak in July-August shown by the stations data driven estimates. Estimates from both sources are close during September, October, and early November but differ strongly during other seasons.
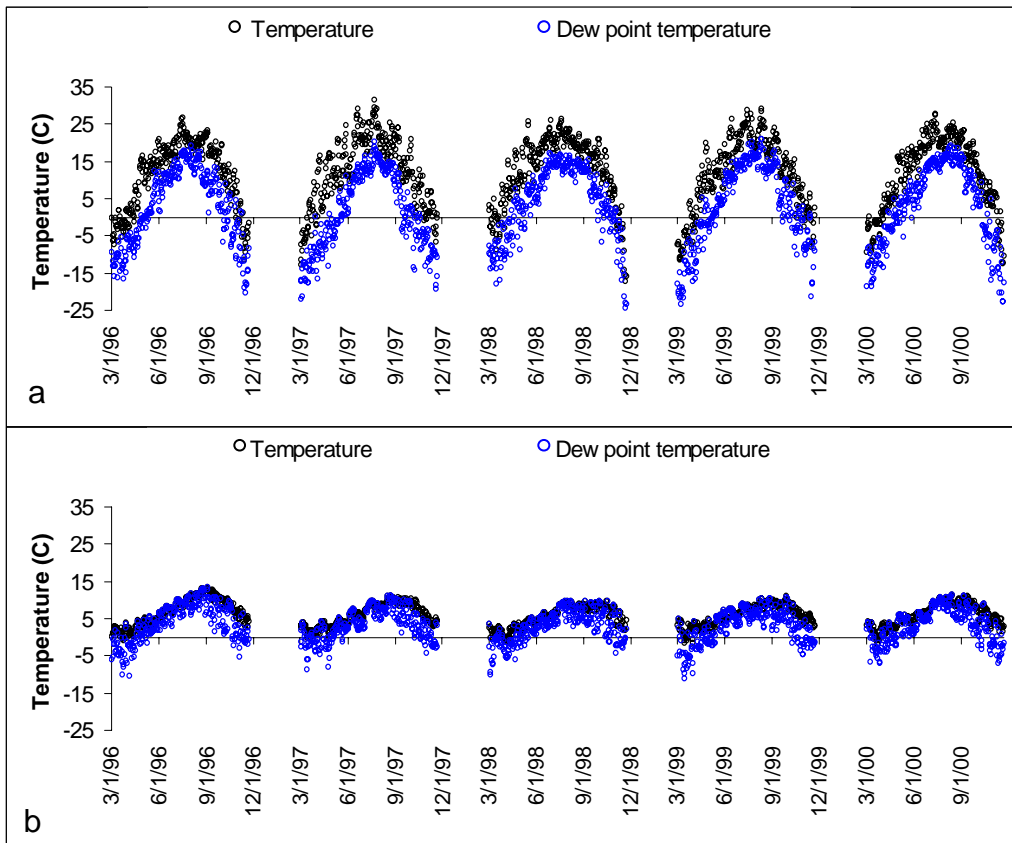
Figure 5-2. Average daily air (black) and dew point (blue) temperature estimates from: a) interpolated point source data using meteorological observations, and b) gridded ECHAM5 modeled data during 1996 – 2000.

Similarly to the estimates of air temperature, there is a large discrepancy between the observational and modeled estimates of humidity. Most noticeably, ECHAM5 driven humidity estimates are much higher leading to dew point temperatures being very close to the air temperatures. Figure 5-2 b shows that the range between ECHAM5 modeled air temperatures and dew point temperatures is particularly narrow during summer months which is consistent with the expected climatology of the region which is dominated by a summer monsoon. However, it differs from the observed values indicative of an overestimation of the Pacific Ocean influence on the RFE in the ECHAM5 parameterization.

The magnitude of the difference between air temperature estimates and dew point estimates is of great importance for fire danger modeling. Fire weather within the fire danger model is assessed using the modified version of the Nesterov Fire Index (NFI_{mod}) (described in chapter 4). In this index, both the absolute measure of air temperature and the difference between the estimates of air temperature and dew point directly influence the magnitude of the NFI_{mod}.

The NFI_{mod} reduces the importance of the actual amount of precipitation. Instead it emphasizes the importance of the frequency of occurrence of precipitation of 3 mm and greater. The analysis shows that the relationship between the observed and modeled amounts of precipitation in the RFE is weak ($R^2 = 0.41$, slope $= 0.23$). The comparison of the monthly mean frequency of precipitation of 3 mm and greater indicates that the discrepancy between observed and modeled estimates is greater during spring and fall than during summer (Figure 5-3).
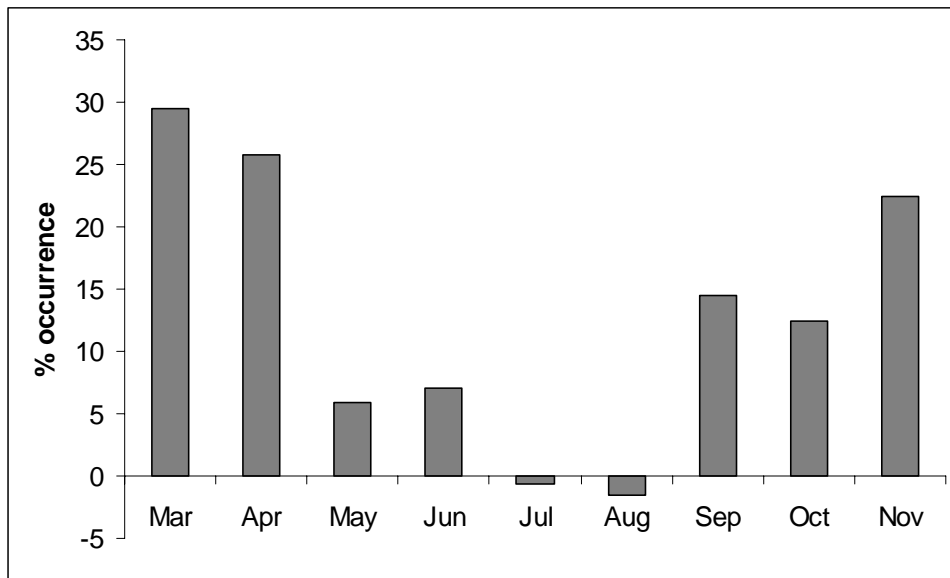
Figure 5-3. Mean monthly difference in occurrence of precipitation of 3 mm and greater according to the ECHAM5 driven estimates compared to the interpolated station observations in 1996-2000.

Spatial patterns of differences in air temperature, dew point temperature, and precipitation are shown in Figure 5-4. No specific pattern in the differences between observed and modeled estimates of precipitation (analyzed as the frequency of precipitation occurrence of 3mm and greater) was found (Figure 5-4 a). Air temperatures interpolated from point source measurements show considerably higher values over the central part of the study area as compared to the ECHAM5 driven estimates (Figure 5-4 b). Dew point temperature estimates from observed data are generally lower than those driven by the ECHAM5, with the exception of the northern part of the study area where they are slightly higher (Figure 5-4 c). Overall the dew point temperature estimates from both sources are closer than the air temperature estimates.
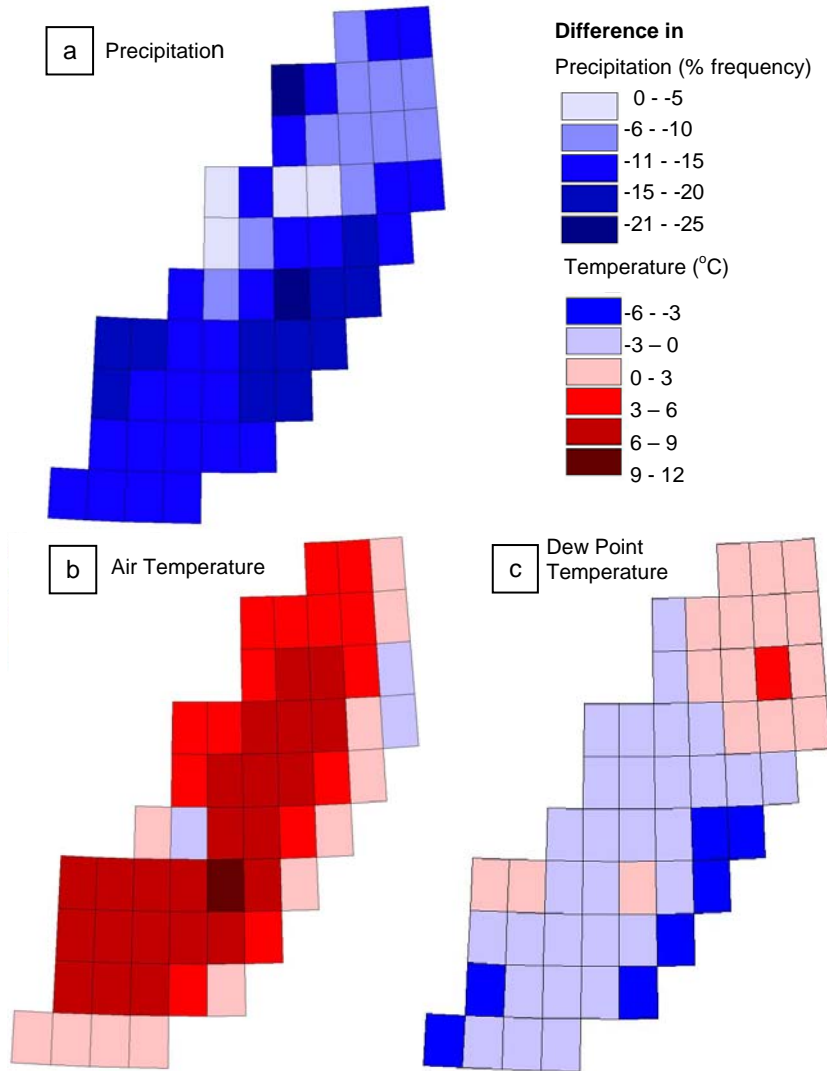
Figure 5-4. Differences in mean year ECHAM5 driven estimates compared to mean
yearly meteorological station measurements driven estimates within 1 degree cells
for: a) precipitation (% frequency), b) air temperature (°C), and c) dew point
temperature(°C). The difference was calculated by subtracting the mean yearly
ECHAM5 estimated parameter within the 1 degree grid from the mean yearly stations
derived estimates.

The large differences between GCM and observational data driven estimates of temperature, dew point temperature, and precipitation are likely to impact fire danger estimates considerably. This analysis shows that by itself fire weather assessed from GCM data is not strongly representative of observed conditions. Therefore, evaluating changes in fire danger throughout the 21st century based on meteorological parameters alone is unlikely to produce a realistic projection. However, coupling GCM based fire weather with risk of ignition and potential fire behavior within a fire danger model is likely to improve the forecast due to contributions from other spatially explicit sources and the fuzzy logic driven decision process. The evaluation of this hypothesis is presented in the next section.

5.3.2. Comparison between Fire Danger Estimates from Observed and Modeled Weather Parameters

The comparison between fire danger estimates from observed and modeled meteorological data was undertaken to evaluate the potential for using GCM modeled data at very coarse resolution for a relatively small region. Because other components of the fire danger model were not adjusted to the pre-2000 period, the estimates of fire danger in the region from either observed or modeled data do not have a truly predictive capability for 1996-2000. In particular, the information on fuel composition and previous disturbances which drive in part the evaluation of potential fire behavior was developed based on data acquired during 2000 – 2005 and does not reflect the state of vegetation during the pre-2000 period. Therefore fire danger modeling results for 1996-2000 should not be viewed as reflecting the actual fire danger in the region during this time-frame.

Fire danger estimates from observational and modeled meteorological information provide comparable results (Figure 5-5 a and b). Both datasets provide a similar view of inter- and intra-annual variability in fire danger in the RFE. Average daily fire danger estimates, ranging between 0 (no danger) and 1 (extreme danger), from both datasets cover a similar range of values with an average yearly standard deviation of ~0.09 for both the observed and modeled weather parameters. However,
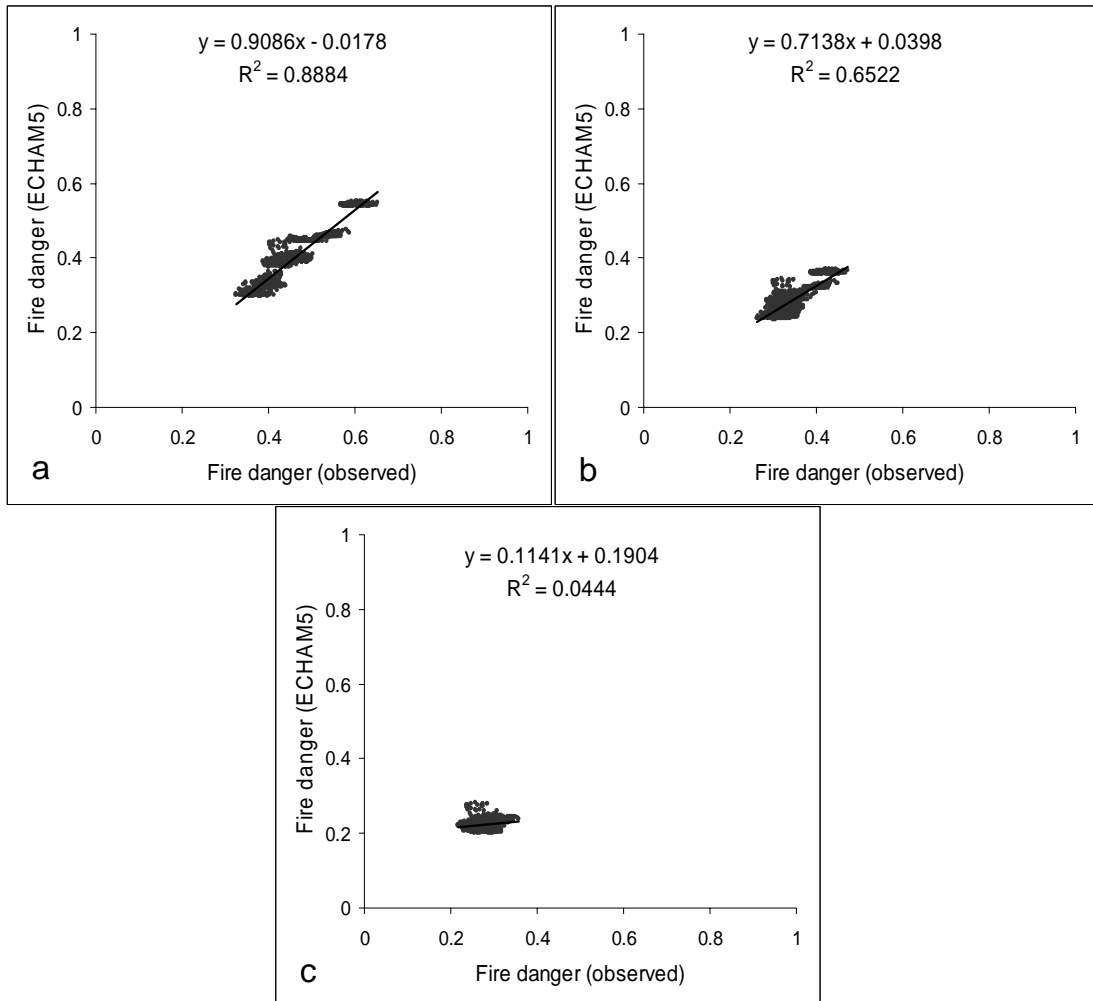
Figure 5-5. Direct comparison of average daily estimates of fire danger during 1996 – 2000 for 3 model scenarios: a) "worst case", b) "trade off", c) "best case".

the ECHAM5 modeled weather observations tend to lower the projected fire danger rate over the entire region, with an average mean for the 3 potential scenarios of ~ 0.36 for the meteorological station driven fire danger estimates as compared to ~ 0.30 for the ECHAM5 modeled data driven estimates.

The direct comparison of individual scenarios of fire danger from the two data sources shows that the estimates for the "worst case" scenario, that reflect the upper limit of uncertainty, are very closely matched (slope ~0.91, R^2 ~ 0.89) (Figure 5-5 a). However, this close relationship deteriorates in the comparison of "trade off" scenarios (slope ~0.71, R^2 ~ 0.66) and dissipates completely for the "best case" scenario (slope ~0.11, R^2 ~ 0.04) (Figure 5-5 b and c). The diminishing slopes of the relationships also show that the ECHAM5 driven estimates tend to underestimate fire danger (consistent with previous findings). These relationships, derived from the 1996 – 2000 record, remain relatively unchanged during each of these years analyzed individually, thus providing a consistent view of meteorological conditions from which a reliable bias in fire danger assessment can be estimated.

A strong relationship of the "worst case" scenario assessment of fire danger in the RFE in combination with a lack of a relationship for the "best case" scenario indicates that weather conditions incorporated through the fire weather assessment play a different role within each of the fire danger scenarios. The deterioration of the relationship is expected with increasing contribution from the fire weather component of the fire danger model along the "worst case" – "trade off" – "best case" scenario continuum. Although the fire danger value presents a sum of equally weighted risk of ignition, potential fire behavior, and fire weather values, the input values for the risk

126

of ignition and potential fire behavior differ for the three output scenarios. The

"worst case" scenario contains higher values for the risk of ignition and potential fire

behavior than the "trade off" scenario. The values for the risk of ignition and

potential fire behavior within the "trade off" scenario are in turn higher than those

within the "best case" scenario. Considering that the fire weather value is the same

within all three scenarios, its contribution to the total fire danger value changes in

relation to the magnitude of other input parameters (risk of ignition and potential fire

behavior). For example in a hypothetical case of the risk of ignition value of 10,

potential fire behavior value of 7, and fire weather value of 5, the fire weather value

contributes ~23% of the total fire danger value. If the hypothetical risk of ignition

value is 3, potential fire behavior value is 3, and the fire weather value is still 5, the

total contribution of the fire weather value is ~45%.

The results in figure 5-5 b and c show that with a weakening relationship in

the "trade off" and "best case" scenarios, the range of predicted fire danger values

narrows. Consequently, even with weak relationships, the predicted fire danger

values are still found within the same general range of fire danger.

Fire danger estimates, ranging between 0 and 1, were further binned to ten

qualitative levels: 1) none $\leq$ 0.1, 2) very low (VL) 0.1-0.2, 3) low ("L") 0.2-0.3, 4)

moderate low (ML) 0.3-0.4, 5) moderate (M) 0.4-0.5, 6) moderate high (MH) 0.5-0.6,

7) high (H) 0.6-0.7, 8) very high (VH) 0.7-0.8, 9) severe (S) 0.8-0.9, 10) catastrophic

(C) > 0.9. Monthly frequencies of binned fire danger values also show a good

correspondence between the station and model driven datasets (Figure 5-6).

Consistent with the previous findings, while retaining a close resemblance in inter-

and intra-annual patterns of fire danger, ECHAM5 driven fire danger values are lower that those driven by observed values for all three scenarios.
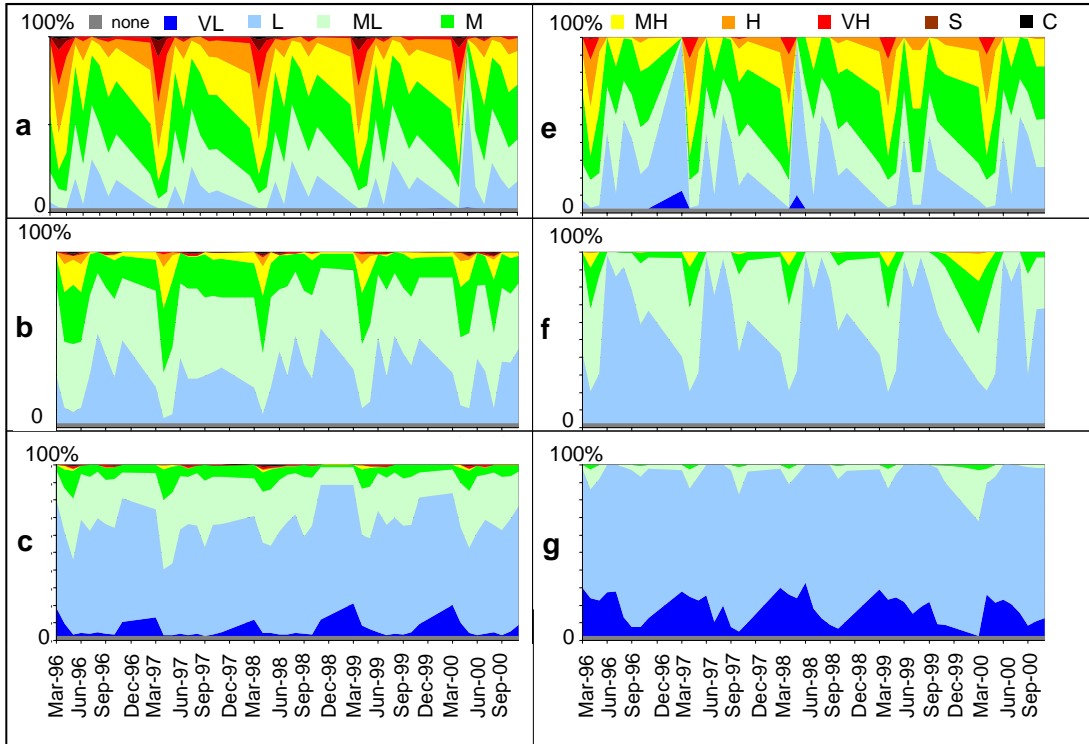
Figure 5-6. Monthly frequencies of fire danger values from observed and modeled weather parameters for three scenarios: a) "worst case" - observed, b) "trade off" - observed, c) "best case" – observed, d) "worst case" - modeled, e) "trade off" – modeled, f) "best case" - modeled.Fire danger values ranging from 0 to 1 were binned to 10 qualitative values: 1) none ≤ 0.1, 2) very low (VL) 0.1-0.2, 3) low ("L") 0.2-0.3, 4) moderate low (ML) 0.3-0.4, 5) moderate (M) 0.4-0.5, 6) moderate high (MH) 0.5-0.6, 7) high (H) 0.6-0.7, 8) very high (VH) 0.7-0.8, 9) severe (S) 0.8-0.9, 10) catastrophic (C) >0.9.

On average during 1996 – 2000 the modeled weather parameter driven estimates of fire danger were 13%, 17%, and 21% lower for "worst case", "trade off" and "best case" scenarios, respectively, compared to the fire danger estimates driven by observational data. Figure 5-7 shows that greater difference (up to 18, 23, and 26 % for "worst case", "trade off", and "best case" respectively in June) is found during warm months (May - September), and the difference is less pronounced during colder periods (as little as 7, 9, and 11% for "worst case", "trade off", and "best case" respectively in November).
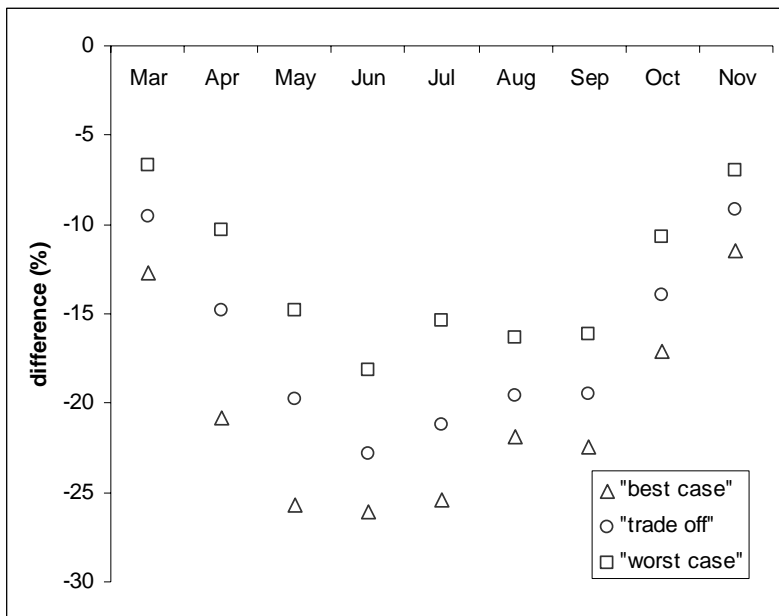
Figure 5-7. Differences in the monthly mean modeled data driven estimates of fire danger in the RFE, compared to observational data driven values in percent.

Geographic accuracy of fire danger estimates was evaluated using mean daily, monthly, and yearly estimates of fire danger within 1 x 1 degree cells. The previous

analysis has shown little inter-annual variation in the relationships between modeled

and observational data driven mean yearly values and monthly frequencies of fire

danger estimates during 1996 - 2000.The analysis shows that the relationships of the

daily mean 1 degree estimates vary within the region and among the three scenarios

(Figure 5-8). Consistent with the previous findings, the "worst case" scenario outputs

have the strongest relationship (mean R^2 ~0.72, mean slope ~0.75) which weakens

substantially in the "trade off" scenario (mean R^2 ~0.41, mean slope ~0.45), and

becomes non-existent in the "best case" scenario (mean R^2 ~0.1, mean slope ~0.14).
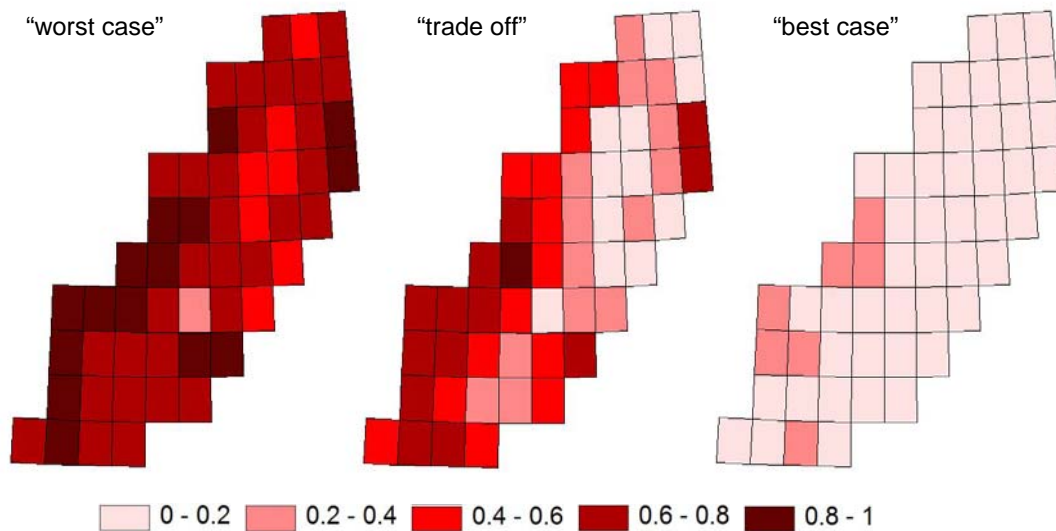
Figure 5-8. The strength of relationships between the modeled and observational data

driven daily mean 1 degree estimates of fire danger in the RFE expressed through R^2

values.

In general, the relationships are found to be stronger on the edges of the study area rather than in the central parts. But the patterns for the three scenarios are explained by different drivers. The strong relationships ($R^2 > 0.8$) of the "worst case" scenario match the patterns of population distribution in the RFE. Population distribution in this region is highly uneven with a large concentration of towns, and transportation routes in the western and eastern part of the study area leaving the central part very sparsely populated (see chapter 2). Subsequently, fire danger for the western and eastern edges of the study area often experiences stronger influences of anthropogenic presence, expressed through the risk of ignition, land use, and previous disturbances rather than weather conditions. In contrast, the comparatively stronger relationships of the "best case" scenario are driven by smaller differences in precipitation and temperature estimates within those 1 degree cells (Figure 5-4).

While daily mean 1 degree estimates show little consistency for the two of the three scenarios, yearly and monthly means within 1 degree cells show more stability. All three scenarios have a similar pattern of mean yearly difference (%) from the observational data driven estimates with the mean 12, 16, and 20% and the standard deviation from the mean of 4, 5, and 6% for the "worst case", "trade off", and "best case" scenario respectively. Monthly mean estimates within 1 degree cells show more variability with the mean standard deviations over the March – November period of 6, 7, and 8 % for the "worst case", "trade off", and "best case" scenario respectively.

In summary, fire danger estimates driven by the ECHAM5 modeled weather parameters give a consistent and representative assessment of fire danger in the RFE.

These estimates capture inter- and intra-annual patterns of fire danger change well. The modeled data driven fire danger assessment provides a close approximation for the upper range of potential fire danger values but underestimates mean and particularly lower range values. Modeled data driven estimates also represent the geographic distribution of fire danger values reasonably well particularly at monthly and yearly mean levels. Therefore, overall ECHAM5 data driven estimates of fire danger are considered suitable for exploring future changes in fire danger in the RFE under the projected scenarios of climate change.

5.3.3. Estimates of Changes in Fire Danger during the 21st Century Using A2 and B1 Climate Change Scenarios

Mean fire danger (averaged over the entire study area in 5-year periods – 1996-2000, 2046-2050, and 2096-2100) is projected to increase by less than 1% by the middle of the 21st century and by 5.2% (A2 scenario) or 2.5% (B1 scenario) by the end of the 21st century. The increase of the lower "best case" scenario is projected to be slightly higher (6.7% and 3.3% for A2 and B1 scenarios by the end of the 21st century, respectively). At the same time the upper "worst case" scenario range will increase at a lower rate (3.7% and 1.8% for the A2 and B1 scenarios by the end of the 21st century, respectively) effectively narrowing the range of uncertainty in fire danger estimates by 3% and 1.5% for the A2 and B1 scenarios, respectively. According to the results, fire danger will follow the same inter- and intra-annual pattern as was observed at the end of the 20th century (Figure 5-9).

Fire danger values will rise over the 21st century throughout the year with the most noticeable increases projected to occur by the end of the 21st century in August,

132

September, and October (13%, 10%, and 8% respectively) according to the A2

scenario (Figure 5-10). The range of potential danger values ("worst case" to "best

case") remains constant throughout the 21st century and resembles closely that of the

end of the 20th century.
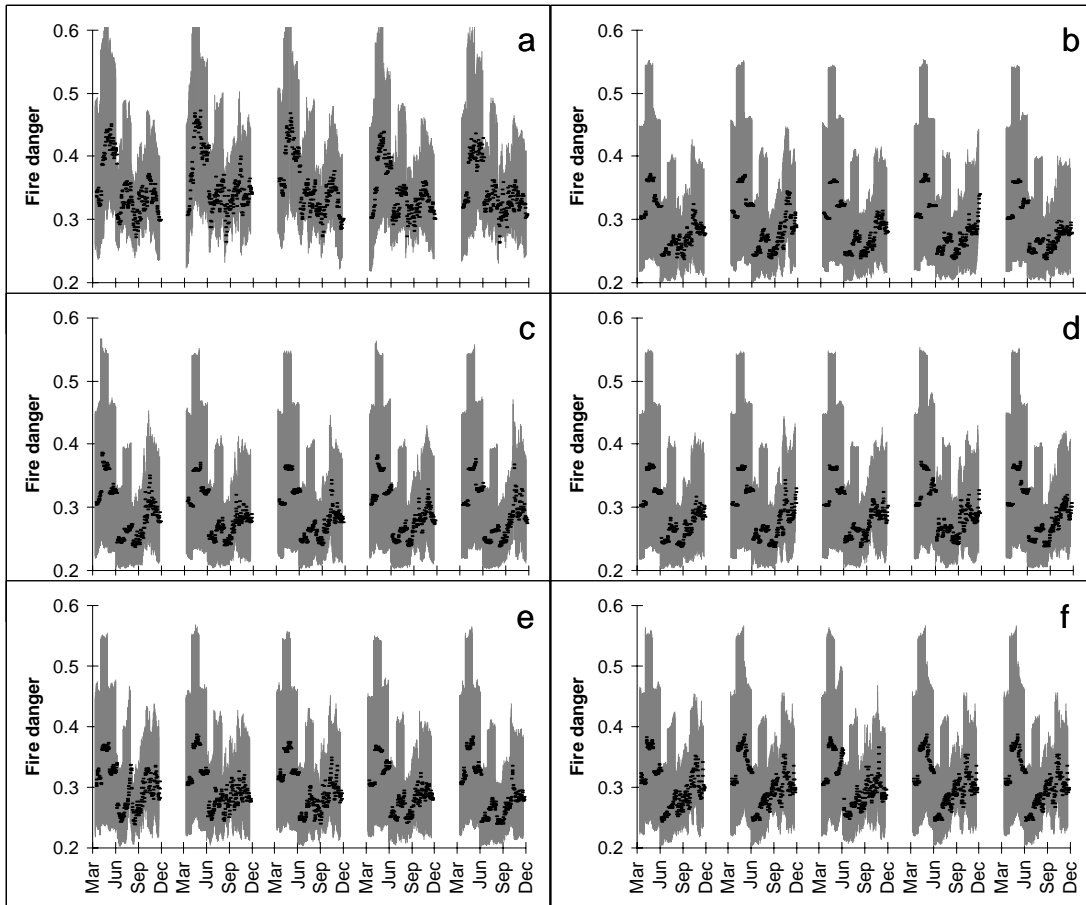
Figure 5-9. Fire danger patterns over 5 year periods: a) 1996-2000 – observed

meteorological data, b) 1996-2000 – 20c3m scenario, c) 2046-2050 – B1 scenario, d)

2046-2050 – A2 scenario, e) 2096-2100 – B1 scenario, f) 2096-2100 – A2 scenario.

Mean values are shown as dots and uncertainty range is shown in grey.
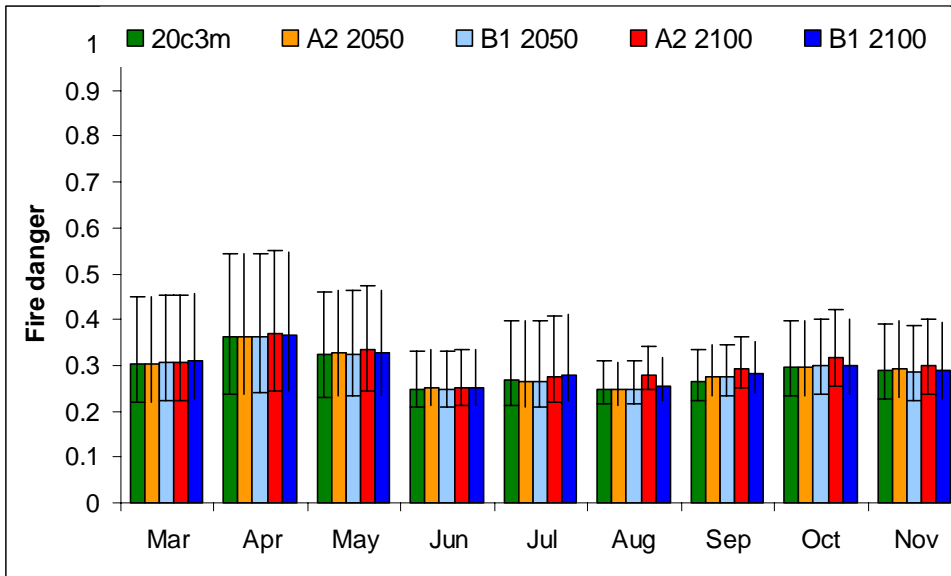
Figure 5-10. Monthly increases in mean fire danger (averaged over 5 year periods 1996-2000, 2046-2050, 2096-2100) in the 21st century over the RFE projected by A2 and B1 scenarios compared to the 20c3m estimates.

Frequency of monthly and yearly mean values binned into ten fire danger categories, ranging from "none" to "catastrophic" (described in section 5.3.2), also shows negligible change in fire danger by 2050 (A2 and B1 scenarios) and a noticeable increase in frequency of occurrence of higher fire danger conditions (relative to "worst case", "trade off", and "best case" scenarios) in March, April, May, August, September, and October (A2 scenario) (Figure 5-11). No marked increase in the frequency of high fire danger conditions was noted for the B1 scenario.
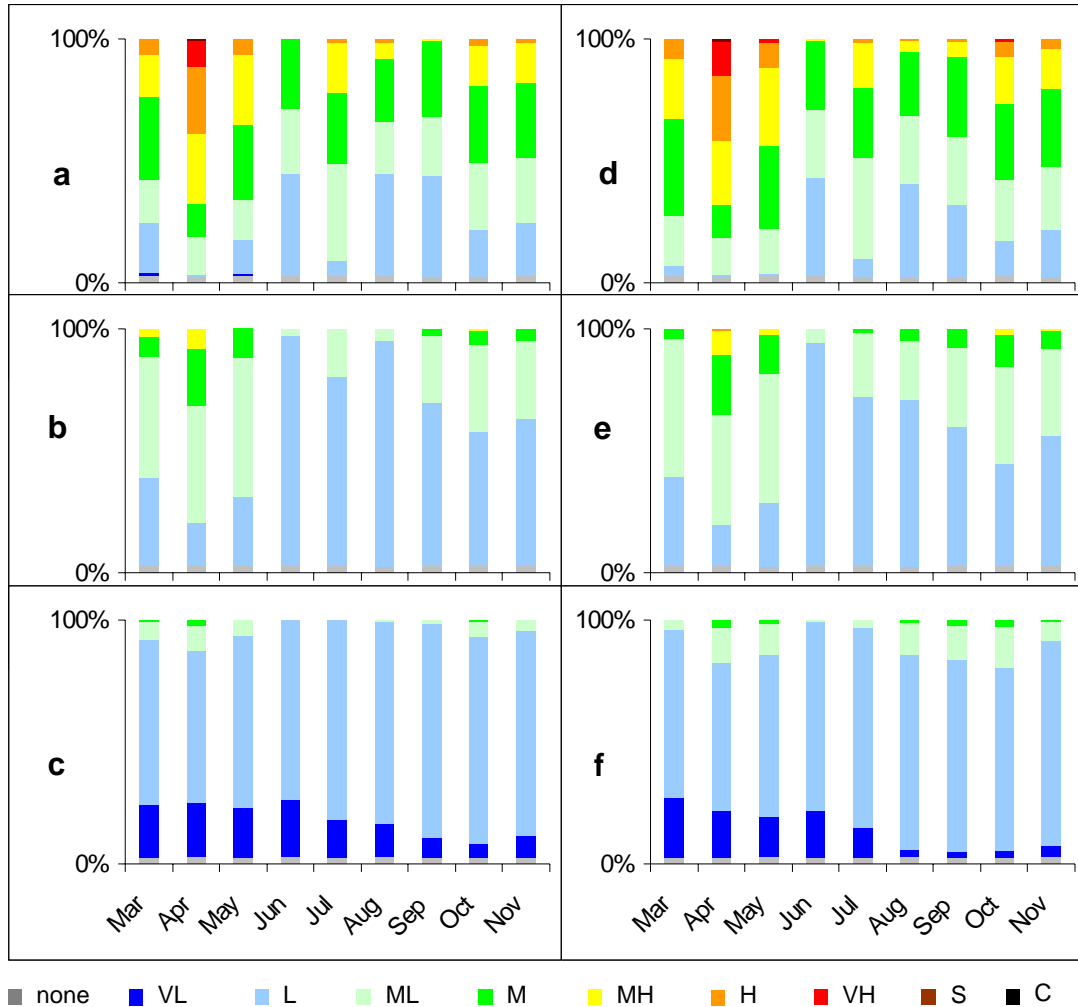
Figure 5-11. Increase in frequency of higher fire danger occurrence projected by the A2 scenario by the end of the 21st century: a) "worst case" – 20c3m scenario, b) "trade off" – 20c3m scenario, c) "best case"– 20c3m scenario, d) "worst case" – A2 scenario, e) "trade off" – A2 scenario, f) "best case" – A2 scenario. Fire danger values are binned into 10 equal-size qualitative bins: 1) none ≤ 0.1, 2) very low (VL) 0.1-0.2, 3) low ("L") 0.2-0.3, 4) moderate low (ML) 0.3-0.4, 5) moderate (M) 0.4-0.5, 6) moderate high (MH) 0.5-0.6, 7) high (H) 0.6-0.7, 8) very high (VH) 0.7-0.8, 9) severe (S) 0.8-0.9, 10) catastrophic (C) >0.9.

The spatial pattern of fire danger change in the RFE under A2 and B1 climate change scenarios show pronounced differences (Figure 5-12). By the mid 21st century, spatial patterns of fire danger increase are similar for both A2 and B1 scenarios of climate change. A slight (1-5% mean annual value) increase in fire danger is observed over the southern third of the region while no significant change is expected in the northern and central parts. However, by the end of the 21st century the impact of climate change under the A2 scenario is observed over the entire region with a particularly noticeable increase (up to 15% mean annual value) in the southern part of the region.

The 10-15% mean yearly increase is distributed unevenly throughout the year. The 1 degree cells in the southern part of the region show 20-38% increase in mean monthly fire danger during July or August and 10 – 20% increase in May, September, and October. Even the 38% increase during August within a 1 degree cell raises the total monthly mean fire danger level from "low" to only "moderate low". However, the change in the frequency of occurrence of various levels of fire danger changes dramatically. Frequencies of fire danger values, calculated by 10 bins, were described previously in this paper. Within the 1 degree grid these frequencies showed the largest (38%) increase in monthly (August) mean fire danger. At the end of the 20th century 96% and 4% of August fire danger values in that cell were within "low" and "moderate low" fire danger bins, respectively. By the end of the 21st century under the A2 scenario only 34% of August fire danger values remained in the "low" bin while 42% were in the "moderate low" and 23% moved to the "moderate" fire danger bins. A small number of grid cells (0.2%) were within "moderate high" fire

danger with the values forecasted for 2097, 2099, and 2100. No fire danger values

above "moderate low" were recorded during 1996-2000 within this cell.
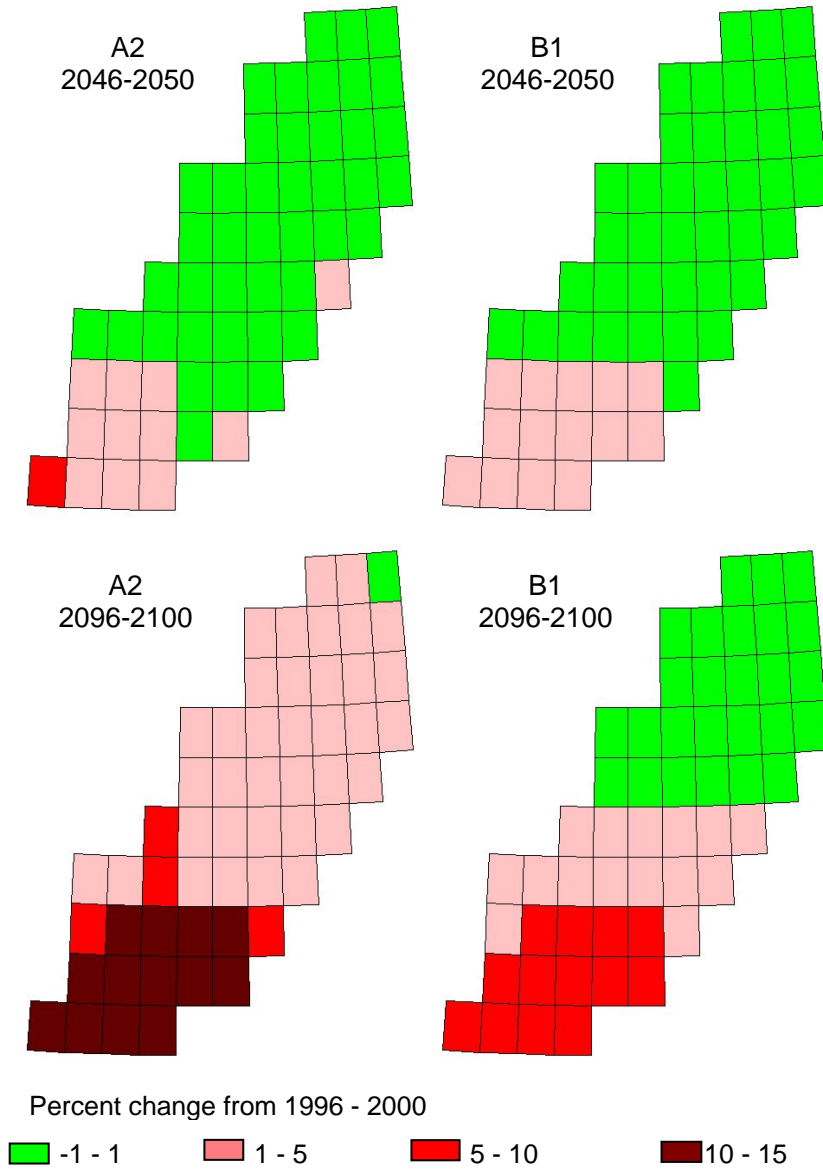
Figure 5-12. Change in mean yearly fire danger by 1 degree cells as percent from

1996 values for 2050 and 2100 using A2 and B1 scenarios.

A noticeable (5-10% mean annual value) increase in fire danger over the southern part of the study area is expected even under the B1 scenario. A smaller increase is expected over the central part and no increase is likely to be observed in the northern part of the study area.

5.4. Discussion

This analysis evaluates climate driven change in fire danger through climate change impact on fire weather and its subsequent contribution to the overall fire danger. Fire weather is the only variable parameter in this assessment. While other components of the fire danger model including the risk of ignition and potential fire behavior are also likely to be affected by climate change, evaluation of compound effects of climate change on fire danger is outside the scope of this current work. The study rather focuses on isolating the climate change impact on weather conditions conducive to fire occurrence.

The climate of the RFE separates this area from other boreal and temperate forests of Northern Eurasia. The bulk of the large (500 – 1500 mm/year) amount of precipitation arrives during the warmest time of year (June-August) thus considerably lowering fire danger in the RFE during these months. Wet summers and moderately warm spring and fall periods result in the overall moderately-low fire weather characteristic for the RFE. It is likely that the region's proximity to the Pacific Ocean will mitigate against sharp increases in fire danger projected for other areas of Siberia (Stocks et al., 1998). Our study shows that even under the worst case scenario of climate change (A2), the overall increase in fire danger in the RFE will not be considerable. These findings are consistent with the results by Malevsky-Malevich et

al. (2008). Even the maximum projected 5 percent total regional increase by the end of the 21st century will still keep the mean regional fire danger within "low" and "moderate low" range, with the highest level of uncertainly just marginally entering into the "moderate" fire danger zone. The rate of change is likely to be slow. Our estimates show that in the next 50 years fire danger will increase by less than 1% under both A2 and B1 scenarios. According to our finding, the most aggressive A2 and the most favorable B1 scenarios project comparable rates of change in fire danger in the RFE by 2050. The outcomes of the two scenarios are nearly identical for the mid 21st century and show little difference (~4%) in mean yearly estimates by the end of the 21st century.

Change in fire danger under B1 scenario is negligible. Under this scenario fire danger in the RFE will be the same as fire danger at the mid 21st century ±1% for the majority of the areas. Fire danger levels will rise slightly in the southern part of the region by the end of the 21st century. However, even with the 5-10% increase in the southern part (compared to the end of the 20th century) fire danger will stay within "low" and "moderately low" categories.

Under the A2 scenario, climate change will drive fire danger higher. Similarly under the B1 scenario, the initial rate of fire danger increase will be slow. However, the rate will increase from the mid 21st century resulting in the noticeably more frequent occurrence of "high" – "severe" fire danger conditions, particularly in the late summer and fall. According to the projected scenarios, the fire season is likely to become more active beginning in August and going through October. Late season fire danger increase has a potential to increase the amount of burned area, burn

intensity, and burn severity due to higher fuel accumulation at the end of the growth season and the compound effects of longer period of higher fire danger levels. At the end of the 20th century, the period of "low" fire danger lasted from June through September. Climate projections show that this period will shorten to only two months, June and July, allowing the fuels to dry out considerably more by the expected increase in fire activity in October and November. October is already projected to experience the largest increase in fire danger within a year; however, this increase is driven only by the changes in daily weather conditions and does not take into account the compound changes in the state of fuels which results from an increase in fire danger during the two preceding months. The compound effects are likely to increase fire danger further pushing it beyond the projected 8% increase compared to the 1996-2000 values.

Fire danger increase by the end of the 21st century will not be uniformly distributed across the region. The study shows that the yearly mean fire danger increase over the southern part of the region could be considerably larger than the elsewhere. In this area, monthly mean fire danger values in July or August may rise as high as 37% in some of the 1 degree cells. While fire occurrence during summer months is rather uncharacteristic for the area, it often leads to large severe fires like those that occurred in July of 2003 (see chapter 4). A nearly 40% increase in fire danger during July and August at the end of the 21st century may be indicative of similar conditions developing over 24% of the study area, that would subsequently lead to potentially catastrophic fires in the RFE. Fire danger in the northern part of the study area will experience little change under both A2 and B1 scenarios.

Overall, this study has shown that climate driven change in fire weather is unlikely to result in considerable increase in fire danger at the regional scale for the RFE even under the worst scenario of climate change (A2). Fire danger under the B1 scenario will be similar to the conditions at the end of the 20th century. Under the A2 scenario, fire danger will increase more substantially by the end of the 21st century. The range of increase will vary within the region is more likely to affect fire danger during July - October.

5.5.   *Conclusions*

The results show that in the RFE GCM driven fire danger estimates are lower than those driven by observational data interpolated from point source weather parameters. However, the estimates are consistent at yearly and monthly temporal resolutions for the entire region and its individual parts assessed using a 1 degree grid. In addition, while mean GCM driven fire danger levels are noticeably lower, the range of uncertainty is close to observational data driven estimates. Overall, ECHAM5 provides sufficient inputs for producing estimates of fire danger in the RFE comparable to those from observational meteorological data.

The projected mean yearly changes in climate driven fire danger during in the 21st century in the RFE are small. Changes in mean yearly and mean monthly fire danger under B1 scenario are negligible. Under A2 scenario fire danger change during the first part of the 21st century is close to that projected under B1 scenario but increases more sharply by the end of the 21st century. The magnitude of the increase varies spatially and temporally. The greatest increase in fire danger is projected to occur in the southern part of the RFE where monthly mean fire danger estimate for

individual cells can be up to nearly 40% higher in a single month compared to the values observed at the end of the 20th century. July, August, and October are likely to experience the largest increase in fire danger by the end of the 21st century in individual 1 degree cells under A2 scenario.

This study evaluates potential changes in fire danger driven only by climate induced changes in fire weather and assumes stationary vegetation, population, economic development, and land use. Each of these multiple stressors has a potential to change the fire regime. Therefore, further development of coupled models, with a capability to account for direct contribution from each of these components as well as feedbacks from their interactions, is necessary to develop a suite of realistic future scenarios of change in fire danger. The model's predictive capability in the RFE could also be furthered by improved understanding of the monsoon and the resiliency of this meso scale climate system to emissions induced change.

In summary, this chapter establishes the feasibility of regional fire danger modeling and subsequently regional fire threat modeling based on very coarse resolution GCM inputs. It offers a proof of concept to start considering the long term viability of endangered species under a changing climate. The considerable fire danger increase over the southern portion of the study area under the A2 scenario raises concerns regarding the potential impact on the Amur tiger meta-population because it affects a large portion of the known tiger range. The results also indicate that further modeling fire threat to the Amur tiger can be narrowed down to only one scenario of climate change (A2) since fire danger change is not likely to increase significantly under the B1 scenario.

Chapter 6: Estimating Wildland Fire Threat to the Amur Tiger and Its Habitat: Current Levels and Future Scenarios under the Influence of Climate Change

The focus of the research, described in this chapter, is aimed at completing parameterization of the fire threat model and using its predictive capability to assess the current and future potential wildland fire threat to the Amur tiger and its habitat. Here the resource-oriented modules of the fire threat model (values at risk and rehabilitation potential) are defined in terms of their relevance to the tiger meta-population. The model of fire threat to the Amur tiger is assembled and used to address the major research questions of the doctoral research defined in chapter 1.

6.1.   Introduction

High rates of economic development combined with climate change are pushing the limits of stable ecosystem functioning and threatening global biodiversity (Millennium Ecosystem Assessment, 2005). Recent studies estimate that gradual shifts in species ranges under changing climate may lead to wide spread extinction by the end of the 21st century (Thomas et al., 2004; Sekercioglu et al., in press; Pimm, 2008).   With the projected increase in fire danger over Northern Eurasia (Stocks et al., 1998; Malevsky-Malevich et al., 2008; chapter 5 of this dissertation) the rates of habitat conversion in boreal and temperate ecosystems are likely to be amplified by wildland fire. Sudden and extensive habitat loss from wildland fire can potentially

undermine species conservation efforts aimed at policy ensured protection of habitat and its connectivity.

The forests of the RFE contain large contiguous Amur tiger (*Panthera tigris altaica*) habitat patches up to 183,237 km² (Dinerstein et al., 2007). The remaining tiger meta-population of approximately 500 tigers occupies ~160,000 km² (Miquelle et al. 1999a). Low prey densities found even in best quality habitats in the RFE necessitate ~ 500km^2 home ranges for individual tigers, thus requiring availability of large contiguous sections of habitat to support the minimum viable population – 876 individuals (Reed et al, 2003).

Recent studies have shown that in comparison with other areas of Northern Eurasia, overall mean fire danger is not predicted to increase in the RFE dramatically (Malevsky-Malevich et al., 2008). However, a more detailed assessment of fire danger trends driven by climate change scenarios, described in chapter 5, projects a considerable increase in fire danger under SRES A2 scenario in the southern portion of the region which currently constitutes the bulk of the highest quality Amur tiger habitat.

This chapter describes a spatially explicit and temporally dynamic model of wildland fire threat to the Amur tiger developed within the framework of fire threat assessment presented in chapter 2. The model parameterization incorporates knowledge about regional fire specifics (developed in chapter 4) and expert knowledge of tiger habitat use and post-fire vegetation recovery in the RFE (described in this chapter). First, this chapter details the components, parameterization, data flow, and sensitivity assessment of the full fire threat model.

Second, it describes fire threat to the Amur tiger during the 2005-2007 period based on observed meteorological conditions. Finally, it presents projections of fire threat driven by outputs of the ECHAM5 model over two 5-year periods. ECHAM5 model output from the 20th Century climate experiment (20c3m) scenario are used to develop a base-line of fire threat over the 1996-2000 time frame and to evaluate large scale trends in climate induced fire threat change under A2 SRES scenario by 2096-2100.

6.2.   *Fire Threat Model*

The conceptual framework of fire threat modeling provides the necessary structure to develop an understanding of fire impacts on a specific resource (chapter 2). The emphasis of the modeling effort moves from forecasting the presence, extent, and generic severity of wildland fire (achieved by fire danger modeling) towards modeling the pressure from fire effects on well-being of the resource of interest. The conceptual framework identifies four major contributors to the overall fire threat (FT) – fire danger (FD), values at risk (VAR), Recovery Potential (RP), and Fire Suppression Capabilities (FSC). The FSC component has a negligible contribution in assessing fire threat to the Amur tiger because the majority of the tiger habitat is remote and inaccessible. Therefore, the FSC component was removed from the model. At the conceptual level, VAR and RP components are identified in general and need to be better defined to reflect the sensitivity of the Amur tiger meta-population to fire impacts.

The Amur tiger (*Panthera tigris altaica*) distribution at the regional scale is most closely related to the distribution of its prey and availability of suitable habitat

(Miquelle et al, 1999a).   Therefore, for the Amur tiger the VAR module, renamed

Tiger Risk (TR), evaluates the combined impact of fire threat to the tigers (Direct

Threat subcomponent) and the major prey species (Indirect Threat subcomponent) -

red deer (*Cervus elaphus*), wild boar (*Sus scrofa*), and moose (*Alces alces*) (Miquelle

et al, 1999a) (Figure 6-1). Both tigers and their prey are affected by fire in two ways.

First, the flaming front, heat, and smoke pose a direct threat to less mobile (e.g.

young) individuals leading to their mortality and thus affecting the animals directly.
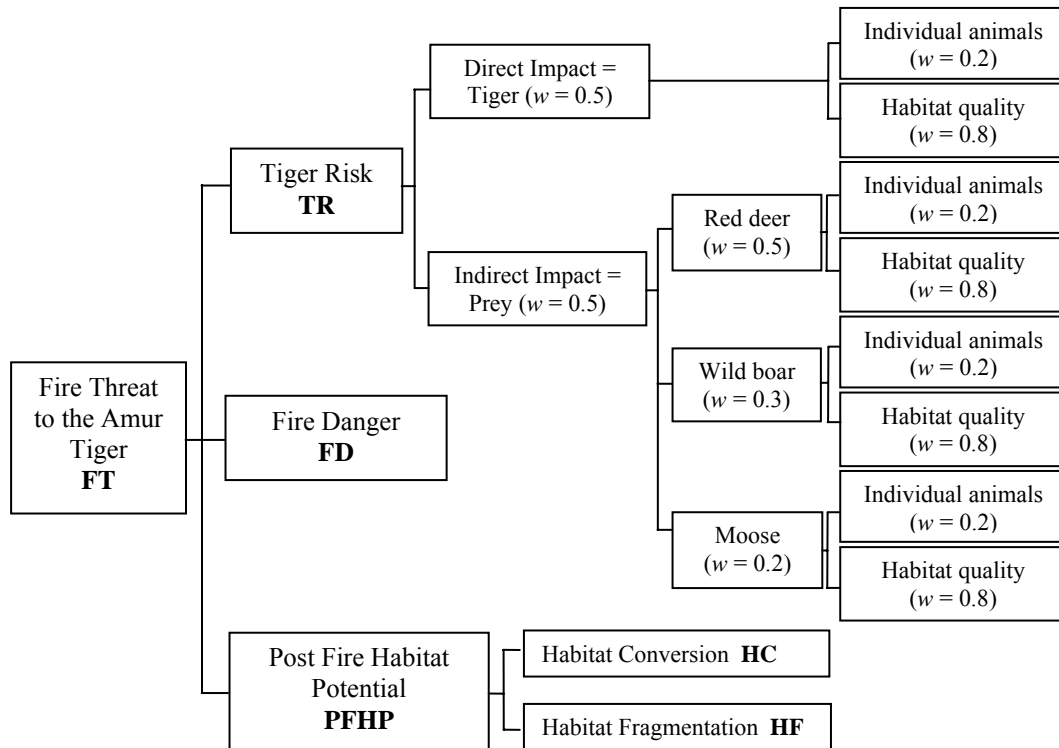
Figure 6-1. Components of the Fire threat model defined for the Amur tiger. The

acronyms in bold are used to reference respective modules throughout this chapter.

However, a more pronounced fire effect is often reflected in destruction or modification of the preferred habitat leading to a broader impact on a large number of animals.

The generic Recovery Potential module for the Amur tiger is driven primarily by the long-term post-fire habitat quality and availability for tigers and their prey. In this sense the recovery potential translates into the Post Fire Habitat Potential (PFHP) and is referred to it that way throughout the chapter. The components of the PFHP evaluate post-fire habitat quality by assessing habitat suitability for tigers and prey species and fragmentation (Figure 6-1). The development of the FD module is described in chapters 2 and 4. Detailed descriptions for the TR and PFHP modules including their parameterization are provided below.

6.2.1. Tiger Risk Module

Each of the sub-components within the Direct and Indirect Threat components of the TR module describes the spatial variability of fire threat through habitat ranking and temporal variability through the impacts of the burning front and smoke on the animals. Habitat ranking (HR) evaluates the species preference for particular habitats and relates to habitat quality. HR is calculated as a sum of geographically overlapping parameters, developed from a literature review, statistical assessments, and expert opinion (D. Miquelle, A. Kulikov, personal comm.). It ranges between 0 and 1 indicating unfavorable and highly preferred habitat, respectively.

Although species use various segments of their habitat differently throughout the year, the exact timing of fire impact on the intra-annual scale is of little importance because ecosystems of the RFE do not recover quickly. The impacted

147

areas of the habitat remain unavailable to the animals during all seasons. However, the TR module has temporal variability determined by the vulnerability of the young animals to the direct impacts of the flaming front and smoke. For a certain time period after birth young animals are susceptible to impacts from flaming front and smoke inhalation due to their limited mobility. During these periods of limited mobility the contribution from the *Individual animal* inputs is switched on (Figure 6-1). Outside the time window of the limited mobility of the young, these inputs are turned off and the overall threat to a species is considered to be lower.

The weights of *Individual animals* and *Habitat quality* parameters reflect the assessment of the relative impact of these parameters on a population of tigers and their prey species. Fire-induced change of habitat presents a long-term impact which has the potential to affect all members of a population found within the affected area. In comparison, fire threat posed to the young animals by flaming fire has a limited impact on a small subgroup within the species population prone to higher mortality rates than other age groups. On average tiger cubs present approximately 20% of the total tiger population (Smirnov and Miquelle, 2005). Although young boar piglets represent on average 40% of the total boar population, non-fire related mortality rates during the first year of life are at a minimum of 30-50% of the young animals (Zaumyslova, 2005). Therefore, the fire is likely to present direct threat to approximately 20% of the boar population. Similar to wild boar, very high mortality rates are characteristic for deer calves. Although no direct information is available for calf mortality rates in the RFE, similar studies of red deer calf mortality throughout Russia cite between 30 and 50% levels (Heptner et al, 1988). Indirect

148

assessment of moose population structure through bear kill and tracking produces a similar estimate of moose population structure with calves presenting ~ 20% of the herd (Heptner et al, 1988). The 2005 tiger track survey estimates the tiger meta-population to consist of 331-393 adults and 97-109 cubs (Miquelle et al., 2007). With the estimated cub mortality rate of 41-47% (Kerley et al., 2003) the expected adult to cub ratio is ~ 80%/20% and is similar to that of the ungulate prey species.   Based on these assessments the young mobility parameter is weighted at 0.2.

6.2.1.1. Indirect Threat Assessment

Indirect Threat is evaluated through potential fire impact on three major prey species. The weights assigned to each of the prey species reflect the importance of the species in the Amur tiger diet. Red deer (*Cervus elaphus*) is the major prey species which accounts for approximately 60 - 65% of the total tiger diet (Miquelle et al, 2005) and largely drives the distribution of the tiger meta-population (Miquelle et al., 1999a). Wild boar (*Sus scrofa*) is considered the tiger's favorite prey (Zaumyslova, 2005). Moose (*Alces alces*) presents a significant source of the tigers' diet in the northern part of the Amur tiger habitat (A. Kulikov, personal comm., 2006). Red deer distribution correlates significantly with the distribution of the tiger – 61% of tiger distribution in the RFE overlaps with the distribution of red deer (Miquelle et al., 1999a). In comparison, only 37% of tiger habitat overlaps with wild boar habitat. No similar assessment for the overlap between tiger and moose habitats is available; however, we estimate from the maps of species distribution (Miquelle et al., 1999a) that it does not exceed 30%. Subsequently, the weights for the red deer, wild boar, and the moose subcomponents were set to 0.5, 0.3, and 0.2. The total

value of Indirect Threat presents a weighted sum of the three subcomponents which reflects the improved relationship between the distribution of tiger and prey for combination of several species (Miquelle et al, 1999a).

6.2.1.1.1. Assessment of the Mobility of the Young

New born piglets of the wild boar appear in the RFE between early March (D. Miquelle, personal comm. 2006) and mid April (Baskin and Danell, 2003). They become highly mobile in 2 – 3 weeks (Heptner et al, 1989) when they start traveling with the herd daily. Based on these data we set temporal window of animals' susceptibility to flaming and smoking fires to March 1 – May 10.

Female red deer fawn between mid April and early May (Baskin and Danell, 2003). Fawns become truly mobile when 3 weeks old (Heptner et al., 1989) and reach the levels of mobility comparable to the adults by the age of 1 month. Subsequently, the temporal window of animals' susceptibility to flaming front impacts is set between April 10 and June 10.

Moose calving generally occurs during May (Heptner et al., 1989). Calves develop quickly and begin moving freely on the third day of their life. By the 10th day their mobility is no longer inferior to that of their mothers (Heptner et al., 1989). The time period of heightened risk for the moose is set between May 1 and June 10.

6.2.1.1.2. Prey Habitat Ranking

Habitat ranking methodology is based primarily on converting qualitative descriptions of species habitat preference to a set of weighted parameters using expert opinion. The information was acquired from a combination of literature research and spatial analysis of land cover types within the known distribution of the Amur tiger

and its prey species. The presented approach is valid for mapping habitat preferences at the regional scale when prey species habitat preference can be directly linked to the geographic distribution of land cover types (Stephens et al, 2005a, Stephens et al, 2005b, Baskin and Danell, 2003). A review of literature provided the bases for identifying the major drivers of species habitat preference and inferring their relative importance. We accounted for all major drivers with the exception of snow depth - an important limiting factor for tigers and prey species distribution (Baskin and Danell, 2003; Heptner et al, 1989, Myslenkov, 2005). Spatially explicit information on snow depth is not available and therefore could not be included in the ranking methodology.

Habitat ranking (*HR*), ranging between 0 and 1, is calculated following:

$$HR = \Sigma(t,\ lc,\ we,\ fe,\ nb,\ ob) \tag{6.1}$$

where *t* represents terrain defined by the slope and elevation boundaries, *lc* is land cover, *we* - water edge, *fe* – forest edge, *nb* – new burns and *ob* – old burns. The parameterization of these inputs is detailed in the text below.

As the strongest predictor of species presence, land cover type was set to account for 40% of the total habitat rank value. Species use of habitat within various land cover types was evaluated by comparing the area occupied by a given land cover within the known distribution of a species (as shown in Miquelle et al. (2005)) and the total available area occupied by the same land cover within the study area. The fraction (*f*) was calculated following equation 6.2:

$$f = a_i\ /\ A_i \tag{6.2}$$

151

where a_i is the area of land cover type i within the species distribution map and A_i is the area of land cover type i within the study area. The land cover map, used in this analysis, was developed from 3 remotely sensed data products described in detail in chapter 4. Land cover fractions, ranging primarily between 0 and 0.8, were linearly stretched between 0 and 0.4 (the maximum allowed contribution from the land cover components to the *HR* value). Although two land cover types within the moose distribution were found to have fractional weight over 0.8, they were included in the lower ranking group ($w = 0.4$) because of a very small geographic sample of these land covers available within the study area. The full list of land cover assignments by weight for each species is presented in Table 6-1.

Table 6-1. Weight (*w*) assignment for various parameters included in prey habitat ranking. Land covers were ranked based on their fractional assessment (*f*), other parameters were assessed qualitatively through the analysis of literature sources.

Parameters	Moose		Red deer		Wild boar	
	f	*w*	*f*	*w*	*f*	*w*
shrublands	0.64	0.4	0.13	0.1	0.03	0.0
grasslands	0.19	0.3	0.12	0.1	0.05	0.0
riparian vegetation	0.39	0.2	0.13	0.1	0.00	0.0
tundra	0.87	0.4	0.26	0.2	0.00	0.0
wetlands	0.14	0.1	0.24	0.2	0.04	0.0
barren and sparsely vegetated	0.70	0.0	0.09	0.0	0.00	0.0
croplands and cropland complexes	0.04	0.0	0.11	0.1	0.10	0.1
urban	0.00	0.0	0.00	0.0	0.01	0.0
water bodies	0.24	0.0	0.02	0.0	0.01	0.0
dark coniferous forests (sparse)	0.76	0.4	0.22	0.2	0.02	0.0
pine forests (sparse)	0.00	0.0	0.00	0.0	0.00	0.0
larch forests (sparse)	0.59	0.3	0.18	0.1	0.02	0.0
broadleaf forests (sparse)	0.03	0.0	0.24	0.2	0.33	0.2
siberian dwarf pine forests (sparse)	0.77	0.4	0.18	0.1	0.00	0.0
mixed forests (sparse)	0.43	0.3	0.46	0.3	0.18	0.0
dark coniferous forests (dense)	0.73	0.4	0.28	0.2	0.05	0.0
pine forests (dense)	0.00	0.0	0.00	0.0	0.00	0.0

larch forests (dense)	0.74	0.4	0.26	0.2	0.07	0.0
broadleaf forests (dense)	0.11	0.1	0.63	0.4	0.64	0.4
siberian dwarf pine forests (dense)	0.84	0.4	0.18	0.1	0.00	0.0
mixed forests (dense)	0.31	0.2	0.62	0.4	0.44	0.3
terrain		0.3		0.2		0.2
old burns		0.0		0.1		0.1
new burns		-0.1		-0.1		-0.2

Literature descriptions of the habitats for each ungulate species emphasized the importance of water- and forest-edge habitats in species habitat preferences (Voloshina et al, 2006; Baskin and Danell, 2003; Heptner et al, 1989). Forest edge was defined as a 1 km (A. Kulikov, personal comm., 2006) buffer from all land cover types identified as sparse or dense forest and land cover type "forest/natural vegetation". Water edge coverage was estimated as 1 km buffer from land cover type "water" and a map of large rivers. The importance of water edge was emphasized for all three species and its weight was set at 0.2. Forest edge is considered to be of higher importance for red deer and boar ($w = 0.2$) and of lesser importance for moose ($w = 0.1$).

Literature sources reference recently burned areas as undesirable habitat for ungulates (Stephens, 2005b). Based on the field observations made during the 2006 field work, recent burns (burns with little regrowth) were identified as ~2 year old burns. Wild boar is reported to avoid recent burns completely (Zaulmyslova, 2005b) and therefore this parameter received a negative weight ($w = -0.2$) in the overall boar habitat ranking scheme. The recent burns have lower (although still negative) impact on deer and moose use of the habitat ($w = -0.1$). Areas burned ~3 years prior to mapping and older were considered old burns (covered with some type of vegetation – grass or shrub). Unlike recent burns, regrowing burns present an attractive land

153

cover for some ungulates and specifically red deer (Astafiev et al, 2006). Old burns

were assigned a weight of 0.1 for red deer and boar. For moose burned area is

considered to be usable with the appearance of dense shrubby vegetation. Based on

the data collected during field surveys and literature review, shrubby vegetation does

not appear in considerable amounts in areas burned more recently than ~7-10 years

prior to mapping. Therefore, in the moose habitat ranking all burns mapped by the

MODIS burned area algorithm since 2001 (chapter 3) were defined as new burns.

The category "old burns" was eliminated because burns older than 2001 were mapped

as specific land cover classes (chapter 4).

Elevation and slope are known to influence species distribution (Baskin and

Danell, 2003; Heptner et al, 1989). The specific slope/elevation combinations

limiting species use of habitat are presented in Table 6-2. The weights for slope and

elevation were assigned based on the restrictions imposed by the terrain on the

species' use of the habitat. For example, moose are found only in areas with gentle

slopes (defined in this study as slopes <=15%). In comparison, red deer are not

restricted by the gradient of the terrain and can freely move across the landscape.

Consequently, the terrain restriction is weighted greater for moose habitat ranking (w

= 0.3) rather than red deer habitat ranking (w = 0.2). The maps of ranked habitat are

presented in Figure 6-2.

Table 6-2. Slope and elevation composition defining terrain as an input to tiger and

prey habitat ranking.

Prey species	Slope (%)	Elevation (m)
moose	0 -15	200 - 1700
red deer	0 - 50	300 - 700

wild boar	0 - 15	200 - 2000
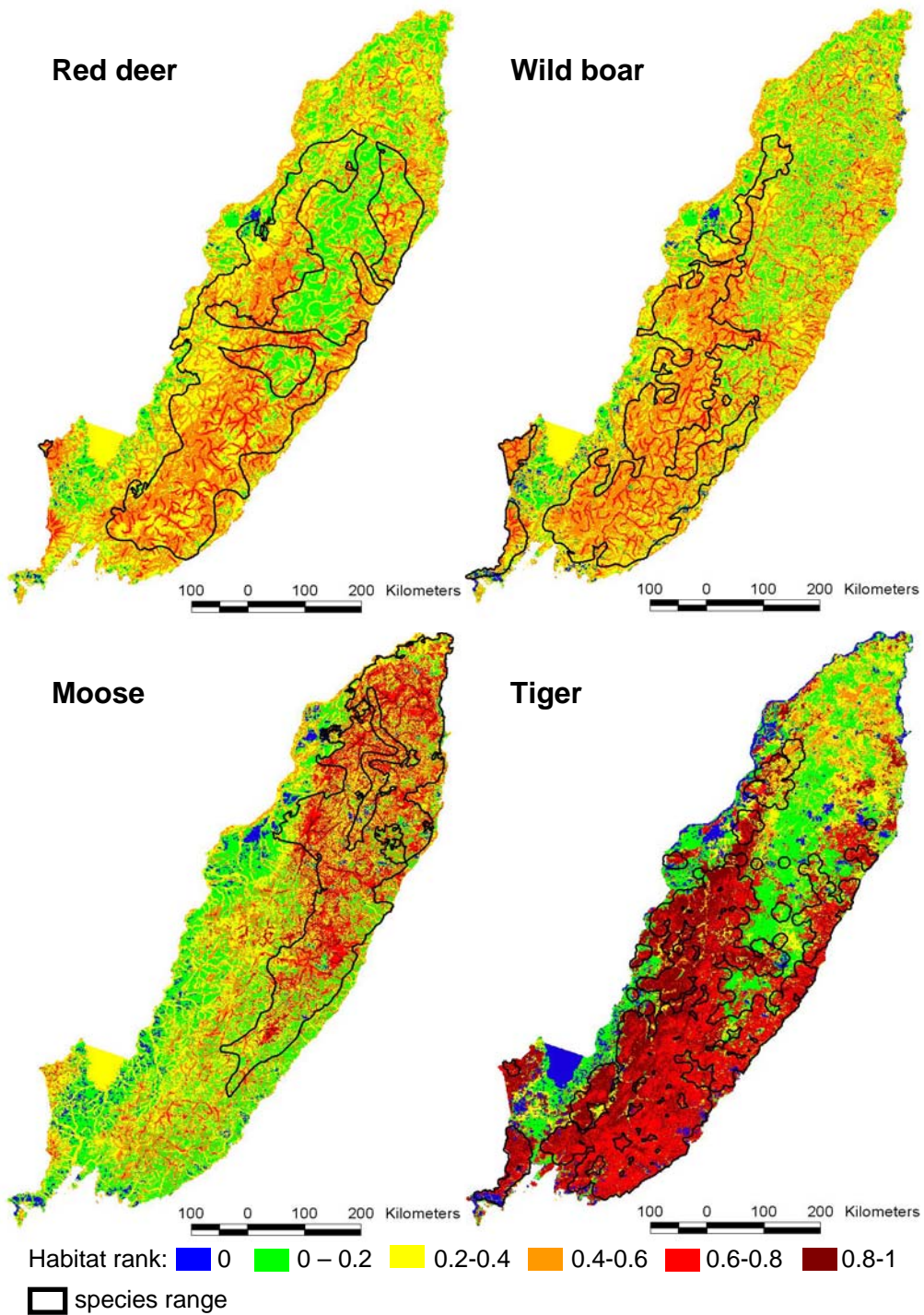
Figure 6-2. Distribution of highly ranked habitats within the known area of presence

of a) red deer, b) wild boar, c) moose, and d) the Amur tiger (Miquelle et al., 2005).

6.2.1.2. Direct Threat Assessment

6.2.1.2.1. Assessment of the Mobility of Tiger Cubs

The literature overview and radio tracking data provided by Kerley et al

(2005) cite large discrepancies in reported seasons of birthing for the Amur tiger.

The period of relative immobility of the young (when they stay in the immediate

vicinity of the den) ranges between 21 and 67 days. Generally tiger cubs start

traveling with their mothers once they reach 3 months of age (D. Miquelle, personal

communication, 2006). It is hard to determine a specific window in time within a

year when fires pose higher levels of risk to the meta-population of tigers based on

limited mobility of the young. Consequently, the direct threat component of the TR

representing fire impact on tigers remains stable in time and does not show temporal

variability.

6.2.1.2.2. Tiger Habitat Ranking

Land cover rating for the tiger habitat was conducted following a similar approach to

the fractional assessment described in prey habitat ranking. In addition to land cover,

tiger habitat preference is also driven by terrain. Multiple literature sources name

areas along river valleys (defined in this study as river flood plains and surrounding

slopes <= 10% at elevations >=100m and <=700m) as highly preferred habitat by the

Amur tiger (Miquelle et al, 1999a, Astafiev et al, 2006, Smirnov, 2005). Because

river valleys define preference rather than limitation in tiger distribution the weight

was set at 0.2. River valleys influence the overall tiger distribution as topographic

features rather than distance from water which was found to be unimportant

(Miquelle et al, 1999a). Tigers are known to avoid recently (0 – 5 year old) burned

areas (Miquelle et al, 2004) which includes all burns since the development of land cover map (w = -0.2).

Because of the small number of known factors contributing to tiger habitat preference ranking, the weights of various land covers were assigned based on their fractional assessment with an additional adjustment. The fractional assessment values (*f*) were adjusted based on the most recent evaluation of tiger habitat preference inferred from tiger track density surveys in the RFE (Miquelle et al, 2007). In this assessment tiger habitat preference was ranked on a qualitative scale in four categories – "extremely low", "low", "moderate", and "high". Comparison of the results of fractional assessment of land covers within the known tiger distribution showed that "high" importance designation was roughly equivalent to the 0.6 – 0.8 fraction and the "extremely low" was equivalent to <0.1 fraction. The *f* values were rounded to one decimal place and were adjusted if their qualitative importance was lower (-0.1) or higher (+0.1) than that suggested by the *f* value. If the qualitative importance was considerably higher or lower than the estimated *f* (e.g. *f* = 0.1 and importance is "high") the weights were adjusted by 0.2. Table 6-3 shows the adjustment of the initial fractional land cover assignments by the qualitative assessments in Miquelle et al (2007) and the final land cover weighting for all input parameters. Tiger habitat ranking (*THR*) follows:

$$THR = \Sigma(t, lc, nb) \tag{6.3}$$

where t is terrain variables representing river valleys, lc – land cover, nb – new burns. The map of ranked tiger habitat and the fractional assessment of habitat within the known species distribution are presented in Figure 6-2 d.

Table 6-3. Land cover grouping by habitat inclusion in the distribution for the Amur tiger and the weight adjustments based on the habitat importance (Miquelle et al, 2007).

Input parameters	f	Importance	w
barren and sparsely vegetated	0.0	extremely low	0.0
broadleaf forests (dense)	0.8	high	0.8
broadleaf forests (sparse)	0.5	high	0.6
croplands and cropland complexes	0.1	extremely low	0.0
dark coniferous forests (dense)	0.2	low	0.1
dark coniferous forests (sparse)	0.1	low	0.1
forest-natural vegetation complex	0.2	moderate	0.3
grasslands	0.1	low	0.1
larch forests (dense)	0.2	moderate	0.3
larch forests (sparse)	0.1	moderate	0.2
mixed forests (dense)	0.7	high	0.7
mixed forests (sparse)	0.5	high	0.6
pine forests (dense)	0.1	high	0.3
pine forests (sparse)	0.0	high	0.2
riparian vegetation	0.1	moderate	0.2
shrublands	0.1	moderate	0.2
siberian dwarf pine forests (dense)	0.0	extremely low	0.0
siberian dwarf pine forests (sparse)	0.0	extremely low	0.0
tundra	0.0	extremely low	0.0
urban	0.0		0.0
water bodies	0.1		0.0
wetlands	0.2	moderate	0.3
terrain (valley)			0.2
new burns			-0.2

6.2.2. Post Fire Habitat Potential

PFHP assessment combines several methods. The full data flow chart (Figure 6-3) identifies the major components of PFHP and describes their relationships. These components include Fire Impact (FI), Post-Fire Habitat Rank (PFHR), Habitat Conversion (HC), and Habitat Fragmentation (HF). Definitions, parameterization,

and sources for these components range from statistical analyses of remotely sensed

data sources to literature-based look up table compilation.
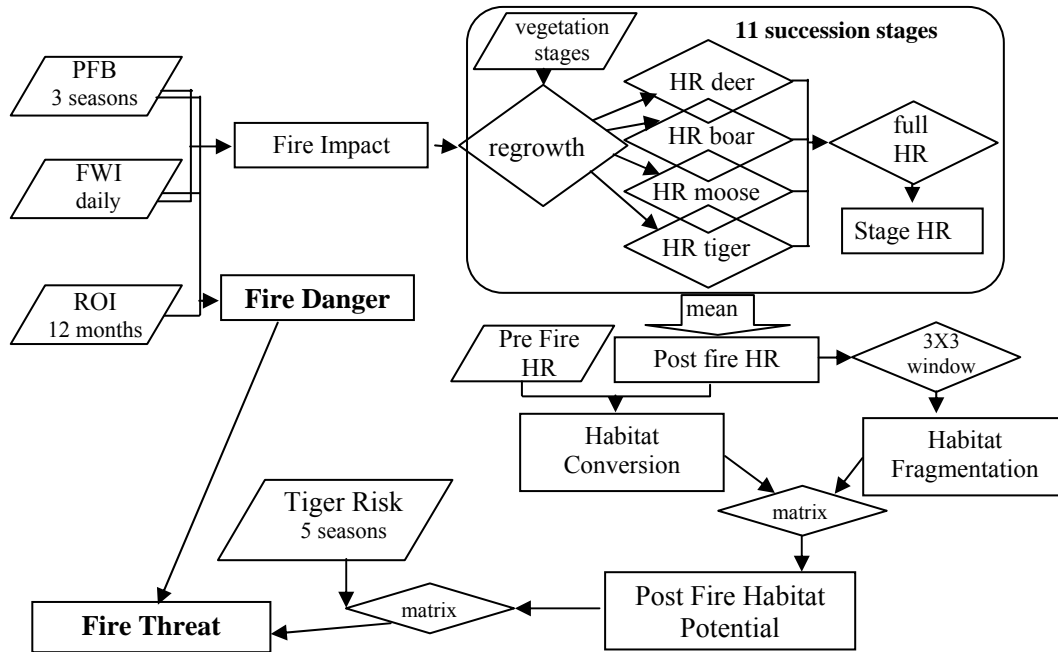
Figure 6-3. Full FTM Data flow

6.2.2.1. Fire Impact Assessment

Fire impact (FI) presents a binary identifier of model grid cells where fire can

result in a stand replacing event or high burn severity conditions. For this study we

adopted the differenced Normalized Burn Ratio (dNBR) index which has been

correlated with the field measurements of burn severity assessed through the

Composite Burn Index (CBI) across various ecosystems of the continental US (Key

and Benson, 2006; Zhu et al., 2006). Although numerous recent studies demonstrated

the variability of dNBR measurements due to changing solar and view angles (Roy et al, 2006; Walz et al., 2007), site conditions (Wimberly and Reilly, 2007), and its ability to detect burn severity across all vegetation types (Epting et al, 2005), dNBR based burn severity estimates are considered reliable in tree dominated landscapes where it is directly related to tree mortality (Epting et al., 2005; vanWagtendonk et al., 2004; Waltz et al, 2007, Wimberly and Reily, 2007).

A limited field sample collected during the 2006 field work supports applicability of dNBR burn severity assessment for identifying stand replacing fires. A transect of ~3 km was surveyed within a 2003 burn scar in spruce/fir forest (Figure 6-4 a and b). Along the transect, 12 points were opportunistically selected to capture the variability of observed burn severity levels within the MODIS burned area 500 m (25 ha) mapping grid cells. The number and density of observations were determined through a visual assessment of variability of conditions within a 360º view from the starting point and each subsequent point along the transect. Very low density (1 point) was set in uniformly burned areas with no standing living trees (Figure 6-4 c). 50 m radius plots were established around each point and the number of dead, living, and downed trees within broadleaved and coniferous categories were counted and converted to percent tree mortality (by category and total). Field observations show that areas with dNBR below 0.2 demonstrate patchy fire effects with no dominant tree mortality; areas with dNBR between 0.2 and 0.3 include sizable pockets of unburned vegetation; and areas with dNBR greater than 0.4 (corresponding to "moderate-high" burn severity class (Key and Benson, 2006)) are characterized by complete tree mortality.
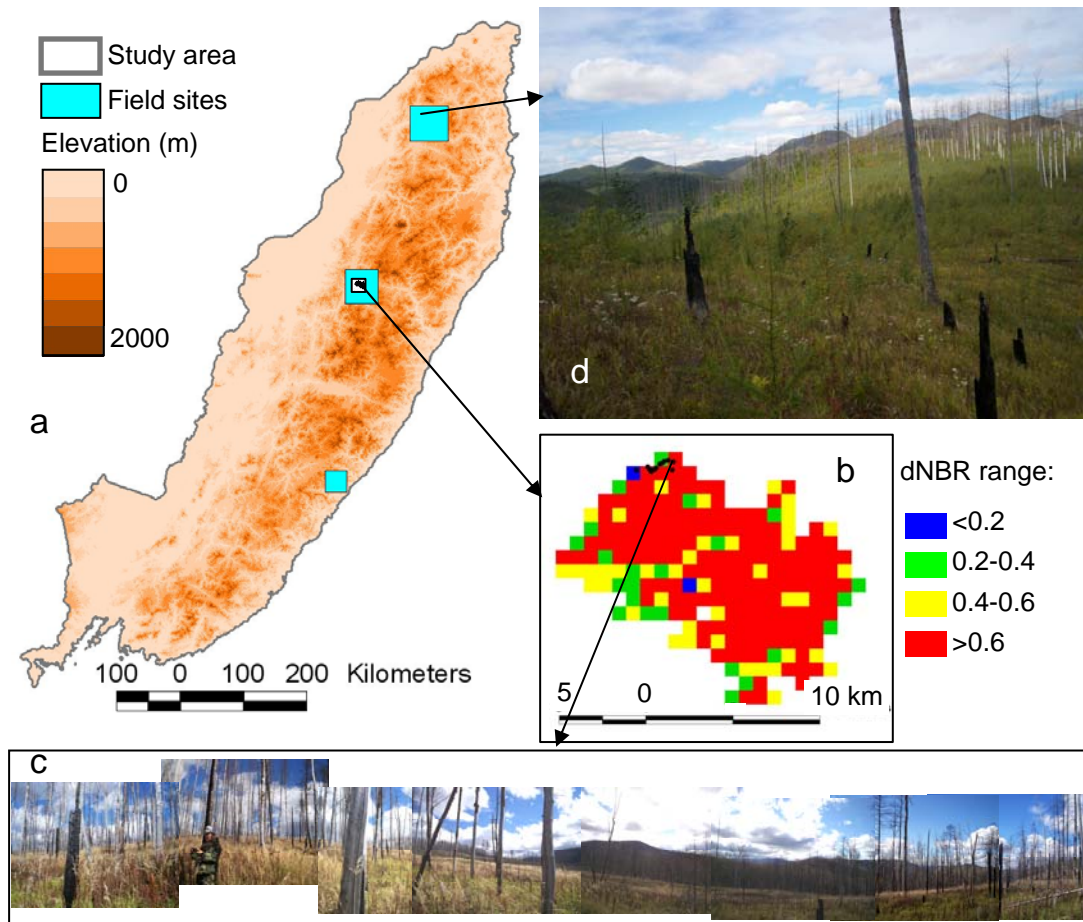
Figure 6-4. Field sites surveyed in 2006 to collected data on post-fire vegetation regrowth and burn severity: a) distribution of the 3 survey areas (shown larger than actual size) in the RFE, b) the burned severity levels within a 2003 burn scar and location of field transect; c) 360º view of severely burned area from single field point within a MODIS 500 m grid cell, d) homogenous vegetation regrowth in 1998 burn scars.

Although originally developed for the Landsat imagery (30 m spatial resolution), dNBR retains its ability to map general patterns of impact severity at much coarser (500 m) resolution of the Moderate Resolution Imaging

Spectroradiometer (MODIS) (Walz etal., 2007).   The MODIS dNBR estimates were produced within burned area mapping in the RFE for 2001-2005 (chapter 3).

Burn severity and particularly tree mortality, are driven by a combination of numerous factors including broad categories such as fuel load, rainfall and humidity, topography, climate (Whelan, 1995). Specific conditions such as stand age class, tree composition, vertical structure of the stand, fuel continuity, and local wind patterns also impacts burn severity (Johnson, 1992). Burn severity is nearly as much influenced by fire residency time as by fire intensity (Johnson, 1992) and specific patterns of fire spread (e.g. up or down hill burning) (Fuller, 1991). The influence of the broad categories is modeled within the Potential Fire Behavior and Fire Weather modules of the FTM. However, the information on the specific conditions and fire residency time is not available and cannot be obtained reliably from the satellite record. Therefore, the FI index, calculated as a sum of fire weather and potential fire behavior, presents an approximation of conditions leading to stand replacing fires and is likely to underestimate the extent of moderate high and high burn severity rather than overestimate it.

The high mortality FI threshold was identified by comparing FI to dNBR values over areas burned during 2005 fire season. The exact date of burning for each grid cell necessary for FI calculation was assigned based on its proximity to active fire detections (Giglio et al., 2003). The sample was stratified by 6 land covers (Table 4) and a separate assessment was conducted for each type. In each case distribution of values was positively skewed making standard deviation based metrics non-applicable. Subsequently, minimum observed FI corresponding to moderate high

or high burn severity category was accepted as the high mortality FI threshold. A complete set of FI thresholds for each land cover type is shown in Table 6-4.

Table 6-4. Minimum Fire Impact (FI) levels for moderately-high and high burn severity occurrence within various land cover types of the RFE.

Land cover type	min FI
dark coniferous forest	980
larch forest	938
mixed forest	868
forest/natural vegetation	1146
shrublands	1149
wetlands	1156

6.2.2.2. Post Fire Habitat Potential

Grid cells exceeding the FI threshold are further used to evaluate vegetation succession, using a look up table developed from the patterns of vegetation recovery described in the literature for the RFE (Krestov, 2003; Sheingauz, 1996; Sheshukov, 1996; Gossow, 1996) and field observations. Trends of vegetation recovery following stand replacing fires were defined within a look up table (LUT) (Table 6-5) for 11 successional stages - immediate (first season post fire), 5, 10, 15, 20, 25, 30, 35, 40, 45, and 50-year assessments. The 50-year window is selected based on the time frame required for establishment of tree dominated land covers post fire for the majority of land cover types in the RFE (Krestov, 2003).

Post-fire succession of various land covers is affected by climatic patterns (e.g. moisture availability and temperatures), soil erosion and organic content, seed bank richness in the soils, successful seed producing season during the year of fire

163

occurrence, during the preceding year, or the first and second post-fire years, reoccurrence of fire over the burns within 1-3 years, competition from other native or exotic species (Krestov, 2003; Sheshukov, 1996).

Table 6-5. Look up table for 11 stages of post-fire successional stages over a 50-year period

Land cover type	mixed forest (MF) south	mixed forest (MF) north	spruce-fir forest (SFF)	spruce-fir forest (SFF) (adjacent to larch)	larch (LF) (moisture deficit)	larch (LF) (no moisture deficit)	larch dominated wetlands (W)	dwarf pine forest (DPF)	broadleaf deciduous forest (BDF)	forest/ natural vegetation (FNV)
1	grass	grass	grass	grass	moss	grass	grass	grass	grass	grass
5	shrub	shrub	grass	grass	grass	shrub	shrub	shrub	shrub	grass
10	shrub	shrub	shrub	shrub	grass	shrub	shrub	shrub	shrub	shrub
15	FNV	shrub	shrub	shrub	grass	shrub	shrub	shrub	FNV	shrub
20	BDF sparse	FNV	shrub	shrub	shrub	FNV	FNV	shrub	BDF sparse	FNV
25	BDF sparse	BDF sparse	FNV	shrub	shrub	LF sparse	LF sparse	shrub	BDF dense	FNV
30	BDF dense	MF dense	BDF sparse	FNV	shrub	LF sparse	LF sparse	shrub	BDF dense	FNV
35	BDF dense	MF dense	MF dense	LF sparse	shrub	LF dense	LF dense	shrub	BDF dense	BDF sparse
40	BDF dense	MF dense	MF dense	LF sparse	shrub	LF dense	LF dense	DPF sparse	BDF dense	MF dense
45	BDF dense	LF dense	MF dense	LF dense	FNV	LF dense	LF dense	DPF sparse	BDF dense	MF dense
50	BDF dense	LF dense	MF dense	LF dense	MF sparse	LF dense	LF dense	DPF sparse	BDF dense	MF dense

(Row label: **Years post fire**)

The LUT is created under the assumption of favorable climatic conditions, sufficient seed availability for coniferous species throughout the entire burned area, and absence of competition with introduced species. However, important general

distinctions are made for areas with expected moisture deficit and moisture accumulation due to topography and proximity of larch stands for the dark coniferous forest regeneration.

Moisture limited areas of regrowth were identified using the ArcINFO© procedure FLOWACCUMULATION which models the amount of rain flowing through each grid cell of a Digital Elevation Model under a hypothetical scenario of uniformly distributed precipitation with no interception, loss to ground water, or evapotranspiration. A threshold (<= 2) was developed from a limited number (n=41) of field observations of regrowth patterns during the field work of 2006. Regrowth information including height and count of tree species, type and height of ground cover and shrubs in 10 m radius plots were recorded at each point in 5 field transects within burns of 1996, 1998, and 2003. Due to limited area and ragged terrain access points were selected opportunistically. However, the observed regrowth patterns across large areas of similar burn ages were highly homogenous (Figure 6-4 d).

The proximity to larch stands was evaluated in a 5X5 window. The expected post-fire land covers were further ranked for habitat suitability using the habitat ranking system described in the Values at Risk section and averaged over the 11 successional stages into the Post Fire Habitat Rank. Habitat Conversion (HC) was calculated following $HC = HR_{post-burn} - HR_{pre-burn}$ where HR is habitat rank and compares the mean quality of the habitat during the 50-year succession to the pre-fire habitat quality. Negative HC indicates declining habitat quality while positive HC indicates an improvement in the post-fire habitat value for the Amur tiger.

Habitat Fragmentation (HF) is assessed for each individual cell within a 3X3

moving window over the post-fire habitat ranking. Evaluation of habitat

fragmentation as a function of habitat quality presents a more reasonable alternative

to habitat fragmentation as a function of land cover. Changes in quality of the habitat

are more likely to impact the use of the habitat and animals' ability to move freely

across landscape. HF is calculated as a mean of absolute values of differences

between the value of the given cell n_{ij} and the eight surrounding cells. The resultant

HF index ranges between 0 and 1 and provides quantitative assessment of uniformity

and amplitude of variations in habitat quality for each grid cell. Low HF values

correspond to homogenous habitat quality and high values indicate fragmented

habitat with high differences in habitat quality among the adjacent cells. HF and HC

estimates per grid cell are further combined through a matrix (Table 6-6) into the

Post-Fire Habitat Potential (PHFP) (Figure 6-3).

Table 6-6. Matrix for calculating Post Fire Habitat Potential

PFHP		Habitat Fragmentation									
		<= .1	.1 - .2	.2 -.3	.3 -.4	.4 -.5	.5 -.6	.6 - .7	.7 - .8	.8 - .9	> .9
Habitat Conversion	< -.5	0.5	0.4	0.3	0.2	0.1	0	0	0	0	0
	-.3 - -.5	0.6	0.5	0.4	0.3	0.2	0.1	0	0	0	0
	-.1 - -.3	0.7	0.6	0.5	0.4	0.3	0.2	0.1	0	0	0
	-.1 - .1	0.8	0.7	0.6	0.5	0.4	0.3	0.2	0.1	0	0
	.1 - .3	0.9	0.8	0.7	0.6	0.5	0.4	0.3	0.2	0.1	0
	.3 - .5	1	0.9	0.8	0.7	0.6	0.5	0.4	0.3	0.2	0.1
	> .5	1	1	0.9	0.8	0.7	0.6	0.5	0.4	0.3	0.2

PFHP is then combined with the TR values using matrix in Table 6-7 and the result is

converted to a fuzzy set of probabilistic fire threat values through multiplying it by

the three scenarios of fire danger (Malczewski, 1999). The final output Fire Threat

presents a fuzzy set FT[min, mean, max] corresponding to three scenarios "best case"

– minimum, "trade off" –mean, and "worst case" – maximum.

Table 6-7. Matrix for combining Post Fire Habitat Potential and Values at Risk

		Post Fire Habitat Potential									
		<=.1	.1 - .2	.2 -.3	.3 -.4	.4 -.5	.5 -.6	.6 - .7	.7 - .8	.8 -.9	>.9
Tiger Risk	<= .1	0.4	0.35	0.3	0.25	0.2	0.15	0.1	0.05	0	0
	.1 - .2	0.45	0.3	0.35	0.3	0.25	0.2	0.15	0.1	0.05	0
	.2 -.3	0.5	0.35	0.4	0.35	0.3	0.25	0.2	0.15	0.1	0.1
	.3 -.4	0.6	0.55	0.5	0.45	0.4	0.35	0.3	0.25	0.25	0.2
	.4 -.5	0.7	0.65	0.6	0.55	0.5	0.45	0.4	0.3	0.3	0.3
	.5 -.6	0.8	0.75	0.7	0.6	0.55	0.5	0.45	0.35	0.35	0.3
	.6 - .7	0.9	0.85	0.8	0.75	0.7	0.6	0.5	0.4	0.4	0.4
	.7 - .8	1	0.95	0.9	0.85	0.8	0.7	0.6	0.45	0.45	0.4
	.8 - .9	1	1	0.95	0.9	0.85	0.8	0.7	0.5	0.5	0.5
	> .9	1	1	1	0.95	0.9	0.85	0.8	0.6	0.6	0.5

6.2.3. Model Sensitivity Assessment

As a fuzzy set, fire threat value at each $cell_{ij}$ carries an assessment of the range

of uncertainty with the top defined by the "worst case" scenario (max) and the bottom

level defined by the "best case" scenario (min). However, by design this uncertainty

expresses the inherited uncertainty of the fire danger modeling and does not represent

the contribution from other components of the model. A three-step assessment was

designed to better understand the sensitivity of a full fire threat model to values

representing individual model components. The first step presents an analysis of the

relative magnitude of contribution from various components to the overall fire threat

value. The second step addresses the range of possible habitat states during the 50-

year post-fire regrowth. The last step evaluates the range of uncertainty introduced within habitat ranking.

The relative contribution of various factors to the overall fire threat value was assessed using the stepwise linear regression approach. To ensure a representative sample for the full range of fire threat values between 0 (the lowest) and 1 (the highest), a stratified random sample of 1000 points was created. Fire threat values were stratified by equal intervals of 0.1 into 10 bins and 100 randomly selected points in space and time were collected for each of the bins for 3 output scenarios of fire threat during the 2007 fire season. Fire threat values for the "worst case" scenario covered the entire range (0-1), values for "trade off" scenario did not exceed 0.8, and values for the "best case" scenario did not exceed 0.7. As a preparatory step we plotted the 3 components (fire danger, values at risk, and post fire habitat potential) and 2 independent parameters constituting the post fire habitat potential (habitat conversion and habitat fragmentation) against fire threat values individually (Figure 6-5). Values of all components range between 0 and 1 allowing for an easy visual interpretation of the relationships.

The individual parameter evaluation shows that the strongest relationships with fire threat exist for fire danger, values at risk, and habitat conversion values. These plots also show that these parameters have a different magnitude of impact at different levels of fire threat. The variability of moderate and high fire threat values is strongly dependant on fire danger assessment (Figure 6-5 a), whereas the variability of the lower fire threat value is more dependant on tiger risk (Figure 6-5 b) and habitat conversion (Figure 6-5 d). Habitat fragmentation at an individual cell

level is fairly uniform and therefore does not appear to have a significant relationship

with the fire threat values (Figure 6-5e).

Stepwise linear regression analysis confirms these relationships (Table 6-8).

In this analysis the PHFP component was substituted with its parts HC and HF in the

equation. Both forward and backward linear regressions were preformed for the three

output fire threat scenarios. In each case FD and HC components are identified as the

most influential followed by the HF component. Although the TR component is

shown to have the lowest amount of influence on the fire threat values, this may be

explained by the spatial autocorrelation between TR and HC components (~0.75

residual). Autocorrelation of two independently strong predictors within a stepwise

regression results in omitting the contribution of one of the correlated parameters.

Table 6-8. Results of the stepwise linear regression assessment for the model

sensitivity testing.

	Max	Mean	Min
Coefficients			
FD	0.7657196	0.72697	0.713942
TR	0.1249285	0.093342	0.094991
HC	-1.099934	-0.72031	-0.57166
HF	0.5838579	0.498266	0.293825
n (df)*	1000 (995)	800 (795)	700 (695)
RMSE	0.112	0.06784	0.05391
R^2	0.8435	0.906	0.9249
p-value	0.0000	0.0000	0.0000

*n represents the sample size, df is degrees of freedom
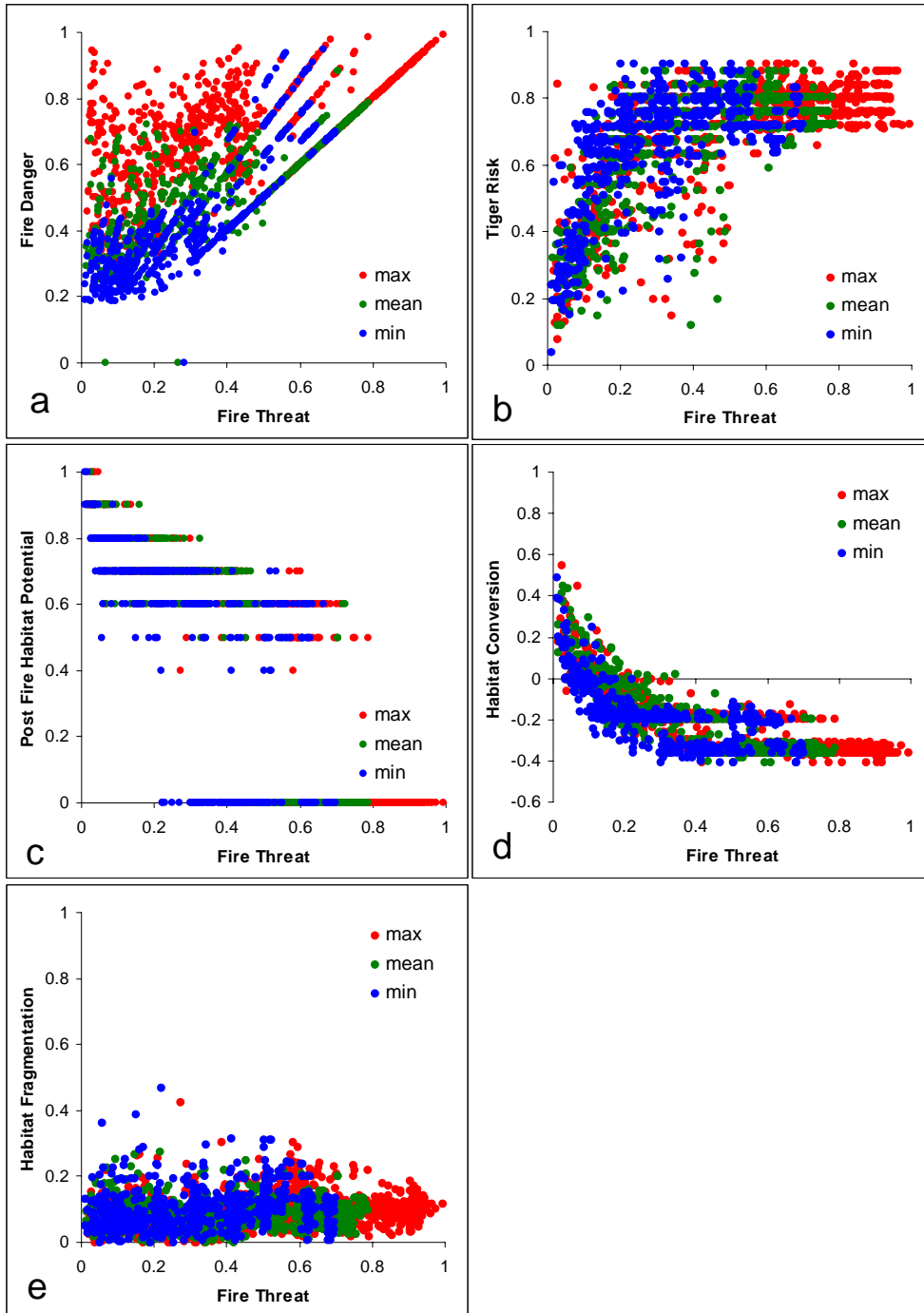
Figure 6-5. Relationships between fire threat values for three output scenarios "worst case" (max) - red, "trade off" (mean) - green, and "best case" (min) – blue and individual parameters of the FTM: a) fire danger, b) tiger risk, c) post fire habitat potential, d) habitat conversion, e) habitat fragmentation.

Variability of the state of the Amur tiger habitat during the 50-year regrowth period produces additional uncertainty within fire threat estimates. Habitat ranking is averaged over the 11 successional stages to calculate a long-term post-fire habitat rank. To evaluate the full possible range of magnitude in fire threat throughout the 50-year regrowth period, two more scenarios to the PFHP modeling producing a fuzzy set [min, mean, max] for post-fire habitat ranking and propagating it through the model were added to the fire threat calculation. The "min" and "max" scenarios represent the worst and best state in habitat quality respectively during the 50-year period. The fuzzy PFHP[min, mean, max] was combined with crisp TR datasets and then merged with the fuzzy FD[min, mean, max] dataset. Opposite to the PFHP scenarios, FD "min" and "max" scenarios correspond to the "best case" and "worst case" of fire danger, respectively. Therefore evaluation of the broadest possible range of scenarios required combining PFHP/TR(max) with FD(min) and PFHP/TR(min) with FD(max) scenarios.

Figure 6-6 shows that the fullest range of potential fire threat values, driven by the contribution from the best and worst post fire habitat stages, is not much greater than that covered by the fuzzy set FT[min, mean, max] for a 50-year mean post fire habitat potential. The difference between the FT_{max} with the mean 50-year PFHP and FT_{max} with the lowest PFHP, representative of the worst post fire habitat stage (usually immediately after burning), is greater than that of the FT_{min} with the mean 50-year PFHP and FT_{min} with the highest PFHP, representative of the best post fire habitat stage. This indicates that the highest quality habitat value is closer to the

mean value for the 11 stages of regrowth compared to the lowest habitat quality value.
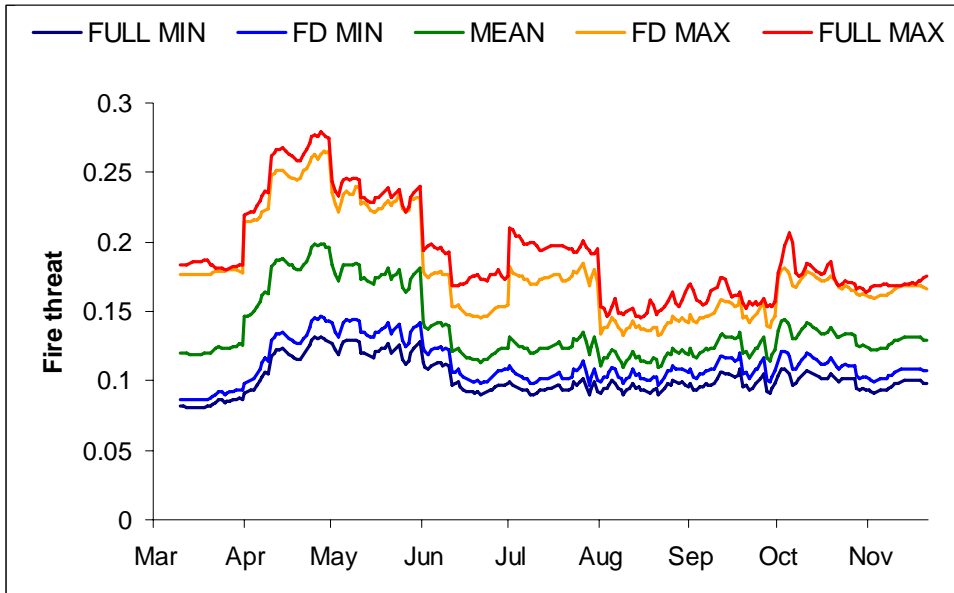
Figure 6-6. Mean daily regional fire threat estimates for 2007, where FULL MIN results from the best quality habitat stage and the lowest fire danger, FD MIN is driven by the lowest fire danger only, MEAN is calculated from the mean fire danger, FD MAX is driven by the highest fire danger, and FULL MAX is a combination of the worst fire danger and the lowest quality of habitat.

This finding is consistent with the observed post-fire habitat use by ungulates (Peek, 1997; Kie et al, 2003). Field studies have demonstrated that ungulate densities increase rapidly within regrowing burns, starting at ~ 5 year post burn. Habitat use peaks at ~15 - 25 years after the burn, possibly reaching 2-3 times higher ungulate densities than in non-burned forests, and then begins to decline reaching the near equilibrium state ~ 50-70 years after then burning when a new tree dominated land

172

cover is established. Thus the 50-year mean estimate of post-fire habitat rank is expected to be closer to the peak level habitat use than to the lowest level habitat use post fire – a pattern reproduced by the model.

The qualitative nature of weightings within the habitat ranking methodology also carries a range of uncertainty associated with the magnitude of assigned weights. A set of ranking systems based on varying weights assigned to the input parameters was created and compared to the habitat ranking described in section 6.2.1. To evaluate the largest possible variability in fire threat introduced by habitat ranking uncertainty, the set that produced the greatest difference from the original habitat ranking, driven exclusively by land cover types, was selected and processed through the fire threat model for the three output scenarios during 2007 season.

The results show that modifications in habitat ranking can affect fire threat values considerably (Figure 6-7). Habitat ranking driven by land cover increases the mean rank value within 1 degree cells (n = 54) throughout the study area linearly by nearly 30% (R^2 ~0.96, slope ~1.3) (Figure 6-7 a). This increase propagates linearly through the fire threat model consistently raising mean fire threat values within 1 degree cells for each of the output scenarios by ~36% (R^2 ~0.95 for each scenario) (Figure 6-7 b, c, and d) and mean fire threat values for the entire study area by 20 – 25% (R^2 > 0.99 for each scenario) for "worst" and "best case" scenarios, respectively.

The large increase in fire threat under the land cover driven habitat ranking is not surprising. With elimination of other contributing factors, over 28% of the entire study area is ranked above 0.8 habitat quality (ranging between 0 and 1) compared to only 4% under the ranking that considers importance of overlapping of fine spatial

173

patterns such as water edge and forest edge. Although the land cover driven habitat

ranking presents an oversimplified approach to habitat ranking, it allows for

establishing the top level of habitat ranking driven range of uncertainty.
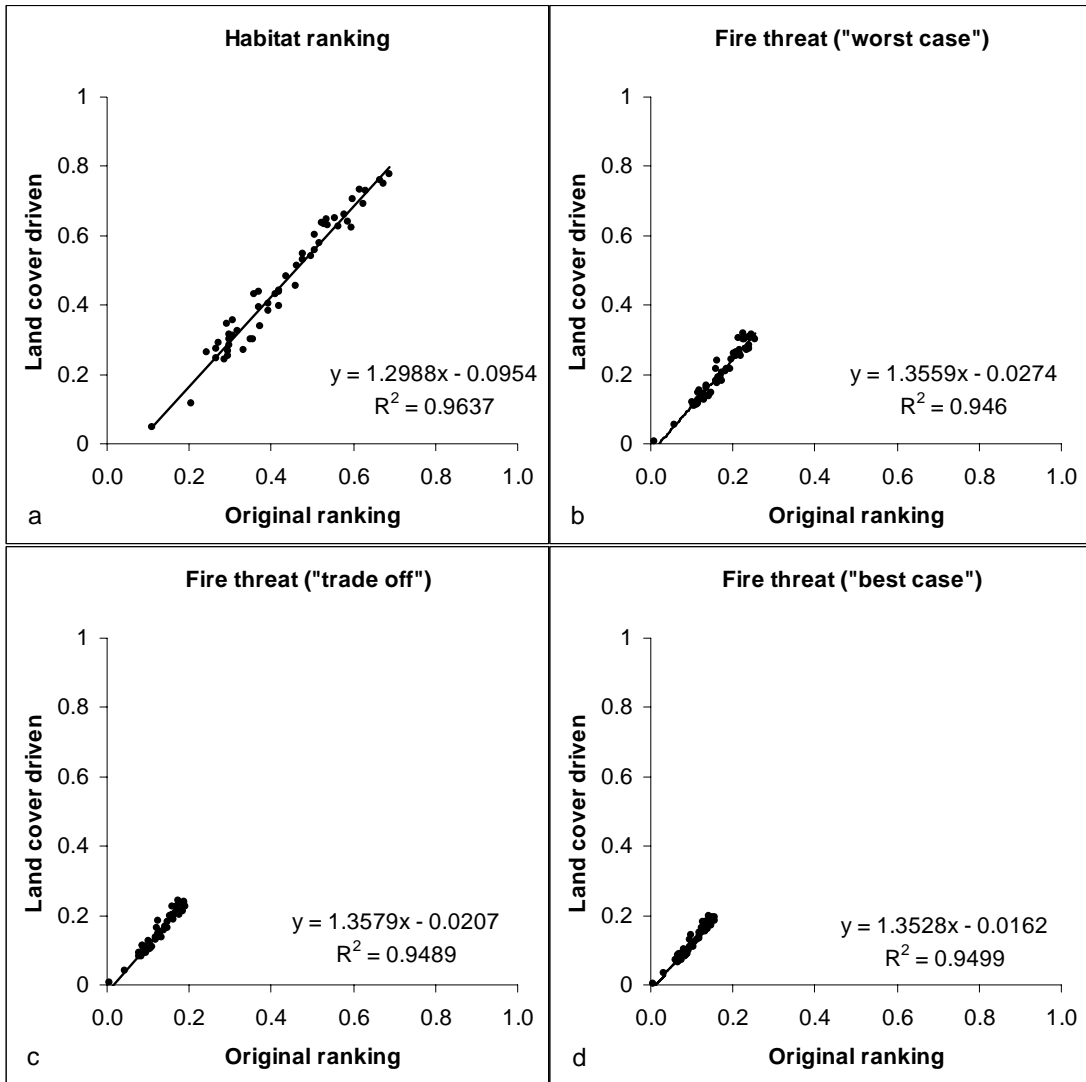
Figure 6-7. Changes introduced by weights assigned to various inputs in habitat

ranking (a) and fire threat for b) "worst case" –max, c) "trade off" – mean, and d)

"best case" – min scenarios.

6.3.1. Current Levels of Fire Threat to the Amur Tiger

Current levels of fire threat to the Amur tiger were evaluated based on the data

record for 2005-2007 when a complete dataset of updated information, including

daily weather measurements and yearly information about fire occurrence, was

available. This analysis includes a comparison of daily 1km grids of fire threat values

ranging between 0 (the lowest) and 1 (the highest). Fire threat during the months of

December, January, and February is considered negligible due to the presence of

snow cover which impedes fire ignition and propagation. Subsequently, fire threat is

only modeled during March - November time frame. The analysis was focused on

identifying magnitude and general spatial and temporal trends of fire threat to the

Amur tiger under current climatic conditions within the entire study area and within

the known area of tiger presence (or tiger range). Recolonization of the RFE by tigers

is an on-going process. Therefore, it is important to consider the study area as a

whole because it includes many potential areas of habitat for tigers that have not yet

been colonized. However, an analysis of fire threat within the current tiger range

allows for evaluating fire threat in the most suitable tiger habitat that often serves as a

source of tiger meta-population and thus has a particularly significant role.

Mean fire threat to the Amur tiger over the entire study area during 2005-2007

was low. Even under the "worst case" scenario mean projected levels of fire threat

did not rise above 0.3 while the "best case" scenario values remained below 0.15.

The mean confidence range (the difference between the "best case" and "worst case"

scenarios) was relatively narrow (0.07) and stable (standard deviation ~0.03). During

2005-2007 fire threat values followed a distinct temporal pattern of intra-annual distribution with a tall peak in April-May and two small peaks in July and October, respectively. This pattern was observed during all three years with only minor variations resulting from weather driven change in fire danger.

In the areas of known tiger presence mapped during a winter tiger track survey (Miquelle et al., 2005) the observed patterns of fire threat distribution were similar to those over the entire RFE. However, the mean fire threat values were on average slightly higher (+0.03) for all three scenarios. This increase is driven by elimination of areas of poor habitat where tigers are not found thus removing the lowest values of fire threat from averaging. With the exception of the increase in magnitude, other parameters describing the mean regional fire threat including the range between "worst" and "best" case scenarios and its stability as well as seasonality are nearly identical to those obtained for the entire RFE (Figure 6-8).

Fire threat values of individual 1km cells were binned to 10 equal ranges to evaluate frequency distribution of various fire threat level occurrences at monthly scales. The bins were assigned qualitative values to assist in easier interpretation of their magnitude: 1) 0-0.1 – none, 2) 0.1-0.2 – very low (VL), 3) 0.2-0.3 – low (L), 4) 0.3-0.4 – moderate low (ML), 5) 0.4-0.5 – moderate (M), 6) 0.5-0.6 – moderate high (MH), 7) 0.6-0.7 – high (H), 8) 0.7-0.8 – very high (VH), 9) 0.8-0.9 – severe (S), 10) 0.9-1 – catastrophic (C). The analysis shows that most of the time, fire threat to the Amur tiger in the study area was between very low and moderately low (Figure 6-9 a, b, c). Noticeable spikes in fire threat occur in April and May when up to 15% (under the "worst case scenario - Figure 6-9 a) of values are at or above moderate fire threat

level. This pattern repeats throughout the 2005-2007 time period and is characteristic for all three output scenarios, although the magnitude of change is smaller under the "trade off" and even smaller under the "best case" scenarios.
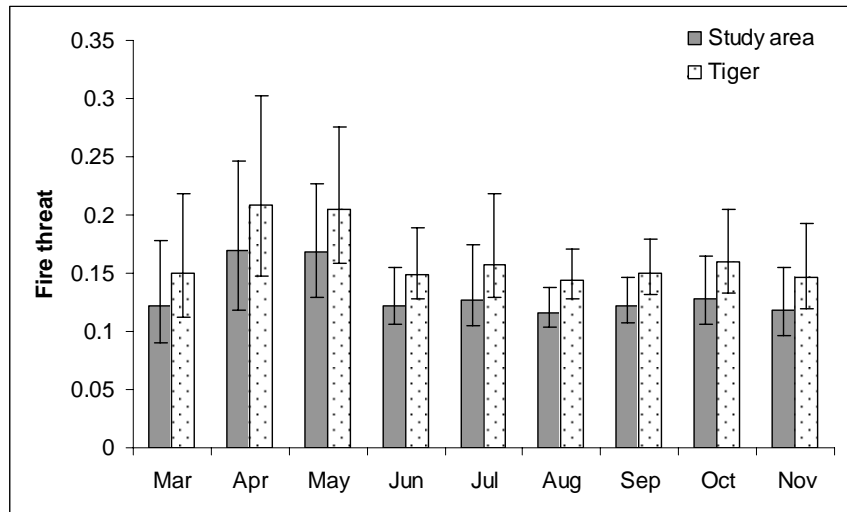
Figure 6-8. Mean monthly fire threat levels (2005-2007) within: a) the entire study area and b) the known area of tiger presence. The "trade off" scenario is used as the basis with the "best case" and the "worst case" scenarios representing error bars.

Monthly frequency distribution of threat levels provides a smoothed view of the fire threat over the entire area. At daily time scales and over isolated areas fire threat reaches the highest "catastrophic" levels in all 3 years of observation. During September, October, and November of 2005 3, 50, and 57 1km grid cells, respectively, registered "catastrophic" levels of fire threat under the "worst case" scenario. Even under the assumption that the same cell experienced "catastrophic" levels of fire threat during half of each month, during November of 2005 it translates

into ~ 4 km^2 of the study area under the "catastrophic" threat level, 24 km^2 under the
"severe" threat level, 89 km^2 under "very high" and 373 km^2 under "high" fire threat.
Using similar assumptions, even under the "best case" scenario ~45 km^2 are found at
or above "high" fire threat level in 2005. However, in 2006 and 2007 this number is
considerably smaller and can be as low as 1km^2.
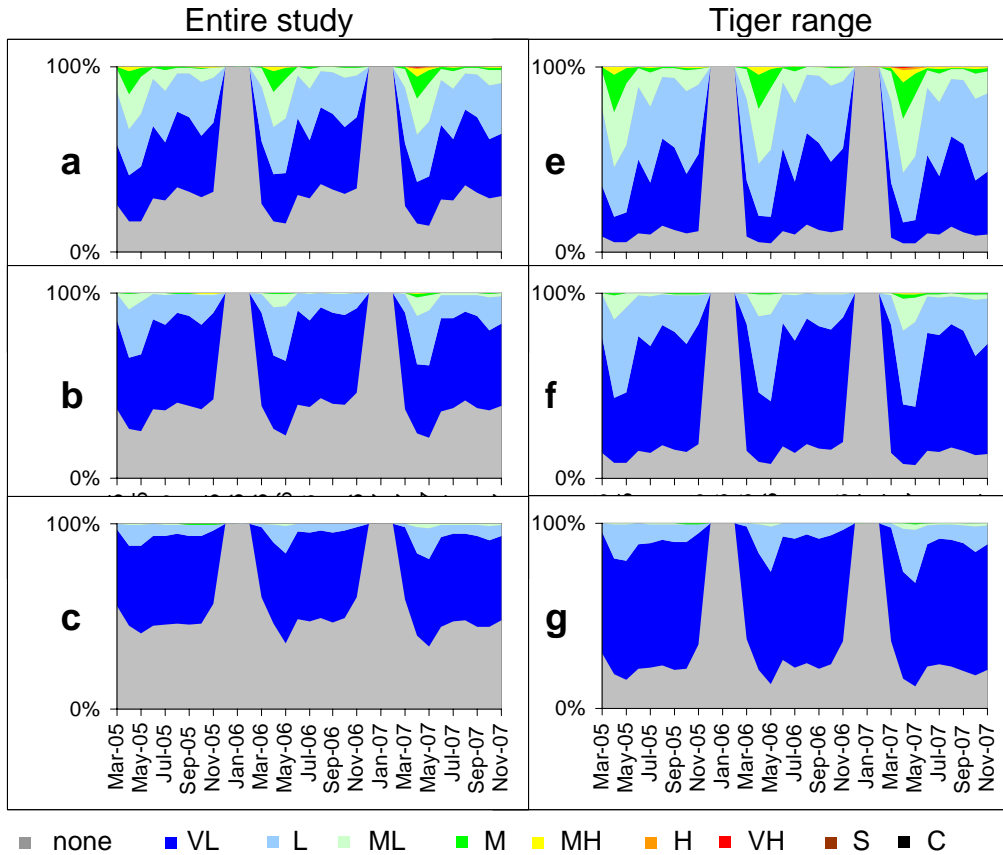
Figure 6-9. Frequency distribution of monthly fire threat levels in the entire study
area: a) "worst case", b) "trade off", and c) "best case" scenarios; and within the
known area of tiger presence: e) "worst case", f) "trade off", g) "best case" scenarios.

Compared to the entire study area, fire threat levels registered within the areas
of known tiger presence are higher (Figure 6-9 e, f, g). The known area of tiger

presence excludes the areas not suitable for tigers, for example agricultural and urban areas, thus leading to a large reduction in the number of cells with "none" fire threat level. However, these are primarily replaced with "low" and "very low" fire danger areas with only a very moderate (1% or less) increase in the higher ranges of fire threat values.

Fire threat varies considerably in space and time. Spatial patterns of fire threat observed during 2005-2007 demonstrate both consistency (Figure 6-10 a, b, c) and variability (Figure 6-10 e, f, g). A large increase in fire ignitions during April, connected to anthropogenic activity in the RFE (chapter 2), raises the overall fire danger and subsequently fire threat in a predictable pattern observed on anniversary dates during each of the three years (Figure 6-10 a, b, c). In contrast, weather driven changes in fire danger result in localized increases with changing spatial pattern and fire threat levels (Figure 6-10 e, f, g). While seasonally consistent increases in fire threat level are wide spread and persistent in time, weather driven events generally cover smaller areas for short periods of time and, therefore, do not raise fire threat levels at coarser spatial scales.

Fire threat distribution, analyzed within a 1X1 degree grid, showed little variability in spatial patterns at yearly or monthly scales. Spatial patterns of yearly mean fire danger in 1 degree cells are similar for the entire RFE and within the known area of the Amur tiger presence (Figure 6-11).
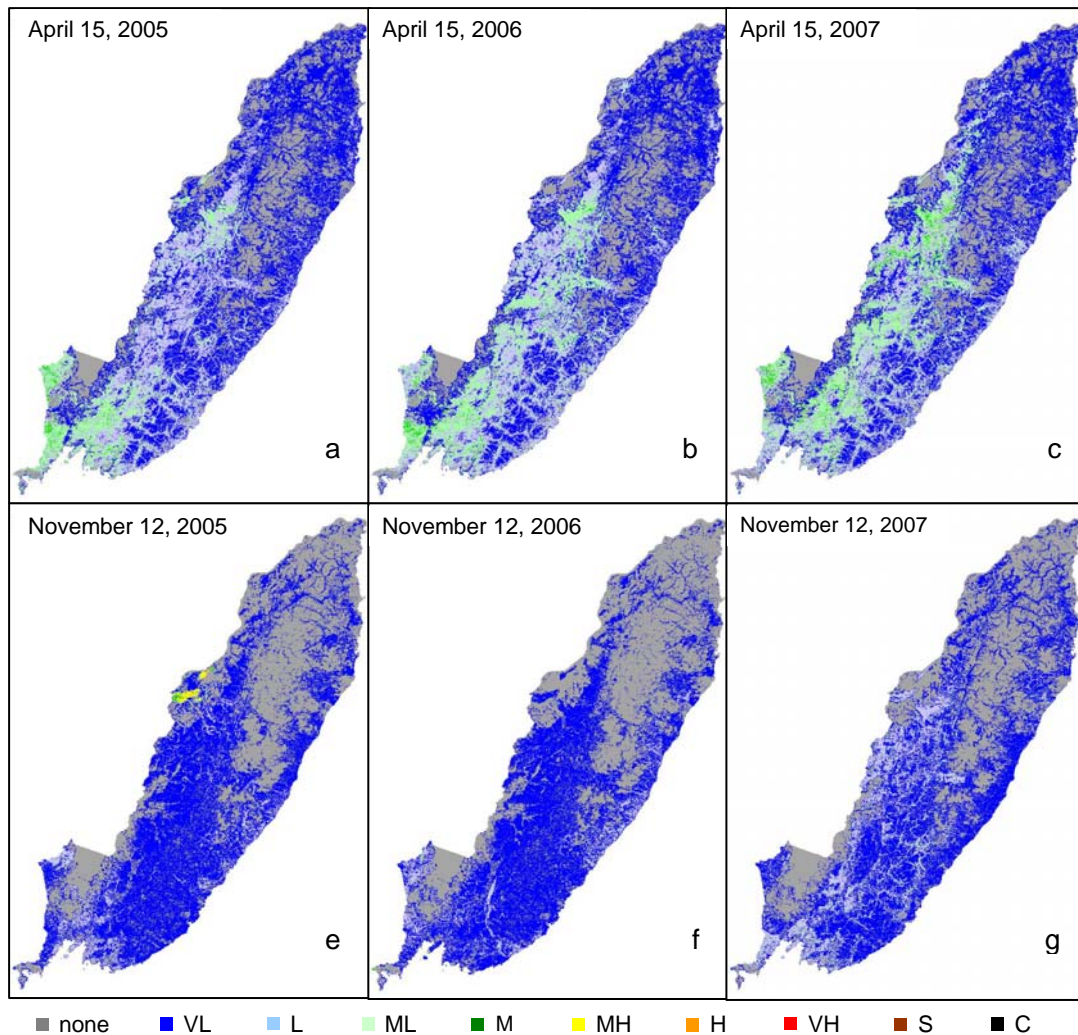
Figure 6-10. Daily fire threat in the RFE on April 15 of a) 2005, b) 2006, c) 2007, and November 12 of e) 2005, f) 2006, g) 2007.

6.3.2. Fire Threat to the Amur Tiger by the End of the 21st Century

The fire threat model was used to analyze potential changes in fire threat driven by projected climate change during the 21st century. In this analysis, fire danger presents the only variable component in the overall fire threat model. Although tiger habitat is likely to experience additional impact from climate change

particularly in the post-fire recovery phase (e.g. changes in tree species composition),

it is outside the scope of this study.
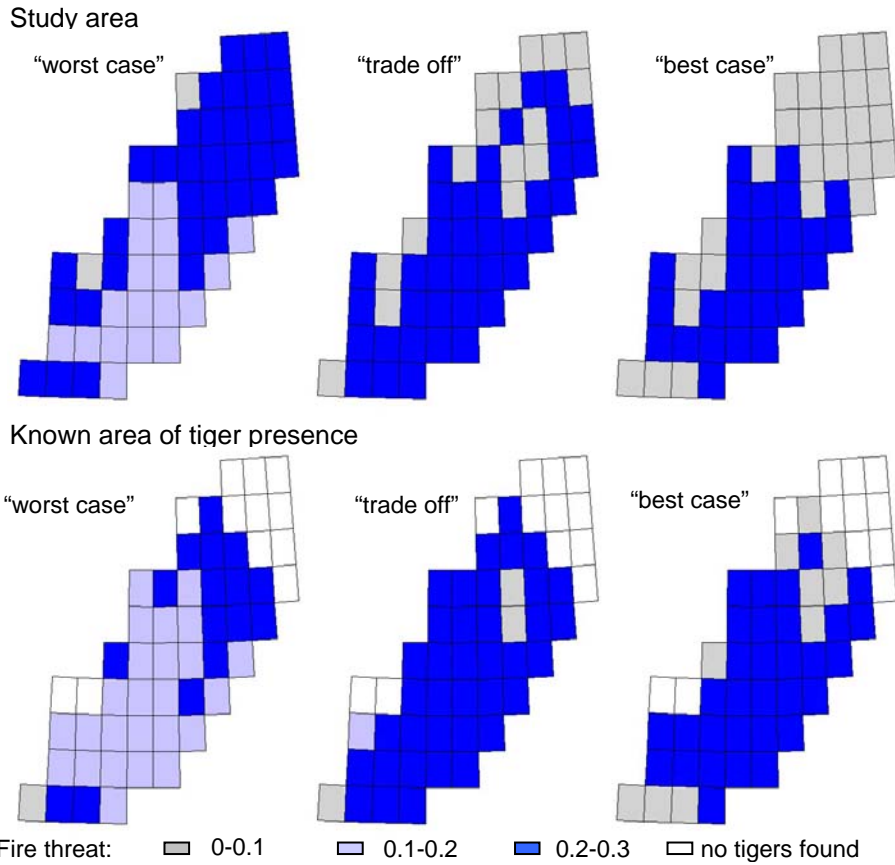
Figure 6-11. Mean yearly fire threat in 1X1 degree cells within the entire study area

and areas of known tiger presence.

ECHAM5 projections of meteorological parameters have been shown to

underestimate fire danger compared to observed data (chapter 5). Due to this

underestimation, the direct comparison of modeled fire threat at the end of the 21st

century and observed conditions in the beginning of the 20th century is not an

acceptable approach. Instead, ECHAM5 driven estimates of fire threat observed over

a 5-year period at the end of the 20th century (1996-2000) are compared with

ECHAM5 driven estimates over 2096-2100.   The analysis is focused on

understanding the general trends observable at coarser spatial and temporal resolution

to minimize uncertainty introduced at the fire threat model's 1km daily resolution.

Under the A2 scenario fire threat is expected to rise throughout the RFE with a

particularly pronounced increase in the southern potion of the region (Figure 6-12).
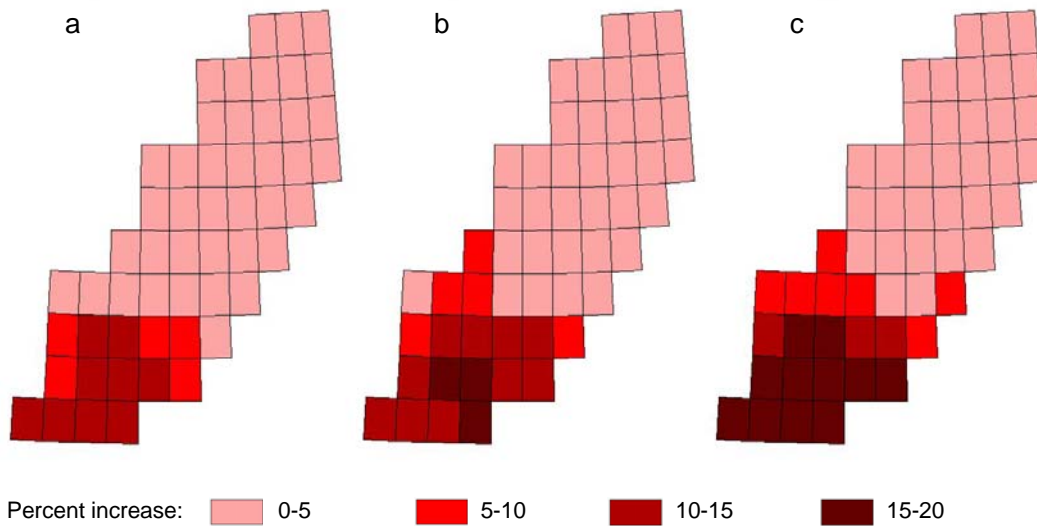
Figure 6-12. Fire threat change under the A2 scenario by the end of the 21st century

compared to the conditions at the end of the 20th century for 3 output scenarios: a)

"worst case", b) "trade off", and c) "best case".

The pattern of the increase is similar to that of fire danger (chapter 4 figure 5-12);

however, the magnitude of fire threat increase is up to 5% larger.   The rates of

increase will be the highest for the "best case" scenario and the lowest for the "worst

case" scenario thus narrowing the range of uncertainty in fire threat estimates. Mean regional yearly fire threat will rise by ~6% ("trade off" scenario) compared to values at the end of the 20th century. This moderate yearly increase will be driven by large increases (6-17% range) in regional fire threat in August – October counterbalanced by small increases (2-4%) in March, April, and June and moderate (4-6%) increases in May, July, and November (Figure 6-13).
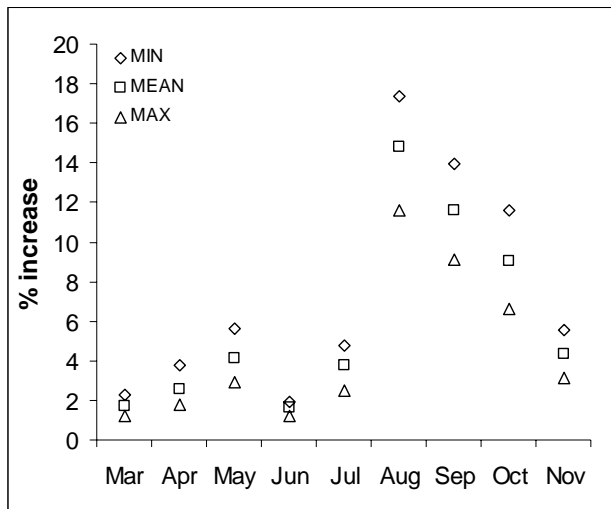
Figure 6-13. Percent increase in average monthly fire threat levels by the end of the 21st century for the 3 output scenarios MIN – "best case", MEAN – "trade off", and MAX – "worst case".

Frequency distribution of the 10 fire threat levels (described in the previous section) show that in August and September fire threat is likely to increase over large areas and become persistent (Figure 6-14). In contrast, a larger increase of fire threat at "moderate high" and above values will occur in March, April, May, July and

November. During these months a greater number of localized high fire threat conditions similar to those shown in Figure 6-11 e are expected.
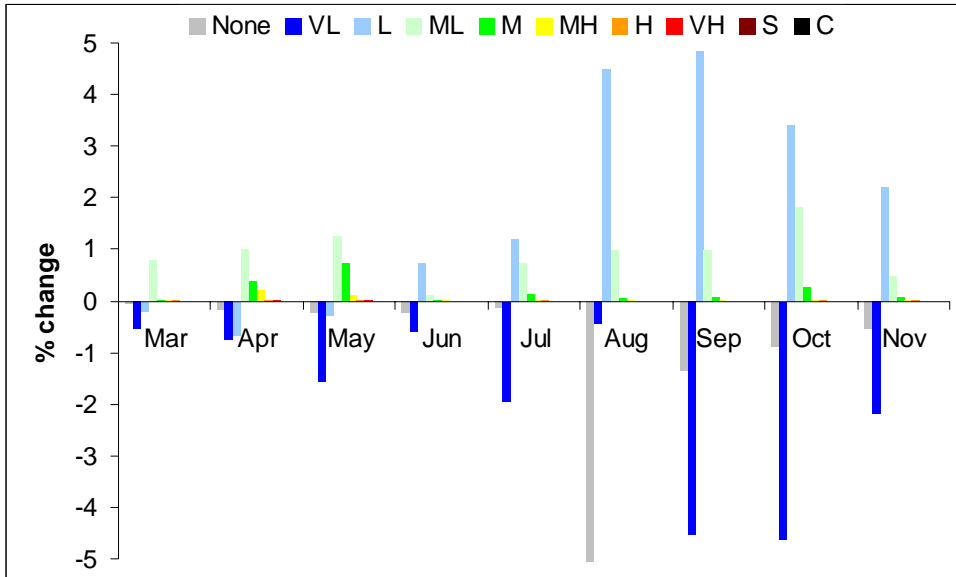
Figure 6-14. Percent change in frequency distribution of fire threat levels by the end of the 21st century compared to the conditions at the end of the 20th century.

Monthly fire threat change will also vary spatially over the RFE (Figure 6-15). While the northern and central sections of the area will experience only mild (<5%) fire threat increases in most months and even decreases in June and July, fire threat change in the southern part will be persistent throughout the year and much larger reaching nearly 40% in August over the southwester section of tiger habitat.

Frequency distribution of fire threat levels within the three cells with mean increase in fire threat > 35% show that in addition to the overall increase in fire threat levels compared to the end of the 20th century, inter-annual variability of threat

levels will also increase (Figure 6-16). This may be indicative of a higher frequency

of high fire threat years in the southern part of the RFE compared to the conditions at

the end of the 20th century.
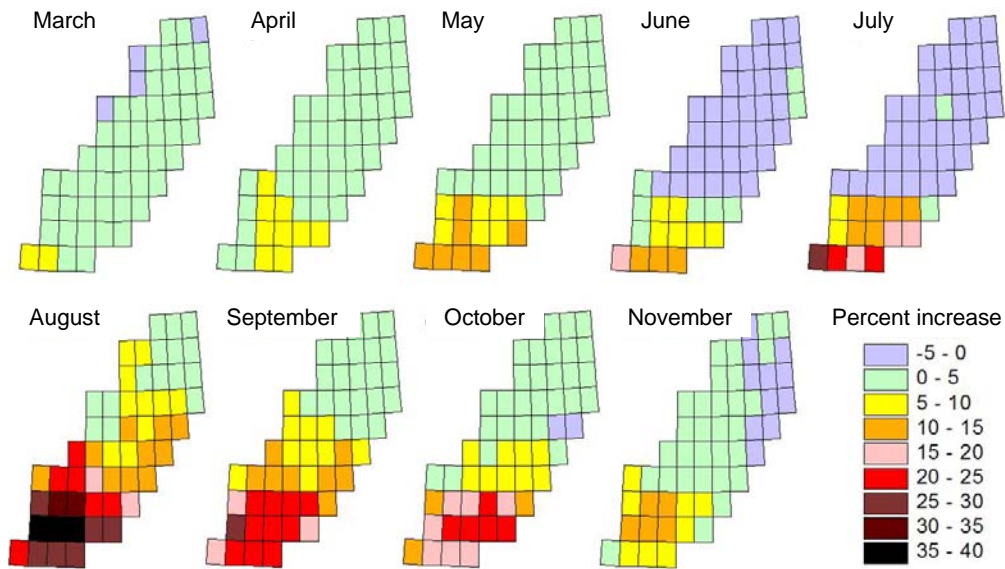
Figure 6-15. Monthly mean change in fire threat compared to the end of the 20th

century within 1 degree grid.

6.4.   *Discussion*

The predictive capability of fire threat modeling is regulated by several

independent components which require detailed understanding of patterns and

dependencies between fire, landscape, and tigers. The RFE is a relatively sparsely

populated remote region with limited access to many areas. This remoteness and

inaccessibility serves both a positive and a negative role at the same time. On the one

hand, it allows for preserving large contiguous areas of anthropogenically unaltered habitat critical for supporting a meta-population of a large solitary carnivore. On the other hand, it limits significantly our ability to develop detailed knowledge of wildland fire, its impacts on the habitat, specific patterns of post-fire recovery, and the tiger habitat suitability. Satellite based observations provide the basis for regional assessment of various fire and habitat related parameters. However, it is difficult to relate the results of landscape level field studies to coarse resolution remotely sensed products. This model presents a methodology and a feasibility study for modeling landscape scale processes at the regional scale using remotely sensed data.
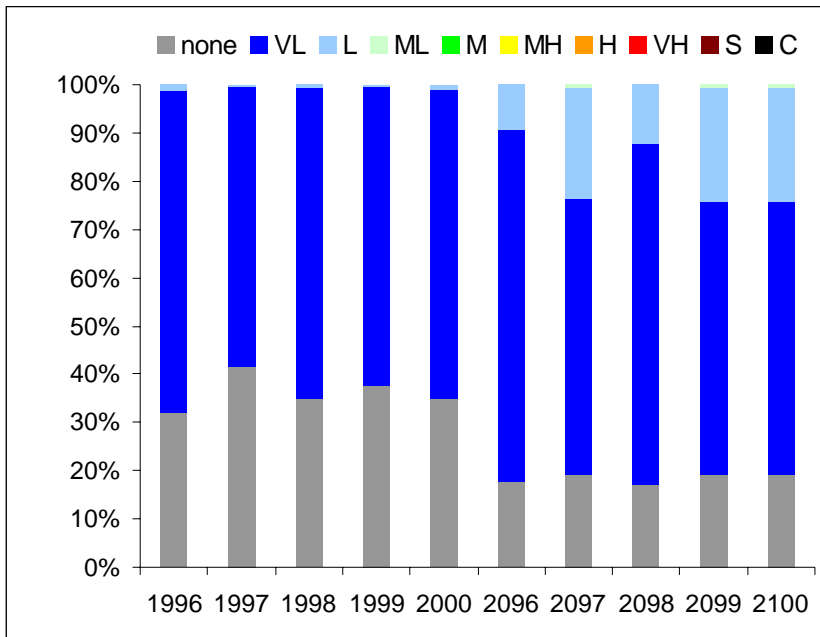
Figure 6-16. Frequency distribution of fire threat levels in the three 1 degree cells with monthly mean fire threat increase > 35% in August by the end of the 21st century.

Model sensitivity assessment shows a large uncertainty in fire threat estimates associated with the accuracy of habitat ranking. The presented methodology of habitat ranking is expected to provide a more realistic assessment of habitat importance for the tiger and prey species compared to that driven exclusively by land cover distribution, because it accounts for a number of contributing parameters known to impact habitat use. However, the relative contributions from each of the parameters may differ from the ones used in this study. Therefore, fire threat modeling accuracy can be further improved by development of spatially explicit maps of habitat suitability based on the field surveys of density distribution of animals during all seasons as a factor of various environmental parameters.

Assessment of fire threat during 2005-2007 provides the first view of the extent and severity of wildland fire impact on the Amur tiger and its habitat. According to satellite observations of fire activity, 2005-2007 fire seasons during this time frame were typical with relatively few large fires. Therefore, this analysis presents an assessment of fire threat under typical conditions for the RFE and does not include fire threat during seasons of uncharacteristically high fire occurrence (e.g. 2003, 1998 – chapter 4). Since large fire seasons are repeated, periodic events, their omission limits our knowledge of fire threat to the tiger to only moderate seasons of fire activity. However, it is likely that the most significant damage to the tigers and their habitat would occur during large fire seasons.

One of the limitations of the current fire threat model is its inability to deal with fire induced habitat degradation. Our present state of knowledge about post-fire vegetation recovery is primarily based on forest rehabilitation after a stand-replacing

fire. Little has been published in the literature regarding moderate and low severity

fire impacts and post-fire habitat rehabilitation. Even less is currently known about

tiger and prey species use of fire degraded habitat in comparison to its use during pre-

fire period. Incorporation of these parameters into fire threat modeling is likely to

enhance our understanding of a broader spectrum of fire impact on the tigers and their

habitat.

Modeling uncertainty can be further reduced with development of a regionally

tuned suite of remotely sensed products. Mapping of individual parameters related to

the important tiger habitat descriptors, such as Korean pine, which is specific to this

geographic region, instead of fitting the existing globally generic land cover datasets

for habitat suitability modeling is likely to improve the model's predictive

capabilities.

Potential climate change scenarios show that the RFE is less likely to be

strongly affected by climate change, as compared to other areas in Northern Eurasia

(Malevsky-Malevich et al., 2008). Under the most favorable SRES scenario B1, fire

danger and subsequently fire threat in the RFE will remain close to their current

levels (chapter 5). However, under the least favorable SRES scenario A2 fire threat

will rise considerably in the southern part of the RFE impacting large tracts of high

quality tiger habitat. The A2 scenario seems to be a more likely outcome for the

study area because of its geographic position next to massive and fast growing

economies and population of South-East and South Asia. Therefore, although the

chapter presents estimates for the most unfavorable scenario, they are not unrealistic

considering the regional dynamics of the past 10 years (Auffhammer and Carson, in press).

The results of this study shows that current levels of fire threat to the Amur tiger in the RFE are fairly low during a typical year. At present elevated levels of fire threat are connected to two main factors. The first factor presents wide spread anthropogenically driven increase in fire occurrence in the RFE during spring months. The second factor represents primarily localized weather driven increases in fire danger at daily scales. Fires connected to the second factor are more likely to occur in remote and particularly important sections of tiger habitat, thus resulting in higher fire threat. These weather dependant fire events are likely to increase in number and extent by the end of the 21st century over the southern part of the habitat covering 2/3 of the known area of tiger distribution. Based on the trajectories of post-fire recovery described in the literature (Krestov, 2003) with 12-15 year frequency of large fire seasons observed in the 20th century (Sheingauz, 1996), the fire impacted areas generally recovered to a suitable (although not necessarily highest quality) habitat before a new section of the habitat was impacted. Increased frequency of such seasons in the 21st century is likely to result in potentially higher fragmentation of the habitat with considerable loss of connectivity.

6.5. *Conclusions*

Fire threat modeling provides a structure for incorporating wildland fire into resource management and resource protection framework. It draws linkages between generic fire impacts and specific responses to those characteristic for the Amur tiger. A remotely sensed data driven model is applied to analyze fire threat to the tiger

meta-population based on the patterns observed during 2005 – 2007. As a modeling tool, this approach can be used to analyze a variety of potential scenarios including management decision and future forecasting. In this research, the model's predictive capability was used to evaluate potential long-term changes in fire threat under the future scenarios of climate change produced by the ECHAM5 model.

The results show that at present in low to moderate fire years the Amur tiger habitat is rarely threatened by wildland fire. The combination of fairly low fire activity with trajectories of vegetation recovery within the existing tiger habitat, results in overall low fire threat throughout the year. Only relatively small and localized high fire threat occurrences were observed in the RFE during 2005-2007. The range of potential change in fire threat by the end of the 21st century, projected by various climate change scenarios, is considerable. Under B1 scenario, fire threat is likely to remain at the present low levels. However, under the most unfavorable A2 scenario fire threat to the Amur tiger and its habitat will rise. The magnitude of change will vary in space and time with the most pronounced increase in the southern part of the known Amur tiger habitat. Fire threat is expected to rise considerably throughout late summer and fall. However, the frequency of episodic high fire threat events is likely to increase throughout the year.

The results presented in this chapter reflect an assessment of potential fire threat to the Amur tiger under the changing climate based on the currently available datasets. The predictive capabilities of the presented model can be further improved through development of better understanding of post-fire habitat use by tigers and their prey species, recovery of fire degraded forests, more precise habitat suitability

modeling, and fine-tuning remotely sensed products to represent the drivers of the

resource well-being more adequately. The analysis will be strengthened by a longer

monitoring period and inclusion of catastrophic fire years.   Our ability to model

climate induced change in fire threat to the Amur tiger will be further improved with

the development of regional high resolution climate models capable of capturing

regional specifics and spatial variability of climate change in the RFE.

Chapter 7: Operational and Scientific Potential for Fire Threat Modeling for the Amur Tiger and Its Habitat and Areas for Future Research

7.1. Implications of this research for tiger conservation

The Russian Far East currently presents a stronghold for tiger conservation (Dinerstein et al., 2006). The RFE contains two of 20 Global Priority Tiger Conservation Landscapes (TCL), described as regions offering a high probability of long-term persistence of at least 100 individual tigers with evidence of breeding and minimal-moderate threat levels. The strategic document for tiger conservation defines preservation of whole landscapes including core areas, buffer zones, and dispersal routes as the goal of tiger conservation in the wild (Dinerstein et al., 2006). This document cites habitat destruction and degradation as one of the highest threats to the tigers and underlines the importance of preserving every remaining portion of the habitat necessary to facilitate movement of tigers across landscape. A habitat protection plan for the Amur tiger was developed to ensure the long-term existence of interlinked core conservation units spread across the RFE with an intent to "guard against catastrophic events and minimize the effects of long-term habitat and genetic erosion" (Miquelle et al., 1999b).

Wildland fire presents the dominant and recurring natural catastrophe affecting the Amur tiger habitat with the yearly amount of burned area ranging between 200,000 ha and nearly 1,000,000 ha during low and high fire severity seasons, respectively. The fire threat model, developed within this research, provides

a useful tool for operational monitoring of fire threat to the Amur tiger at the daily time scale (driven by changes in weather), assessment of management decisions aimed at ensuring habitat availability and connectivity, and strategic planning for tiger conservation and landscape protection.

This research has demonstrated that "protected area" status does not limit catastrophic fire occurrence in core areas of tiger habitat. Despite a close link between fire ignitions and anthropogenic activity in the RFE in general, large fires that occur during uncharacteristically dry years, burn in remote areas with limited human access. These fires can result in extensive (over 500,000 ha in the summer of 2003) conversion of tree dominated land to open landscapes thus considerably modifying the available tiger habitat. Over 3% of the area within the habitat protection plan burned during the 2001-2005 period with nearly 2% burned during a single catastrophic season of 2003. Considering that fires are recurrent events in the RFE, it is important that fire modification of the habitat (specifically within the core areas, buffers, and dispersal routes, identified in the TCL approach) is monitored on a yearly basis and is reflected in the habitat protection plan. The habitat protection plan should be treated as a dynamic strategic document and adjusted to reflect current habitat availability and connectivity of its individual sections and to be updated approximately every 5 years.

The repeated burning in broadleaf forests of the southern tip of the tiger range, identified in this study (Figure 7-1), may be contributing to the decline in tiger numbers in these areas reported by field surveys (Miquelle, 2006). Repeated low intensity surface fires observed in these forests do not kill the dominant trees but

remove the understory and surface layers, impeding forest regeneration and degrading the browsing base for large prey species such as red deer (~140-250 kg (Heptner et al., 1989)). Although the resultant increase in herbaceous cover within these forests is beneficial for smaller prey species (e.g. sika deer, ~60 - 131 kg (Heptner et al., 1989)) (Dr. John Seidensticker, personal comm.., 2008), the increase in prey biomass associated with distribution density for sika deer in the oak forests of the RFE (from ~ 0.3 to ~1 individuals per km^2 between 1992 and 2002) is not comparable to the decrease in densities of red deer (from ~ 4 to ~2 individuals per km^2 between 1992 and 2002) (Stephens et al., 2005a).
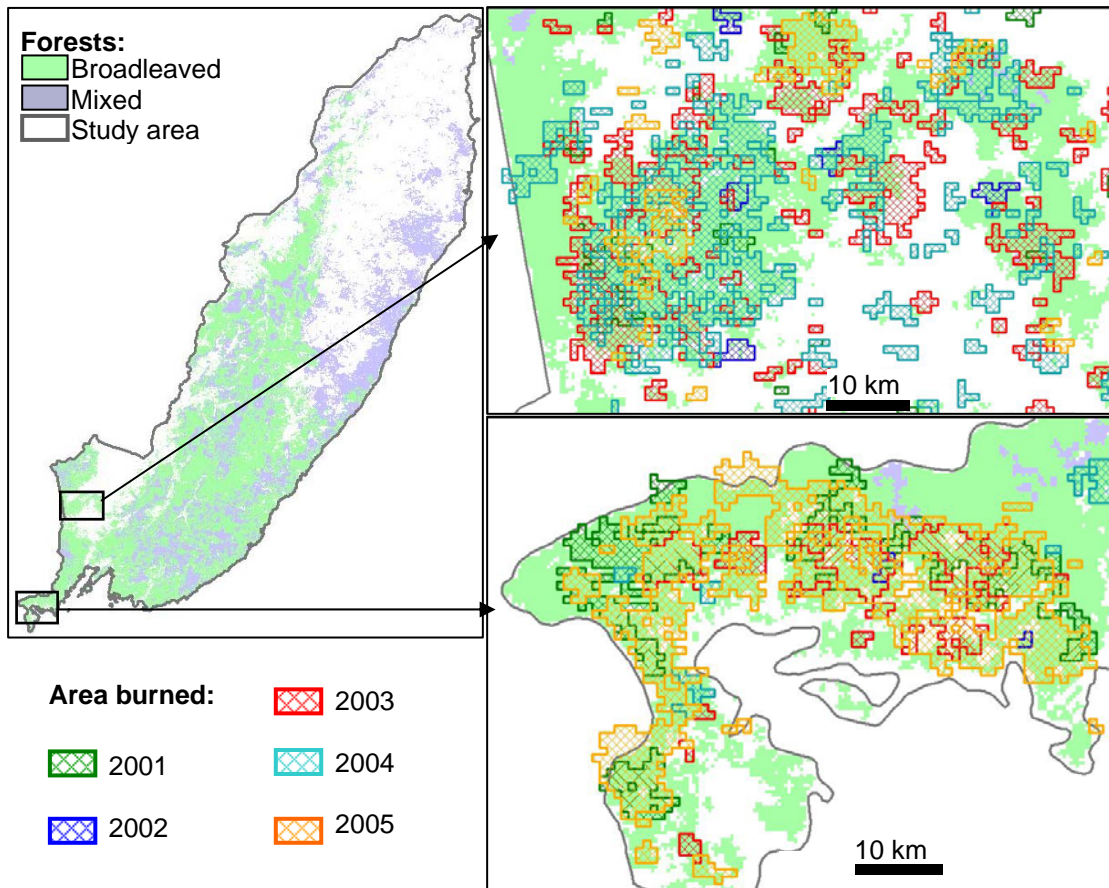
Figure 7-1. Multi-year burning in broadleaved forests of the southern RFE

In certain cases wildland fire occurrence has a positive effect, improving tiger habitat by converting larch and spruce/fir forests, which provide a substandard habitat for tigers, to shrub dominated communities supporting higher prey densities. These fires frequently occur during large fire seasons (exceptionally dry conditions) and lead to extensive habitat conversion with short-term negative but long-term positive influence on tiger habitat quality. However, the impact of these fires on spatial habitat connectivity and subsequently tiger dispersal is not well understood and requires further investigation.

The pressing nature of the decline in the number of tigers and extent of their habitat (Dinerstein et al., 2006) consumes the current tiger conservation operations and leaves little room for long-term studies aimed at evaluation of climate change impacts on future habitat availability and sustainability of the species. This research presents one of the first contributions to the extension of the strategic framework for tiger conservation. Although the current levels of fire threat to the Amur tiger are generally low, the stability of the Amur tiger habitat in the RFE, crucially important for long-term tiger survival, is uncertain under the influence of changing climate. The currently projected climate change results in little change in fire threat under the B1 and a noticeable increase under the A2 SRES IPCC scenarios. Although the A2 scenario is considered the "worst case" story line of the SRES suite, it appears the most likely to occur, based on the observed rates of economic development in South and South-East Asia.

The results indicate that the southern portion of the tiger habitat is likely to experience a considerable increase in fire threat (up to 20% mean annual increase and

up to 40% increase in mean August fire threat) by the end of the 21st century,

compared to the levels at the end of the 20th century. Several core areas included in

the habitat protection plan are likely to see more frequent and severe wildland fires.

In particular, wildland fires are likely to impact the established protected areas,

including Lasovsky and Ussuri State Reserves, Kedrovaya Pad' Zapovednik, and

Barsovy Zakaznik, which may subsequently lose their role as a stronghold and source

of tiger population in the tiger conservation landscapes. The existing and proposed

protected areas (Upper Ussuri National Park, Southern Primorye Nature Park, and

Borisovskoe Plateau Zakaznik) and proposed ecological corridors (Lazovsky, Nature

Park , and Southern Sikhote-Alin) in the southern section of the RFE are small (~

25,000-180,000 ha) and narrow (15-44 km across). The width of these narrow

protected areas is not sufficient to ensure habitat connectivity under the current levels

of fire occurrence (Figure 7-2) and is likely to become less sufficient under the 10-

20% annual increase in fire occurrence, projected for the end of the 21st century.

Based on the sizes of observed fire scars in catastrophic year of 2003, protected areas

larger than 50,000 ha and broader (in their narrowest part) than 35 km may be

required to maintain habitat connectivity under the projected increase in wildland fire

occurrence. While no significant change in fire threat to the tigers is expected over

the northern part of the RFE, these areas currently represent low quality habitat types

(larch and dark coniferous forests) and thus are unlikely to provide a reasonable

substitute for the lost range in the south.

Since the designation of additional protected areas may not be practical or

possible due to competing land uses and economic development, habitat connectivity

can be ensured through strategic planning of forest use aimed at maintaining a

sufficient portion of connected forested landscapes at various stages of regrowth

necessary to support sufficient prey densities and ensure distribution of tigers across

landscapes.
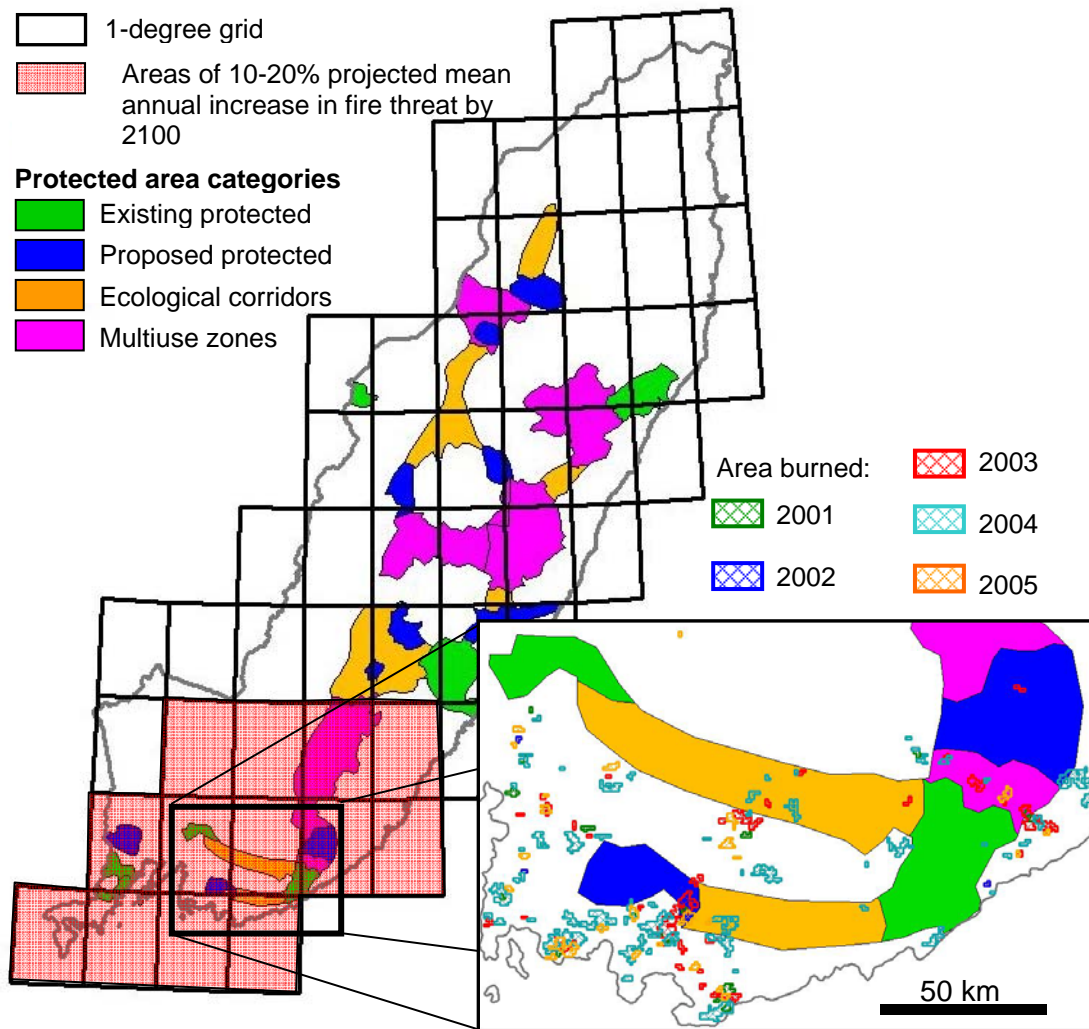
Figure 7-2. Burned areas detected during 2001-2005 within the areas of the habitat

protection plan (habitat protection plan is adapted from Miquelle et al., 1999b)

However, this strategic planning will require close collaboration from various stakeholders, including timber harvesting industries, forest management, recreational hunting, and wildlife protection, and the regional and federal government support.

Because tigers are a conservation dependant species (Dinerstein et al., 2006), their survival depends on our ability to develop a flexible and comprehensive approach to strategic planning for habitat availability. Modeling allows for development of scenarios aimed at evaluating impacts of various aspects of anthropogenic and environmental phenomena beyond the range of our current experience. The fire threat model developed in this research presents a tool and provides a framework for expanding the modeling capabilities to further investigate threat assessment in the context of tiger conservation.

7.2. Modeling fire and impacts of climate change on terrestrial ecosystems

Future functioning of terrestrial ecosystems under changing climate is an important question in Earth system science. Numerous national and international programs focus on developing an understanding of drivers of ecosystem change and forecasting ecosystems development in the future. The research carried out within this project presents methodological advancements enabling an assessment of the drivers and potential future scenarios of change in ecosystem functioning in the RFE through fire threat modeling.

 The fire threat model, developed as part of this research, provides a flexible environment that can support evaluation of fire threat to various resources across the globe and develop future scenarios of fire impact under changing climate or land use.

The availability of global satellite observations ensures the applicability of this modeling framework worldwide. Remotely sensed data driven parameterization of the fire danger model has been shown to provide realistic fire danger estimates in the RFE. This is particularly important as there is no reliable long-term record of fire occurrence or supporting high resolution information available to apply other conventional fire danger rating methods.

The fire danger and fire threat models also provide a framework for evaluating potential future scenarios. Fire danger modeling using outputs from a Global Circulation Model (GCM) enables the assessment of changing fire regimes under various emission scenarios. However, the accuracy and the resolution of the future scenarios are limited by the resolution and accuracy of the existing GCM outputs. This research showed a large discrepancy between the GCM modeled weather parameters and the observed meteorological conditions in the RFE at the end of the 20th century. In this region the ECHAM5 model appears to significantly overestimate oceanic influence on the area's climate expressed through temperature, humidity, and precipitation. Further development of high resolution regional climate models fine-tuned to realistically represent climatic processes at the regional scale, with a particularly important ability to forecast extreme or uncharacteristic climatic conditions, is imperative to improving our future predictive capabilities. Similarly, increased emphasis is needed to sustain and enhance in-situ meteorological measurements in this region and their real time availability.

Accuracy, resolution, and availability of satellite products present the second most important limiting factor in our modeling capabilities. In many areas of the

world satellite observations present the only reliable and consistent source of information about the state of terrestrial ecosystems. The development of early warning systems for wildland fire, emphasized by the Food and Agricultural Organization (FAO, 2001) and the Northern Eurasia Earth Science Partnership Initiative (NEESPI, 2004), require the development of a suite of standardized and validated satellite-based products to support a global view of fire drivers and post-fire impacts on ecosystem functioning. In particular, products detailing fuel availability and structure, live vegetation moisture content, and integrated fire intensity and burn severity are of critical importance.

In summary, the fire threat model, developed in this research, provides a suitable framework for developing global early warning systems of fire danger and fire threat. The existing approaches can be applied to successfully monitor fire danger at the regional scale. However, improvement of satellite-based products, including development of region- and application-specific land cover classifications, mapping 3-dimentional vegetation structure, development of a consistent long-term record of land cover and land use change, and production of reliable estimates of air temperature, humidity, and precipitation, in addition to an increase in density of meteorological observations in remote areas will further our understanding of fire ecology worldwide and improve the model's predictive capabilities. GCM scenarios of climate change currently produce an oversimplified view of regional climate of the RFE. Development of realistic scenarios of fire danger/threat change directly comparable to observed conditions require considerable investment in building regional climate models operating at high resolution (~1 km) with reliable accuracy.

Given the importance of the monsoon in ameliorating the potential impacts of fire in this region it will be important for the climate models to realistically simulate the monsoon processes and investigate any potential shifts or changes in the regional climate.

7.3. Future research directions

Future research will continue the assessment of long-term habitat availability in the RFE within the framework of tiger conservation landscapes. This study addressed the threat to tigers and their habitat arising from potential future climate driven increase in natural catastrophes and specifically wildland fire. A comprehensive assessment of compound effects from multiple drivers of habitat modification (such as climate induced vegetation change, timber harvesting, human population growth, etc) and their feedbacks will help to evaluate the feasibility of reaching the goals of increasing the tiger population in the RFE tiger conservation landscapes and maintaining the population long-term (i.e. MVP). This comprehensive approach will allow for identification of newly developing areas, capable of supporting tiger presence, as well as sections of habitat, lost to fire or timber harvesting, thus providing a structure for habitat monitoring and projecting dynamic shifts in habitat availability and potential for habitat management.

The immediate objectives of future research will address the uncertainties remaining within the potential impacts of wildland fire on habitat availability. In particular, the short record of data availability for fire threat modeling (2005-2007) limits our understanding of potential fire impacts on the Amur tiger and its habitat during years of large fire occurrence. The analysis of fire regimes presented in this

work shows that these seasons result in 3-5 times greater amounts of burned area than low fire severity seasons.   In addition, these large burns occur in remote areas of tiger habitat as opposed to areas close to human presence, which is typical of mild fire seasons. Future research will focus on extending the modeling record forward and backward in time to incorporate several high fire severity seasons and improve our understanding of wildland fire threat to the Amur tiger.

This research focused on evaluating fire danger and fire threat under climate induced changes on fire weather. However, climate change impacts on ecosystems are multi-dimensional and are likely to impact vegetation composition, trajectories of post fire vegetation recovery and species composition, and the ranges for tigers and their prey as well. These changes can be addressed using the existing structure of the fire threat model by coupling the model with a suite of related models aimed at understanding climate change impact on individual ecosystem components. A modeling initiative for coupling the fire threat model with a vegetation model to evaluate potential scenarios of changes in habitat restoration and connectivity under increasing pressures from climate change is currently underway in collaboration with the University of Virginia.

Further development of the model's predictive capabilities will also involve addition of a land use modeling component (Messina and Cochrane, 2007). This addition will allow for evaluation of a compound climate and land use impact on fire threat to the Amur tiger as well as development of a set of land use management scenarios aimed at minimizing climate induced fire threat increase.

Finally, the flexible structure of fire danger and fire threat modeling and developed methodologies for remotely-sensed data model parameterization allow for easy expansion of fire danger and fire threat modeling to other regions, particularly those within Northern Eurasia. Future research will evaluate fire danger as a function of socio-economic and environmental drivers across various ecosystems of Northern Eurasia, develop an early warning system for wildland fire within the modeling framework of fire threat, and evaluate potential future wildland fire impacts.

Bibliography

Achard F, Stibig H-J, Laestadius L, Roshchanka V, Yaroshenko A, Aksenov D (Eds)
(2005). 'Identification of "Hot Spot Areas" of Forest Cover Changes in Boreal
Eurasia.' Office for Publications of the European Communities, Luxembourg

Allgőwer B, Carlson JD, van Wagtendonk JW (2003) Introduction to fire danger
rating and remote sensing – will remote sensing enhance wildland fire danger
rating. In Chuvieco E (Ed) 'Wildland fire danger estimation and mapping: the
role of remote sensing data.', 1-20. World Scientific, Singapore.

Amatulli G, Rodrihues MJ, Trombetti M, Lovreglio R (2006) Assessing long-term
fire risk at local scale by means of decision tree technique. *Journal of
Geophysical Research* 3**,** doi:10.1029/2005JG000133

Andrews PL, Queen LP (2001) Fire Modeling and Information System Technology.
International Journal of Wildland Fire **10**, 343-352.

Arino O, Rosaz J (1999) 1997 and 1998 World ATSR Fire Atlas Using ERS- 2
ATSR-2 Data. In Neuenschwander LF, Ryan KC, Goldberg GE (Eds)
'Proceedings of the Joint Fire Science Conference', 177–182. Boise, Idaho 15–17
June, 1999. University of Idaho and the International Association of Wildland
Fire.

Astafiev AA, Potikha EV (2006) History and the Research Activities of the Nature
Reserve. In Astafiev AA, Gromyko MN (Eds) 'Flora and Fauna of the Sikhote-
Alin Zapovednik', 5-13. Primpoligraphcombinat Ltd., Vladivostok, Russia. <in
Russian>

Astafiev AA, Zaitsev VA, Kostoglod VE, Matyushkin EN (2006) Carnivora. In Astafiev AA, Gromyko MN (Eds) 'Flora and Fauna of the Sikhote-Alin Nature Reserve', 306-347. Primpoligraphcombinat Ltd., Vladivistok, Russia. <in Russian>

Auffhammer and Carson (in press) Forecasting the path of China's CO_2 emissions using province-level information. *Journal of Environmental Economics and Management*, doi:10.1016/j.jeem.2007.10.002

Backer DM, Jensen SE, McPherson GR (2004) Impacts of Fire-Suppression Activities on Natural Communities. *Conservation Biology* **18 (4)**, 937-946.

Barber VA, Juday GP, Finney BP (2000) Reduced Growth of Alaskan White Spruce in the Twentieth Century from Temperature-Induced Drought Stress. *Nature* **405**, 668-673.

Bartalev S, Ershov D, Isaev A, Potapov P, Turubanova S, Yaroshenko A (2004) Russia's Forests. TerraNorte Information System. RAS Space Research Institute. <terranorte.iki.rssi.ru> 08/05/2005

Bartalev SA, Belward AS, Erchov DV, Isaev AS (2003) A New SPOT4-VEGETATION Derived Land Cover Map of Northern Eurasia. *International Journal of Remote Sensing* **24 (9)**, 1977 – 1982.

Baskin L, Danell K (2003) 'Ecology of Ungulates: A Handbook of Species in Eastern Europe and Northern and Central Asia'. Springer-Verlag Berlin Heidelberg, Germany.

Bonazountas M, Kallidromitou D, Kassomenos PA, Passas N (2005) Forest Fire Risk Analysis. *Human and Ecological Risk Assessment* **11**, 617–626.

Bonan GB, Pollard D, Thompson SL (1992) Effects of Boreal Forest Vegetation on Global Climate. *Nature* **359**, 716 – 718.

Bond WJ, Woodward FI, Midgley GF (2005) The Global Distribution of Ecosystems in a World Without Fire. *New Phytologist* **165**, 525-538.

Brivio PA, Maggi M, Binaghi E, Gallo I (2003) Mapping Burned Surfaces in Sub-Saharan Africa Based on Multi-Temporal Neural Classification. *International Journal of Remote Sensing* **24 (20)**, 4003−4018.

Buchholtz G, Weidemann D (2000) The Use of Simple Fire Danger Rating Systems as a Tool for Early Warning in Forestry. *International Forest Fire News* **23**, 33-36.

Chapin FS, McGuire AD, Randerson J, Pielke R, Baldocchi D, Hobbie SE, Roulet N, Eugster W, Kasischke E, Rastetter EB, Zimov A, Running SW (2000) Arctic and Boreal Ecosystems of Western North America as Components of the Climate System. *Global Change Biology* **6**, 211-223.

Chuvieco E, Cocero D, Riano D, Martin P, Martinez-Vega J, de la Riva J, Perez F (2004) Combining NDVI and Surface Temperature for the Estimation of Live Fuel Moisture Content in Forest Fire Danger Rating. *Remote Sensing of Environment* **92**, 322-331.

Chuvieco E, Martin MP (1994) Global fire mapping and fire danger estimation using AVHRR images. *Photogrammetric Engineering and Remote Sensing* **60 (5)**, 563−570.

Cocke AE, Fule PZ, Crouse JE (2005) Comparison of Burn Severity Assessments
Using Differenced Normalized Burn Ratio and Ground Data. *International
Journal of Wildland Fire* **14 (2)**, 189−198.

Cohen JD (1999) Reducing the Wildland Fire Threat to Homes: Where and How
Much. USDA Forest Service Gen.Tech.Rep. PSW-GTR-173.
<www.nps.gov/fire/download/pub_pub_reducingfirethreat.pdf> 03/30/2008

Conard SG, Sukhinin AI, Stocks BJ, Cahoon DR, Davidenko EP, Ivanova GI (2002)
Determining Effects of Area Burned and Fire Severity on Carbon Cycling and
Emission in Siberia. *Climatic Change* **55**, 197–211.

Davis FW, Burrows DA (1994) Spatial Simulation of Fire Regime in Mediterranean-
Climate Landscapes. In Moreno JM, Oechel WC (Ed.) 'The Role of Fire in
Mediterranean-Type Ecosystems', 117-139. Ecological Studies, vol. 107.
Springer-Verlag Press.

de Groot WJ, Bothwell PM, Carlsson DH, Logan KA (2003) Simulating the Effects
of Future Fire Regimes on Western Canadian Boreal Forests. *Journal of
Vegetation Science* **14**, 355 - 364.

de la Riva J, Perez-Cabello F, Lana-Renault N, Koutsias N (2004) Mapping Wildfire
Occurrence at Regional Scale. *Remote Sensing of Environment* **92**, 363-369.

Dinerstein E, Loucks C, Heydlauff A, Wikramanayake E, Bryja G, Forrest J,
Ginsberg J, Klenzendorf S, Leimgruber P, O'Brien T, Sanderson E, Seidensticker
J, Songer M (2006) Setting Priorities for the Conservation and Recovery of Wild
Tigers: 2005–2015. A User's Guide. WWF, WCS, Smithsonian, and NFWF-STF,
Washington, D.C. – New York.

Dinerstein E, Loucks C, Wikramanayake E, Ginsberg J, Sanderson E, Seidensticker J,
Forrest J, Bryja G, Heydlauff A, Klenzendorf S, Leimgruber P, Mills J, O'Brien
TG, Shrestha M, Simons R, Songer M (2007) The Fate of Wild Tigers.
BioScience **57 (6)**, 508-514.

Egorov VA, Bartalev SA, Loupian EA (2004) Algorithm for Burned Area Detection
and Assessment of Fire-Induced Vegetation Damage from SPOT-Vegetation
Data. Conference proceedings of the International Scientific-Technical conference
dedicated to 225 anniversary of Moscow State University of Geodesy and
Cartography (MIIGAiK), 199−204. Moscow, Russia <in Russian>

Epting J, Verbyla D, Sorbel B (2005) Evaluation of Remotely Sensed Indices for
Assessing Burn Severity in Interior Alaska Using Landsat TM and ETM+.
Remote Sensing of Environment **96**, 328−339.

Fairbrother A, Turnley JG (2005) Predicting Risks of Uncharacteristic Wildfires:
Application of the Risk Assessment Process. *Forest Ecology and Management*
211, 28–35.

FAO (2001) Global Forest Fire Assessment 1990-2000. Forest Resources
Assessment Working Paper - 055, AD653/E.
<http://www.fao.org/docrep/006/AD653E/ad653e105.htm> 03/30/2008

Flannigan MD, Logan KA, Amiro BD, Skinner WR, Stocks BJ (2005) Future area
burned in Canada. *Climatic Change* **72**, 1–16.

Flannigan MD, Vonderhaar TH (1986) Forest-Fire Monitoring Using NOAA Satellite
AVHRR. *Canadian Journal of Forest Research* **16 (5)**, 975−982.

Friedl MA, McIver DK, Hodges JCF, Zhang XY , Muchoney D, Strahler AH, Woodcock CE, Gopal S, Schneider A, Cooper A, Baccini A, Gao F, Schaaf C (2002) Global Land Cover Mapping from MODIS: Algorithms and Early Results. *Remote Sensing of Environment* **83**, 287 - 302.

Fuller M (1991) 'Forest Fires: An introduction to wildland fire behavior, management, firefighting, and prevention.' John Wiley & Sons, New York, USA.

Gao BC (1996) NDWI - A Normalized Difference Water Index for Remote Sensing of Vegetation Liquid Water from Space. *Remote Sensing of Environment* **58 (3)**, 257−266.

George C, Rowland C, Gerard F, Balzter H (2006) Retrospective Mapping of Burnt Areas in Central Siberia Using a Modification of the Normalized Difference Water Index. *Remote Sensing of Environment* **104**, 346−359.

Gerard F, Plummer S, Wadsworth R, Sanfeliu AF, Iliffe L, Balzter H, Wyatt B (2003) Forest Fire Scar Detection in the Boreal Forest with Multitemporal SPOT-VEGETATION Data. *IEEE Transactions on Geoscience and Remote Sensing* **41 (11)**, 2575−2585.

Giglio L, Descloitres J, Justice CO, Kaufman YJ (2003) An Enhanced Contextual Fire Detection Algorithm for MODIS. *Remote Sensing of Environment* **87 (2-3)**, 273-282.

Giglio L, van der Werf GR, Randerson JT, Collatz GJ, Kasibhatla P (2006) Global Estimation of Burned Area Using MODIS Active Fire Observations. *Atmospheric Chemistry and Physics* **6**, 957−974.

Gill AE (1982) 'Atmosphere-Ocean Dynamics.' Academic Press, New York.

Gillett NP, Weaver AJ, Zwiers FW, Flannigan MD (2004) Detecting the Effect of Climate Change on Canadian Forest Fires. *Geophysical Research Letters* **31 (18)**, Art. No. L18211.

Gossow H (1996) Fire-Vegetation-Wildlife Interactions in the Boreal Forest. In Goldammer JG, Furyaev VV (Eds) 'Fire in Ecosystems of Boreal Eurasia', 431-444. Kluwer Academic Publishers, Dodrecht, Netherlands.

Groisman PA, Sherstyukov BG, Razuvaev VN, Knight RW, Enloe JG, Stroumentova NS, Whitfield PH, Førland E, Hannsen-Bauer I, Tuomenvirta H, Aleksandersson H, Mescherskaya AV, Karl TR (2007) Potential Forest Fire Danger over Northern Eurasia: Changes During the 20th Century. *Global and Planetary Change* **56 (3-4)**, 371-386.

Gromyko MN (2006) Climate Change and Catastrophic Disturbances of Forest Ecosystems in the Sikhote-Alin State Nature Reserve. In Darman YuA, Kokorin AO, Minin AA (Eds) 'Climate Change Impact on Ecosystems of the Amur River Basin', 52-67. Moscow: WWF-Russia, 2006. <in Russian>

Gutman G, Bartalev S, Korovin G (1995) Delineation of Large Fire Damage Areas in Boreal Forests Using NOAA AVHRR Measurements. *Natural Hazards: Monitoring and Assessment Using Remote Sensing Technique Advances in Space Research* **15 (11)**, 111−113.

Hanes TL (1971) Succession after Fire in the Chaparral of Southern California. *Ecological Monographs* **41 (1)**, 27−52.

Hansen MC, DeFries RS, Townshend JRG, Carroll M, Dimiceli C, Sohlberg RA (2003) Global Percent Tree Cover at a Spatial Resolution of 500 Meters: First

Results of the MODIS Vegetation Continuous Fields Algorithm. *Earth Interactions* **7 (10)**, 1 - 15.

Harden JW, Manies KL, Turetsky MR, Neff JC (2006) Effects of Wildfire and Permafrost on Soil Organic Matter and Soil Climate in Interior Alaska. *Global Change Biology* **12**, 2391–2403.

Harris GA (1967) Some Competitive Relationships Between Agropyron spicatum and Bromus tectorum. *Ecological Monographs* **37 (2)**, 89−111.

Heptner VG, Nasimovich AA, Bannikov AG (1989) 'Mammals of the Soviet Union: Ungulates'. Amerind Publishing Co. Pvt. Ltd., New Deli.

Howard SM, Lacasse JM (2004) An Evaluation of Gap-Filled Landsat SLC-Off Imager for Wildland Fire Burn Severity Mapping. *Photogrammetric Engineering and Remote Sensing* **70**, 877−880.

Humphrey LD (1984) Patterns and Mechanisms of Plant Succession After Fire on Artemisia-Grass Sites in Southeastern Idaho. *Vegetation* **57 (2–3)**, 91−101.

Iliadis LS (2005) A Decision Support System Applying an Integrated Fuzzy Model for Long-Term Forest Fire Risk Estimation. *Environmental Modeling and Software* **20**, 613-621.

IPCC (2007) IPCC Fourth Assessment Report: Climate Change 2007. <http://www.ipcc.ch/ipccreports/ar4-syr.htm> 03/10/2008

IUCN (2001) World Heritage Nomination − IUCN Technical Evaluation: Central Sikhote-Alin (Russian Federation): 19-24. <whc.unesco.org> 08/21/2004

Ivanova GA, Ivanov VA (1999) Fire and Fire Regimes in the Forests of Central Siberia. Papers from the poster session. The Joint Fire Science Conference and

Workshop, Boise Idaho, June 15-17, 1999.

<http://jfsp.nifc.gov/conferenceproc/P-06Ivanovaetal.pdf> 4/01/2008

Jayaweera KOLF, Ahlnas K (1974) Detection of Thunderstorms from Satellite
Imagery for Forest Fire Control. *Journal of Forestry* **72 (12)**, 767−770.

Johnson EA (1992) 'Fire and Vegetation Dynamics: Studies from the North
American Boreal Forest.' Cambridge University Press, Cambridge, UK.

Jolly WM, Graham JM, Michaelis A, Nemani R, Running SW (2005) A Flexible,
Integrated System for Generating Meteorological Surfaces Derived from Point
Sources Across Multiple Geographic Scales. *Environmental Modeling and
Software* **20**, 873-882.

Justice CO, Vermote E, Townshend JRG, Defries R, Roy DP, Hall DK, Salomonson
VV, Privette J, Riggs G, Strahler A, Lucht W, Myneni R, Knjazihhin Y, Running
S, Nemani R, Wan Z, Huete A, van Leeuwen W, Wolfe R (1998) The Moderate
Resolution Imaging Spectroradiometer (MODIS): Land Remote Sensing for
Global Change Research. *IEEE Transactions on Geoscience and Remote Sensing*
36 (4), 1228−1249.

Kasischke ES, Hyer EJ, French NHF, Suchinin AI, Hewson JH, Stocks BJ (2004)
Carbon Emissions from Boreal Forest Fires − 1996 to 2002. *Global
Biogeochemical Cycles* **19**, GB1012, doi:10.1029/2004

Kaufman YJ (1988) Atmospheric Effect on Spectral Signature \ Measurements and
Corrections. *IEEE Transactions on Geoscience and Remote Sensing* **26 (4)**,
441−450.

Kaufman YJ, Justice CO, Flynn LP, Kendall JD, Prins EM, Giglio L, Ward DE, Menzel WP, Setzer AW (1998) Potential Global Fire Monitoring from EOS-MODIS. *Journal of Geophysical Research – Atmospheres* **103 (D24)**, 32215-32238.

Kerley LL, Goodrich JM, Miquelle DG, Smirnov EN, Quigley HB, Hornocker MG (2003) Reproductive Parameters of Wild Female Amur (Siberian) Tigers (*Panthera tigris altaica*). *Journal of Mammalogy* **84 (1)**, 288-298.

Kerley LL, Goodrich JM, Nikolaev IG, Miquelle DG, Schleyer BO, Smirnov EN, Quigley HB, Hornocker MG (2005) Reproductive Statistics for Female Amur Tigers in the Wild. In Miquelle DG, Smirnov E, Goodrich J (Eds) 'Tigers of the Sikhote-Alin Nature Reserve: Ecology and Conservation', 61-69. Vladivostok, Russia. <in Russian>

Key CH, Benson NC (2006) FIREMON Landscape Assessment: Sampling and Analysis Methods. USDA Forest Service General Technical Report RMRS-GTR-164-CD. 2006 <http://frames.nbii.gov/projects/firemon/FIREMON_LandscapeAssessment.pdf> 04/05/2008

Kie JG, Bowyer RT, Stewart KM (2003) Ungulates in Western Coniferous Forests: Habitat Relationships, Population Dynamics, and Ecosystem Processes. In Zabel CJ, Anthony RG (Eds) 'Mammal Community Dynamics: Management and Conservation in the Coniferous Forests of Western North America', 296-340. Cambridge University Press, New York, NY, USA.

Kielland K, McFarland J, Olson K (2006) Amino Acid Uptake in Deciduous and Coniferous Taiga. *Plant Soil* **288**, 297 – 308.

Korontzi S, McCarty J, Loboda T, Kumar S, Justice C (2006) Global Distribution of Agricultural Fires in Croplands from 3 Years of Moderate Resolution Imaging Spectroradiometer (MODIS) Data. *Global Biogeochemical Cycles* **20**, GB2021, doi:10.1029/2005GB002529

Korovin GN (1996) Analysis of the Distribution of Forest Fires in Russia. In Goldammer JG, Furyaev VV (Eds) 'Fire in Ecosystems of Boreal Eurasia', 112-128. Kluwer Academic Publishers, Dodrecht, Netherlands.

Kotlyakov V (2003) Climate. In Stolbovoi V , McCallum I (Eds) 'Land Resources of Russia.' CD-Rom. International Institute for Applied Systems Analysis and the Russian Academy of Science. Laxenburg, Austria.

Kovacs K, Ranson J, Sun G, Kharuk VI (2004) The Relationship of the Terra MODIS Fire Product and Anthropogenic Features in the Central Siberian Landscape. *Earth Interactions* **8 (18)**, 1–25.

Krestov P (2003) Forest Vegetation of Easternmost Russia (Russian Far East). In Kolbek T, Srutek M, Box EO (Eds) 'Forest Vegetation of Northeast Asia.', 93-180. Kluwer Academic Publishers, Dodrecht, Netherlands.

Kruse FA, Lefkoff AB, Boardman JW, Heidebrecht KB, Shapiro AT, Barloon JP, Goetz AFH (1993) The Spectral Image Processing System (SIPS) - Interactive Visualization and Analysis of Imaging Spectrometer Data. *Remote Sensing of Environment* **44**, 145−163.

Lee TM, Jetz W (2007) Future Battlegrounds for Conservation under Global Change. *Proceedings of the Royal Society*, 1-10. doi:10.1098/rspb.2007.1732.

Loboda TV (in press) Modeling Fire Danger in Data-Poor Regions: A case study from the Russian Far East. *International Journal of Wildland Fire*.

Loboda TV, Csiszar IA (unpublished) Inter-comparison of Burned Area Estimates in Central Siberia derived from Various Coarse Resolution Satellite Data Sources.

Loboda TV, Csiszar IA (2005) Estimating Burned Area from AVHRR and MODIS: Validation Results and Sources of Error. Proceeding of the 2nd Open All-Russia Conference: Current Aspects of Remote Sensing of Earth from Space   (Physical basics, methods and monitoring technologies of an environment, potentially of dangerous phenomena and objects), Moscow, Russia, 2004, Volume 2: 415–421. Space Research Institute of the Russian Academy of Sciences, Publishing House GRANP, Moscow 2005.

Loboda TV, Csiszar IA (2007a) Assessing the Risk of Ignition in the Russian Far East within a Modeling Framework of Fire Threat. *Ecological Applications* **17 (3)**, 791-805.

Loboda TV, Csiszar IA (2007b) Reconstruction of fire spread within wildland fire events in Northern Eurasia from the MODIS active fire product. *Global and Planetary Change,* **56 (3-4)**, 258-273.

Loboda TV, O'Neal KJ, Csiszar IA (2007) Regionally Adaptable dNBR-based Algorithm for Burned Area Mapping from MODIS Data. *Remote Sensing of Environment* **109**, 429-442.

Logan JA, Régnière J, Powell JA (2003) Assessing the Impacts of Global Warming on Forest Pest Dynamics. *Frontiers in Ecology and Environment* **1**, 130- 137.

Lopez-Garcia MJ, Caselles V (1991) Mapping Burns and Natural Reforestation Using Thematic Mapper Data. *Geocarto International* **6**, 31-37.

Lynham TA (2005) International Wildland Fire Danger Rating Early Warning Through the Use of Satellite Remote Sensing Data. White paper for the Committee on Earth Observation Sattelites (CEOS) meeting April 20-22, 2006 Japan.

Mack RN (1981) Invasion of Bromus-tectorum L into Western North America - An Ecological Chronicle. *Agro-Ecosystems* **7 (2)**, 145−165.

Malczewski J (1999) 'GIS and Multicriteria Decision Analysis.' John Wiley and Sons, New York, New York, USA.

Malevsky-Malevich SP, Molkentin EK, Nadyozhina ED, Shklyarevich OB (2008) An Assessment of Potential Change in Wildfire Activity in the Russian Boreal Forest Zone Induced by Climate Warming During the Twenty-First Century. *Climatic Change* **86**, 463–474.

Martell DL (2001) Forest Fire Management. In Johnson EA, Miyanishi K (Eds) 'Forest Fires: Behavior and Ecological Effects', 527-583. Academic Press, San Diego, CA, USA.

Matyushkin EN (2006) Carnivora: the Amur tiger. In Astafiev AA, Gromyko MN (Eds) 'Flora and Fauna of the Sikhote-Alin Nature Reserve', 335-341. Primpoligraphcombinat Ltd., Vladivistok, Russia. <in Russian>

Meehl GA (2007) Global Climate Projections: The 2007 IPCC Assessment.

Statement before the Committee on Science and Technology of the United States

House of Representatives. February 8, 2007.

<www.ucar.edu/oga/pdf/meehl_testimony%202-07.pdf> 03/29/2008

Messina JP, Cochrane MA (2007) The Forests are Bleeding: How Land Use Change

is Creating a New Fire Regime in the Ecuadorian Amazon. *Journal of Latin

American Geography* **6 (1)**, 85-100.

Millennium Ecosystem Assessment (2005) Ecosystems and Human Well-Being:

Biodiversity Synthesis. Washington, DC: Millennium Ecosystem Assessment.

World Resources Institute.

Minnich RA (1983) Fire mosaics in Southern California and Northern Baja

California. *Science* **219 (4590)**, 1287−1294.

Miquelle DG (2006) Monitoring Amur Tigers 2005 – 2006. Final Report to the

National Fish and Wildlife Foundation, Save the Tiger Fund from the Wildlife

Conservation Society (Grant # 2005-0013-026).

<http://www.savethetigerfund.org/AM/Template.cfm?Section=Home&CONTEN

TID=8564&TEMPLATE=/CM/ContentDisplay.cfm> 04/02/2008

Miquelle DG, Smirnov EN, Merrill TW, Myslenkov AE, Quigley HB, Hornocker

MG, Schleyer B (1999a) Hierarchical Spatial Analysis of Amur tiger Relationships

to Habitat and Prey. In Seidensticker J, Christie S, Jackson P (Eds) 'Riding the

Tiger: Tiger Conservation in Human Dominated Landscapes', 71-99. Cambridge

University Press, UK.

Miquelle DG, Merrill TW, Dunishenko YM, Smirnov EN, Quigley HB, Pikunov DG, Hornocker MG (1999b) A Habitat Protection Plan for the Amur Tiger: Developing Political and Ecological Criteria for a Viable Land-use Plan. In Seidensticker J, Christie S, Jackson P (Eds) 'Riding the Tiger: Tiger Conservation in Human Dominated Landscapes', 273-289. Cambridge University Press, UK.

Miquelle DG, Murzin A, Hotte M (2004) An Analysis of Fires and Their Impact on Leopards in Southwest Primorye. Attachement to the final report 'Habitat Assessment and Land-use Planning for Siberian Tigers and Amur Leopards in the Russian Far East' to PIN-MATRA. (D. Miquelle, personal comm.)

Miquelle DG, Kerley LL, Goodrich JM, Schleyer BO, Smirnov EN, Quigley HB, Hornocker MG, Nikolaev IG, Matyushkin EN (2005) Specifics of Food Base of the Amur Tiger in the Sikhote-Alin Nature Reserve and the Russian Far East and the Conservation Opportunities. In Miquelle DG, Smirnov E, Goodrich J (Eds) 'Tigers of the Sikhote-Alin Nature Reserve: Ecology and Conservation', 125-131. Vladivostok, Russia. <in Russian>

Miquelle DG, Pikunov DG, Dunishenko YM, Aramilev VV, Nikolaev IG, Abramov VK, Smirnov EN, Salkina GP, Seryodkin IV, Gaponov VV, Fomenko PV, Litvinov MN, Kostyria AV, Yudin VG, Korkisko VG, Murzin AA (2007) A Survey of Amur (Siberian) Tigers in the Russian Far East, 2004-2005. A Final Report Provided to the Save the Tiger Fund. <http://www.savethetigerfund.org/AM/Template.cfm?Section=Final_Reports&TEMPLATE=/CM/ContentDisplay.cfm&CONTENTID=8590> 03/07/2008

Moreno JM, Oechel WC (1994). Fire Intensity as a Determinant Factor of Postfire

    Plant Recovery in Southern California Chaparral. In Moreno JM, Oechel WC

    (Eds) 'The Role of Fire in Mediterranean-Type Ecosystems' Ecological Studies,

    vol. 107: 26-45. Springer-Verlag Press.

Myslenkov AI (2005) Ungulates. In Utenkova AP, Astafiev AA (Eds) 'Structural

    Organization and Dynamics of Natural Complexes of the Sikhote-Alin Biosphere

    Reserve', 213-233. Vladivostok, Russia. <in Russian>

Nakicenovic N, Alcamo J, Davis G, de Vries B, Fenhann J, Gaffin S, Gregory K,

    Grübler A, Jung TY, Kram T, La Rovere EL, Michaelis L, Mori S, Morita T,

    Pepper W, Pitcher H, Price L, Riahi K, Roehrl A, Rogner H-H, Sankovski A,

    Schlesinger M, Shukla P, Smith S, Swart R, van Rooijen S, Victor N, Dadi Z

    (2000). Special Report on Emissions Scenarios: A Special Report of Working

    Group III of the Intergovernmental Panel on Climate Change, Cambridge

    University Press, Cambridge, UK

    <http://www.grida.no/climate/ipcc/emission/index.htm> 03/14/2008

National Climatic Data Center (NCDC) Dataset 9290c (2005a) Global Synoptic

    Climatology Network. C. The Former USSR, 2005. Data documentation. Version

    1.0 <http://www1.ncdc.noaa.gov/pub/data/documentlibrary/tddoc/td9290c.pdf>

National Climatic Data Center (NCDC) Dataset 9813 (2005 b) Daily and Sub-daily

    Precipitation for the Former USSR, 2005. Data documentation. Version 1.0

    <http://www1.ncdc.noaa.gov/pub/data/documentlibrary/tddoc/td9813.pdf>

National Research Council (1995) Science and the Endangered Species Act. Committee of Scientific Issues in the Endangered Species Act. National Academy Press, Washington DC.

NCEP/NCAR Reanalysis1. Data provided by the NOAA-CIRES Climate Diagnostics Center, Boulder, Colorado, USA, from their Web site at <http://www.cdc.noaa.gov/>

NEESPI (2004) The NEESPI Science Plan Executive Overview. <http://neespi.org/>

Oldford S, Leblon B, Maclean D, Flannigan M (2006) Predicting Slow-Drying Fire Weather Index Fuel Moisture Codes with NOAA-AVHRR Images in Canada's Northern Boreal Forests. *International Journal of Remote Sensing* **27 (18)**, 3881-3902.

Peek JM (1997) Habitat Relationships. In Franzmann AW, Schwartz CC (Eds) 'Ecology and Management of the North American Moose', 351-376. Smithsonian Institution Press, Washington DC.

Pimm SL (2008) Biodiversity: Climate Change or Habitat Loss - Which Will Kill More Species? *Current Biology* **Vol 18:** 117-119, doi 10.1016/j.cub.2007.11.055

Prater MR, Obrist D, Arnone JA III, DeLucia EH (2006) Net Carbon Exchange and Evapotranspiration in Postfire and Intact Sagebrush Communities in the Great Basin. *Oecologia* **146**, 595−607.

Preisler HK, Brillinger DR, Burgan RE, Benoit JW (2004) Probability Based Model for Estimation of Wildfire Risk. *International Journal of Wildland Fire* **13**, 133-142.

Prins EM, Feltz JM, Menzel WP, Ward DE (1998) An Overview of GOES-8 Diurnal Fire and Smoke Results for SCAR-B and the 1995 Fire Season in South America. *Journal of Geophysical Research -Atmospheres* **103 (D24)**, 31821−31836.

Rauster Y, Herland E, Frelander H, Soini K, Kuoremaki T, Ruokari A (1997) Satellite-Based Forest Fire Detection for Fire Control in Boreal Forests. *International Journal of Remote Sensing* **18 (12)**, 2641−2656.

Reed DH, O'Grady JJ, Brook BW, Ballou JD, Frankham R, (2003) Estimates of Minimum Viable Population Sizes for Vertebrates and Factors Influencing Those Estimates. *Biological Conservation* **113**, 23-34.

Roads J, Kanamitsu M, Stewart RE (2002) Continental-Scale Experiment Water and Energy Budgets in the NCEP-DOE Reanalysis II. *Journal of Hydrometeorology* **3**, 227-248.

Roy DP, Frost P, Justice CO, Landmann T, Le Roux J, Gumbo K, Makungwa S, Dunham K, Du Toit R, Mhwandagara K, Zacarias A, Tacheba B, Dube O, Pereira J, Mushove P, Morisette J, Vannan S, Davies D (2005a) The Southern Africa Fire Network (SAFNet) Regional burned area product validation protocol. International Journal of Remote Sensing **26**, 4265−4292.

Roy DP, Jin Y, Lewis PE, Justice CO (2005b) Prototyping a Global Algorithm for Systematic Fire-Affected Area Mapping Using MODIS Time Series Data. *Remote Sensing of Environment* **97 (2)**, 137−162.

Roy DP, Boschetti L, Trigg SN (2006) Remote Sensing of Fire Severity: Assessing the Performance of the Normalized Burn Ratio. *IEEE Geoscience and Remote Sensing Letters* **3**, 112-116.

Rundel PW (1998) Landscape Disturbance in Mediterranean-type Ecosystems: An
Overview. In Rundel PW, Montenegro G, Jaksic FM (Eds) 'Landscape
Disturbance and Biodiversity in Mediterranean-Type Ecosystems', Ecological
Studies, vol. 136, 4-22. Springer-Verlag Press.

Sampson RN, Sampson RW (2005) Application of Hazard and Risk Analysis at the
Project Level to Assess Ecologic Impact. *Forest Ecology and Management* **211**,
109–116.

San-Miguel-Ayanz J, Carlson JD, Alexander M, Tolhurst K, Morgan G, Sneeuwjagt
R, Dudley M (2003) Current Methods to Assess Fire Danger Potential. In
Chuvieco E (Ed) 'Wildland fire danger estimation and mapping: the role of
remote sensing data', 21-62. World Scientific, Singapore.

Sasikala KR, Petrou M, Kittler J (1996) Comparison of Different Fuzzy Logic Rules
for Uncertain Reasoning with a GIS. In Binaghi E, Brivio PA, Rampini A (Eds)
'Soft Computing in Remote Sensing Data Analysis', Series in Remote Sensing,
Vol. 1, 121-128. World Scientific Press, MA, USA.

Savin I (2003) Climatic Stations Database. In Stolbovoi V, McCallum I (Eds) 'Land
Resources of Russia.' CD-Rom. International Institute for Applied Systems
Analysis and the Russian Academy of Science. Laxenburg, Austria.

Seidensticker J, Christie S, Jackson P (1999) Tiger Ecology: Understanding and
Encouraging Landscape Patterns and Conditions Where Tigers Can Persist. In
Seidensticker J, Christie S, Jackson P (Eds) 'Riding the Tiger: Tiger Conservation
in Human Dominated Landscapes', 55-60. Cambridge University Press, UK.

Sekercioglu CH, Schneider SH, Fay JP, Loarie SR (in press) Climate Change, Elevational Range Shifts, and Bird Extinctions. *Conservation Biology*.

Shao G, Yan X, Bugmann H (2003) Sensitivities of Species Compositions of the Mixed Forest in Eastern Eurasian Continent to Climate Change. *Global and Planetary Change* **37 (3-4)**, 307-313.

Sheingauz AS (1996) The Role of Fire in Forest Cover, Structure, and Dynamics in the Russian Far East. In Goldammer JG, Furyaev VV (Eds) 'Fire in Ecosystems of Boreal Eurasia', 186-190. Kluwer Academic Publishers, Dodrecht, Netherlands.

Sheshukov MA (1996) Importance of Fire in Forest Formation Under Various Zonal-Geographic Conditions of the Far East. In Goldammer JG, Furyaev VV (Eds) 'Fire in Ecosystems of Boreal Eurasia', 191-196. Kluwer Academic Publishers, Dodrecht, Netherlands.

Shriner DS, Street RB (Eds) (1998) North America. In Watson RT, Zinyowera MC, Moss RH, Dokken DJ (Eds) 'The Regional Impacts of Climate Change: An Assessment of Vlunerability', IPCC Special Report <http://www.grida.no/Climate/ipcc/regional/index.htm> 04/20/2008

Simon M, Plummer S, Fierens F, Hoelzemann JJ, Arino O (2004) Burned Area Detection at Global Scale Using ATSR-2: The GLOBSCAR Products and Their Qualification. *Journal of Geophysical Research - Atmospheres*, **109 (D14)**, Art. No. D14S02.

Sirois L, Payette S (1991) Reduced Postfire Tree Regeneration Along a Boreal Forest-Tundra Transect in Northern Quebec. *Ecology* **72 (2)**, 619-627.

Smirnov EN (2005) The Tiger. In In Utenkova AP, Astafiev AA (Eds) 'Structural Organization and Dynamics of Natural Complexes of the Sikhote-Alin Biosphere Reserve', 202-205. Vladivostok, Russia. <in Russian>

Smirnov EN, Miquelle DG (1999) Population Dynamics of the Amur Tiger in Sikhote-Alin Zapovednik, Russia. In Seidensticker J, Christie S, Jackson P (Eds) 'Riding the Tiger: Tiger Conservation in Human Dominated Landscapes', 61-70. Cambridge University Press, UK.

Smirnov EN, Miquelle DG (2005) Population Dynamics of the Amur Tiger in the Sikhote-Alin Biosphere Reserve: 1966 – 2003. In Miquelle DG, Smirnov E, Goodrich J (Eds) 'Tigers of the Sikhote-Alin Nature Reserve: Ecology and Conservation', 75-82.   Vladivostok, Russia. <in Russian>

Soja AJ, Tchebakova NA, French NHF, Flannigan MD, Shugart HH, Stocks BJ, Sukhinin AI, Parfenova EI, Chapin III FS, Stackhouse Jr PW (2007) Climate-Induced Boreal Forest Change: Predictions Versus Current Observations. *Global and Planetary Change* **56**, 274–296.

Solichin, Goldammer JG, Hoffmann AA, Rucker G (2003) Fire Threat Analysis in West Kutai District of East Kalimantan, Indonesia. 4th International Workshop on Remote Sensing and GIS Applications to Forest Fie Management: Innovative Concepts and Methods in Fire Danger Estimation, 123-127. Ghent, Belguim, Ghent University – EARSeL.

Stephens FA, Zaumyslova OYu, Hayward GD, Miquelle DG (2005a) Estimating the density of ungulates in Sikhote-Alin Zapovednik, In Miquelle DG, Smirnov E,

Goodrich J (Eds) 'Tigers of the Sikhote-Alin Nature Reserve: Ecology and Conservation', 97-112.   Vladivostok, Russia. <in Russian>

Stephens FA, Zaumyslova OYu, Hayward GD, Miquelle DG (2005b) Ungulate abundance in Sikhote-Alin Zapovednik: trends and causal factors. In In Miquelle DG, Smirnov E, Goodrich J (Eds) 'Tigers of the Sikhote-Alin Nature Reserve: Ecology and Conservation', 113-124.   Vladivostok, Russia. <in Russian>

Stocks BJ (1991) The Extent and Impact of Forest Fires in Northern Circumpolar Countries. In Levine, J. S. (Ed) 'Global Biomass Burning: Atmospheric, Climatic, and Biospheric Implications', 197-202. MIT Press, Cambridge, MA.

Stocks BJ (1993) Global Warming and Forest Fires in Canada. *The Forestry Chronicle* **69 (3)**, 290-293.

Stocks BJ, Fosberg MA, Lynham TJ, Mearns L, Wotton BM, Yang Q, Jin J-Z, Lawrence K, Hartley GR, Mason JA, McKenney DW (1998) Climate Change and Forest Fire Potential in Russian and Canadian Boreal Forests. *Climatic Change* **38**, 1-13.

Stolbovoi V, Fischer G, Ovechkin VS, Rozhkova (Kravets) S (1998) Vegetation. In Stolbovoi V, McCallum I (Eds) 'Land Resources of Russia.' CD-Rom. International Institute for Applied Systems Analysis and the Russian Academy of Science. Laxenburg, Austria.

Stolbovoi V, McCallum I (2003) Land Resources of Russia. CD-Rom. International Institute for Applied Systems Analysis and the Russian Academy of Science. Laxenburg, Austria.

Sukhinin AI, French NHF, Kasischke ES, Hewson JH, Soja AJ, Csiszar IA, Hyer E J, Loboda T, Conard SG, Romasko VI, Pavlichenko EA, Miskiv SI, Slinkina OA (2004) Satellite-based Mapping of Fires in Russia: New Products for Fire Management and Carbon Cycle Studies. *Remote Sensing of Environment* **93 (4)**, 546-564.

Tansey K, Gregoire JM, Stroppiana D, Sousa A, Silva J, Pereira JMC, Boschetti L, Maggi M, Brivio PA, Fraser R, Flasse S, Ershov D, Binaghi E, Graetz D, Peduzzi P (2004) Vegetation Burning in the year 2000:Global Burned Area Estimates from SPOT VEGETATION Data. *Journal of Geophysical Research - Atmospheres* **109 (D14)**, Art. No. D14S03.

Taylor SW, Alexander ME (2006) Science, Technology, and Human Factors in Fire Danger Rating: The Canadian Experience. *International Journal of Wildland Fire* **15**, 121-135.

Thomas CD, Cameron A, Green RE, Bakkenes M, Beaumont LJ, Collingham YC, Erasmus BFN, Ferreira de Siqueira M, Grainger A, Hannah L, Hughes L, Huntley B, van Jaarsveld AS, Midgley GF, Miles L, Ortega-Huerta MA, Townsend Peterson A, Phillips OL, Williams SE (2004) Extinction Risk from Climate Change. *Nature* **427**, 145-148.

Thornton PE, Running SW, White MA (1997) Generating Surfaces of Daily Meteorological Variables Over Large Regions of Complex Terrain. *Journal of Hydrology* **190**, 214-251.

UNESCO (2001) Conventions Concerning the Protection of the World Cultural and Natural Heritage: World Heritage Committee report. Helsinki, Finland,

December 11-16, 2001. <http://whc.unesco.org/archive/repcom01.htm#766rev>
08/26/2004

USGS. Reprocessing by the GLCF, 2004. 3 Arc Second SRTM Elevation,
Reprocessed to GeoTIFF. College Park, Maryland: The Global Land Cover
Facility. Version 1.0.

Vadrevu KP, Eaturu A, Badarinath KVS (2006) Spatial Distribution of Forest Fires
and Controlling Factors in Andhra Pradesh, India Using Spot Satellite Datasets.
Environmental Monitoring and Assessment **123**, 75-96.

Vajda A, Venalainen A (2005) Feedback Processes Between Climate, Surface and
Vegetation at the Northern Climatological Tree-line (Finnish Lapland). *Boreal
Environment Research* **10 (4)**, 299-314.

van Wagtendonk JW, Root RR, Key CH (2004) Comparison of AVIRIS and Landsat
ETM+ Detection Capabilities for Burn Severity. *Remote Sensing of Environment*
92 (3), 397-408.

Vermote EF, El Saleous NZ, Justice CO (2002) Atmospheric Correction of MODIS
Data in the Visible to Middle Infrared: First Results. *Remote Sensing of
Environment* **83 (1-2)**, 97−111.

Voloshina IV, Myslenkov AI, Zaitsev VA, Zaumyslova OYu (2006) Artiodactyla. In
Astafiev AA, Gromyko MN (Eds) 'Flora and Fauna of the Sikhote-Alin Nature
Reserve', 350-377. Primpoligraphcombinat Ltd.,Vladivistok, Russia. <in Russian>

Walz Y, Maier SW, Dech SW, Conrad C, Colditz RR (2007) Classification of Burn
Severity Using Moderate Resolution Imaging Spectroradiometer (MODIS): A

Case Study in the Jarrah-Marri Forest of Southwest Western Australia. *Journal of Geophysical Research* **112**, G02002, doi:10.1029/2005JG000118.

Warren AJ, Collins MJ (2007) A Pixel-Based Semi-Empirical System for Predicting Vegetation Diversity in Boreal Forest. *International Journal of Remote Sensing* **28 (1)**, 83–105.

WDPA Consortium (2005) World Database on Protected Areas 2005 – Copyright World Conservation Union (IUCN) and UNEP-World Conservation Monitoring Centre (UNEP-WCMC).

Wein RW, de Groot WJ (1996) Fire-Climate Change Hypotheses for the Taiga. In Goldammer JG, Furyaev VV (Eds) 'Fire in Ecosystems of boreal Eurasia', 505-512. Kluwer Academic Publishers, Dodrecht, Netherlands.

Whelan RJ (1995) 'The Ecology of Fire.' Cambridge University Press, Cambridge, UK.

Williams LJ, Shaw D, Mendelsohn R (1998) Evaluating GCM Output with Impact Models. *Climatic Change* **39 (1)**, 111-133.

Wimberly MC, Reilly MJ (2007) Assessment of Fire Severity and Species Diversity in the Southern Appalachians Using Landsat TM and ETM+ Imagery. *Remote Sensing of Environment* **108**, 189–197.

Wirth TA, Pyke DA (2006) Monitoring Post-Fire Vegetation Rehabilitation Projects: A Common Approach for Non-Forested Ecosystems. USGS Scientific Investigations Report 2006-5048. <http://pubs.usgs.gov/sir/2006/5048/> 07/28/2007

Yager RR (1988) On ordered weighted averaging aggregation operators in multi-criteria decision making. *IEEE Transactions on Systems, Man and Cybernetic*s **18 (1)**, 183–190.

Young JA, Allen FL (1997) Cheatgrass and Range Science: 1930–1950. *Journal of Range Management* **50 (5)**, 530−535.

Zaumyslova OYu (2005) Wild Boar Ecology within the Sikhote-Alin Biosphere Reserve. In Miquelle DG, Smirnov E, Goodrich J (Eds) 'Tigers of the Sikhote-Alin Nature Reserve: Ecology and Conservation', 83-96. Vladivostok, Russia. <in Russian>

Zhang Y H, Wooster MJ, Tutubalina O, Perry GLW (2003) Monthly Burned Area and Forest Fire Carbon Emission Estimates for the Russian Federation from SPOT VGT. *Remote Sensing of Environment* **87 (1)**, 1−15.

Zhu Z, Key C, Ohlen D, Benson N (2006) Evaluate Sensitivities of Burn-Severity Mapping Algorithms for Different Ecosystems and Fire Histories in the United States: Final Report to the Joint Fire Science Program <http://frames.nbii.gov/metadata/documents> 03/05/2008